UM-HSRI-PF-75-1-2

VEHICLE-IN-USE LIMIT PERFORMANCE AND TIRE FACTORS

TECHNICAL REPORT

CONTRACT NUMBER DOT-HS-031-3-693

THE TIRE-IN-USE

JAMES E. BERNARD
PAUL S. FANCHER
RAJIV GUPTA
HOWARD MONCARZ
LEONARD SEGEL

HIGHWAY SAFETY RESEARCH INSTITUTE
THE UNIVERSITY OF MICHIGAN
ANN ARBOR, MICHIGAN 48105

JANUARY 31, 1975

PREPARED FOR:

THE NATIONAL HIGHWAY TRAFFIC SAFETY ADMINISTRATION
U.S. DEPARTMENT OF TRANSPORTATION
WASHINGTON D. C. 20590

TECHNICAL REPORT STANDARD TITLE PAGE

1. Report No.	2. Government Accession No.	3. Recipient's Catalog No.
UM-HSRI-PF-75-1-2		

4. Title and Subtitle	5. Report Date
Vehicle-In-Use Limit Performance and Tire Factors The Tire in Use	Jan. 31, 1975 6. Performing Organization Code

7. Author(s)	8. Performing Organization Report No.
James E. Bernard, Paul S. Fancher, Rajiv Gupta, Howard Moncarz, Leonard Segel	UM-HSRI-PF-75-1-2

9. Performing Organization Name and Address	10. Work Unit No.
Highway Safety Research Institute The University of Michigan Huron Parkway & Baxter Road Ann Arbor, Michigan 48105	11. Contract or Grant No. DOT-HS-031-3-693

12. Sponsoring Agency Name and Address	13. Type of Report and Period Covered
National Highway Traffic Safety Administration U.S. Department of Transportation Washington, D.C. 20590	Final Technical Report 6/73 - 1/75 14. Sponsoring Agency Code

15. Supplementary Notes

16. Abstract The influence of tire-in-use factors (inflation pressure, replacement mixes, and wear) on the steering and braking response of automobiles is examined through analysis, simulation, laboratory and over-the-road tire testing, and vehicle testing. Results for a 1971 Mustang and a 1973 Buick station wagon illustrate the influence of tire-in-use factors on (a) the open-loop braking and/or turning performance in drastic maneuvers on wet and dry surfaces, and (b) the understeer/oversteer factor for maneuvers involving lateral accelerations below 0.3 g.

This investigation shows that differences in tire mechanical properties between the front and rear wheels (as caused by tire-in-use factors) can cause significant and potentially dangerous changes in limit response and from the stability and control characteristics intended by the vehicle manufacturer. The report recommends that (1) inspection limits for inflation pressure be within ±1 psi of the manufacturer's recommended level, (2) minimum tread-groove depth exceed 2/32", and (3) further research be conducted to develop a cost-effective means for indicating the lateral force characteristics of a tire.

17. Key Words	18. Distribution Statement
Tire shear force, vehicle mechanics, tire wear, tire inflation pressure, replacement tire mixes, emergency maneuvers, linear analysis of directional response, vehicle simulation.	Unlimited

19. Security Classif. (of this report)	20. Security Classif. (of this page)	21. No. of Pages	22. Price
Unclassified	Unclassified	224	

Form DOT F 1700.7 (8-69)

DISCLAIMER

The contents of this report reflect the views of the Highway Safety Research Institute which is responsible for the facts and the accuracy of the data presented herein. The contents do not necessarily reflect the official views or policy of the Department of Transportation. This report does not constitute a standard, specification or regulation.

ACKNOWLEDGEMENTS

The Project Technical Manager for NHTSA was Lloyd Emery.

All vehicle testing was done at the Texas Transportation Institute under the direction of Ronald Young and with the assistance of Monroe White. Dr. Young is the author of Appendix E of this report.

Significant contributions to this program were made by Robert Wild, Douglas Brown, and Charles MacAdam of the Highway Safety Research Institute. Messrs. Wild and MacAdam are authors of Appendices D and F of this report, respectively.

PREFACE

The Final Report for this project is divided into two parts, a Summary Report and a Technical Report. This volume contains the Technical Report.

The Technical Report is supported by several extensive appendices. The size of these appendices requires that they be bound under separate covers.

TABLE OF CONTENTS

1.0 INTRODUCTION

This report presents findings and recommendations developed by The University of Michigan Highway Safety Research Institute (HSRI) for the National Highway Traffic Safety Administration (NHTSA) in a project entitled "Vehicle-in-Use: Limit Performance and Tire Factors." The goal of this research was to develop knowledge useful for refining and updating vehicle safety inspection criteria relating to tires. This project concentrated on studying the influence on vehicle performance of the following tire-in-use factors: (1) shoulder wear; (2) inflation pressure; (3) mixed tire construction, including snow tires; and (4) tread wear (tread depth). The effects of these tire-in-use factors were evaluated for tires of bias, belted-bias, and radial construction.

The methodology consisted of tire testing, vehicle testing, and computer simulation. The HSRI flat bed and mobile tire testers were used to obtain shear-force data for a comprehensive set of new and degraded tires. The data were used to assess changes in tire performance caused by tire-in-use factors. Vehicle testing and computer analyses were used to develop an understanding of the influence of changes in tire performance (as brought about by tire-in-use factors) on vehicle performance.

In studying vehicle performance, two questions were addressed: (1) How much do tire-in-use factors change the stability and control of the vehicle from that intended by the manufacturer? and (2) How much does the limit-maneuvering performance of a given vehicle change as a result of front-to-rear tire asymmetries deriving from tire-in-use factors? To answer the first question, vehicle stability and control were examined through the use of linear analysis and vehicle

testing in the normal driving range. Limit-maneuver testing* and computer simulations were used to study accident-avoidance capabilities.

Computer simulations were used extensively to facilitate critical examination of the many possible effects of tire-in-use factors on vehicle performance. Full-scale vehicle test results for a 1971 Ford Mustang and a 1973 Buick Century station wagon were compared to the computed results to verify the accuracy of the computations.

The basic features of the research approach used in this study are described in Section 2 of this volume. The findings derived from the tasks defined in Section 2 are presented in Sections 3, 4, and 5 under the following categories:

1) Influence of tire factors on limit maneuvering performance.

2) Limit performance on wet surfaces.

3) Influence of tire factors on normal driving maneuvers.

The implications of these findings and the recommendations derived from them are presented in Section 6, along with concluding remarks and suggestions for further research.

Seven appendices are included in this report. Appendix A contains a literature survey covering related work. Several other appendices provide detailed documentation of the work done to produce the findings presented in Sections 3, 4, and 5 of this volume.

---

*This report presents material which can be more fully understood if the reader is acquainted with the limit maneuver test methods put forth in an NHTSA-sponsored study entitled "Vehicle Handling Performance" [1]. (Numbers in square brackets indicate references on page 222 .)

Volume II contains appendices A, B, and C which are devoted to a survey of the literature, a description of the tire-vehicle system simulation model, and the vehicle linear analysis program used in this investigation. Appendices D through G treat subjects related to tire testing and vehicle testing. These appendices are contained in Volume III.

All vehicle performance testing, as described in Appendix E, was conducted at the Texas Transportation Institute (TTI) by TTI personnel.

2.0 RESEARCH APPROACH

To assess the importance of tire-in-use factors in vehicle performance, a plan was adopted which divided the research into four major tasks, entitled:

(1) Tire Testing

(2) Linear Performance Study

(3) Simulation of Limit Maneuvers

(4) Limit Maneuver Study

The scope and type of work performed in each of these tasks are described concisely in this section. The important results and findings derived from this work are presented in Sections 3, 4, and 5. Detailed explanations of the methods used and extensive tables and graphs of test data and simulation results may be found in the appendices.

2.1 TIRE TESTING

A schematic diagram indicating the scope of the tire testing is shown in Figure 2-1. A flat-bed tire tester was used to measure the spectrum of cornering stiffnesses for a large number of bias, belted-bias, and radial tires. Based on these data, several tires of each construction type were selected for extensive testing to determine the influence of inflation pressure, tread depth, and shoulder wear on tire performance characteristics such as longitudinal force, lateral force, and aligning torque. Both flat-bed and mobile tire tests were conducted on the selected tires. The flat-bed test results were used to determine the cornering and camber stiffnesses and the aligning torque characteristics of these tires. The mobile tire tester data were used to quantify the influences of velocity and surface (test pad) on tire shear-force performance.

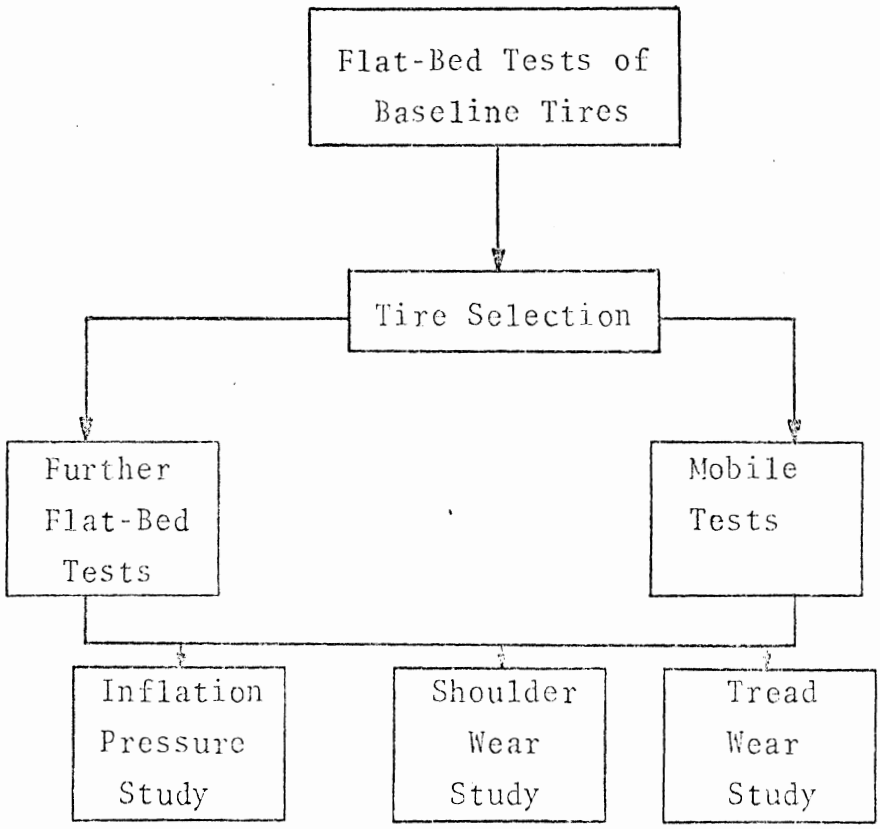

Figure 2-1. Tire test summary

2.1.1 FLAT-BED TIRE TESTING. The HSRI flat-bed laboratory tire tester (shown in Figure 2-2) is an adaptation of a machine developed by B.F. Goodrich [2,3]. It accomodates tires in a size range between 24 in. and 44 in. outside diameter with vertical loadings up to 10,000 lb., and is instrumented to measure all six force and moment components developed by the tire. It is designed to permit low-speed tests at steering angles of up to 90 degrees and camber angles between +20 and -20 degrees. Automatic data scanning and logging using analog-to-digital converters and tape recording equipment provide accurate recording of data for rapid processing on a digital computer.

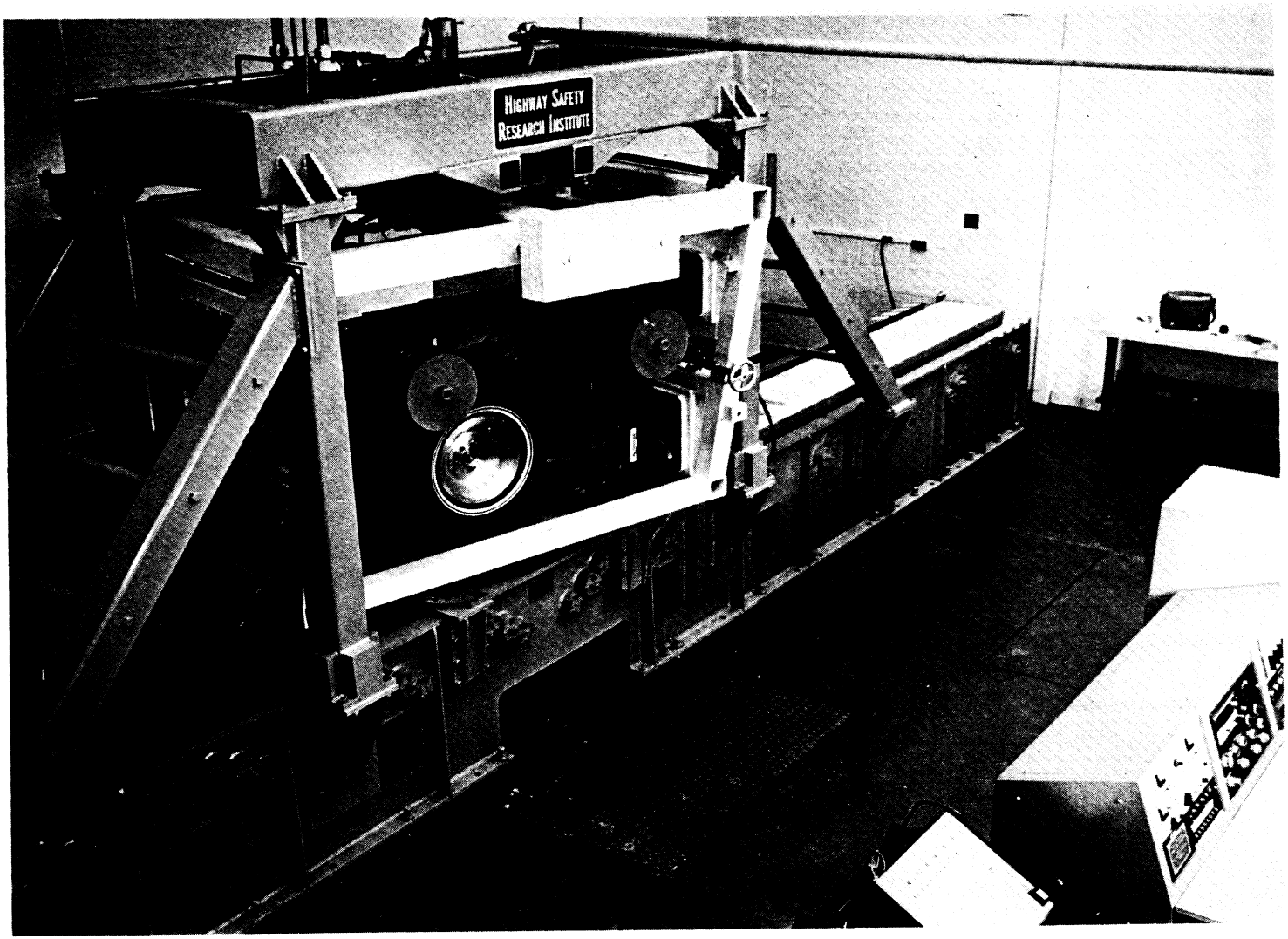

Figure 2-2. Flat-bed tire tester.

The flat-bed tester is intended to provide precise measurements under carefully controlled conditions of the mechanical characteristics of rolling and standing tires. However, since flat-bed data is most useful for quantifying linear elastic tire properties such as cornering stiffness, camber stiffness, and aligning stiffness, the flat-bed tests were concentrated at low values of slip angle and camber angle.

A baseline set of new-tire data gathered on the flat-bed machine was examined to evaluate the probable range of tire properties to be considered. From this baseline, which included over 40 tires, several tires from the radial, bias-belted, and bias categories were selected for further, more comprehensive testing. Each of the tires chosen had a size designation of E or H and an aspect ratio of 78. This latter stipulation was made because the original equipment (OE) tires for the Buick and the Mustang were E78-14 and H78-14, respectively.*

The following tires were selected and tested on the flat-bed machine to establish their elastic properties as a function of load, inflation pressure, and tread wear:

1. Radial—Bridgestone 225SR-14 RD170V, Firestone Town and Country H78-14 (snow), and Pirelli 185-14 CN75 Cinturato.

2. Bias-belted—Firestone Deluxe Champion Sup-R-Belt H78-14 (OE Buick tire), General Belted Jumbo 780 E78-14, General Belted Jumbo 780 H78-14, Goodrich Silvertown belted E78-14 (OE Mustang tire), and Goodyear Custom Power Cushion Polyglas belted E78-14.

*Although aspect ratio and load rating are beyond the scope of this program, it should not be inferred that these are insignificant tire factors. These factors have been studied in another NHTSA-sponsored study [4].

3. Bias—Firestone 500 E78-14, Firestone 500 H78-14, Firestone Town & Country H78-14 (snow).

The data obtained from these flat-bed tests were used in calculations of vehicle performance in the normal driving range. Calculations involving more severe maneuvers require data measured on representative road surfaces at test speeds. Acccordingly, the mobile tire tester was used to gather tire data on the test pads at the Texas Transportation Institute.

2.1.2 MOBILE TIRE TESTING. The HSRI mobile tire tester consists of a retractable test wheel mounted on the rear of a modified tandem-axle commercial tractor (shown in Figure 2-3) which serves as the test bed [2]. The test wheel accommodates tires in the size range from B78-14 to L78-15. A dead-weight, vertical tire load (independent of the test bed) in the range from 600 to 2000 lb. may be used. The test wheel is attached to the test bed through a transducer sensitive to longitudinal and lateral tire forces. Longitudinal and lateral force measurements at all positive values of longitudinal slip, and at slip angles up to 20°, may be made at speeds up to 55 mph. Free-rolling side force measurements may be made up to the maximum speed of the tractor (that is, above 70 mph).

Mobile test data were obtained for a variety of load conditions and speeds for each of the tires studied.

Previous tire test findings [1, 4] have indicated that for many bias and belted-bias tires of current design the measured peak lateral force is a sensitive function of a small amount of test-induced wear. This wear, which occurs primarily in the shoulder region of the tire, is commonly referred to as "shoulder wear."

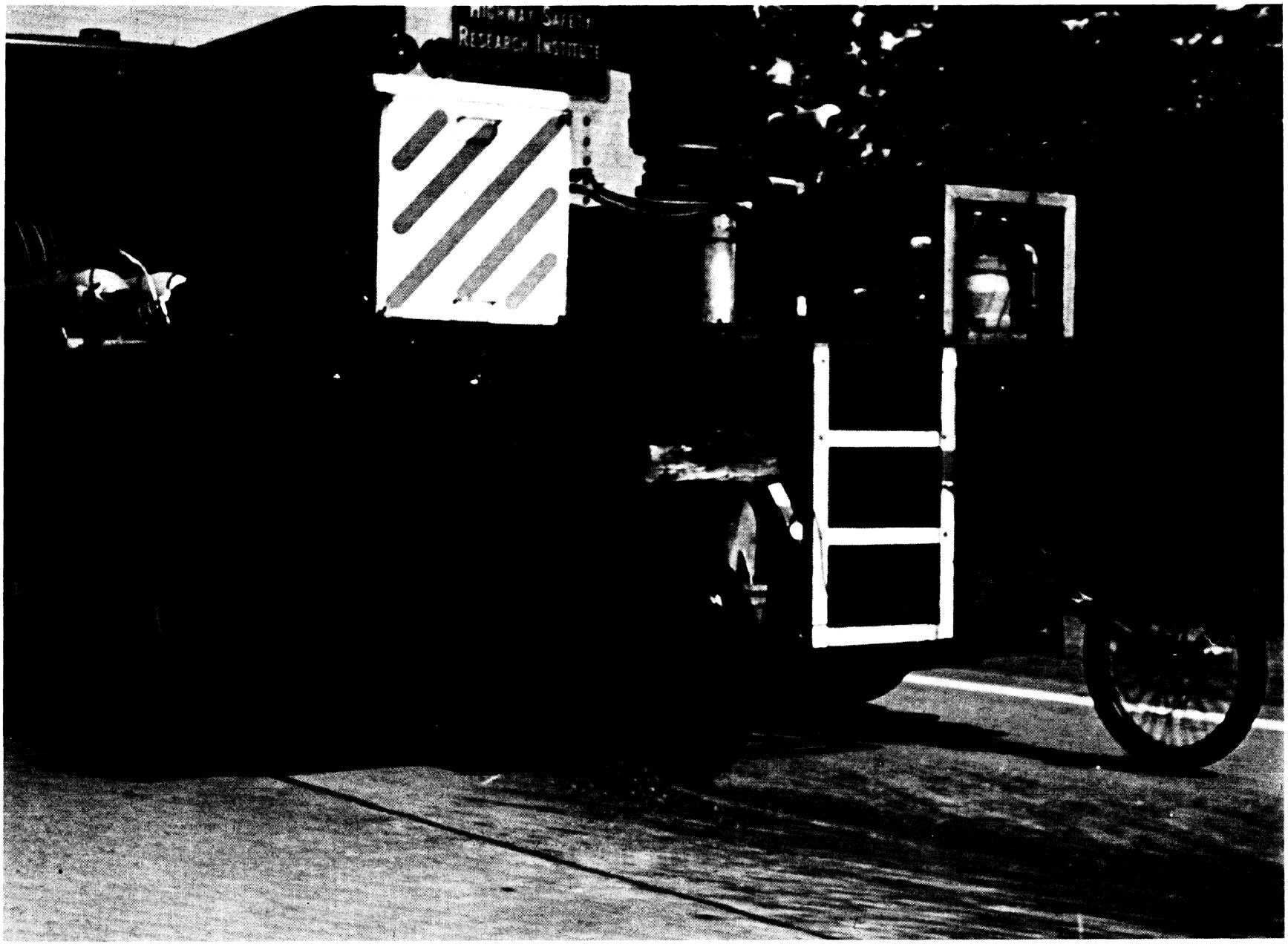

Figure 2-3. Mobile tire tester.

To avoid the build-up of shoulder wear and thereby study the conditions expected to exist on the highway, it was found necessary to structure the mobile tire test program to minimize the number of high-force-level tests performed on a given tire. In addition, special sequences of tire testing were performed to quantify the influence of shoulder wear on peak lateral force as a function of the number of tests performed. This information was used to help plan the vehicle test program, since shoulder-wear effects can also occur during limit-maneuver testing.

The mobile tire tester was also used to gather data on the wet skid pad. The internal watering system on the mobile tire tester was used to wet the test pad directly in front of the test tire. The water delivery rate was varied with vehicle speed to provide a nominal water depth of 0.02 inches. Unfortunately, it was not logistically possible to make tire tests using the external watering system employed for the vehicle tests.

2.2 LINEAR PERFORMANCE STUDY

In the normal driving range (that is, less than about 0.3 g) the directional response of a passenger car can be represented as a linear system. There is an extensive body of literature on this subject. (References [5] to [8] represent a small sample of typical publications.) In addition, the Society of Automotive Engineers (SAE) has developed a proposed recommended set of procedures entitled "Passenger Car and Light Truck Directional Control Response Test Procedures—SAE XJ 266." The following four test methods are described in those procedures.

1. constant radius
2. constant steering wheel angle

3. constant speed
4. constant throttle

The constant-steering-wheel-angle method was chosen for use in this investigation as a guide for linear range testing because (1) the vehicles had to be instrumented and fitted with adjustable steering stops as required for the limit maneuver tests, and (2) the constant-steering-wheel-angle method requires limited driver skill.

The work performed in this task consisted of (1) developing methods for calculating the eigenvalues, eigenvectors, step function response, and steady-state response of the linearized equations of motion for passenger cars; (2) applying the methods developed to analyze the stability and control of the Buick and Mustang as influenced by tire-in-use factors; and (3) testing the two vehicles in several different tire-in-use configurations to give (a) experimental evidence of the extent to which normal driving performance can be altered by tire usage and service factors, and (b) an indication of the extent to which chassis and tire properties have been accurately measured and the linearized description of the tire-vehicle system is adequate for the purposes of this linear performance study.

2.3 SIMULATION OF LIMIT MANEUVERS

A block diagram illustrating the scope of this task is given in Figure 2-4. The purpose of this task was to develop a tire performance model which can be used to represent the complex mechanics of the tire-road interface in a simulation of vehicle response at high levels of steering and braking.

Early in the project, computed results for a 1971 Dodge Coronet and a 1971 Chevrolet Brookwood station wagon were compared to empirical data obtained in an earlier

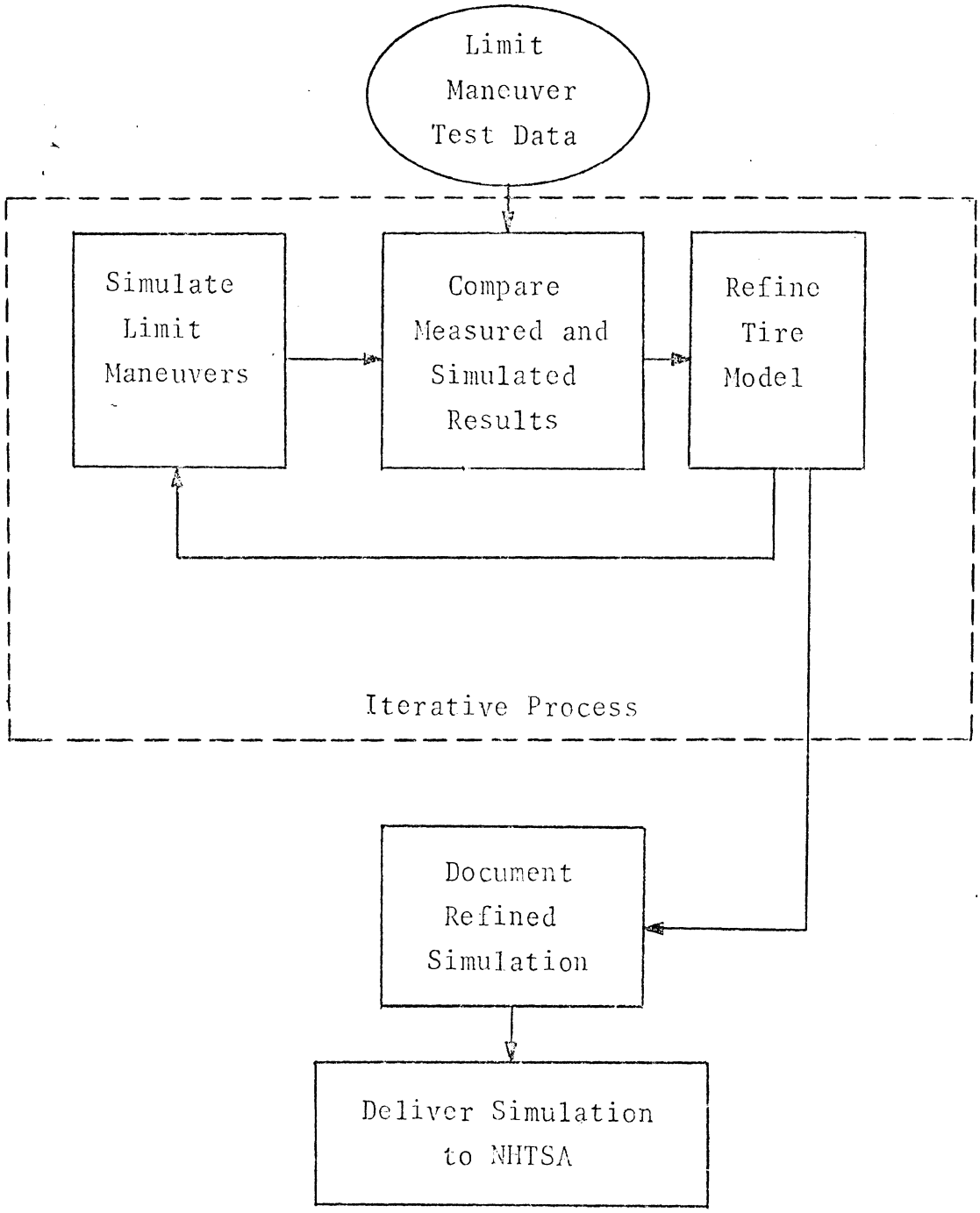

Figure 2-4. Simulation refinement steps.

project, "Vehicle Handling Performance" (VHP) [1]. Based on this comparison, the tire model then used in the simulation was modified to more accurately reproduce the tire shear-force data measured over the range of kinematic variables expected to occur in limit maneuvers. Suitable agreement was obtained between simulated and measured results using the refined tire model.

These efforts yielded a computer simulation well suited for studying the influence of tire-in-use factors on the limit-maneuver performance of the Mustang and Buick. The developed simulation is fully documented in Appendix B.

2.4 LIMIT MANEUVER STUDY

This task was a major endeavor designed to use computer simulations and full-scale vehicle testing to examine the influence of tire-in-use factors on limit-maneuver performance.

The open-loop vehicle test procedures and data processing methodology developed in the VHP study [1] were employed in this task. Accordingly, quantitative measures of vehicle performance in accident avoidance or limit maneuvers were measured using the following six vehicle-handling test procedures:

- straight-line braking
- braking-in-a-turn
- roadholding-in-a-turn
- trapezoidal steer
- sinusoidal steer
- drastic steer and brake

Two types of limit-maneuver tests were performed, depending upon whether the test surface was wet or dry. On

the dry surface all six NHTSA limit-performance maneuvers were used. However, the drastic steer and brake and road-holding-in-a-turn maneuvers were used sparingly for studying tire-in-use factors because (1) these maneuvers are not considered useful for producing tire findings, and (2) the potential for vehicle damage is high.

Wet-surface test procedures were developed for three maneuvers: straight-line braking, braking-in-a-turn, and sinusoidal steer. The velocities used in the wet tests were adjusted to show the influence of tread depth in the sinusoidal steer maneuver.

The scope of the entire limit-maneuver test program is summarized in Tables 2-1 and 2-2. The choices of tire-in-use conditions indicated in Tables 2-1 and 2-2 were based on tire test, simulation, and normal-driving-range results.

The full-scale vehicle simulation was used at two times in this task. First, simulation results were used as an aid in structuring the specific tire-vehicle system tests performed at TTI. Secondly, simulation results were used to provide detailed information on vehicle performance. This information was used in conjunction with the vehicle test results to formulate conclusions concerning the influence of tire-in-use factors on vehicle limit performance.

Extensive support activities were required to perform this task. Vehicle parameters were measured for use in the simulation. Tire parameters and descriptors for the tire model were derived from the tire test data. The vehicles were prepared and instrumented for testing, and an efficient data processing system was worked out.

Furthermore, there were sizeable logistical problems in keeping track of the various tires and tire states to be used in each test procedure. These logistical problems

Table 2-1. Buick Limit-Maneuver Test Matrix

VHP #	Name	Tire Conditions: Original Equipment	Reduced Inflation Pressure (20 psi)	Reduced Inflation Pressure (16 psi)	Replacement Mix (Snow Tires)	Replacement Mix (Radial Tires)	Tread Worn: Tread 2/32"	Groove Depth 4/32"	Groove Depth 6/32"	Shoulder Worn
1	Straight-Line Braking (dry)	A	A	-	R	-	A	-	-	-
2	Braking-in-a-Turn (dry)	A	A	R	R	F	R	-	-	-
3	Roadholding-in-a-Turn (dry)	A	-	R	-	-	-	-	-	-
4	Trapezoidal Steer (dry)	A	A	R	R	F	F	-	-	A
5	Sinusoidal Steer (dry)	A	A	R	R	F	F	-	-	A
6	Drastic Steer and Brake (dry)	-	-	-	-	-	-	-	-	-
7	Straight-Line Braking (wet)	A	A	-	R	-	A	A	A	-
8	Braking-in-a-Turn (wet)	A	A	R	R	F	R	R	R	-
9	Sinusoidal Steer (wet)	A	A	R	R	F	R	R	R	A

Code: A = Test procedure performed with all tires in the indicated tire condition.
R = Test procedure performed with rear tires in the indicated tire condition.
F = Test procedure performed with front tires in the indicated tire condition.
(For cases marked R, the front tires are in OE condition. For cases marked F, the rear tires are in OE condition.)
- = Not in the scope of this test program.

Note: The Buick was also tested in the fully-loaded condition with OE tires and with tires with reduced inflation pressure.

Table 2-2. Mustang Limit-Maneuver Test Matrix

VHP #	Name	Original Equipment	Reduced Inflation Pressure (18 psi)	Replacement Mix (Radial Tires)	Replacement Mix (Brand)	Tread Worn Tread Groove Depths 2/32"	4/32"	6/32"	Shoulder Worn
1	Straight-Line Braking (dry)	A	A	-	-	A	-	-	-
2	Braking-in-a-Turn (dry)	A	A	F	F	R	-	-	-
3	Roadholding-in-a-Turn (dry)	-	-	-	-	-	-	-	-
4	Trapezoidal Steer (dry)	A	R	F	F	F	-	-	A
5	Sinusoidal Steer (dry)	A	R	F	F	F	-	-	A
6	Drastic Steer and Brake (dry)	A	R	-	-	-	-	-	-
7	Straight-Line Braking (wet)	A	A	-	-	A	A	A	-
8	Braking-in-a-Turn (wet)	A	A	F	F	R	R	R	-
9	Sinusoidal Steer (wet)	A	R	F	F	R	R	R	A

Code: A = Test procedure performed with all tires in the indicated tire condition

R = Test procedure performed with rear tires in the indicated tire condition

F = Test procedure performed with front tires in the indicated tire condition

(For cases marked R the front tires are in OE condition. For the cases marked F, the rear tires are in OE condition.)

- = Not in the scope of this test program.

were compounded due to the sensitivity to shoulder wear of the shear force capability of many tires. Consequently, a plan calling for frequent tire changes was developed. The reasons and rationale for this tire-changing plan are discussed in the next section.

3.0 THE INFLUENCE OF TIRE-IN-USE FACTORS ON LIMIT-MANEUVER PERFORMANCE

3.1 THE EFFECTS OF TEST-INDUCED TIRE WEAR ON THE MEASURED RESULTS

Throughout the remainder of this report, analytical and empirical work will be presented to quantify the alteration in braking and handling performance which may be expected to result from changes in tire characteristics. Although some of the conclusions will be based as much on an extension of the tire and vehicle test results through computer simulation as on the test results themselves, it should be emphasized that measurements from the mobile and flat-bed tire test machines and the full-scale vehicle tests are the basis for the "validation" of the computed results. Thus all of the conclusions will depend, to some extent, on an interpretation of empirical results.

Since the conclusions reached in this investigation are intended to apply to vehicles routinely operated on our highways, it is imperative that the relationship between the test vehicles and the general vehicle population be understood. Extreme care was taken in the tire and vehicle testing to ensure that the relationship between the tests and the real world was not irretrievably lost due to test-induced tire wear.

This section re-examines the work of previous researchers who have reported that the peak lateral forces produced by passenger-car tires may be expected to be a function of test-induced wear. It then presents results from the present investigation. These results indicate that forces measured in the linear and intermediate range of slip angles are also subject to significant changes due to test-induced wear, and that these changes may well lead to limit and sub-limit

response characteristics of a tire-vehicle system which are not indicative of the performance of the same vehicle with "non-contaminated" tires. Finally, it presents a tire-test procedure and vehicle-test program designed to minimize these complications.

3.1.1 SHOULDER WEAR. The alteration of the lateral forces produced at large slip angles was found to be a confounding effect in the open-loop measurements conducted in the Vehicle Handling Performance study, which was completed in 1972 [1]. In this study, the investigators sought to analyze a "large variation in peak lateral force capability" which tended to occur with tire usage during limit maneuvers. To provide some insight into this problem, which has come to be called "shoulder wear," the HSRI mobile tire tester was used as the experimental apparatus for (a) providing, in a controlled fashion, a vertical load and slip angle to a tire such that it could be incrementally worn in a manner analogous to that obtained in testing the vehicle, and (b) for gathering tire side-force data concurrent with the wearing process.

The first two tires subjected to this experiment were a Uniroyal L78-15 Fastrak and a Goodyear F78-14 Polyglas. These tires were provided as original equipment on the two test vehicles with which variability in trapezoidal steer data had been first observed. Each tire was subjected to a sequence of runs over both concrete and asphalt by which the mobile tire tester, traveling at 40 mph, lowers the tire onto the pavement at a 20° slip angle and a selected large vertical load. Tire tread profiles were measured by use of a contour copying device and compared with average side forces for each data sample, as illustrated in Figure 3-1. Data sets were gathered in groups of four runs each, designated as a "lap" of the mobile tire tester involving a path over the TTI facility, as shown in Figure 3-2. The very first set of data with the new tire, then, is from tests on concrete, followed by two runs on asphalt, and one more on concrete.

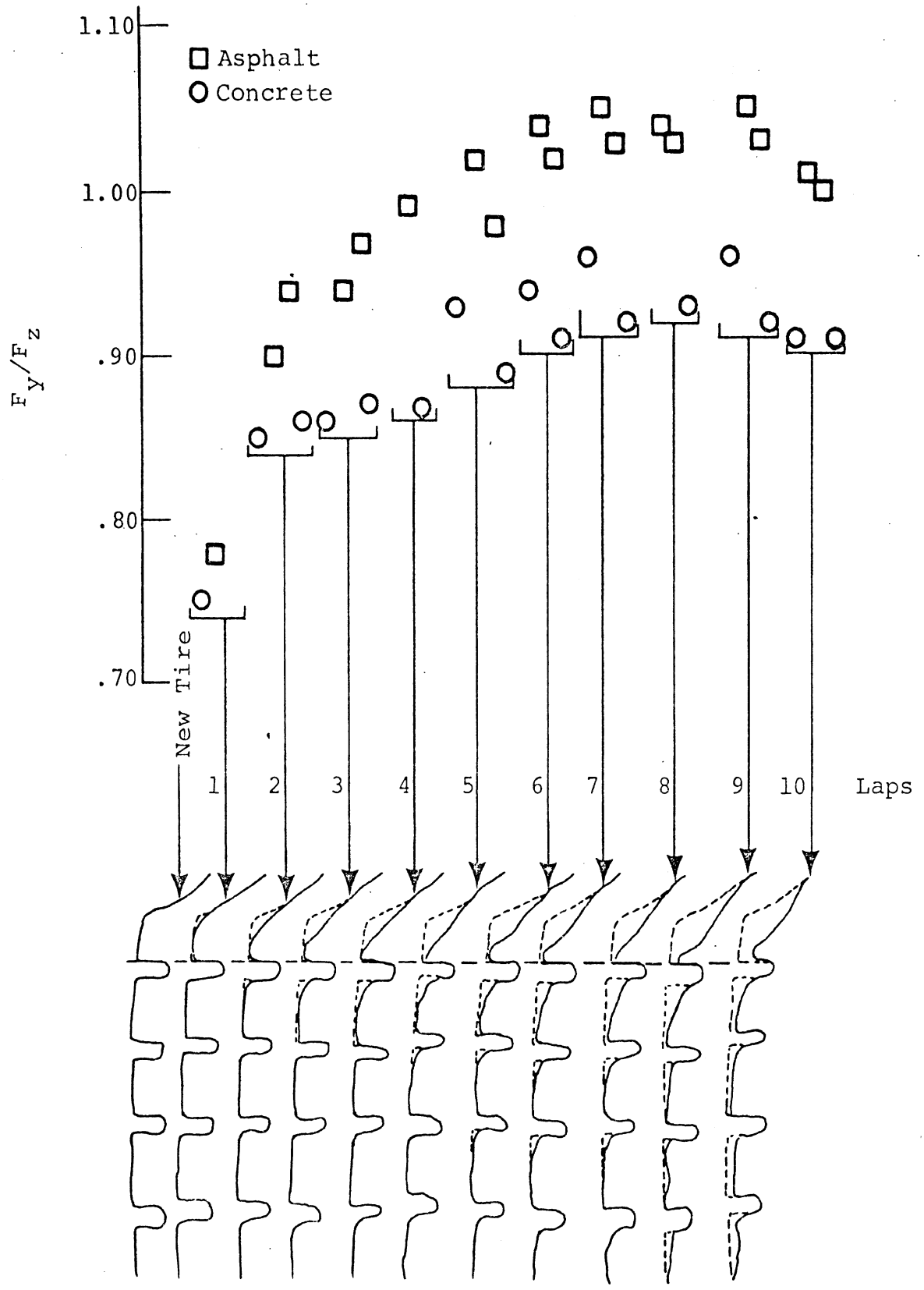

Tread Profile - Outside Shoulder

$\alpha=20°$ $F_z=1550$ Uniroyal L78-15 Fastrak

Tire Sample No. 1

Figure 3-1

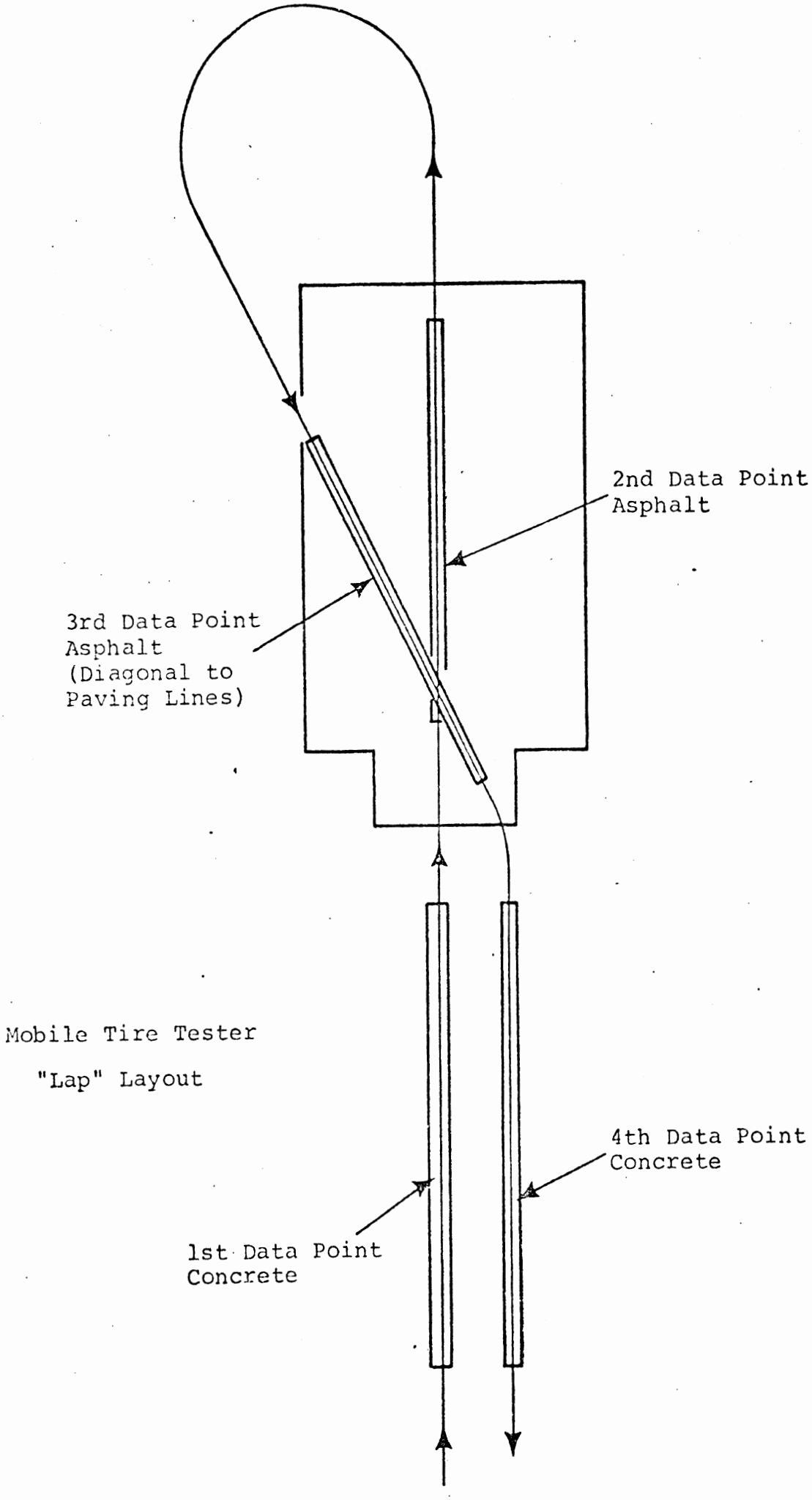
2nd Data Point
Asphalt
3rd Data Point
Asphalt
(Diagonal to
Paving Lines)
Mobile Tire Tester
"Lap" Layout
4th Data Point
Concrete
1st Data Point
Concrete

Figure 3-2

The tire data shown in Figure 3-1 indicates a significant rise in side-force capability with increased wear. (Note that the change in force level from lap one to lap two was accompanied by only barely perceptible tire wear.) It is apparent that the first data point, on concrete, represents a condition whereby a significant improvement in the tire's lateral force capability is taking place, even as the run progresses over nine seconds, as illustrated in Figure 3-3. Note in Figure 3-3 that the force is increasing as runs progress on both concrete and asphalt.

Further data to determine the effects of shoulder wear on lateral force levels at high slip angles were obtained at the TIRF facility of Calspan Corporation [4]. Again, it was found that the lateral forces may change drastically with test-induced wear. In particular, the test results indicated that the average of the lateral forces measured at rated load and six degrees camber and twenty-four degrees slip angle for eleven bias tires and sixteen bias-belted tires increased with shoulder wear, but that the average for nine radial tires decreased.

The spirit of this finding is supported by data produced in the present investigation, in which lateral force measurements were taken for a variety of tires to determine the effect on lateral force of tire wear accrued during mobile tire testing. The following procedure was used to procure these measurements.

1. Lateral force data were obtained at 40 mph for slip angles α = 0, 2, 4, 8, and 16 degrees for a new tire.

2. The procedure in step 1 above was repeated until similar results were obtained in two consecutive passes from α = 0 deg. to α = 16 deg.

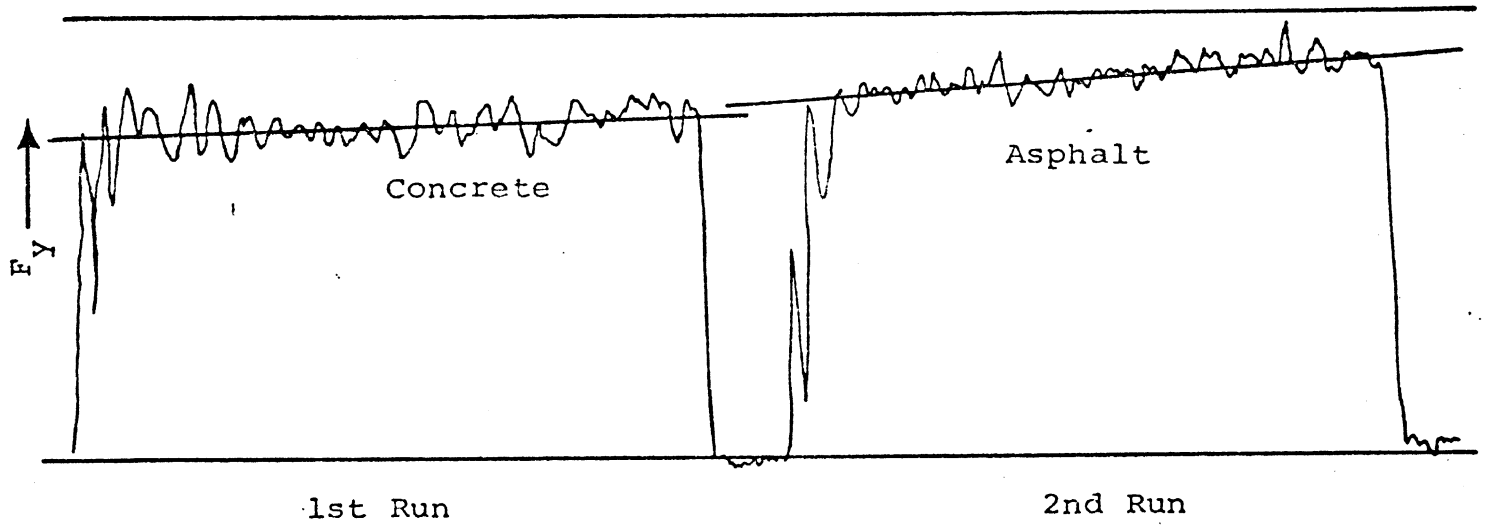

Uniroyal L78-15
Fastrak

Figure 3-3

3. The test data were taken at α of one polarity only; thus the effects of test-induced wear were not symmetric with respect to α. To facilitate analysis of these data, the lateral force points, F_y, were plotted versus the corresponding slip angles with each curve shifted laterally to go through the point $\alpha = F_y = 0$.

The results taken from the Firestone Deluxe Champion Sup-R-Belt H78-14 at 1100-lb. load and the B.F. Goodrich Silvertown E78-17 at 800-lb. load are presented in Table 3-1 and in Figure 3-4. These data indicate an obvious increase in peak lateral force due to a small amount of test-induced wear, a result which might be expected based on [1] and [4].

The radial tires tested in this way exhibited a markedly different trend. Consider Figure 3-5, which presents the data taken from three passes of the Bridgestone radial tire. Clearly, the effect shown here is a slight increase in peak side force, the increase taking place at 8 degrees slip angle, with the worn and new tires achieving approximately equal force levels at 16 degrees slip angle.

In view of these data and the results of previous investigations, it is apparent that a small amount of tire testing can significantly alter the lateral shear force limit of the test tire. Further, the testing of vehicles equipped with shoulder-worn tires of differing construction (for example, radials in front, bias-belted in the rear) cannot be expected to lead to results which are applicable to the same vehicle with non-shoulder-worn tires. It is not so apparent, but nevertheless demonstrable, that the character of the changes in relationship of lateral force to slip angle at slip

Table 3-1. Lateral Force Versus Slip Angle

Firestone Deluxe Champion H78-14
28 psi, 1100 lbs. Load

Angle deg	Pass Number 1	2	3	4	5	6	7
0	0	-32	-35	-75	-87	-117	-100
1	187	145	145	100	45	50	62
2	400	317	260	292	263	270	268
4	625	575	578	555	545	563	525
8	810	863	863	875	870	875	865
16	925	975	1000	1040	1025	1050	1050

B.F. Goodrich Silvertown
24 psi, 800 lbs. Load

Angle deg	1	2	3	4	5
0	0	-32	-38	-75	-75
1	102	102	75	75	68
2	264	230	208	203	203
4	442	403	407	407	416
8	592	623	639	640	651
16	651	702	752	738	774

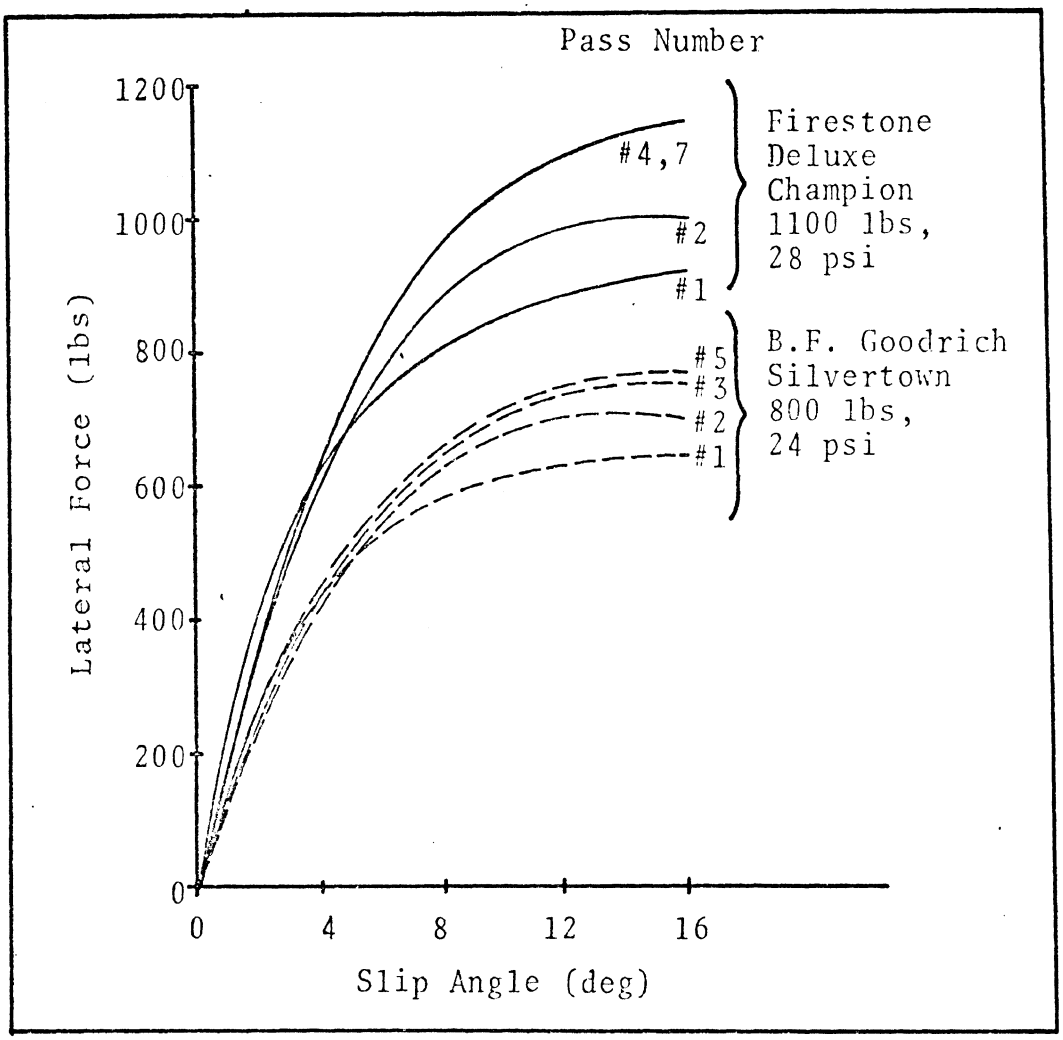

Figure 3-4. Lateral force increase with test-induced wear.

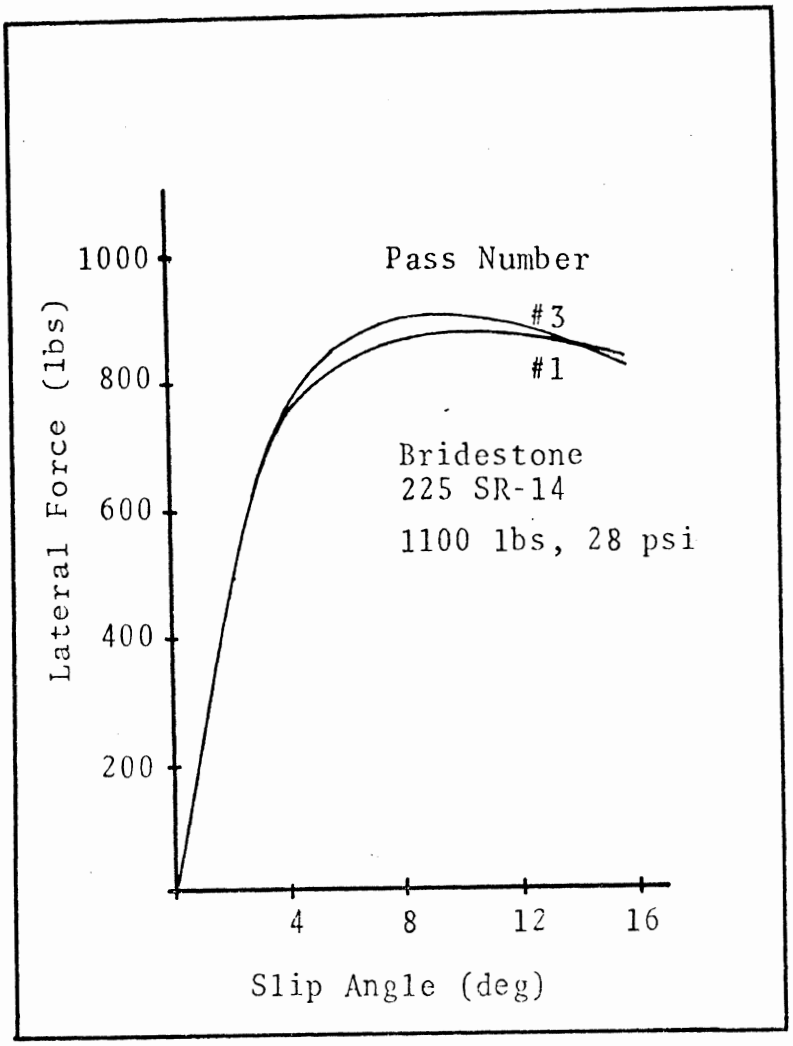

Figure 3-5. Lateral force increase with test-induced wear for a radial tire.

angles significantly below the angle of maximum shear force can have a significant effect on measured vehicle performance.

The following section presents a detailed examination of the possible effects of vehicle- and tire-test-induced wear over the entire free-rolling traction field.

3.1.2 AN EXAMINATION OF THE EFFECTS OF VEHICLE TEST-INDUCED WEAR OVER THE LATERAL TRACTION FIELD. It is reasonable to relate test-induced wear to the distance traveled by a tire while under the action of shear forces at the tire-road interface. Thus, one would expect severe wear to accrue during trapezoidal and sinusoidal steer tests at high-amplitude steer levels on dry surfaces, and during high-speed tire

testing at high slip angles, such as those routinely taking place in the present mobile tire test program. It also seems reasonable to assume that wear accrues much more slowly during less severe vehicle maneuvers and tire tests at low speeds and/or small slip angles.

In this section, data will be presented which have been measured on the HSRI flat-bed test machine for tires previously "shoulder worn" on vehicles in severe maneuvers. These data have been measured on the flat-bed rather than the mobile tire tester, so that laboratory precision may be maintained in the low-slip-angle measurements,* and so no further significant wear is accrued during the test procedure.

The subject tires were worn using the following TTI standard test procedure: Twenty trapezoidal steer maneuvers on dry pavement were run at the highest trapezoidal steer amplitude in the VHTP sequence. The maneuvers were run with an initial set of five turns to the right, then five to the left, then five to the right, then five to the left. At the end of this sequence, the lateral acceleration time histories for the last few runs were compared. If these time histories indicated no significant changes in the peak measured lateral accelerations, the tires are referred to as "shoulder worn."

Four Firestone Deluxe Champion H78-14 and four B.F. Goodrich Silvertown E78-14 tires were subjected to this procedure on the Buick and Mustang, respectively. These tires were then used in the test program at TTI in a rather extensive vehicle test program, including trapezoidal,

---

*We are confident that the angular setting on the mobile tire tester is accurate to ±0.1°. While this is entirely reasonable for large slip angles (say, above 2°), a more precise angular setting is a necessity if comparisons of 1° data are to be made.

sinusoidal, and braking-in-a-turn maneuvers. (The VHTP history of these tires is given in Tables 3-8 and 3-9 of Section 3.2.) At the conclusion of the empirical work at TTI, the left-front and left-rear tires were flat-bed tested at HSRI for comparison with similar measurements of a new tire from the same lot.*

The tread profiles of the new and worn tires may be compared in Figure 3-6. Note that the interior tread elements are severely worn, as are the "shoulders," and that the grooves appear wider and shallower in the worn cases.

A summary of some of the data measured on the flat-bed tester for each of these tires is presented in Tables 3-2 and 3-3. (All the measured data are presented in Appendix D.) Note that the lateral forces measured at the mid-range and high slip angles are much higher in the worn cases. In addition, note that most of the low slip angle values are also significantly higher for the worn tires, indicating that the cornering stiffness has increased by at least ten percent. The lone exception to this trend appears to be the B.F. Goodrich Silvertown at 1400 lbs. load.

3.1.3 SOME ADDITIONAL COMMENTS ON TEST-INDUCED TIRE WEAR. An analysis of the work of previous researchers and of the data generated in the present investigation can leave no doubt that significant tire wear may be expected to accrue during the course of trapezoidal and/or sinusoidal steer tests on a dry surface. In addition, data presented in this program, such as shown in Figures 3-4 and 3-5, and data from previous programs (such as [1] and [4]) indicate that frequent test tire changes seem to be necessary if the new tire condition is to be preserved during tire testing at

*Our tests have indicated that the Buick and Mustang OE tires from the same lot exhibit remarkably similar properties.

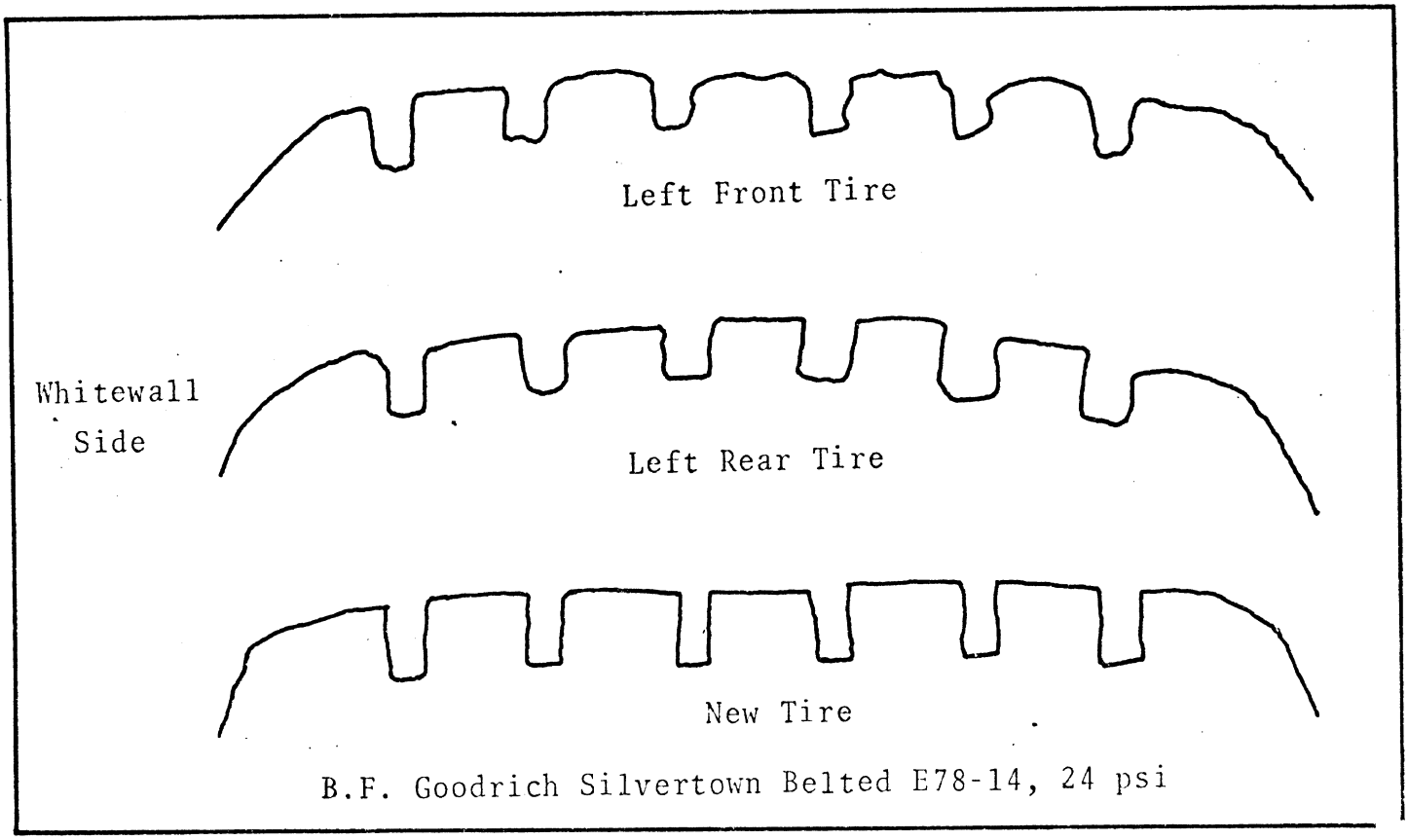

Figure 3-6a. Tread profile for new and worn tires.

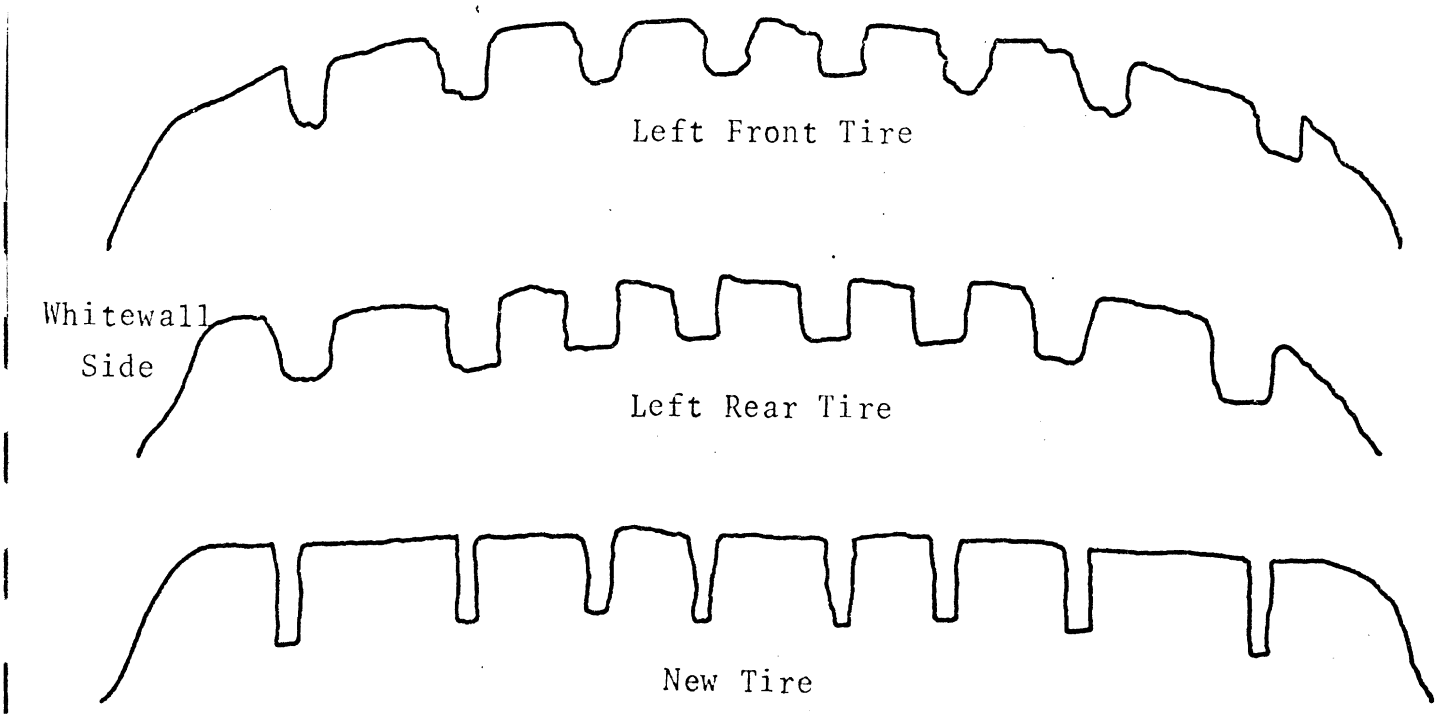

Figure 3-6b. Tread profile for new and worn tires.

Table 3-2 Flat-Bed Lateral Force Measurements for New and Shoulder-Worn Firestone Deluxe Champion Sup-R-Belt H78-14, 28 psi

Vertical Load (lbs)	Lateral Force (lbs) at the Indicated Steer Angle (deg)						(New) (Worn Front) (Worn Rear)		
	0	+1	-1	+2	-2	+4	8	12	18
	-30	-210	-146	-338	-291	-476	-610	-652	-688
800	-35	-232	163	-392	332	-604	-824	-888	-889
	-53	246	163	-393	333	-608	-753	-850	-826
	33	-236	165	-392	339	-586	-797	-888	-958
1100	40	-250	185	-434	376	-716	-1043	-1167	-1208
	-59	-261	180	-452	367	-719	-992	-1111	-1129
	34	-236	164	-404	351	-645	-940	-1085	-1196
1400	39	-247	185	-425	379	-750	-1181	-1398	-1458
	-44	-260	167	-451	374	-769	-1160	-1358	-1366
	35	-228	157	-398	346	-667	-1048	-1250	-1407
1700	27	-228	176	-408	367	-739	-1267	-1561	-1681
	-38	-247	172	-444	358	-775	-1263	-1517	----

Table 3-3 Flat-Bed Lateral Force Measurements for the New and Shoulder-Worn B.F. Goodrich Silvertown E78-14, 24 psi

Vertical Load (lbs)	Lateral Force (lbs) at the Indicated Steer Angle (deg)						(New)	(Worn Front)	(Worn Rear)
	0	1	-1	2	-2	4	8	12	18
	-7	-127	96	-211	190	-306	-382	-403	-420
500	-33	-159	118	-250	220	-393	-559	-605	-637
	-19	-158	126	-254	240	-386	-495	-561	-614
	-7.7	-151	118	-267	237	-408	-560	-633	-679
800	-18	-174	136	-304	265	-495	-784	-909	-991
	-29	-170	143	-303	286	-502	-793	-871	-975
	-7.7	-150	114	-274	252	-448	-683	-819	-912
1100	-18	-155	125	-279	264	-521	-888	-1130	-1286
	-26	-164	136	-292	268	-523	-878	-1096	-1297
	-7.1	-141	108	-264	235	-444	-756	-950	-1120
1400	-9	-142	114	-254	239	-496	-951	-1228	-1449
	-14.2	-133	107	-238	209	-504	-936	-1215	-1446

highway speeds. In this section we will consider in detail the changes that accrued in two tires as a result of a seemingly nominal amount of high-speed tire testing.

A General Belted Jumbo G78-15 was tested on the TIRF facility of Calspan Corporation as part of the Experimental Validation of the Calspan Tire Research Facility [9]. That tire, referred to as #02 in Reference 9 was tested under the conditions listed in Table 3-4. That tire and a new tire from the same lot were then tested on the HSRI flat-bed tire tester to ascertain the effects of the TIRF-induced wear. The tread profiles of the new tire and the worn tire are shown in Figure 3-7, and the measured side forces are presented in carpet plot form in Figure 3-8.

Note that while the high-slip-angle forces of the worn tire are substantially increased, as expected, the cornering stiffness dropped significantly.

Table 3-4. TIRF Test Program for the General Jumbo G78-15 Tire ID #02

Angles at Each Pressure and Load	Speed (mph)	Pressure (psi)	Normal Load
α = ±10, ±8, ±6, ±4, ±2, ±1, 0	6	28	400, 800, 1200, 1600, 2000, 2200
		32	400, 800, 1200, 1600, 2000, 2200
α = ±10, ±6, ±2, 0	20	24	400, 1200, 2000
		32	400, 1200, 2000
α = ±10, ±6, ±2, 0	40	24	400, 1200, 2000
		32	400, 1200, 2000
α = ±10, ±6, ±2, 0	60	24	400, 1200, 2000
		32	400, 1200, 2000

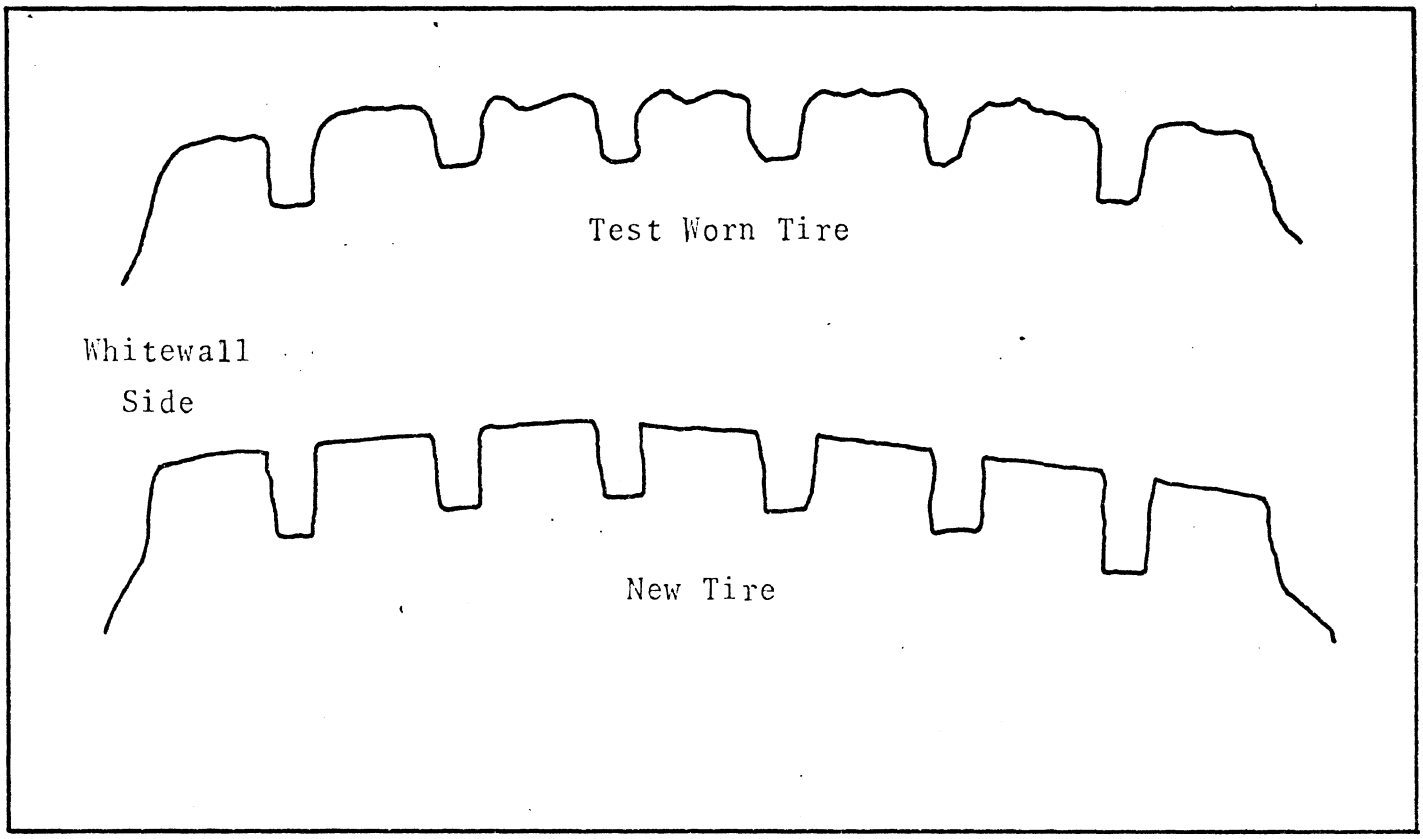

Figure 3-7. Tread profile for new and test-worn General Belted Jumbo G78-15, 28 psi.

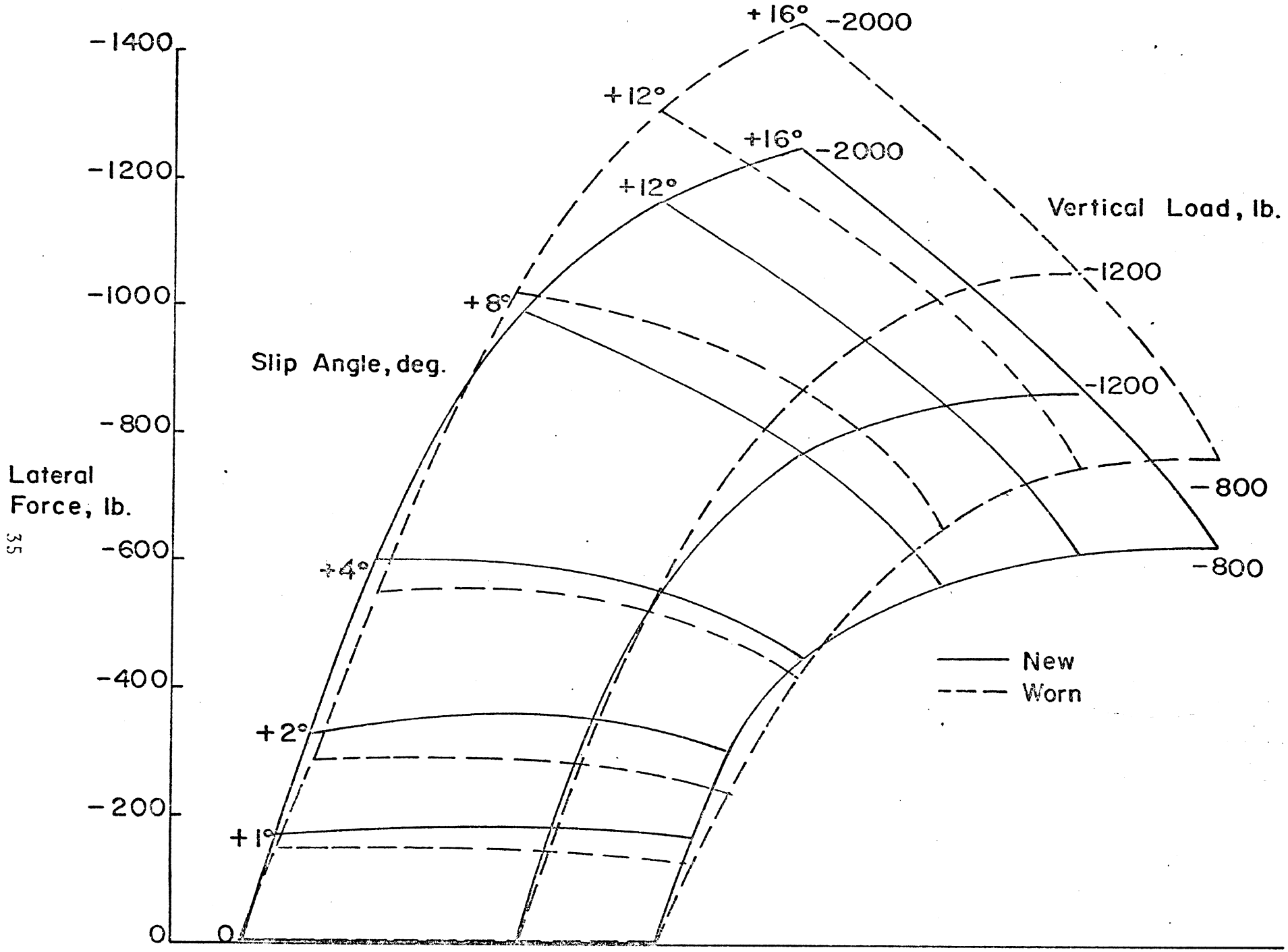

Figure 3-8. Lateral force vs. slip angle and load, General Belted Jumbo G78-15, 28 psi.

A Firestone 500 Steel-Belted Radial JR78-15 was tested under a comparable set of conditions during the TIRF validation program. In this case, the tire referred to as #03 in Reference 9 was flat-bed tested along with a new tire from the same lot to ascertain the effect of TIRF-induced wear. The tread profile of the new tire and the worn tire are shown in Figure 3-9, and the measured side forces are presented in Figure 3-10. In this case, quite similar force levels are measured at low and high slip angles, indicating that the rounded profile of the radial tire is less susceptible to force changes due to test-induced wear. (In this regard, see Figure 3-5.) However, it is evident that substantially lower forces were measured for the worn tire at two and four degrees. These results are a further indication of the need for frequent changes in the test tires during high-speed testing.

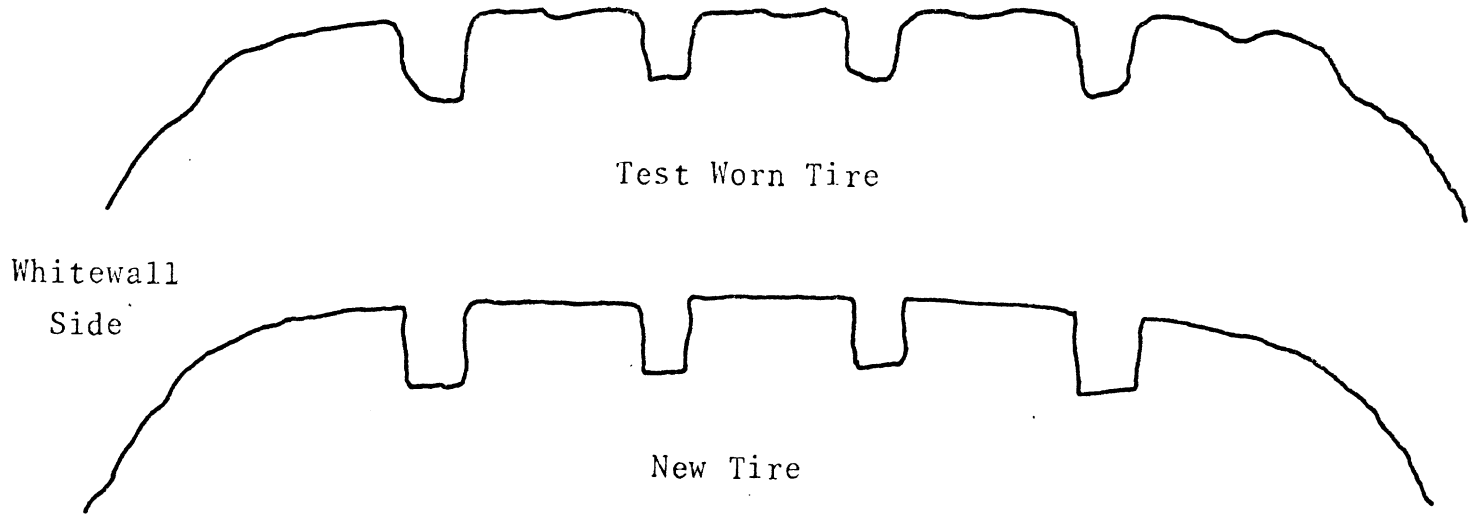

Figure 3-9. Tread profile for a new and test-worn Firestone 500 Steel-Belted Radial JR78-15, 28 psi.

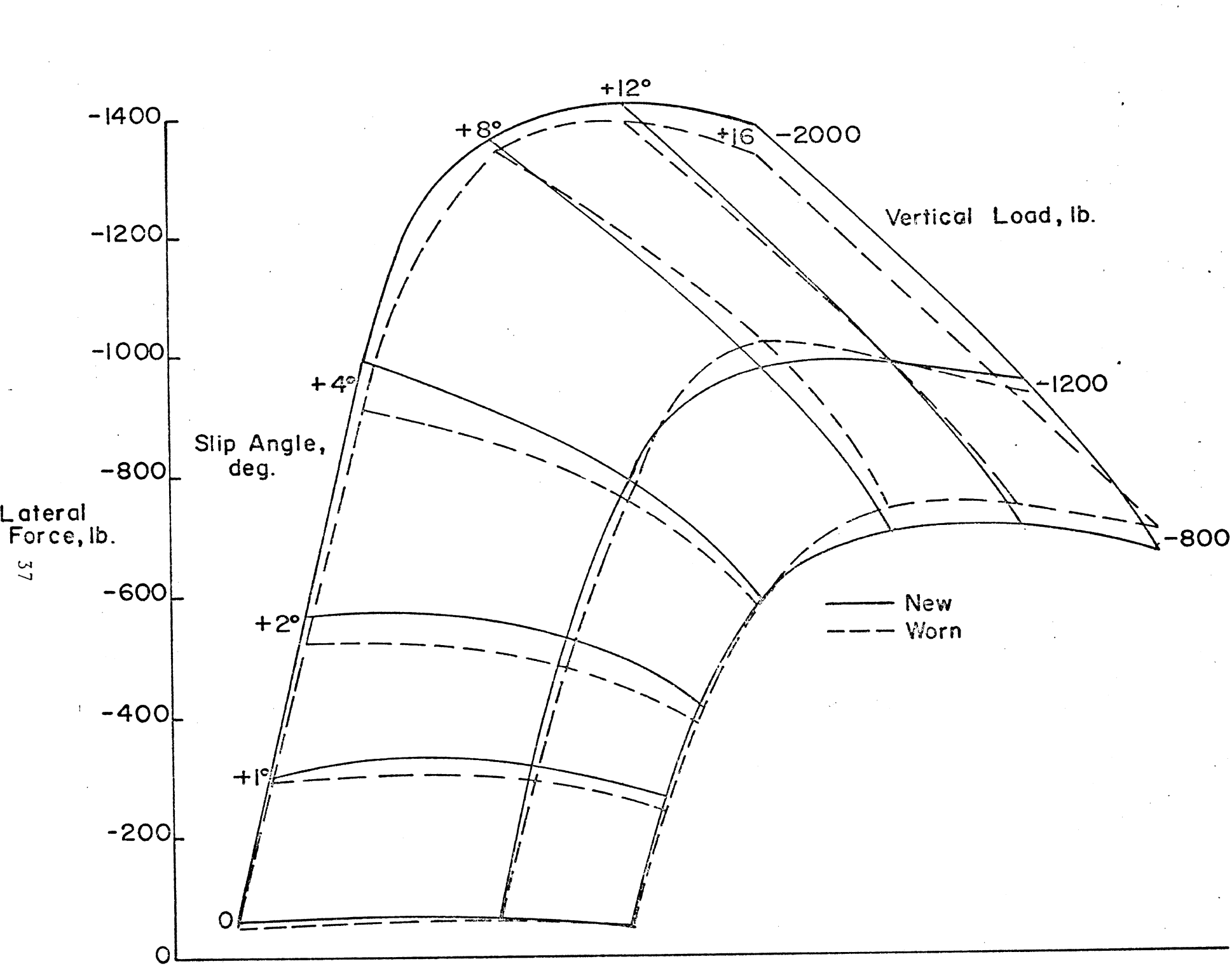

Figure 3-10. Lateral force vs. slip angle and load, Firestone 500 Steel-Belted Radial JR78-15, 28 psi.

3.1.4 A SIMPLIFIED ANALYSIS OF THE EFFECTS OF TEST-WORN TIRES ON VEHICLE TEST RESULTS. This section contains an analysis which demonstrates how a small amount of shoulder wear can have a significant influence on the vehicle sideslip angle attained during a limit or sub-limit turning maneuver. Consider the simplified free-body diagram in Figure 3-11, in which the plan view of a vehicle in a steady turn is presented. (Note that aligning torque is neglected, the side-slip angle, β, is assumed small, and fore-aft forces, as from driving traction or the longitudinal component of the shear forces, FY1, developed at the steered front wheels, are neglected.) Moment equilibrium requires that

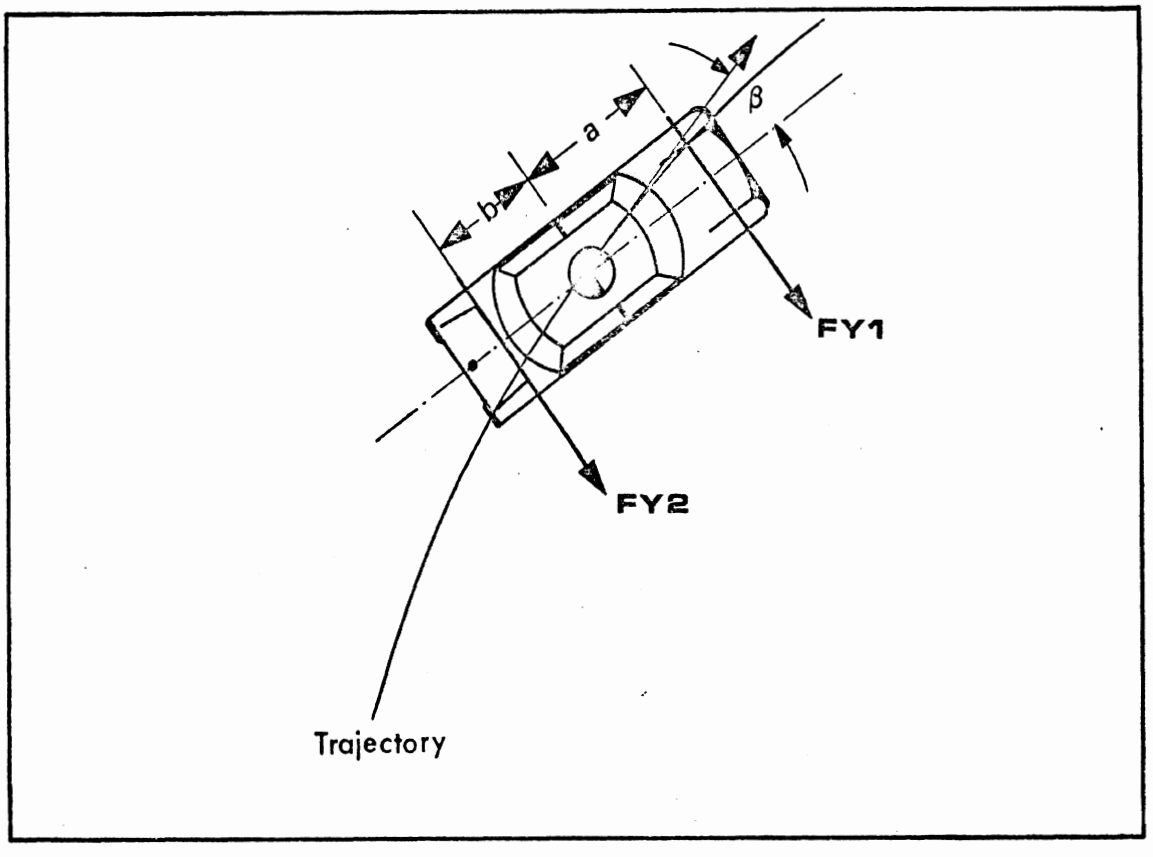

Figure 3-11. Plan view of a vehicle in a steady turn.

$$FY1 \cdot a = FY2 \cdot b \tag{3-1}$$

The sum of the lateral forces must be

$$FY1 + FY2 = M \cdot V \cdot r \tag{3-2}$$

where r is the yaw rate, M is the total mass of the vehicle, and V is the speed. The total normal load on the front tires is FZ1. Moment of equilibrium requires

$$FZ1 = \frac{b \cdot M \cdot g}{a + b} \tag{3-3}$$

Substituting Equations (3-1) and (3-3) into Equation (3-2) yields

$$\frac{FY1}{FZ1} = \frac{V \cdot r}{g} \tag{3-4a}$$

where the right-hand side is the nondimensional lateral acceleration (in units of gravitational acceleration) and the forces are the total lateral and vertical loads on the front tires. In a similar manner it can be shown that

$$\frac{FY2}{FZ2} = \frac{V \cdot r}{g} \tag{3-4b}$$

where FZ2 is the total normal load on the rear tires.

The values of $\frac{FY1}{FZ1}$ and $\frac{FY2}{FZ2}$ may be combined in one plot as a function of slip angle to gain insight into the steady turning behavior of the vehicle in the nonlinear range.* For example, consider Figure 3-12, in which typical $\frac{FY1}{FZ1}$ and $\frac{FY2}{FZ2}$ values are shown as a function of front and rear slip angle, respectively. For the acceleration level, $\bar{a}$, shown in Figure 3-12 the sideslip angles are $\bar{\alpha}_f$ and $\bar{\alpha}_r$. Neglecting small

*This is not a particularly straightforward procedure, since matters are significantly complicated by lateral load transfer. However, the details of these matters have little bearing on this discussion.

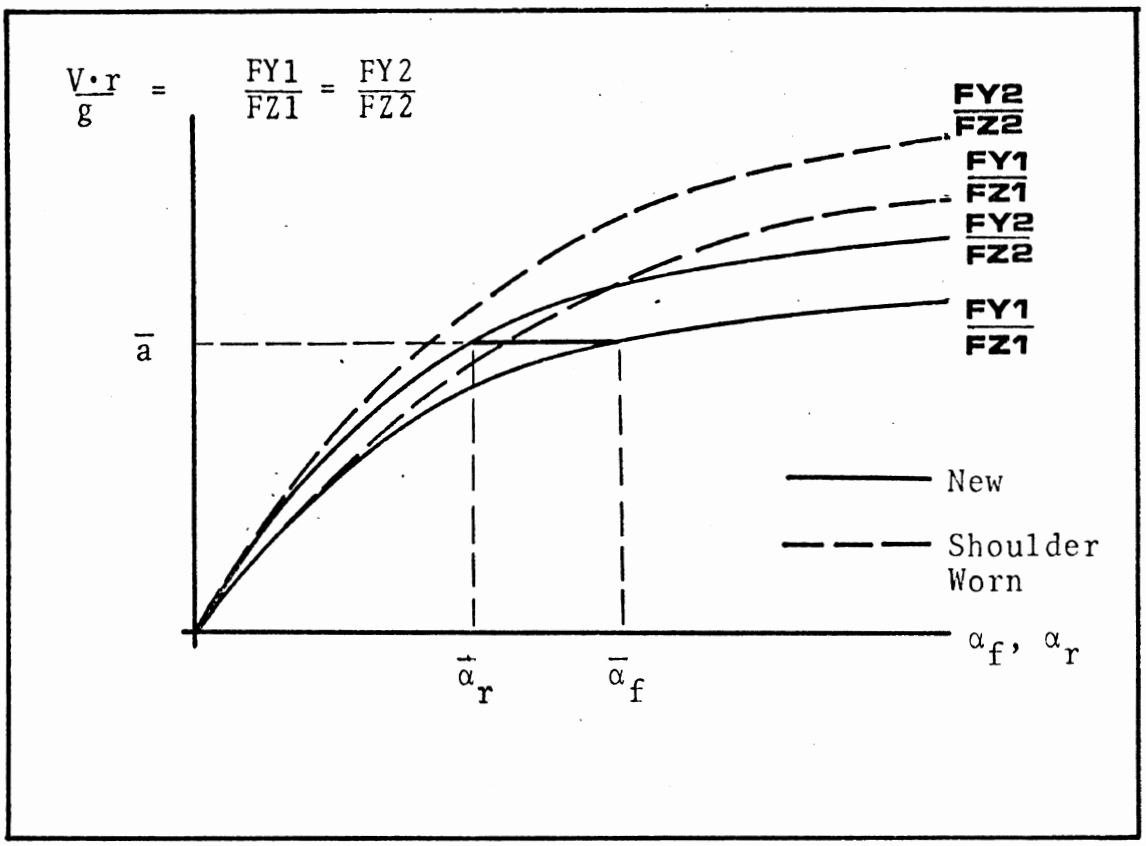

Figure 3-12. Normalized lateral force as a function of front and rear sideslip angles α_f and α_r.

compliance and roll steer effects, the sideslip angle of the rear wheels is

$$\bar{\alpha}_r = \beta - \frac{br}{V} \tag{3-5}$$

Clearly, for a given velocity, V, and a fixed lateral acceleration (Vr) the yaw rate, r, is determined. Thus, for a particular vehicle, the term $\frac{br}{V}$ in (3-5) is constant for a specified level of steady turn, and the value of β attained depends upon $\bar{\alpha}_r$. Inspection of the example presented in Figure 3-12 shows that a smaller β corresponds to lateral acceleration, $\bar{a}$, in the shoulder-worn case.

Now consider the same new tire condition compared to another shoulder-worn state as in Figure 3-13. (Note that the shear force limits are the same in Figures 3-12 and 3-13.) In this case, the shoulder worn tires obviously have a higher steady-state β at lateral acceleration $\bar{a}$.

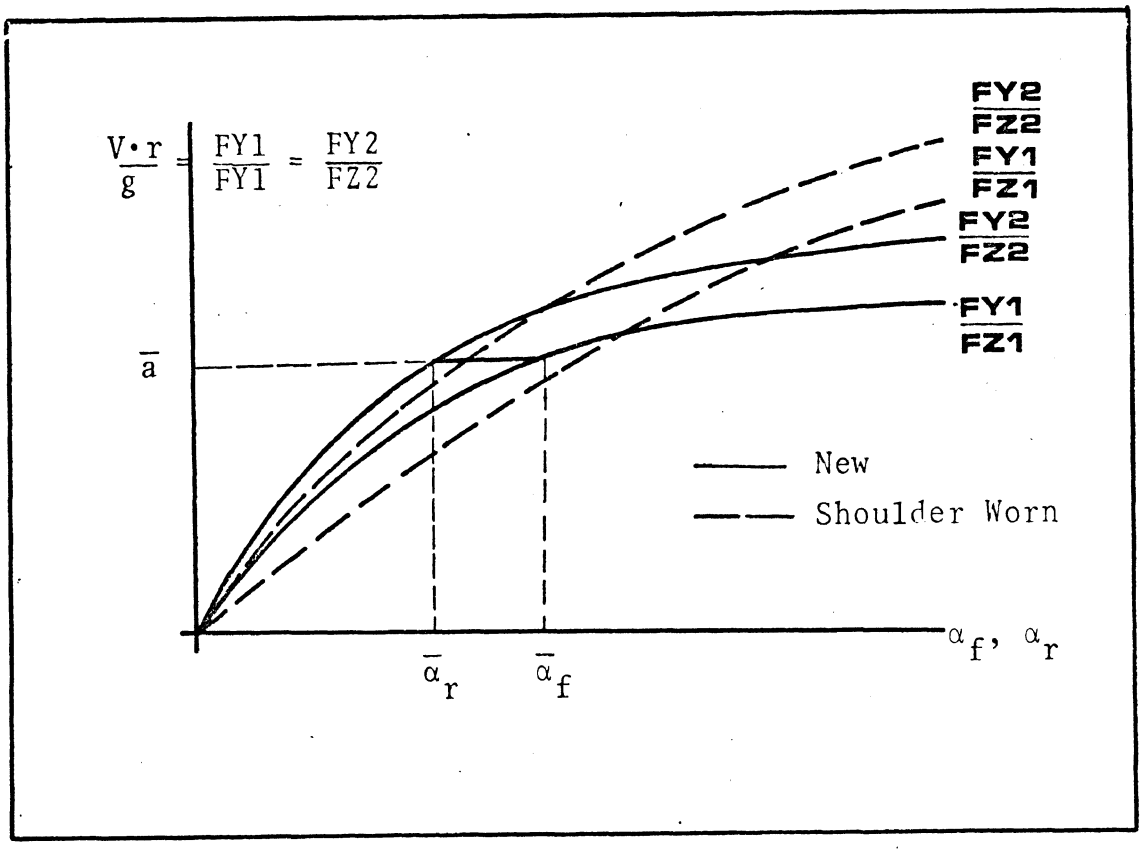

Figure 3-13. Normalized lateral forces as a function of front and rear sideslip angles α_f and α_r.

This rather academic example is not a rigorous statement. (We are, after all, dealing with a very simple model.) Nevertheless, the clear indication here is that if the sub-limit performance of a tire-vehicle system with non-shoulder-worn tires is to be assessed by means of tests run with shoulder-worn tires, the differences between the shoulder-worn tires and the tires to be assessed must be taken into account across the entire range of load and slip angle used in the test procedure.

To avoid these complications in the present investigation, it was decided to attempt to maintain new-tire conditions in the mobile tire testing and in the vehicle testing by changing tires often enough to control the effects of shoulder wear. Details of the steps taken to minimize shoulder wear are given in the following two sections.

3.1.5 THE MOBILE TIRE TEST PLAN. The tires listed in Table 3-5 were tested repeatably through a zero to sixteen-degree slip angle increment on dry concrete. (Some of the data measured during this testing were presented in Figure 3-4 and Tables 3-2 and 3-3. The entire data set is given in

Table 3-5. Tires Tested for the Effects of Shoulder Wear.

B.F. Goodrich Silvertown E78-14
Bridgestone 225R-14
Firestone Deluxe Champion H78-14
Firestone 500 H78-14
Goodyear Custom Power Cushion Polyglas #78-14
Pirelli 185R-14

Appendix D.) These tests indicated that the measured shear forces changed rapidly during testing at high slip angles. Thus it was decided to limit each tire to one sixteen-degree test on a dry surface, thereby producing the mobile tire test matrix shown in Table 3-6 for use at TTI. Note that each entry in this matrix requires one test tire, and thus four tires were required to obtain one set of data for the test matrix given in the table. This added expense is justified, in that the measured data are quite representative of the new tires on the TTI surface. Thus the data have utility

Table 3-6. The Dry-Surface Mobile Tire Test Program

E-78 Tires

Speed (mph)	Load 800	1100	1400
20	μ, X		
40	μ, X	μ, X	X

H-78 Tires

Speed (mph)	Load 800	1100	1700
20		μ, X	
40	μ, X	μ, X	X

X = Free-rolling data at α = 0, 2, 4, 8, 16 deg.
μ = "μ-slip" data α = 0, 4 deg.

for predicting the performance of the test vehicles equipped with new tires and tested on the TTI test surfaces and other similar surfaces.

Note that while the radial tires seemed far less susceptible to wear-induced changes in lateral shear force levels than did the bias tires and the bias-belted tires, the test matrix presented in Table 3-6 was also used for the radial tires. On the wet surface, however, where none of the tires seemed to accrue significant wear, a single tire was used for the entire wet test sequence. The wet tests are discussed in detail in Section 4 of this report.

3.1.6 THE VEHICLE TEST PLAN. The test matrix for the Buick is presented in Table 3-7, and for the Mustang in Table 3-8. Each numerical entry in the matrix refers to a particular set of four tires. Thus it is apparent that the same set of tires was used repeatedly in wet testing and in

Table 3-7. Test Matrix for the Buick

Maneuver Numbers And Names			TIRE CONFIGURATION HEADINGS AND NUMBERS										
			O. E.	P.S.I. 1	P.S.I. 2	Loaded O.E.	Loaded P.S.I.	Snow	Mix	Wear 1	Wear 2	Wear 3	Shoulder Worn
WET	7	St. Line Braking	11	12	X	13	54	14	X	15	16	17	X
	8	Braking In A Turn	11	12	18	13	19	14	20	21	22	23	X
	9	Sinusoidal Steer	24	25	26	27	28	29	30	31	32	33	34
DRY	1	St. Line Braking	11	12	X	13	54	14	X	15	X	X	X
	2	Braking In A Turn	11	12	18	13	19	14	20	21	X	X	X
	5	Sinusoidal Steer	35,36	37	38	39	40	41	42	43	X	X	34
	4	Trapezoidal Steer	44,45	46	47	48	49	50	51	52	X	X	34
	3	Turning on Rough Road	11	18	X	X	X	X	X	X	X	X	X
	6	Drastic Str. & Brake	X	X	X	X	X	X	X	X	X	X	X

Table 3-8. Test Matrix for the Mustang

Maneuver Numbers And Names			TIRE CONFIGURATION HEADINGS AND NUMBERS							
			O. E.	P.S.I.	Mix 1	Mix 2	Wear 1	Wear 2	Wear 3	Shoulder Worn
WET	7	St. Line Braking	11	12	X	X	13	14	15	X
	8	Braking In A Turn	11	12	16	17	18	19	20	X
	9	Sinusoidal Steer	21	22	23	24	25	26	27	28
DRY	1	St. Line Braking	11	12	X	X	13	X	X	X
	2	Braking In A Turn	11	12	16	17	18	X	X	X
	5	Sinusoidal Steer	29,30	31	32	33	34	X	X	28
	4	Trapezoidal Steer	35,36	37	38	39	40	X	X	28
	3	Turning on a Rough Road	X	X	X	X	X	X	X	X
	6	Drastic Steer and Brake	41	42	X	X	X	X	X	X

straight-line braking and braking-in-a-turn on the dry surface. However, in the sinusoidal and trapezoidal steer maneuvers on the dry surface, the test tires were changed frequently.

The exact test history of the tires corresponding to each of the numerical entries in the test matrix are given in Appendix E of this report. In this section, the rationale behind certain important aspects of the vehicle test program will be presented:

1. The procedures are similar to those given in Reference 1, with one major exception—no repeats are run. Thus at each steer level there are just two runs, one each corresponding to right and left polarity.

2. Test-induced wear was not considered to be important in the wet testing, since lateral accelerations and hence the forces generated at the tire-road interface remained relatively low.

3. In the straight-line braking and braking-in-a-turn maneuvers, tne lateral forces at the tire-road interface were expected to remain relatively low. Therefore, the same tires were used throughout this test sequence.

4. For the sinusoidal and trapezoidal maneuvers on the dry surface, new tires* were used in each tire configuration to avoid the accrual of shoulder wear. For example, a new set of tires was used in Buick sinusoidal tests 35 and trapezoidal tests 44, with steer amplitude levels shown in Table 3-9. These tires were then deemed at least partially shoulder worn, i.e., unfit for use in further testing.

*These tires, as all the test tires, were broken in by 100 miles of normal driving.

Table 3-9. Trapezoidal and Sinusoidal Steer Tests

Normalized Steer Amplitude σ	Steer Amplitude (deg) Buick	Mustang
4	95	78
6	140	116
8	175	155
10	210	193
12	240	233
14	280	270
16	310	309
18	340	348
20*	375	386
24*	427	467

*Trapezoidal only

A certain portion of the test matrix for each vehicle was designed to fill out our base of empirical evidence as to the effects of shoulder wear, as will be shown below.

3.1.7 VEHICLE TEST RESULTS INDICATING THE EFFECTS OF SHOULDER WEAR. A comparison of the measured trapezoidal steer response for the Buick with tire configurations 44, 45, and 34 will produce some insight into the effects of shoulder wear for the OE Buick. Test configuration 44 is the OE trapezoidal steer sequence run with the lowest steer angle first, as shown in Table 3-9. (Thus the tests run at the highest amplitude steer levels might be expected to show some effect of the shoulder wear accrued during the lower-level testing.) In test configuration 45, on the other hand, the same steer angles were run, starting with the highest steer level first and working down. (Thus the first test in the sequence, the highest steer level, is truly a non-shoulder-worn test, and wear increases as the steer angles drop.)

In Figure 3-14, the maximum measured peak lateral acceleration levels measured in test configurations 44 and 45 are plotted versus steer angle for comparison with the data measured for shoulder-worn configuration 34. The results presented in the figure correlate well with our understanding of shoulder wear—the shoulder worn points (triangles) from configuration 34 generally lead to the highest lateral acceleration levels, and the partially worn tires, indicated by the solid dots at low steer levels and the open circles at high steer levels, show signs of increasing shoulder wear.

Figure 3-15 shows that somewhat different results were measured in comparable Mustang tests. While the Mustang OE tire is susceptible to shoulder wear (as shown in Figure 3-4), the wear apparently did not build up as rapidly during the course of the Mustang trapezoidal steer tests as it did in the Buick trapezoidal steer tests.

The use of shoulder-worn tires did not always lead to results clearly distinct from the corresponding non-shoulder-worn tires. Consider, for example, the sinusoidal steer results presented in Figure 3-16, in which the peak lateral accelerations during the first and second half of the lane-change steer cycle are plotted as a function of steer amplitude. In this case, the shoulder-worn tires yield results quite characteristic of the unworn original equipment tires.

3.1.8 SUMMARY. Tire wear during the course of tire testing or vehicle testing can significantly alter the shear forces generated at the tire-road interface. This alteration can be an increase or a decrease in lateral force, depending on the characteristics of the unworn tire and the amount of wear.

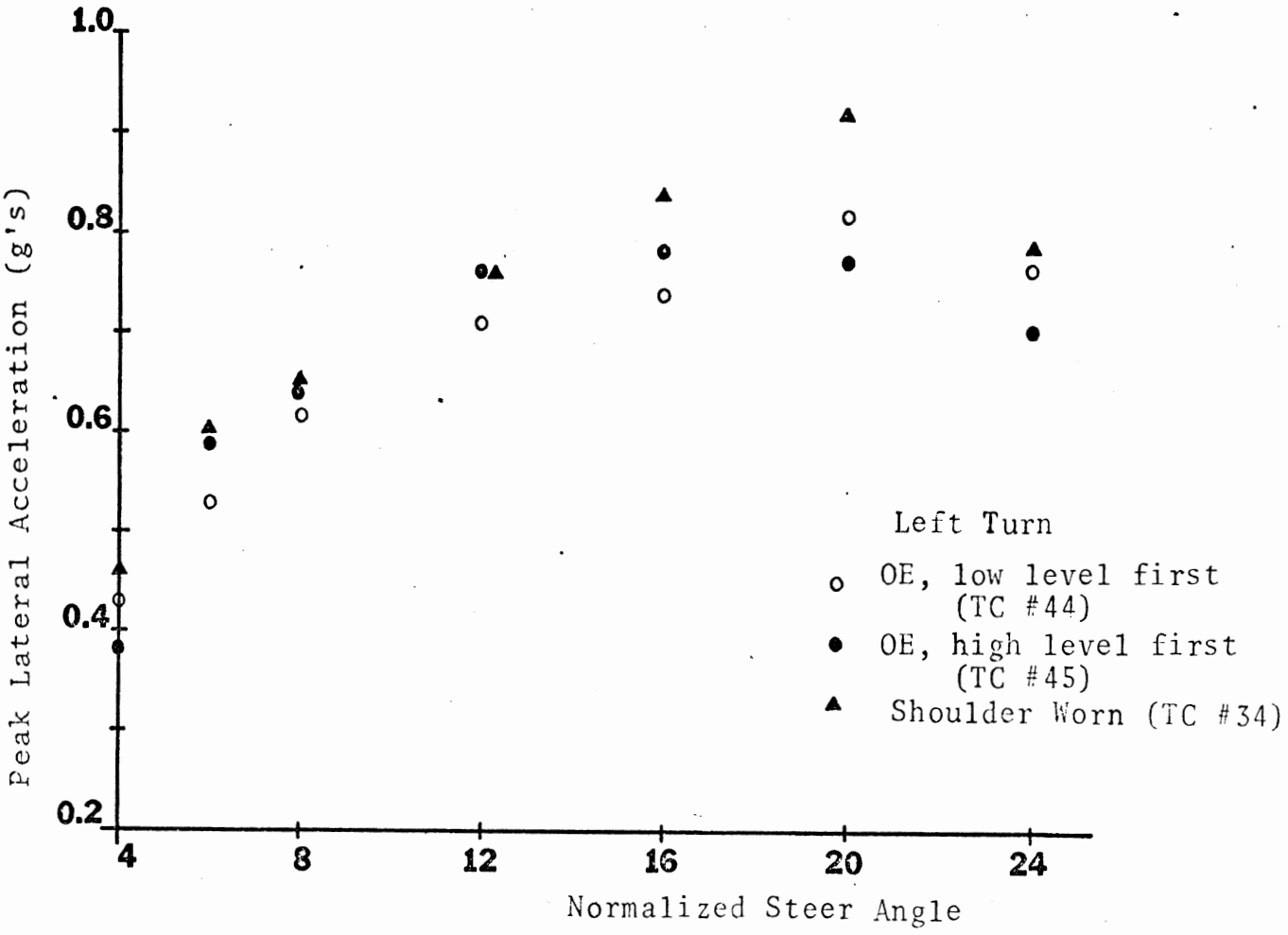

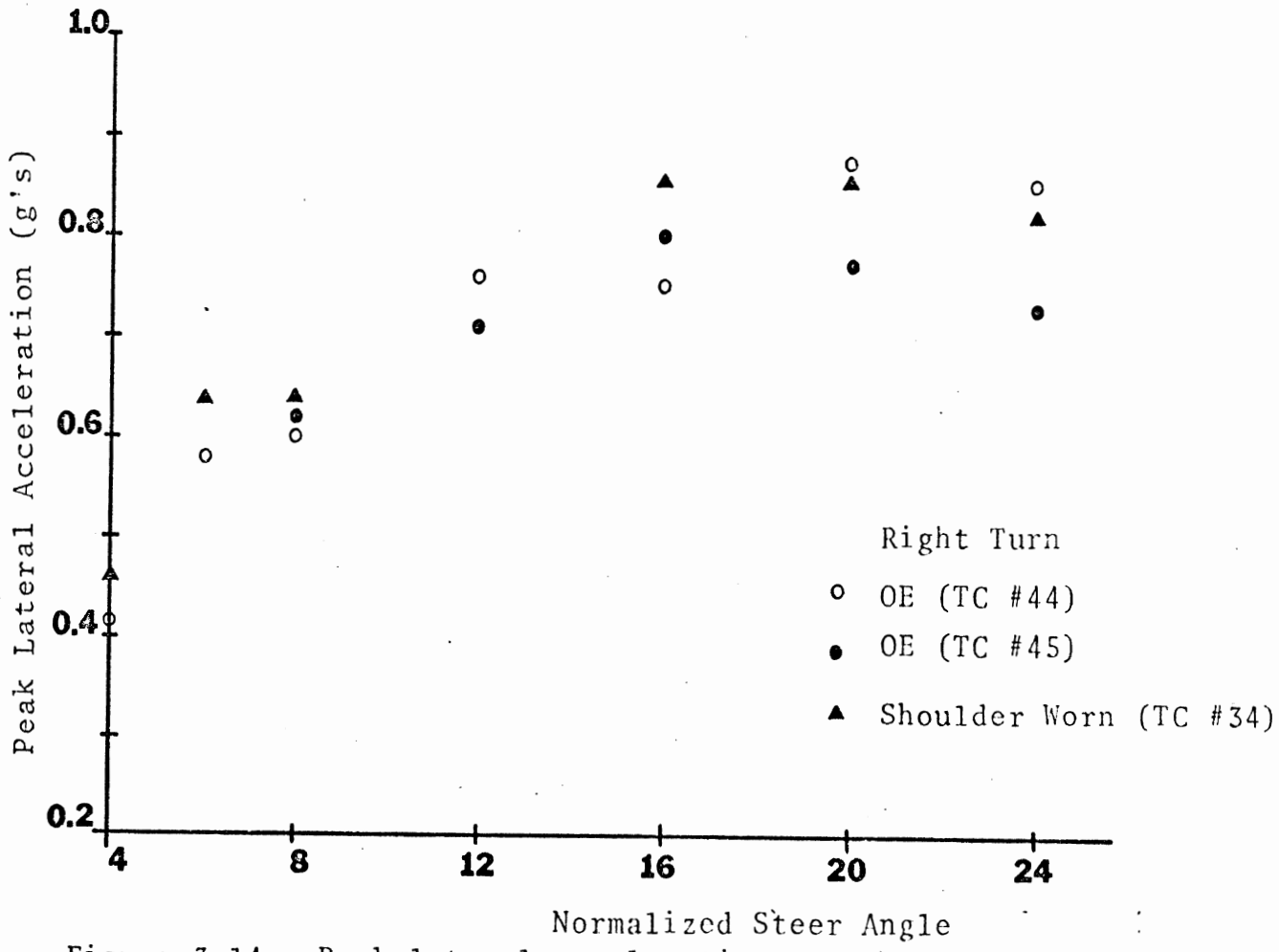

Figure 3-14. Peak lateral acceleration vs. steer angle for the Buick.

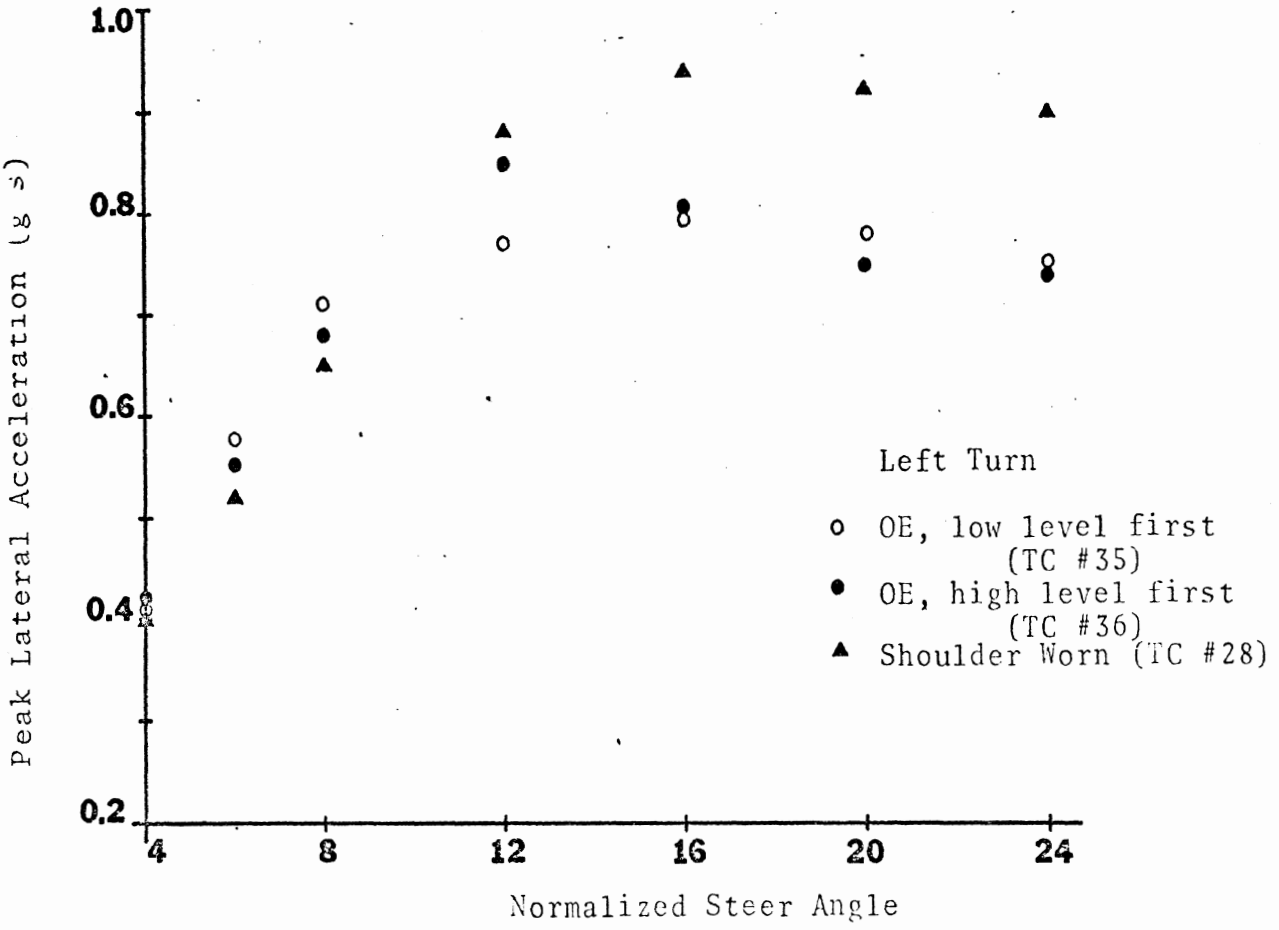

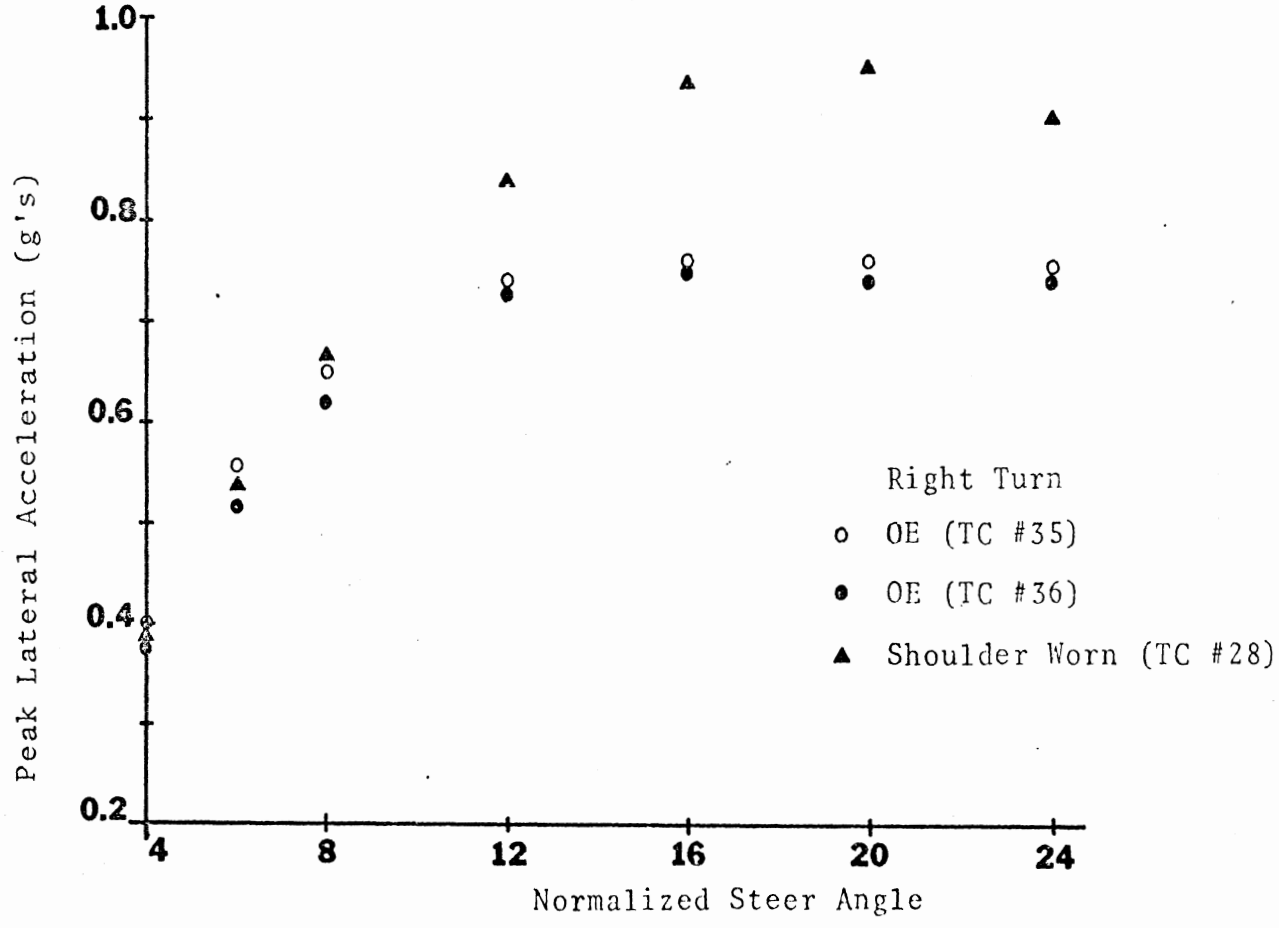

Figure 3-15. Peak lateral acceleration vs. steer angle for the Mustang.

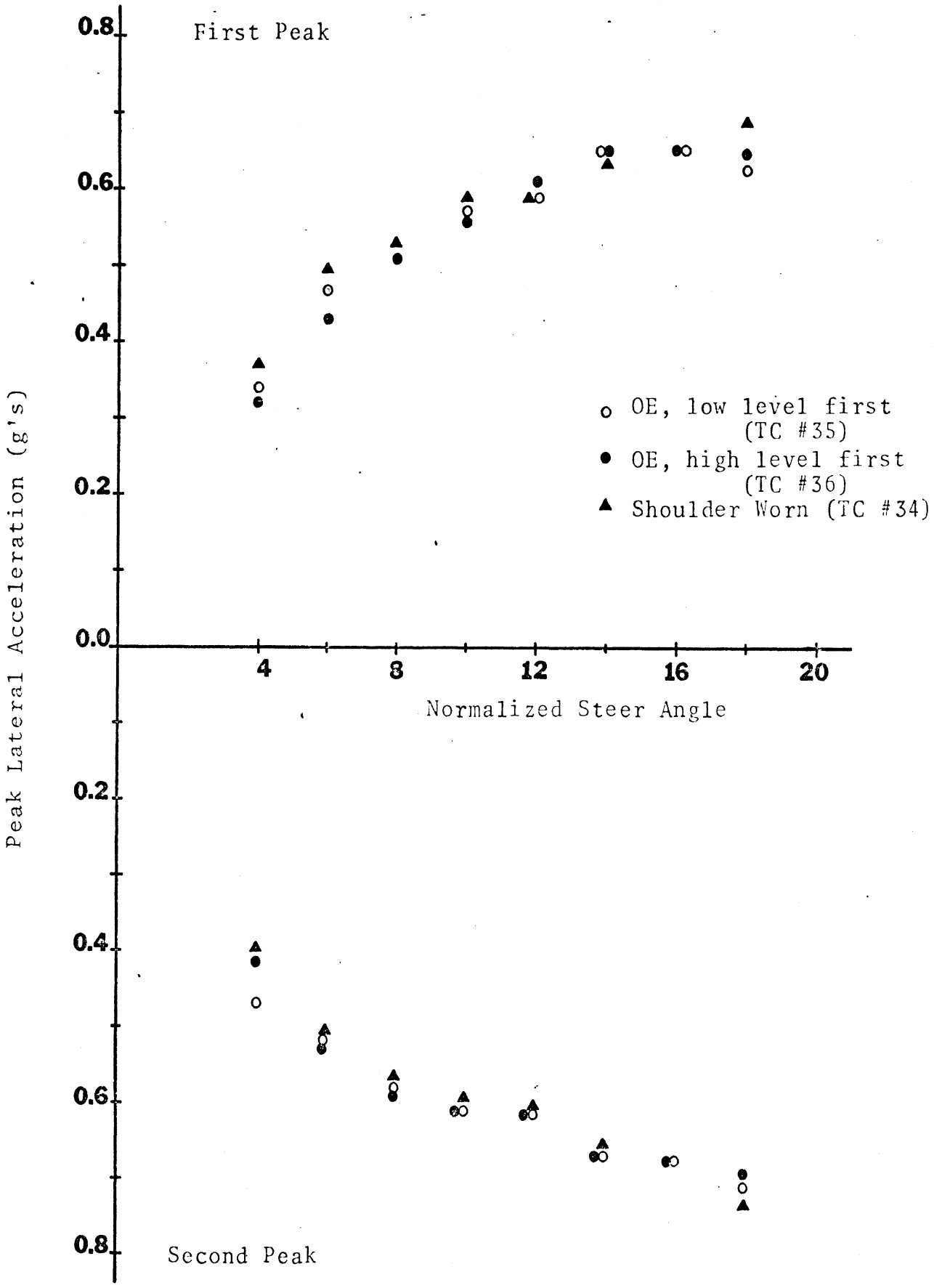

Figure 3-16. Peak lateral accelerations measured in the sinusoidal steer maneuver, Buick, right polarity.

The objectives of the present investigations required the measurement of changes in vehicle-tire system performance resulting from tire-in-use factors. Thus it was particularly desirable to limit the effects of test-induced wear for the various test tires. To this end, the tire and vehicle test programs were designed to limit test-induced wear as much as possible. In addition, tire tests were performed to assess the changes from the new condition resulting from mobile tire test wear, and vehicle tests were performed to assess the effects of intentionally shoulder-worn OE tires on the findings yielded by the vehicle handling test procedures.

3.2 INFLATION PRESSURE

Previous studies have shown that a significant number of vehicles on the road have tires inflated to levels significantly different from that recommended by the manufacturer. For example, it was reported in Reference 10 that of 1620 tires surveyed, 7.5% had cold inflation pressures 5 psi or more below the level recommended by the manufacturers.

Other researchers have presented data in substantial agreement with this finding. For example, consider the data originally presented in Reference 11, listed here in Table 3-10. Note that 12.9% of the cars surveyed had at least one tire with a cold inflation pressure of 18 psi or less, and that over one percent of the cars surveyed had at least one tire at 12 psi or less.

In the present research, analytical and empirical evidence has been gathered indicating an important relationship between inflation pressure and directional response of the Buick and the Mustang. The discussion of this relationship will be facilitated by a detailed consideration of the flat-bed and mobile tire test measurements taken at various inflation pressures.

Table 3-10. Number and Percent of Cars Classified by Number of Underinflated Tires At or Below Specified Pressures.

Total Number of Cars Examined = 1904

Inflation Pressure	Tires per Car and Percent of Population								Total	
	1 Tire	Per-cent	2 Tires	Per-cent	3 Tires	Per-cent	4 Tires	Per-cent	Cars[a]	Per-cent
20	316	16.6	126	6.6	65	3.4	34	1.8	541	28.4
18	170	8.9	48	2.5	21	1.1	7	0.4	246	12.9
16	79	4.1	16	0.8	3	0.2	1	0.1	94	5.2
14	40	2.1	4	0.2	2	0.1	1	0.1	47	2.5
12	20	1.1	3	0.2	0	0	0	0	23	1.2

[a]With one or more underinflated tires

3.2.1 FLAT-BED TEST RESULTS. A summary of some of the flat-bed results for a variety of tires is presented in Table 3-11. The loads given in the table are 800 lb. for the E-size tires (approximately the static load on the tires for the test Mustang) and 1100 lb. for the H-size tires (approximately the static load for the test Buick). The tire test measurements are presented in their entirety in Appendix D of this report.

It should be noted that the normal procedure was to test one tire at the four inflation pressures shown in the table. In four cases, however, some of the data was not measured due to an oversight. The appropriate measurements were subsequently procured from a separate tire taken from a separate lot. Thus the data points noted with an asterisk give some indication of the variability in linear range properties which may be expected from lot to lot for apparently identical tires from the same manufacturers.

Table 3-11. The Effect of Inflation Pressure on Cornering Stiffness, Aligning Stiffness, and Camber Stiffness

Tire	Pressure psi	Cornering Stiffness lb/deg	Aligning Stiffness ft.lb/deg	Camber Stiffness lb/deg
E Size Test Load = 800 lb.				
Firestone 500 E78-14	28	144	12	27
	22	139	16	
	16	119	18	19
	10	101	20	17
General Belted Jumbo E78-14	28	151	10	15
	22	135	21	15
	16	113	25	11
	10	83	26	11
Goodrich Silvertown E78-14 (OE tire)	28	140	14	20
	22	135	18	15
	16	103	21	14
	10	81	23	12
Goodyear Custom Power Cushion Polyglas E78-14	28	165	17	21
	*22	151		
	16	123	24	21
	10	80	25	17
Pirelli 185-14	28	185	18	2
	22	166	21	5
	16	146	25	3
	10	104	30	3
H Size Test Load = 1100 lb.				
Bridgestone 225R-14	34	310	31	8
	*26	264		
	18	257	42	14
	10	174	45	14
Firestone Deluxe Champion H78-14 (OE tire)	34	210	24	41
	26	200	28	38
	18	161	35	31
	10	118	38	24
Firestone 500 H78-14	34	229	25	38
	26	212	29	37
	18	176	32	32
	10	122	34	24
Firestone Town & Country H78-14 (snow)	34	193	15	25
	*26	162		
	18	154	32	28
	10	100	34	23
Firestone Town & Country HR78-14 (snow)	34	191	15	42
	*26	183		
	18	177	19	39
	10	114	28	
General Belted Jumbo H78-14	34	227	31	35
	26	197	36	31
	18	145	35	22
	10	90	21	17

*Tire from a separate lot.

Cornering stiffness, which may be defined as the rate of change of side force with respect to slip angle evaluated at zero slip angle for a free-rolling tire operated at zero inclination angle, is an important tire property, particularly with regard to the normal driving range. The data presented in the table indicates that, as expected, cornering stiffness drops with decreasing inflation pressure for all the tires tested. In addition, note that aligning moment tends to increase and camber stiffness tends to decrease with decreasing inflation pressure for all the tires.

The drop in cornering stiffness with decreasing inflation pressure may be expected to be dependent on the vertical load. As an example, consider Figure 3-17 in which the cornering stiffness of the Firestone 500 H78-14 is plotted as a function of load and inflation pressure. It is clear from the figure that the reduction in cornering stiffness is accentuated by increasing loads. The trend in the data shown in the figure is quite typical of all the tires tested.

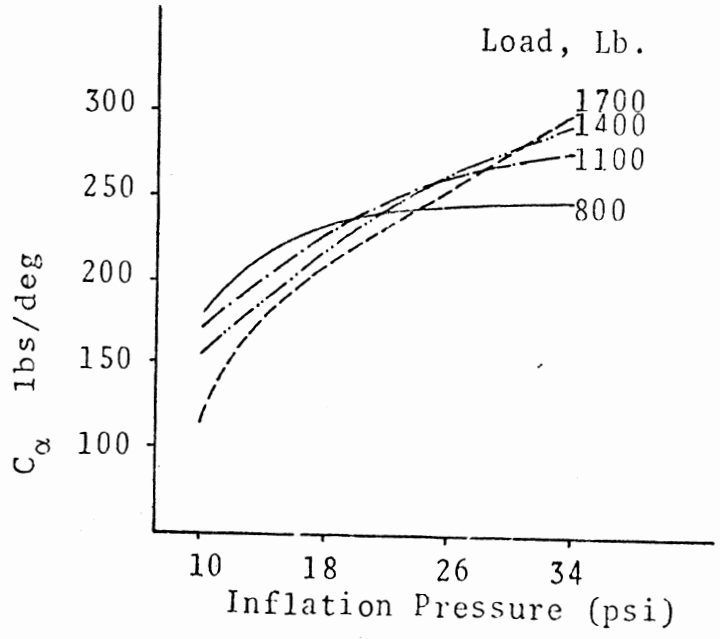

Figure 3-17. Cornering stiffness as a function of inflation pressure and load, Firestone 500 H78-14, 26 psi.

3.2.2 MOBILE TIRE TEST RESULTS. Each of the OE tires, the Firestone Deluxe Champion Sup-R-Belt H78-14 and the Goodrich Silvertown Belted E78-14, have been tested across a wide range of inflation pressures at a variety of load conditions and speeds using the HSRI mobile tire tester. These data, which are summarized in this section, are presented in detail in Appendix D. Initially, the straight-line braking or "μ-slip" data will be considered.

Each OE tire was tested at 800 and 1100 lbs. load, and at two speeds. Some results of these tests, which were performed at TTI on dry concrete, are presented in Tables 3-12 and 3-13.

Table 3-12. Peak and Slide Friction Coefficient (μ_p and μ_s) for the Firestone Deluxe Champion Sup-R-Belt H78-14, Dry Asphalt.

Inflation Pressure (psi)	Speed (mph)	Load (lbs) 800 μ_p	800 μ_s	1100 μ_p	1100 μ_s
12	40	.9	.88	.87	.76
	20			.83	.78
20	40	.92	.85	.90	.80
	20			.92	.79
28	40	.92	.85	.96	.79
	20			.92	.79
36	40	.97	.80	.92	.80
	20			.95	.79

Although friction levels presented in the tables drop with decreasing inflation pressure, the magnitude of the change is not enough to cause detectable changes in braking

Table 3-13. Peak and Slide Friction Coefficient (μ_p and μ_s) for the B.F. Goodrich Silvertown Belted E78-14, Dry Asphalt.

Inflation Pressure (psi)	Speed (mph)	Load (lbs), 800 μ_p	800 μ_s	1100 μ_p	1100 μ_s
12	40	.91	.83	.85	.83
	20	.85	.83		
24	40	.95	.87	.91	.87
	20	1.01	.87		
30	40	.97	.94	.94	.83
	20			---	---

performance due to inflation pressure variations. (Vehicle test data supporting this fact will be presented later.)

The free-rolling mobile tire test data, on the other hand, indicate that important changes take place with varying inflation pressure. The pertinent data are presented graphically in Figures 3-18 and 3-19. (The curves were generated using the semi-empirical tire model contained in the computer simulation, the points marked with an o, ●, or Δ indicate mobile tire tester measurements.) Note that the forces measured across the entire range of slip angles suffer an impressive drop as inflation pressure is decreased, with the most significant changes occurring at the highest loads. This leads to the expectation of a significant relationship between inflation pressure and limit performance. Such a relationship was demonstrated during the vehicle testing, as will be shown below.

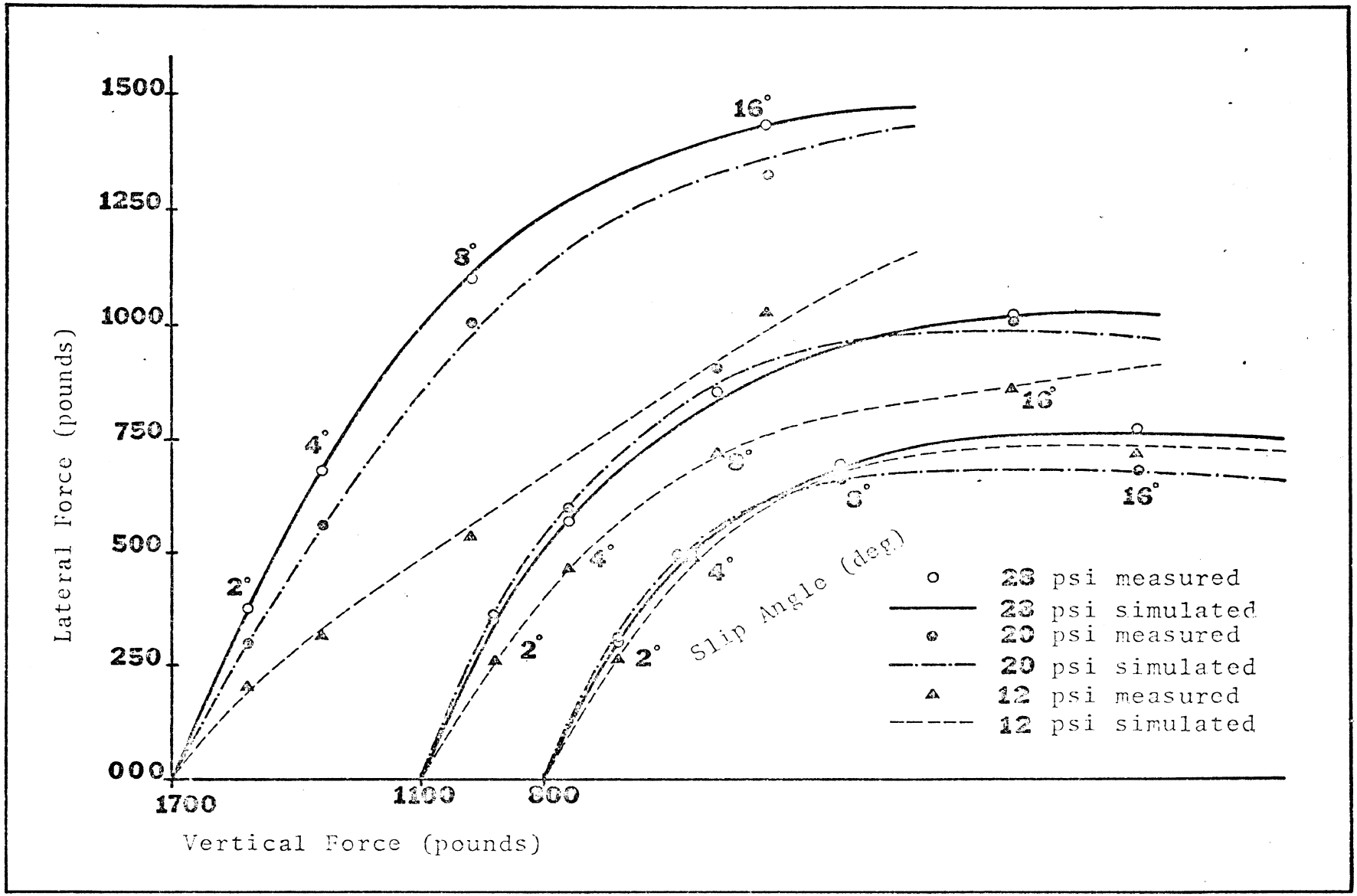

Figure 3-18. Lateral force vs. slip angle at various inflation pressures Firestone Deluxe Champion Sup-R-Belt H78-14, dry asphalt.

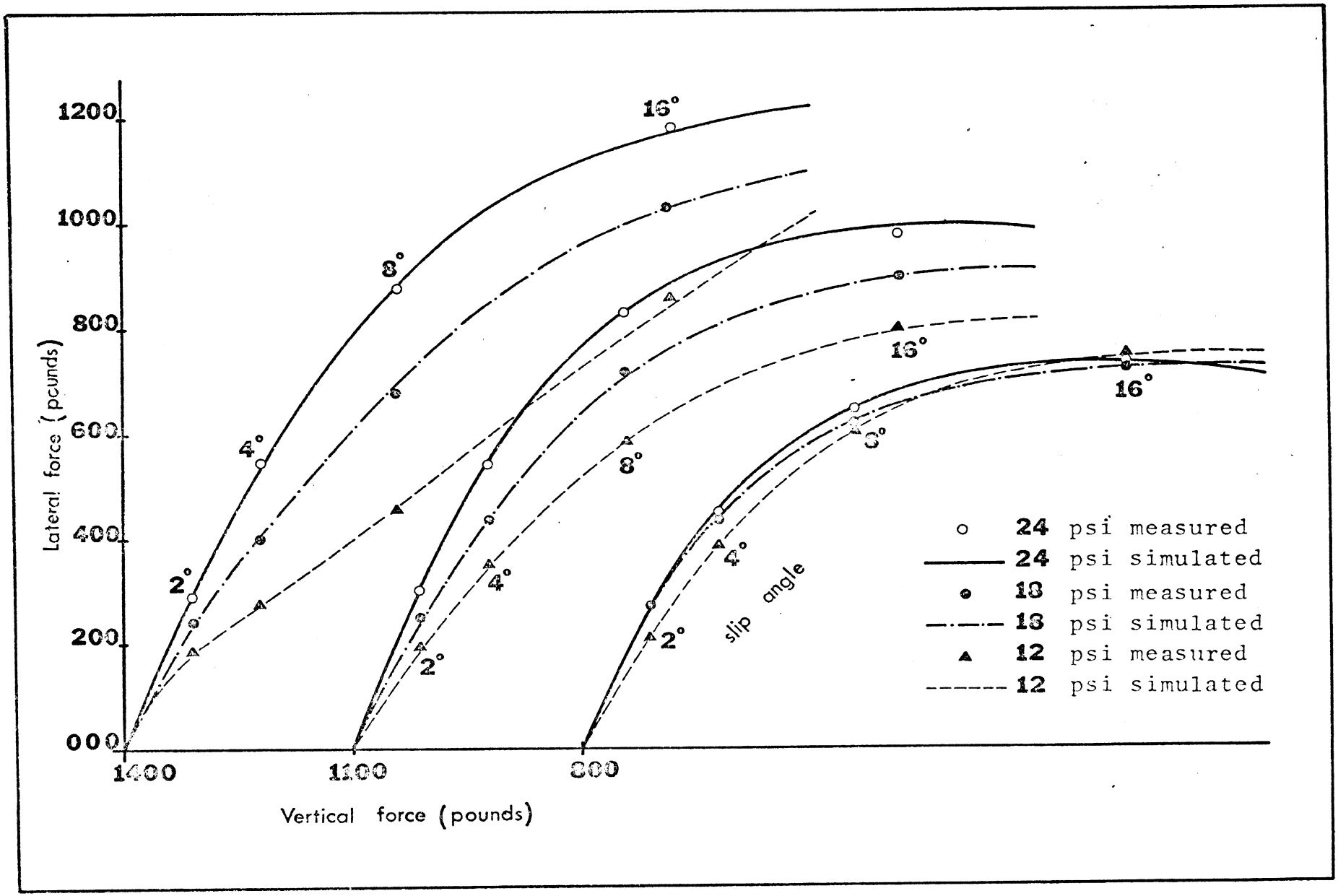

Figure 3-19. Lateral force vs. slip angle at various inflation pressures, B.F. Goodrich Silvertown Belted E78-14, dry asphalt.

3.2.3 MEASUREMENTS AND CALCULATIONS RELATING INFLATION PRESSURE TO LIMIT PERFORMANCE. It was the goal of this investigation to determine, through tire testing, vehicle testing, and analysis, if tire-in-use factors can cause a significant deviation from the OE vehicle performance. In pursuit of this goal, mobile tire testing of the OE Buick and Mustang tires was performed across a wide spectrum of inflation pressures before any limit maneuver testing, and a simulation study (using this mobile tire data) was made to determine the inflation pressures that should be selected to yield a cost-effective and informative test program.

Some results from the pre-test simulation study are presented in Table 3-14 and Figure 3-20(a)-(d). (Note that left and right polarity maneuvers were used to facilitate plotting of the data.) These calculations, and similar calculations for the Buick led to the choice of the inflation and pressure levels listed in Table 3-15 for vehicle testing.

The 24-psi-front, 18-psi-rear configuration was selected for comparison with the OE Mustang. It was believed that, although this pressure differential was not extreme, marked changes from the OE performance would be seen.

Table 3-15 shows that five inflation pressure conditions were selected for the Buick. The OE condition is, of course, the basis for comparison. The PSI1 condition was expected to produce very little change from the behavior exhibited by the OE configuration, in any maneuver, notwithstanding the drop from the OE pressures recommended for the front and rear tires. The PSI2 configuration (OE pressure was maintained in front while dropping the rear pressure level) was, on the other hand, expected to show a marked change from OE performance, particularly in the response to trapezoidal and sinusoidal steer inputs. Significant differences in performance were

Table 3-14. Summary of Computations: Mustang, 232° Trapezoidal Steer.

Inflation Pressure	Steer Polarity	Peak Lateral Acceleration	Peak Sideslip Angle
*24 psi front, 24 psi rear	right	25.51	-6.23
24 psi front, 18 psi rear	right	28.27	-22.70
24 psi front, 12 psi rear	right	29.34	-30.72
*24 psi front, 24 psi rear	left	-26.22	7.2
18 psi front, 24 psi rear	left	-22.34	3.93
12 psi front, 24 psi rear	left	-18.73	2.42

*The measured relationship between steering wheel angle and road wheel angle, which was entered in the simulation, was slightly asymmetric. Thus slight differences appear between these runs.

Table 3-15. Inflation Pressure Levels for Vehicle Tests

Condition	Buick		Mustang	
	Front	Rear	Front	Rear
OE	24	28	24	24
PSI1	20	20	24	18
PSI2	24	16		
Loaded OE	26	32		
Loaded PSI	26	18		

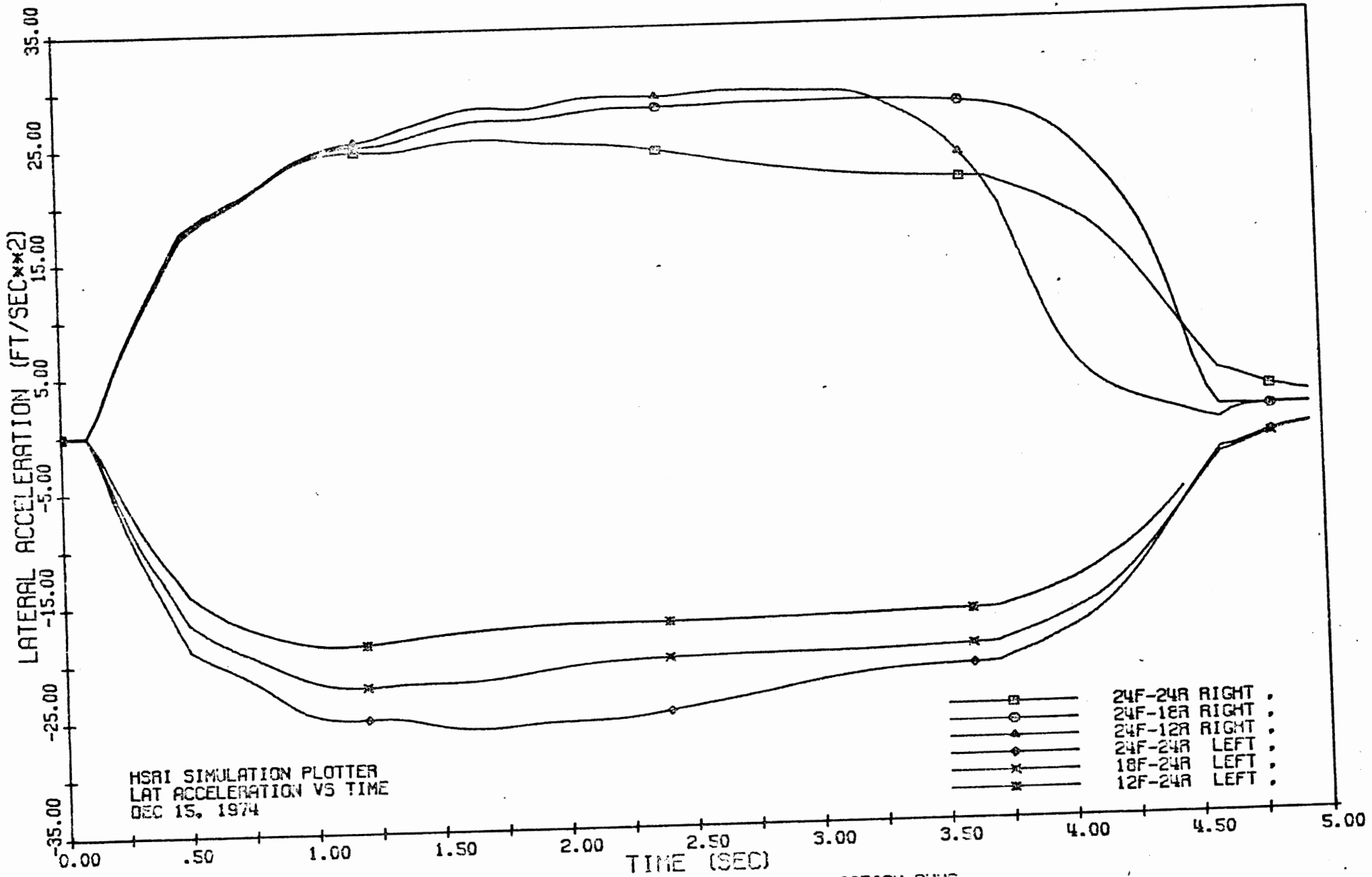

Figure 3-20(a). FORD MUSTANG: 202 DEG T..P., PSI VARIATION RUNS

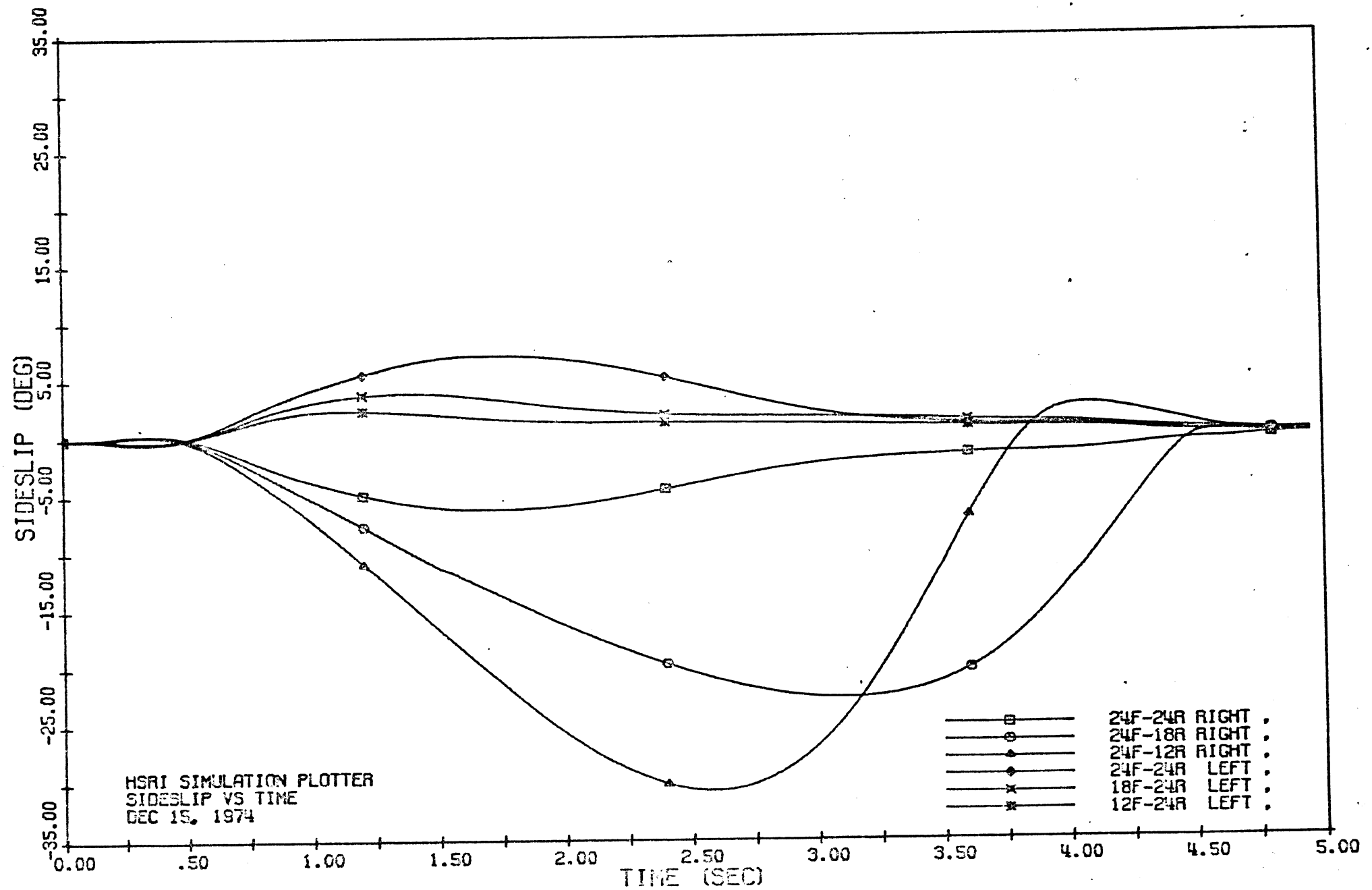

Figure 3-20(b). FORD MUSTANG: 232 DEG TEMP., PSI VARIATION RUNS

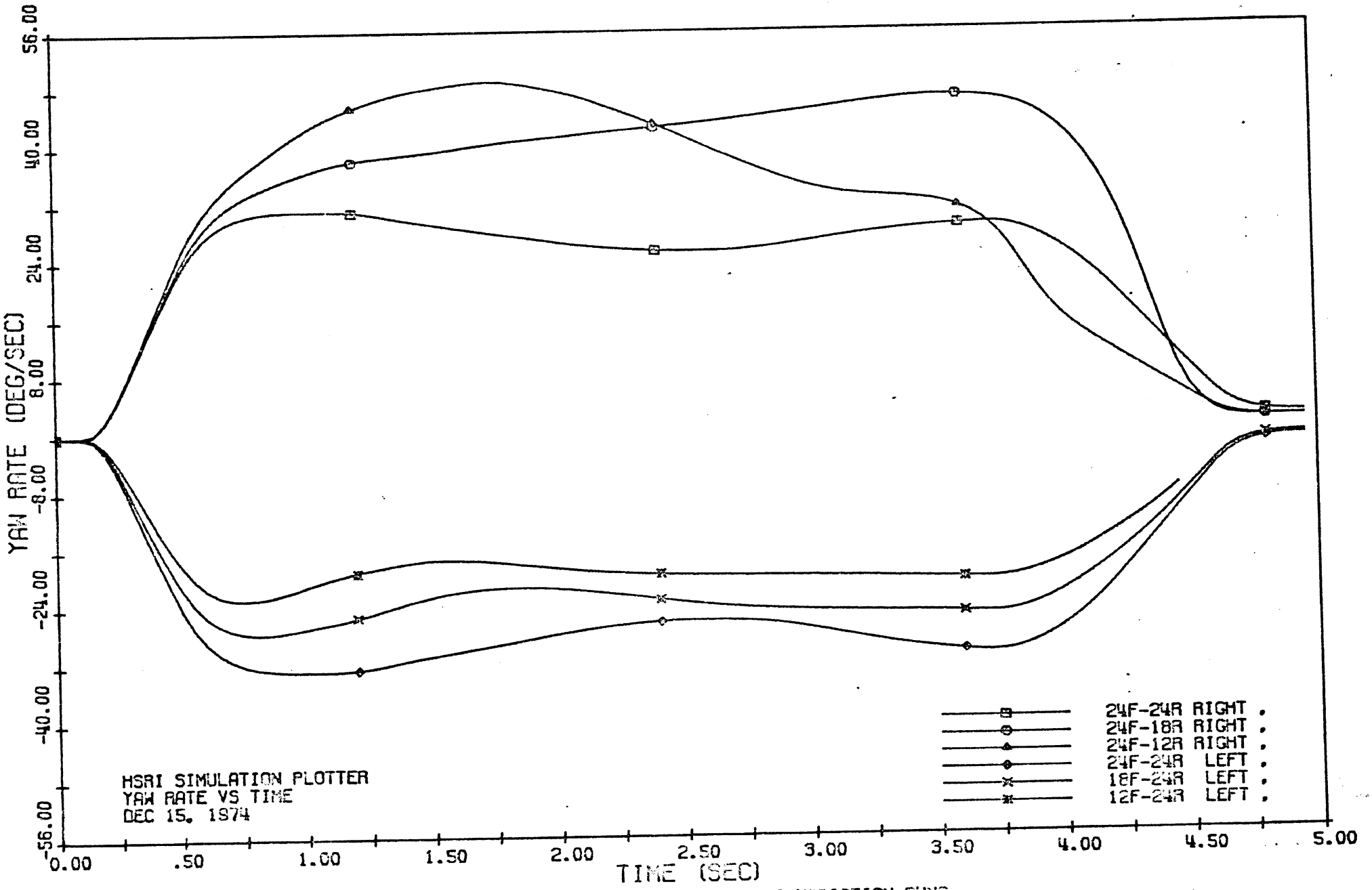

Figure 3-20(c). FORD MUSTANG: 232 DEG TRAP., PSI VARIATION RUNS

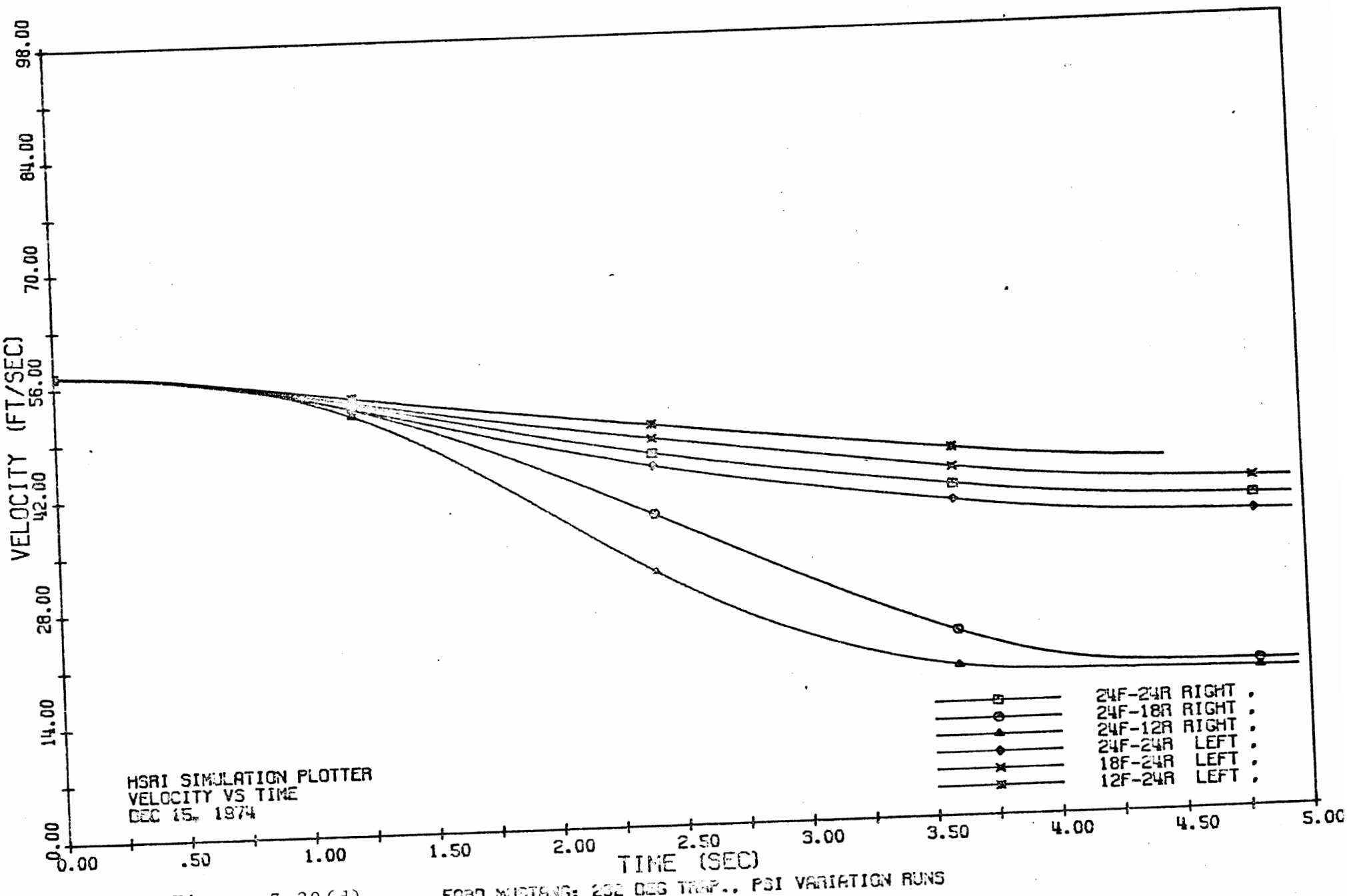
VELOCITY (FT/SEC)
98.00
84.00
70.00
56.00
42.00
28.00
14.00
0.00
0.00
.50
1.00
1.50
2.00
2.50
3.00
3.50
4.00
4.50
5.00
TIME (SEC)
HSRI SIMULATION PLOTTER
VELOCITY VS TIME
DEC 15, 1974
24F-24R RIGHT .
24F-18R RIGHT .
24F-12R RIGHT .
24F-24R LEFT .
18F-24R LEFT .
12F-24R LEFT .
FORD MUSTANG: 232 DEG TRAP., PSI VARIATION RUNS

Figure 3-20(d).

also expected to be demonstrated between the Buick in the loaded OE condition and the loaded PSI condition.

The results of the pre-test simulation study proved to be a realistic indicator of the vehicle test results, as will be shown in the next section.

3.2.4 VEHICLE TEST RESULTS. Each of the six VHTP procedures were performed in an attempt to quantify changes from OE performance deriving from inflation pressure degradations. The results obtained are summarized below for each of the six VHTP's.

3.2.4.1 Straight-Line Braking. The objective of the straight-line braking procedure is to quantify the vehicle's efficiency in utilizing the prevailing surface friction prior to wheel lockup while stopping in a straight line. This measurement is accomplished by sequentially applying an increasing level of braking input to the test vehicle operating at 40 mph until lockup occurs on either the two front or two rear wheels.

Two categories of limit response are commonly observed in this maneuver, as distinguished by the order in which wheel lockup occurs at the limit:

(a) front wheels lock first, thereby degrading the steerability of the vehicle

(b) rear wheels lock first, thereby degrading directional stability.

Braking performance is considered to be degraded if wheel locking is experienced at a lower level of longitudinal acceleration than was achieved in some reference or baseline condition.

The tire data tabulated in Tables 3-12 and 3-13 indicate that changes in peak braking forces on the order of ten percent may be expected to occur as inflation pressure is decreased in the OE tires. Since the straight-line braking procedure seeks peak deceleration levels by incrementing brake line pressure in 25 psi increments, the test procedure does not possess a resolution capability to detect such small changes. Thus is is not surprising that the test results, as summarized in Table 3-16, indicate virtually no change in braking performance on a dry surface deriving from inflation pressure variations.

Table 3-16. Maximum Measured Deceleration Without Locking Two Wheels on One Axle.

	Maximum Deceleration (g's)
	Dry
Mustang	
OE	.73
PSI1	.73
Buick	
OE	.61
PSI1	.61
Loaded	.79
Loaded PSI	.78

The following simplified analysis provides a quantitative evaluation of the influence of peak friction coefficient on the results of the straight-line braking maneuver. In a straight-line braking test the limit deceleration condition is obtained when either the front or rear wheels are on the verge of locking. Consider the case in which the rear wheels are on the verge of locking. In this instance,

$$F_{XR} = \mu_p F_{ZR} \tag{3-6}$$

where

F_{XR} is the total braking force of the rear tires

μ_p is the peak friction coefficient

and F_{ZR} is the vertical load on the rear tires.

and

$$F_{XF} = K \cdot F_{XR} \tag{3-7}$$

where F_{XF} is the total braking force of the front tires and K is a (possibly variable) parameter whose value determines the brake proportioning. The normal load on the rear tires can be found under the assumption of quasi-static load transfer, viz.:

$$F_{ZR} = W_R - \frac{h}{\ell} (F_{XF} + F_{XR}) \tag{3-8}$$

where

W_R is the static load on the rear tires

h is the center of gravity height

and ℓ is the wheel base.

Solving (3-6), (3-7), and (3-8) for F_{XR} yields

$$F_{XR} = \left(\frac{\mu_p W_R}{[1 + \mu_p \frac{h}{\ell} (K + 1)]} \right) \tag{3-9}$$

Let us now consider the OE Mustang braking on a dry surface. The OE Mustang is described by the following parameters:

$\mu_p \approx 1.0$

$K \approx 1.5$ (at high pressure levels)

$W_R = 1620$ lbs.

$\left(\frac{h}{\ell}\right) = 0.187$

The front and rear brake forces obtained from Equations (3-9) and (3-7) are

$F_{XR} = 1105$ lbs.

and

$F_{XF} = 1660$ lbs.

These front and rear braking forces produce a deceleration of 0.755 g on the 3660-lb. Mustang. (Note that the test result was 0.73 g.)

Now assume that $\mu_p = 0.9$ for all tires instead of 1.0. In this case, application of Equations (3-9) and (3-7) yields

$F_{XR} = 1026$ lbs.

$F_{XF} = 1540$ lbs.

and vehicle deceleration is equal to 0.702 g. Thus a 10% reduction in μ_p yields only 0.05 g reduction in maximum deceleration prior to locking the rear wheels.

This 0.05 g change in deceleration is not significantly greater than the resolution of the test procedure. For example, the effectiveness of the rear brakes of the Mustang

is such that, for the range of tire pressure and brake torque under discussion here,

$$T_{BR} \cong P_B \tag{3-10}$$

where T_{BR} is the brake torque in ft/lbs obtained at one rear wheel and P_B is the brake pressure in psi. For rear tire rolling radii of approximately one foot, the total rear brake force is approximately

$$F_{XR} \simeq 2 P_B \tag{3-11}$$

or in terms of incremental changes

$$\Delta F_{XR} = 2\Delta P_B \tag{3-12}$$

For ΔP_B = 25 psi, as specified in the test procedure,

$$\Delta F_{XR} = 50 \text{ lbs.}$$

and $$\Delta F_{XF} = K \cdot \Delta F_{XR} = 75 \text{ lbs.}$$

These changes in braking force lead to 0.034 g change in deceleration. Clearly, the resolution of the test procedure (i.e., 0.034 g) is only marginally adequate to detect a change in the braking performance caused by a change in inflation pressure that reduces μ_p from 1.0 to 0.9.

3.2.4.2 Braking-In-A-Turn. The objective of the braking-in-a-turn maneuver is to characterize the vehicle's ability to attain high levels of longitudinal deceleration without (1) experiencing a large change in path curvature and (2) incurring excessive sideslip. The brakes are applied during a steady .3 g turn at a velocity of 40 mph. The measures of performance employed in this procedure are listed in Table 3-17.

Table 3-17. Measures of Braking-In-A-Turn Performance

Measure	Remarks
A_x	Average deceleration from 40 mph to 10 mph without locking two wheels on the same axle. (Typically both "inside" wheels lock before either "outside" wheels.)
RATIO	The quotient of the average path curvature from 40 mph to 10 mph divided by the pre-braking steady turn path curvature.
β_p	Peak sideslip angle occurring above 10 mph.
$\dot{\beta}_p$	Peak rate of change of sideslip angle occurring above 10 mph.

Some interesting results are summarized in Table 3-18 for the Buick and Mustang. As in straight-line braking, changes in inflation pressure did not yield significantly different results than were measured for the OE vehicle.

Table 3-18. Braking-In-A-Turn Measures for the Buick and Mustang (Left Turn, Right Turn).

	Maximum Deceleration Without Lockup of Both Wheels on an Axle (g's)	RATIO	β_p (deg)	$\dot{\beta}_p$ (deg/sec)
Buick				
OE	.69, .64	2.4, 2.1	6, 9	11, 11
PSI1	.71, .71	2.4, 1.7	14, 7	18, 8
PSI2	.69, .65	1.9, 2.0	8, 8	9, 15
Mustang				
OE	.67, .72	3.3, 2.3	13, 5	43, 12
PSI	.69, .71	2.7, 1.7	20, 4	27, 8

3.2.4.3 Roadholding-In-A-Turn. The objective of this procedure is to evaluate a vehicle's ability to track a curve in the presence of periodic road roughness having excitation frequencies spanning the range of wheel-hop frequencies. The test is performed on a circular course on which rubber strips are positioned at selected intervals. The strips, made of truck tire tread stock, are glued to a paved surface at three sites with spacings designed to provide vertical disturbances of 9, 11, and 14 Hz, respectively, when encountered by the running gear of a vehicle traveling at 30 mph. The vehicle initially contacts the grid from a steady (0.4 g A_y) turn which is nominally at right angles to the first grid element. The test is open-loop in character since the test driver holds the steering input against a stop throughout the curved approach and the traverse of the grid.

The grid frequencies, 9, 11, and 14 Hz, are selected to span the range of wheel-hop frequencies existing in the vehicle population. Thus, limit performance is determined by the presence of a resonant oscillation in the wheel-hop mode, by which a net loss accrues in tire side force.

The Buick in the OE and PSI2 condition was subjected to the roadholding test procedure. Some differences were noted in the lateral accelerations exhibited by the two configurations, both on the grid and upon exit from the grid. These findings were expected, since the wheel-hop frequency is directly dependent on inflation pressure.

The experimental data produced by the roadholding procedure are presented in Appendix F.

3.2.4.4 Trapezoidal Steer. The objective of the trapezoidal steer procedure is to characterize the limit cornering capability of the vehicle in terms of maximum path curvature attainable without excessive sideslipping. This maneuver is

conducted by applying a ramp-fronted step input of steering displacement to the test vehicle while it coasts through a velocity of 40 mph. The test sequence is defined by a set of prescribed steering levels, chosen to sweep from low accelerations to levels sufficiently beyond limit turning performance to assure inclusion of the limit response regime.

The J-turn-type response, though not representative of any realistic highway maneuver, does provide the conditions appropriate for examination of the transition from straight-line motion to a limit turn, such as would occur in the initial phase of an obstacle avoidance maneuver. Typical limit responses exhibited in this test are as follows:

1. Spinout—in which a dramatic yaw divergence is experienced as a result of side force saturation being incurred at the rear tires at an input level which still leaves considerable side force capability on the front tires. (Example time histories are shown in Figure 3-21.)

2. Driftout—in which the front tires saturate in side force prior to the rear tires, resulting in residual unrealized side force capability on the rear tires such that any perturbations of vehicle sideslip beyond this nominal trim condition result in increased side forces on the rear tires. (Example time histories are shown in Figure 3-22.)

3. Rollover—possibly aggravated by contact between wheel rim and pavement.

The tire test data presented in Section 3.2.2 indicates that the lateral forces generated by the free-rolling OE tires suffer an impressive drop as inflation pressure is decreased. Thus it is not surprising that calculations indicate

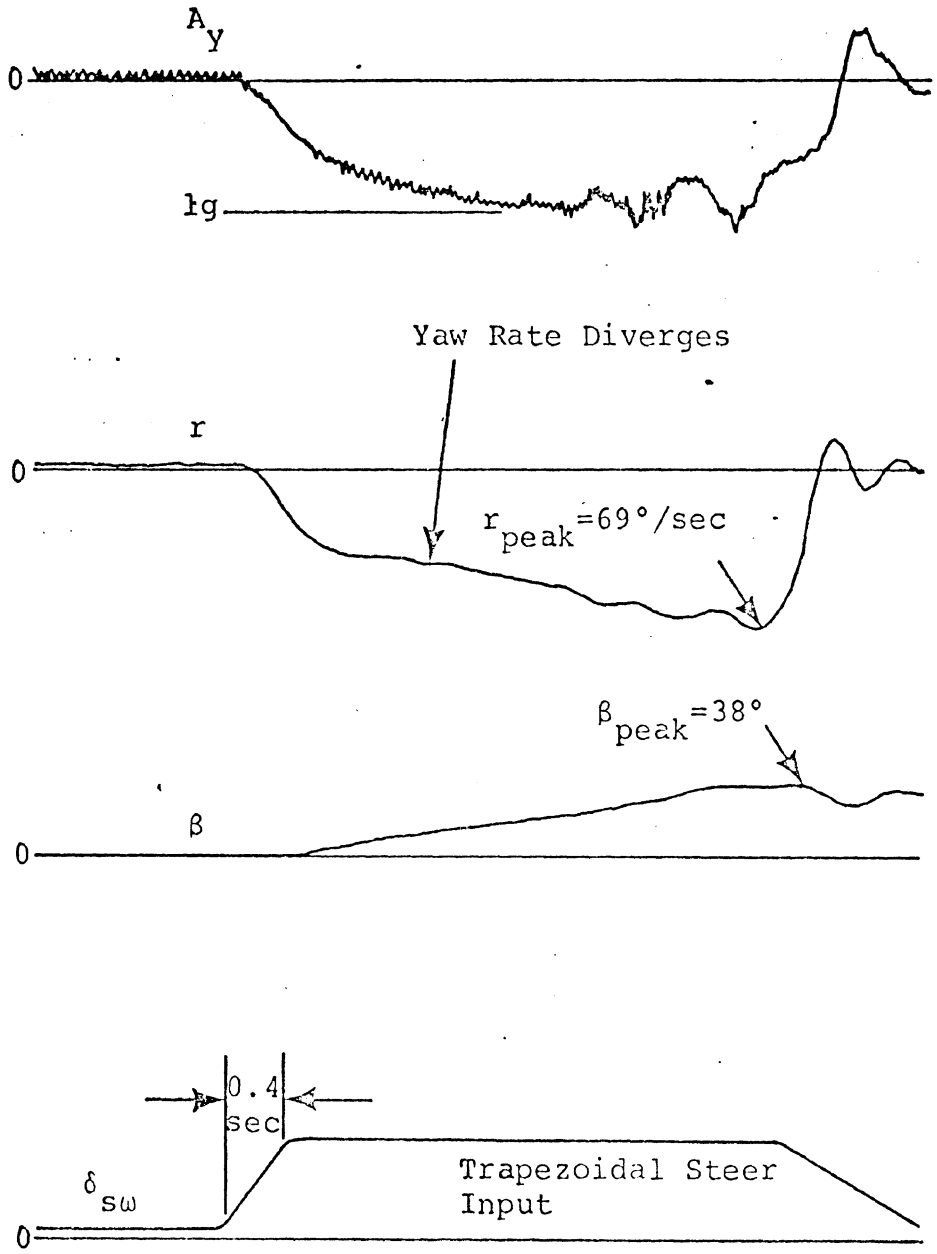

Figure 3-21. Trapezoidal steer rear tire saturation - spinout.

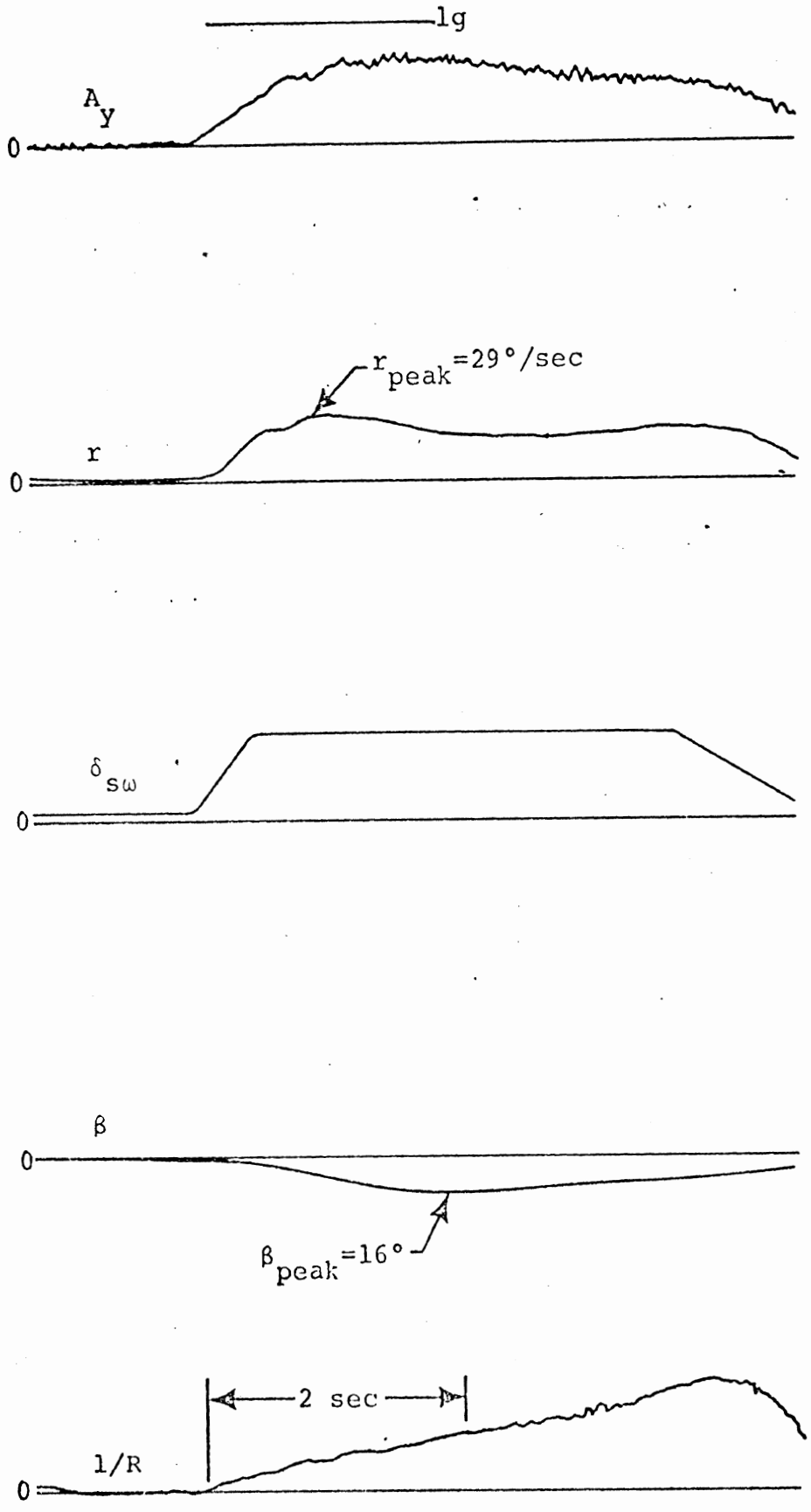

Figure 3-22. Trapezoidal steer front tire saturation - Driftout.

significant changes from the OE trapezoidal-steer response when the inflation pressure is reduced, particularly when the reduction takes place at the rear tires and not the front, thus disturbing the yaw moment balance so critical to this maneuver.

This trend is also apparent in the test results shown in Figures 3-23 and 3-24, in which peak lateral acceleration and peak sideslip angle are plotted versus steering amplitude for various tire inflation pressures on the Buick and Mustang. In Figures 3-23(a) and 3-23(b), the peak lateral accelerations and peak sideslip angles are plotted for the Buick in the OE condition* (24 psi front, 28 psi rear, test configuration #44), the PSI1 condition (20 psi front, 20 psi rear, test configuration #46), and the PSI2 condition (24 psi front, 18 psi rear, test configuration #47).

There are several features to be noted in these figures:

1. The OE condition and the PSI1 condition yield similar performance, reflecting the fact that in the normal driving range the magnitude and the fore-aft balance of the shear forces at the tire-road interface have not been significantly altered in the PSI1 condition.

2. In the PSI2 case, however, the reduced shear force capability of the rear tires has obviously led to higher lateral accelerations and sideslip angles at low steer levels.

---

*Here we refer to the OE test results starting at the lowest steer amplitude, i.e., test configuration #44. Test configuration #45 indicates the OE trapezoidal steer tests run highest steer angle first. See Section 3.2.1 for details.

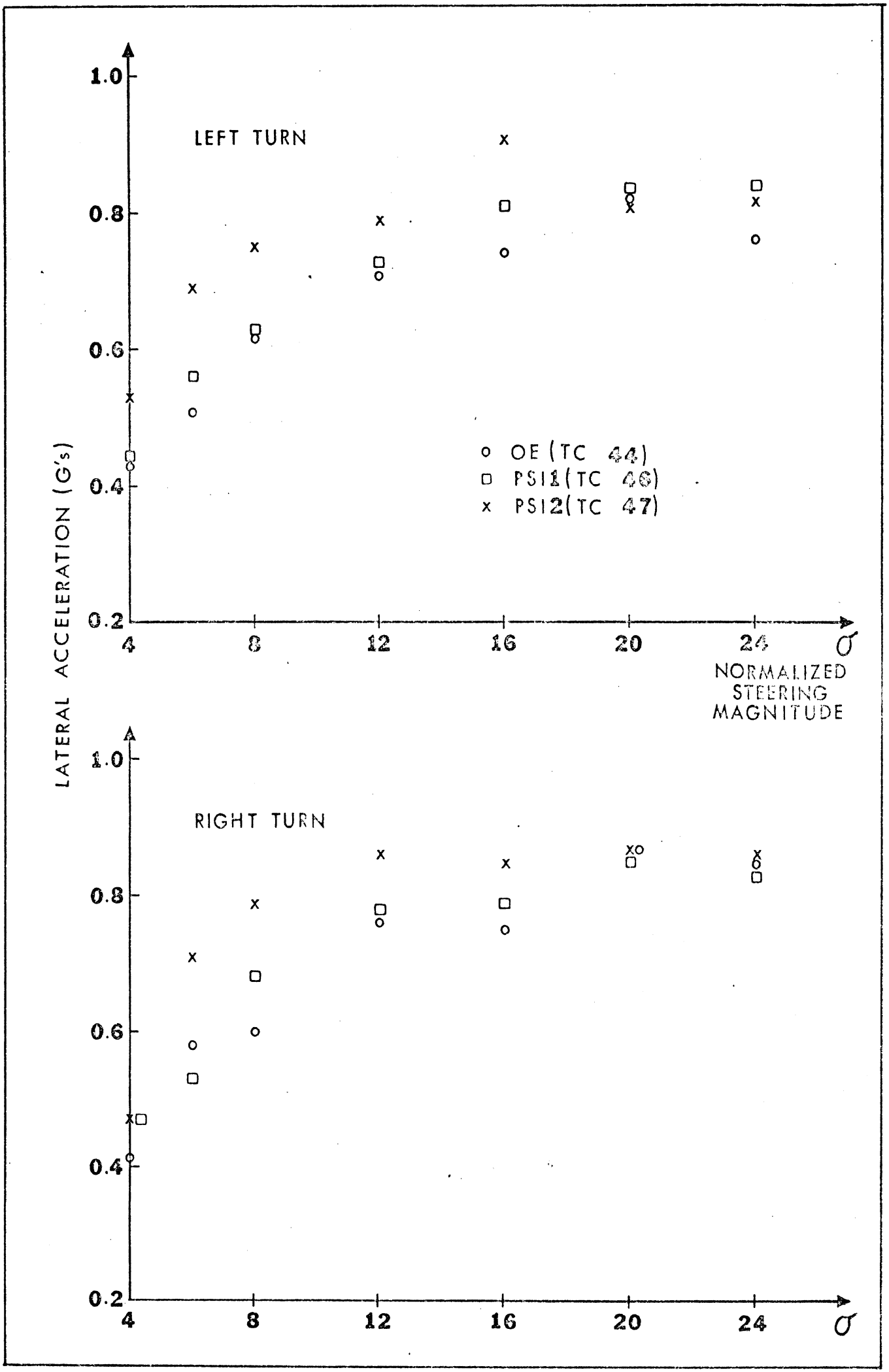

Figure 3-23(a). Peak lateral acceleration vs. steering magnitude, Buick, trapezoidal steer.

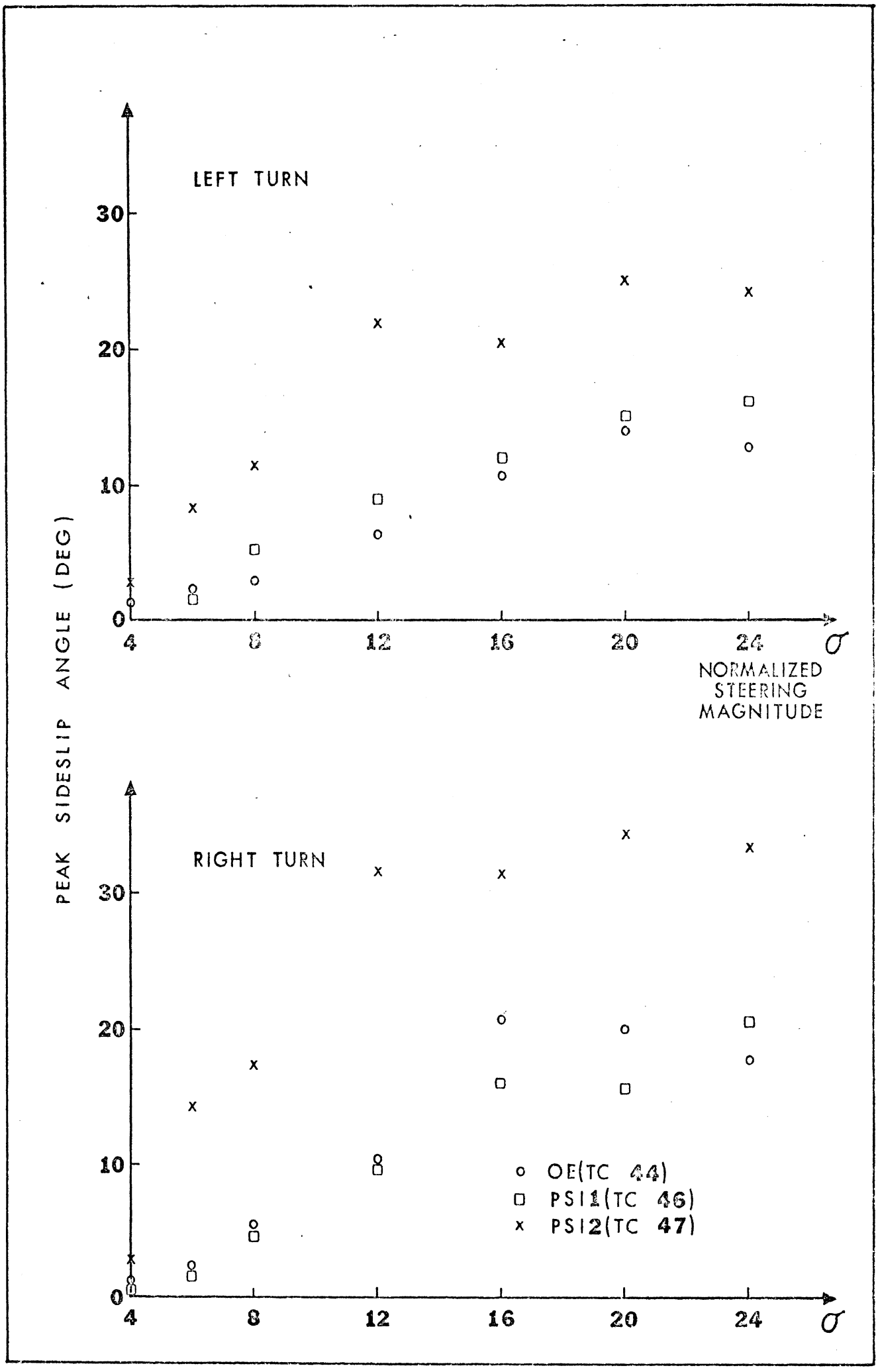

Figure 3-23(b). Peak sideslip angle vs. steering magnitude, Buick, trapezoidal steer.

3. The peak lateral acceleration levels tend to come together with increasing steer levels, suggesting that in this case the saturation levels of the shear forces at the tire-road interface are not significantly altered by the inflation pressure changes. However, the measured sideslip angles corresponding to each lateral acceleration level are obviously increased for the PSI2 runs, indicating that the sideslip angles at the rear tires have been increased to produce the required forces. (This situation has been discussed in some detail in another context in Section 3.1.4.)

This last observation is an important one—the increased sideslip angles produced by the PSI2 configuration indicate that the performance of the Buick has been significantly changed from the performance intended by the manufacturer. There can be no doubt that the change constitutes a severe degradation of the OE vehicle.

This same trend was noted in a comparison between the performance of the loaded Buick with OE inflation pressure levels (26 psi front, 32 psi rear), and in the loaded PSI condition (26 psi front, 20 psi rear). The PSI condition elicited lateral accelerations and sideslip angles far in excess of the OE vehicle at low steer angles. However, while the PSI condition was run over the full range of steer levels, the rear outside tire came off the rim in the first run at $\sigma = 8$, and many times thereafter. This occurrence, to say the least, degraded the rear tires, leaving no possibility of making a clear comparison with the OE condition at higher steer levels. The OE vehicle, on the other hand, remained intact throughout the testing.

The results obtained for the Mustang are presented in Figures 3-24(a) and (b) which compare the OE configuration

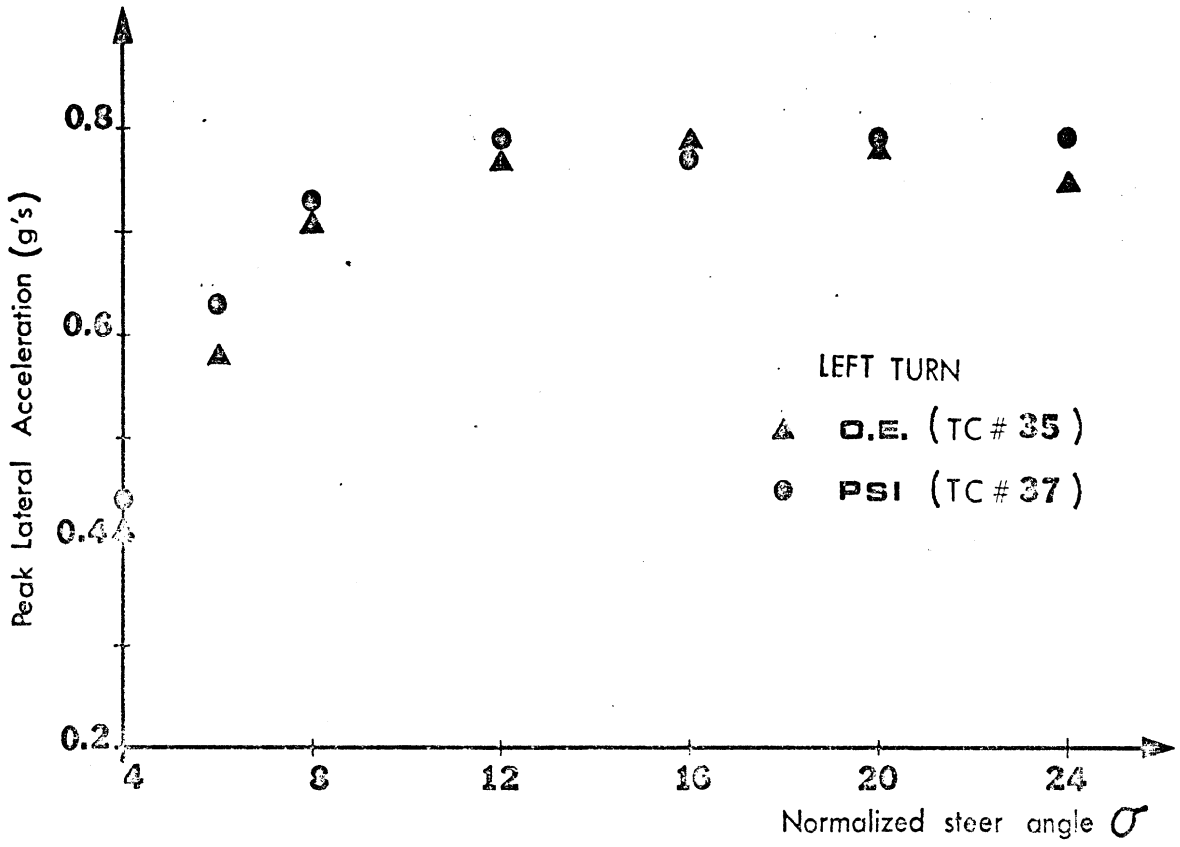

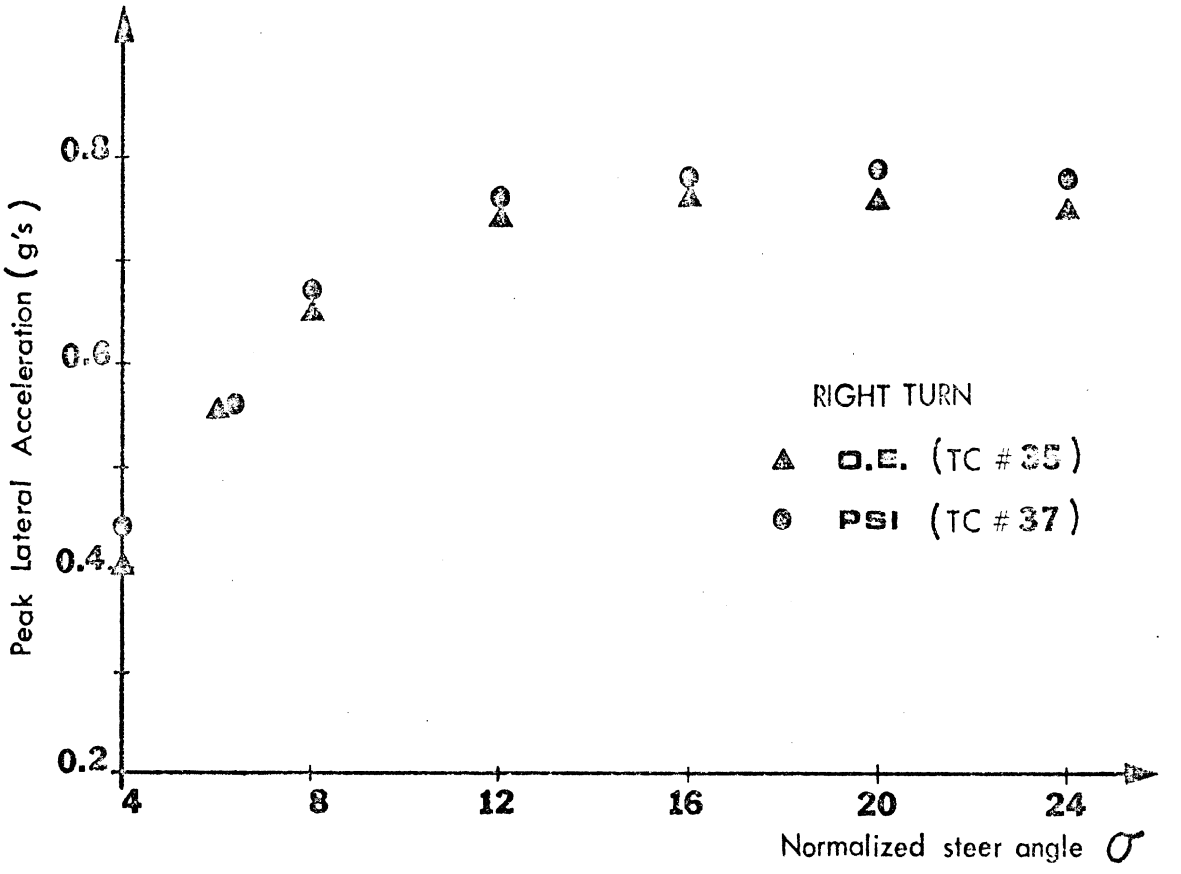

Figure 3-24(a). Peak lateral acceleration vs. steering magnitude, Mustang, trapezoidal steer.

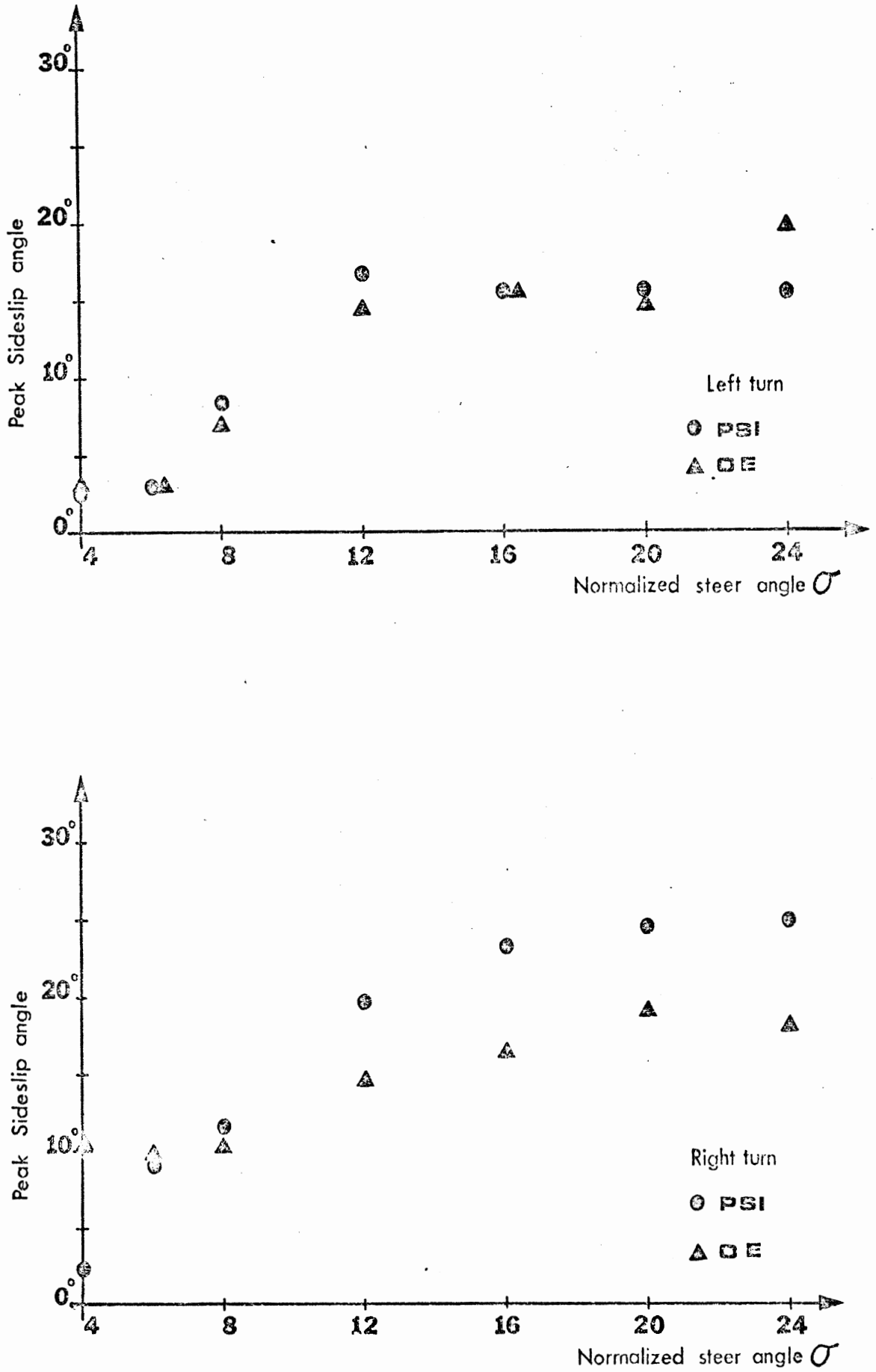

Figure 3-24(b). Peak sideslip angle vs. steering magnitude, Mustang, trapezoidal steer.

(24 psi front, 24 psi rear, test configuration #35) with the PSI configuration (24 psi front, 18 psi rear, test configuration #37). Significant asymmetry in response is obvious for the PSI configuration. Thus, while the difference between the OE and PSI results was nominal in left turns, significantly increased β was measured with the PSI configuration making right turns. (The large sideslip angle recorded at $\sigma = 4$ is probably in error. Note that this finding was not repeated in the left turn, or in configurations #36 or #28. All the trapezoidal steer test results are presented in Appendix F.)

The test results shown in Figures 3-23 and 3-24 show that lowering the inflation pressure in both rear tires from the level recommended by the manufacturers will cause significant deviations from OE performance. The performance changes may be particularly severe if the rear inflation pressure is lower than the manufacturers' recommendation, while the front inflation pressure remains at the manufacturers' recommended level.

These findings may also be shown to be valid if only one rear tire is improperly inflated. Consider Figures 3-25(a)-(d) in which the calculated response to trapezoidal steer inputs of left polarity is presented for the Buick (1) in the OE condition, (2) with the inflation pressure in the left rear tire lowered from the recommended 28 psi to 16 psi, and (3) with the inflation pressure in the right-rear tire lowered to 16 psi. These simulations clearly indicate that a lowered inflation pressure in one rear tire may be expected to result in significant asymmetry between right and left turns, with OE-like performance resulting when the degraded tire is on the inside of the turn, and PSI2-like performance with the degraded tire on the outside of the turn.

Calculations have also been performed to assess the effects of decreasing the front inflation pressure while holding

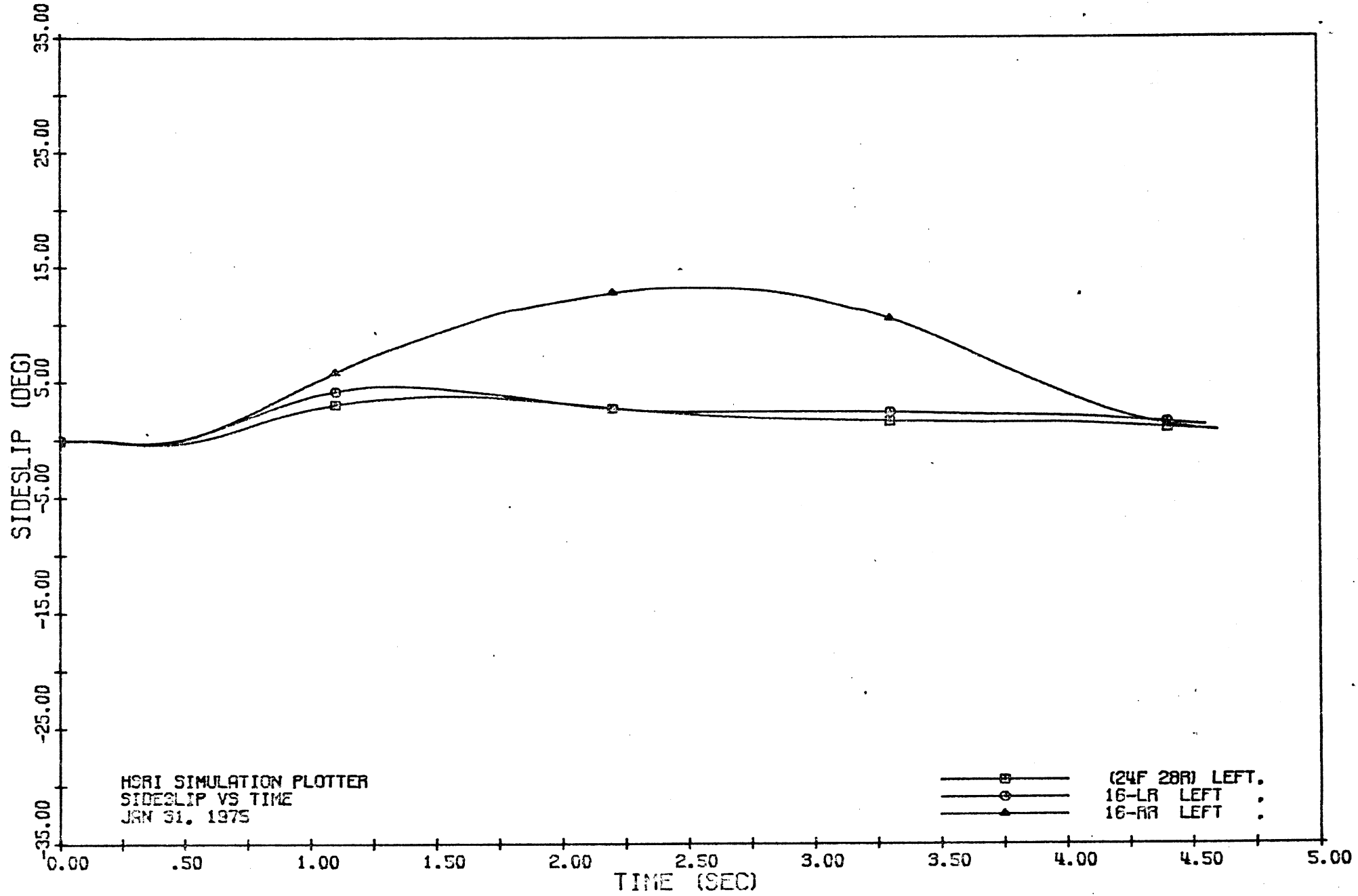

Figure 3-25(a). BUICK WAGON: 240.0 DEG TRAP., PSI ASSYMETRY RUNS

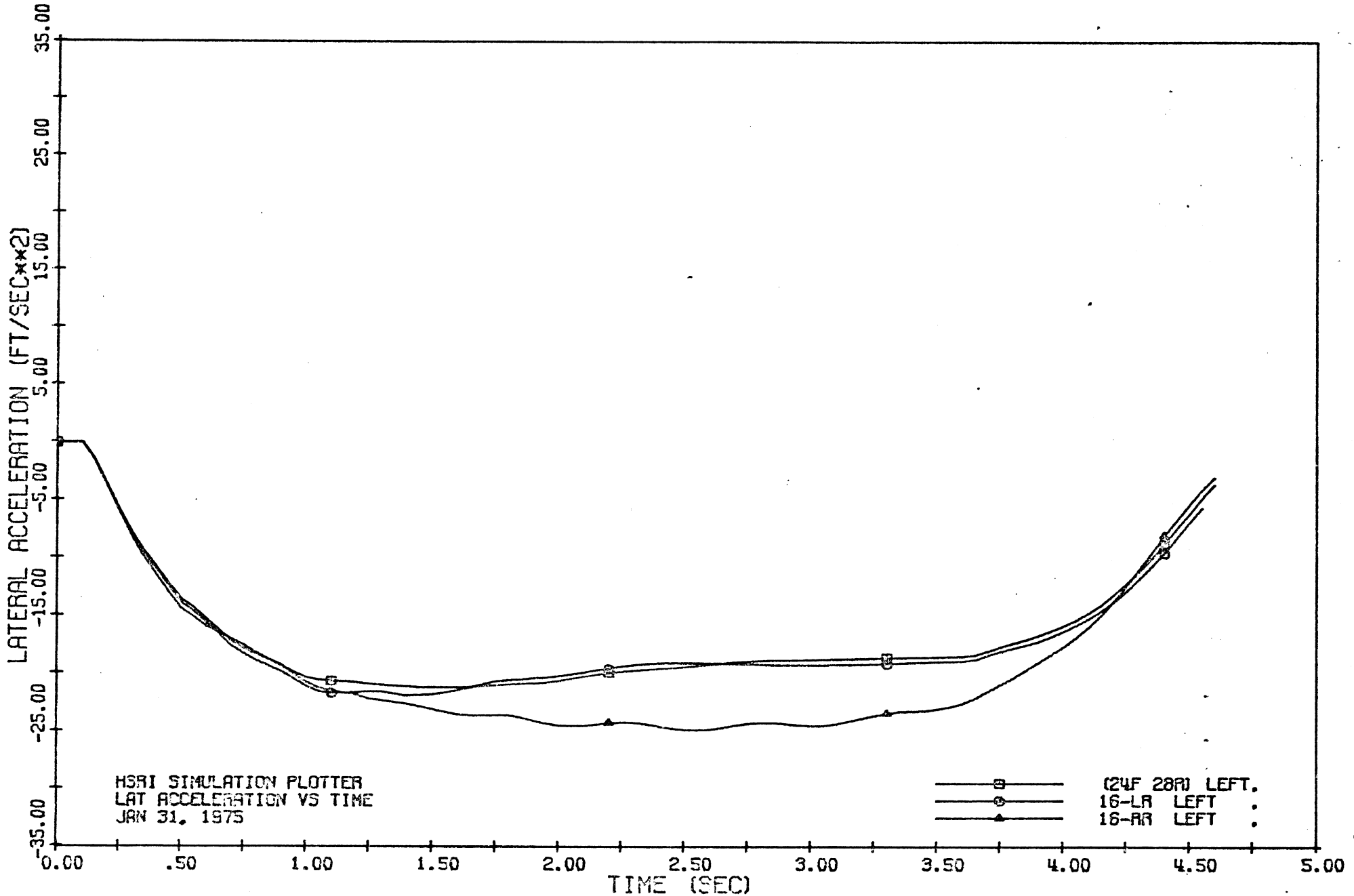

Figure 3-25 (b). BUICK WAGON: 240.0 DEG TRAP., PSI ASSYMETRY RUNS

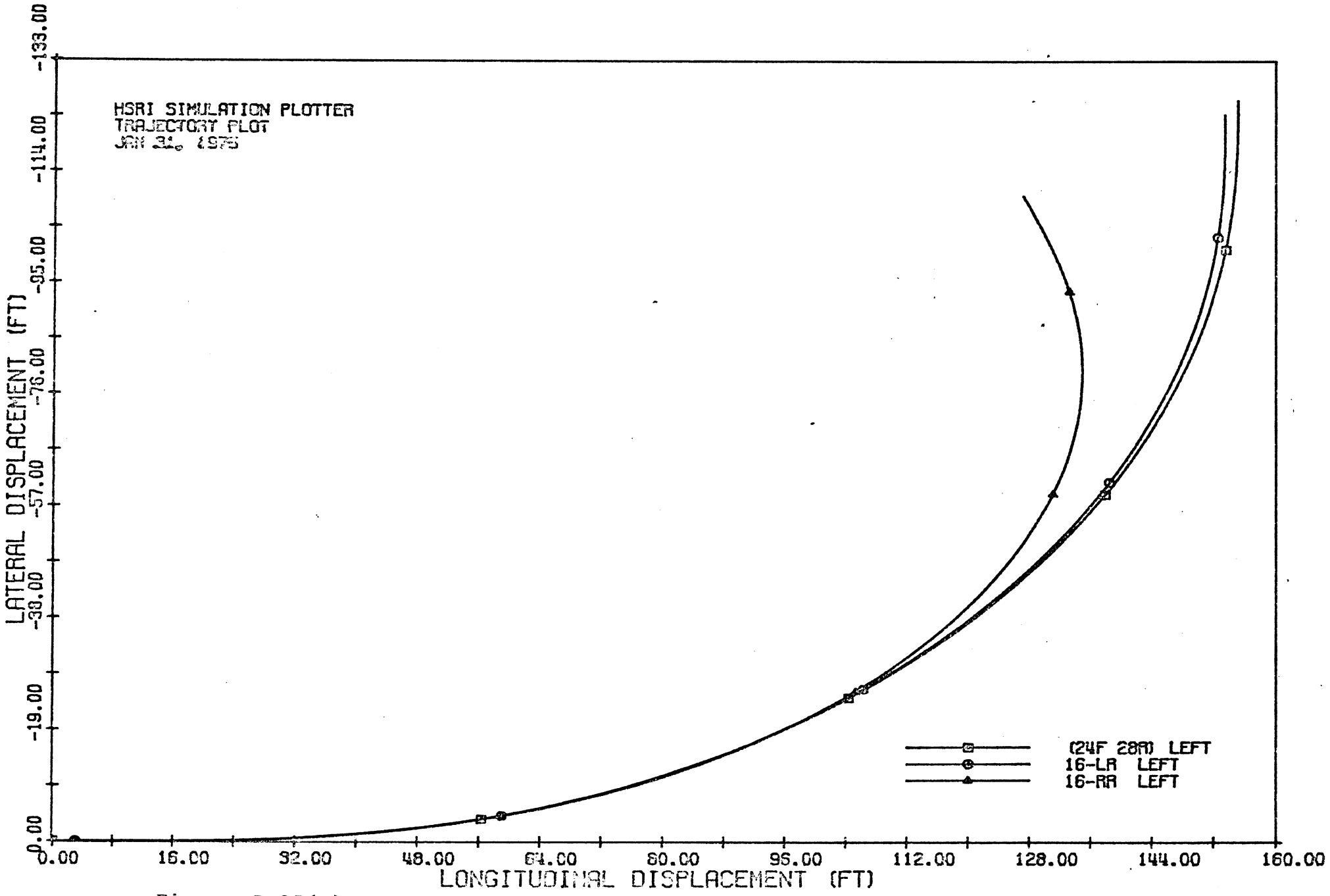

Figure 3-25(c). BUICK WAGON: 240.0 DEG TEMP., PSI ASYMMETRY RUNS

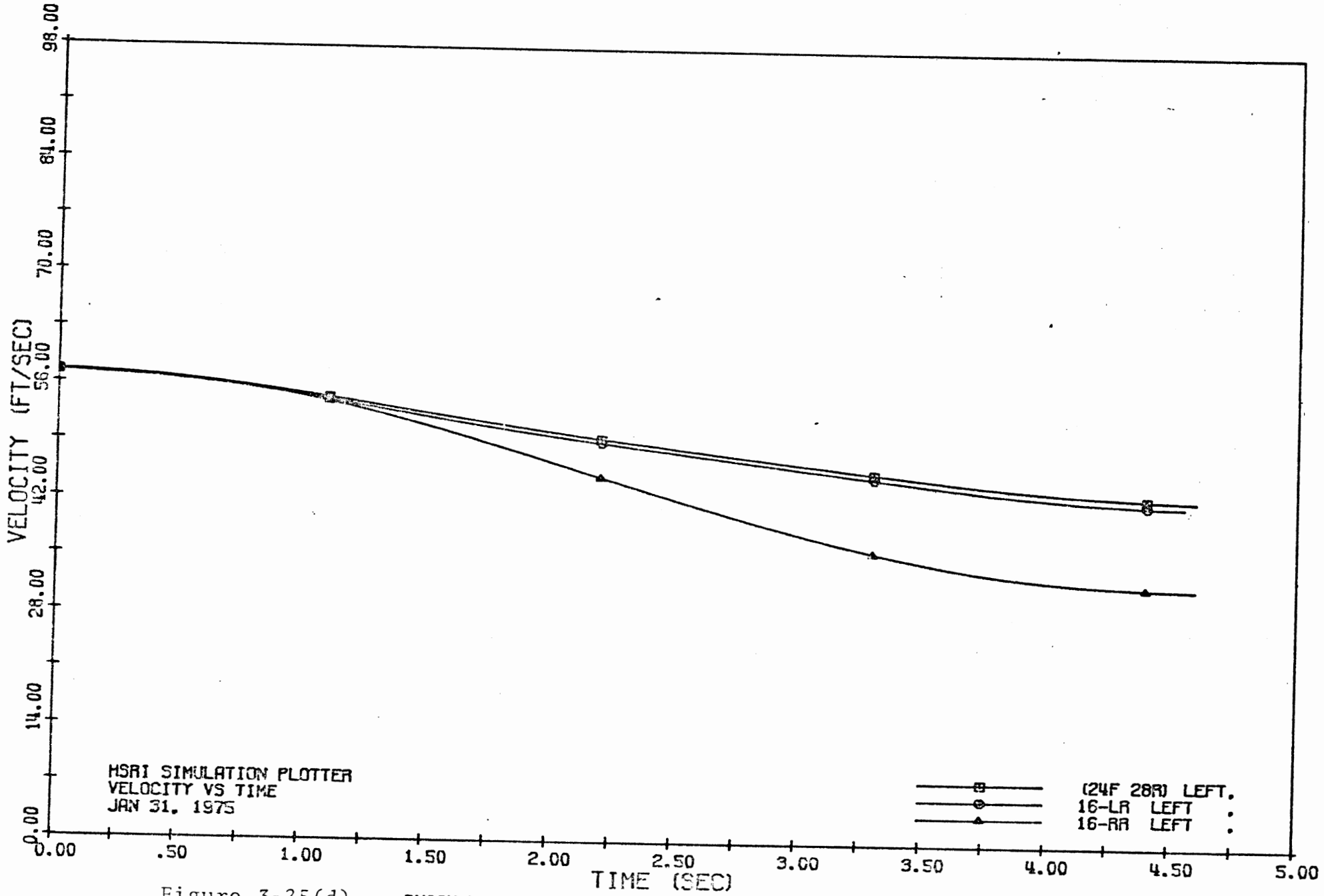

Figure 3-25(d). BUICK WAGON: 240.0 DEG TRAP., PSI ASSYMETRY RUNS

the rear tire at the recommended level. In general, this practice was found to produce less severe changes in performance than are obtained by changing the rear tires. Further, the changes were toward lower lateral accelerations and lower sideslip angles. An example of these calculations was presented previously in Table 3-14 (see Section 3.2.3.)

3.2.4.5 Sinusoidal Steer. The objective of the sinusoidal steer procedure is to evaluate the vehicle's ability to perform a rapid lane change in response to a symmetric input of steering displacement consisting of one cycle of a sine wave. This steering input is applied to a vehicle which is initially moving in a straight-line path. The input is applied at a selected velocity following throttle release. The procedure involves the execution of a large number of runs, performed at increasing steering amplitudes selected such that the trajectories obtained cover the full range of emergency lane change performance.

Two categories of yaw response limit have been previously identified (see Reference 1). These limits have been characterized as asymmetries of directional gain in response to the leading and trailing half-waves of the sinusoidal steer input. These limit responses were categorized as "under-corrective" and "over-corrective" yawing motions in which the second half of the sine wave is viewed as the corrective or recovery stage, during which the driver is attempting to re-establish his initial heading.

In the under-corrective response, the vehicle accumulates a large sideslip angle early in the maneuver, such that the recovery half of the steer input is essentially nullified. Response time histories typical of this condition are shown in Figure 3-26. The front tires, during the second half wave of steering input, experience an insufficient sideslip angle of the recovery polarity to produce a restoring yaw moment of

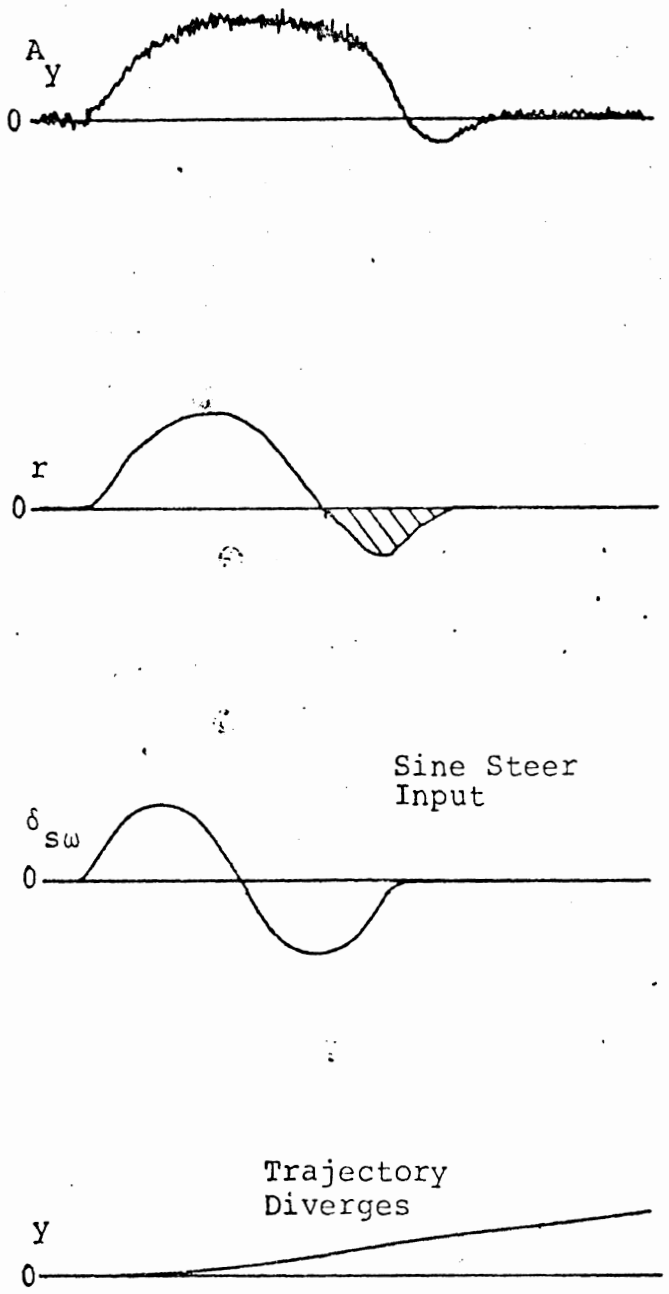

Figure 3-26. Sinusoidal steer under-corrective response.

sufficient magnitude. Carried to the extreme, a spinout is initiated in response to the first half wave of steering and the second half of the symmetric steer input is incapable of arresting the spin.

The over-corrective response, as typified by the time histories shown in Figure 3-27, results in a terminal heading which is directed back toward the original lane from which the maneuver began—the recovery half of the steering input being more effective than the initial steering input.

Several measures of the performance of the vehicle in this maneuver have been discussed by other writers—see, for example, Reference 4. While we have made extensive use of these "metrics," which are listed in Table 3-19, certain new measures have been developed in this program to aid in the analysis of the sinusoidal steer findings.

Table 3-19. Measures of Sinusoidal Steer Performance.

Metric	Definition	Remarks
Δ	Lane change deviation, $\Delta = \frac{1}{3.4}\int^{3.4} \lvert 12 - y \rvert dy$	Lower Δ indicates the vehicle has more successfully moved twelve feet laterally in 3.4 seconds.
$\Delta\psi$	Heading change	Heading of vehicle after 3.4 seconds. Increasing $\Delta\psi$ indicates magnitude of over-correction or under-correction.
β_p	Peak sideslip angle	

Consider Figure 3-28, in which the trajectories from Figure 3-26 and 3-27 are compared. It is apparent that, in these two cases, the $\Delta\psi$ metric gives an adequate indication of the under-corrective or over-corrective nature of the response.

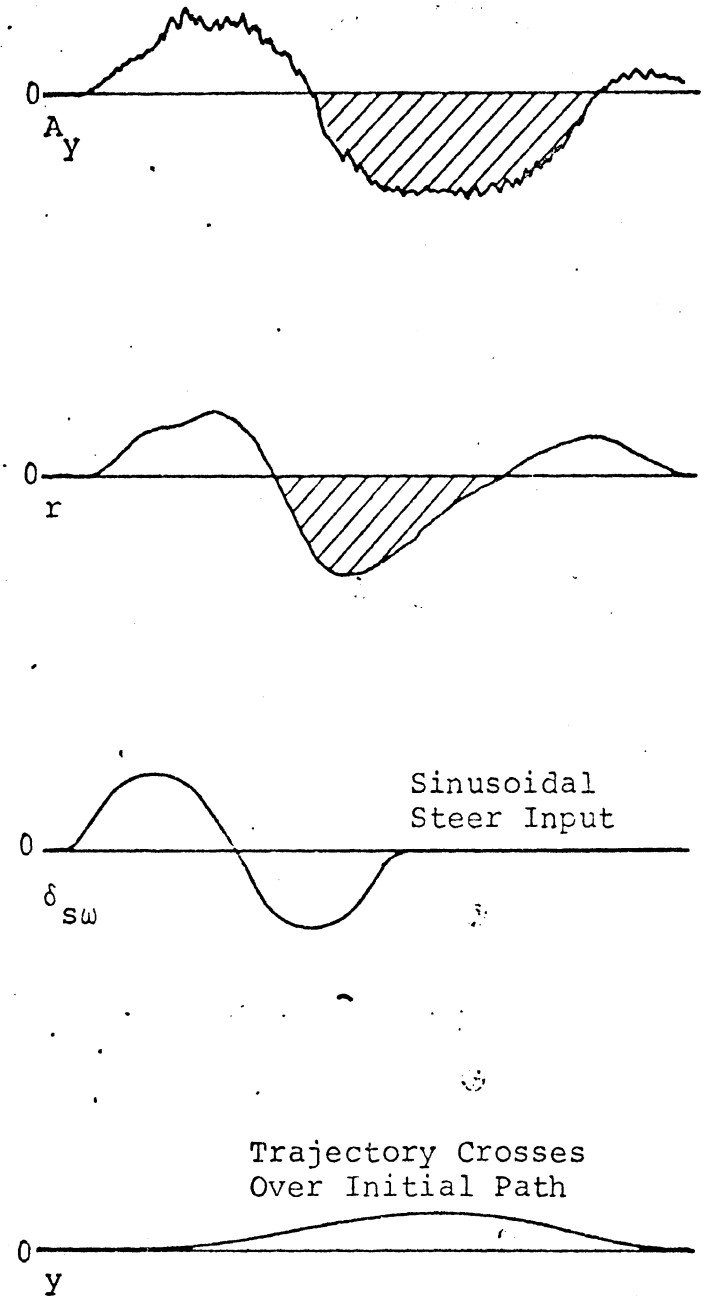

Figure 3-27. Sinusoidal steer over-corrective response.

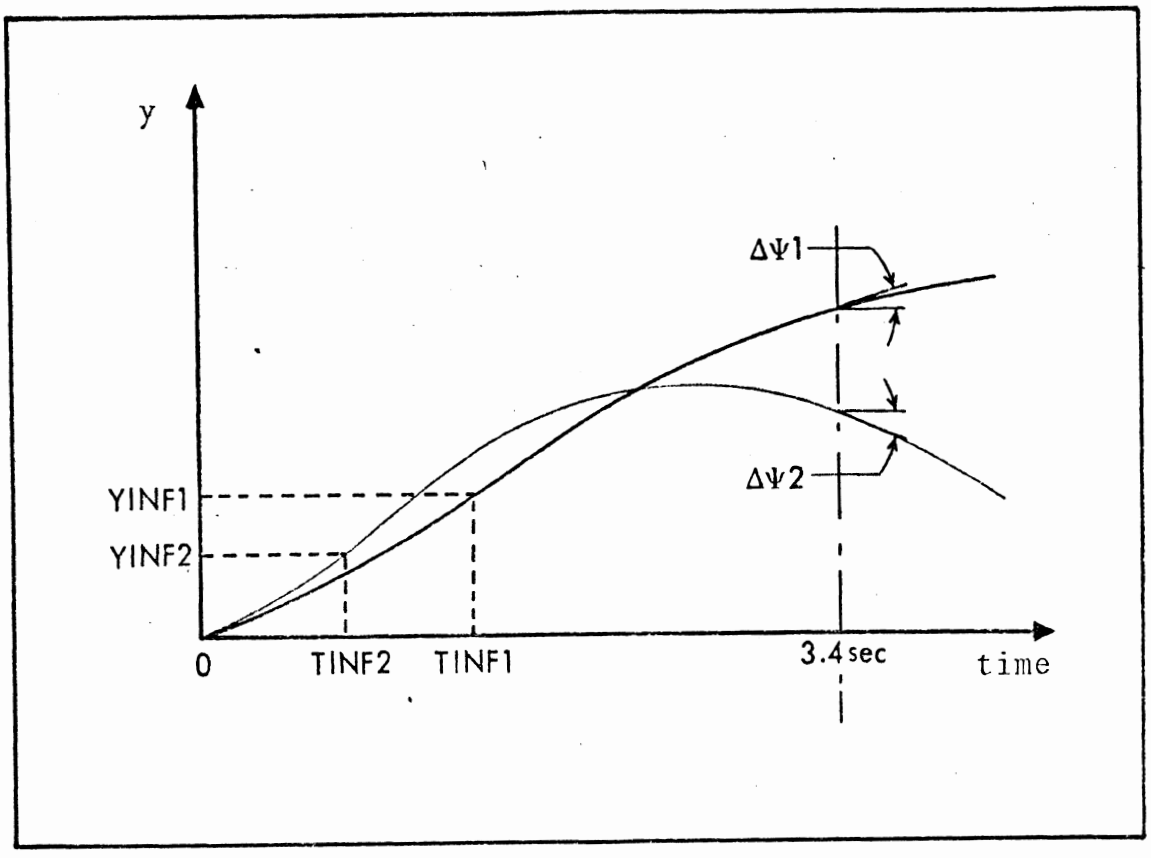

Figure 3-28. Under-corrective and over-corrective trajectories.

However, it will be shown below that low rear inflation pressure can lead to yaw oscillations lagging far behind the end of the steering input, resulting in the conclusion that the $\Delta\psi$ measure becomes a first-order function of the time defined as the end of the maneuver.

In view of these difficulties, it was deemed appropriate to add a new measure, the time at which the path curvature of the trajectory of the mass center changes sign. (This time is shown in Figure 3-28 as TINF.) In addition, a second metric, the lateral coordinate of the mass center at time TINF, is also of interest from an accident avoidance point of view. (This measure is shown in Figure 3-28 as the distance YINF.) It should be noted that, to a very close approximation, the sign change in the path curvature is indicated by a sign change in lateral acceleration. Thus the inflection time, TINF, can be measured using only routine test equipment.

In the following analysis of the measured data, we will make extensive use of β_p to give an indication of the controllability of the vehicle and to detect spinout response. The new metrics TINF and YINF will be used to quantify the time lags between the steer input and the vehicle response to that input, and the lane change deviation, Δ, and the final heading, $\Delta\psi$, will be used as an aid in understanding the net result of the maneuver.

To begin, consider Figures 3-29 through 3-31 in which metrics are presented which quantify the sinusoidal steer response of the Buick in the OE configuration (24 psi front, 28 psi rear, test configuration #35), the PSI1 configuration (20 psi front, 20 psi rear, test configuration #37), and the PSI2 configuration (24 psi front, 16 psi rear, test configuration #38). Note that in each of these figures the response to right and left polarity steering has been averaged, a reasonable simplification in view of the symmetric response of this vehicle under these test conditions. (Details relative to all of the test data are presented in Appendix F of this report.)

In Figure 3-29, the peak sideslip angles are plotted for each of the three test conditions. Clearly, the highest sideslip angles are associated with the OE condition, and the lowest sideslip angles are associated with the PSI2 condition. A similar trend is shown in Figure 3-30 for the final heading angle. This finding does not, however, indicate the PSI2 condition to be desirable, as will be shown below.

In Figure 3-31, the lane change deviation measure is plotted for each test condition. Note that while each configuration elicits a measure of approximately $\Delta = 5$ for a low steer angle, the extreme values listed for the PSI2 condition at high steer angles indicate a substantial departure from the OE condition. More insight into the nature of this change

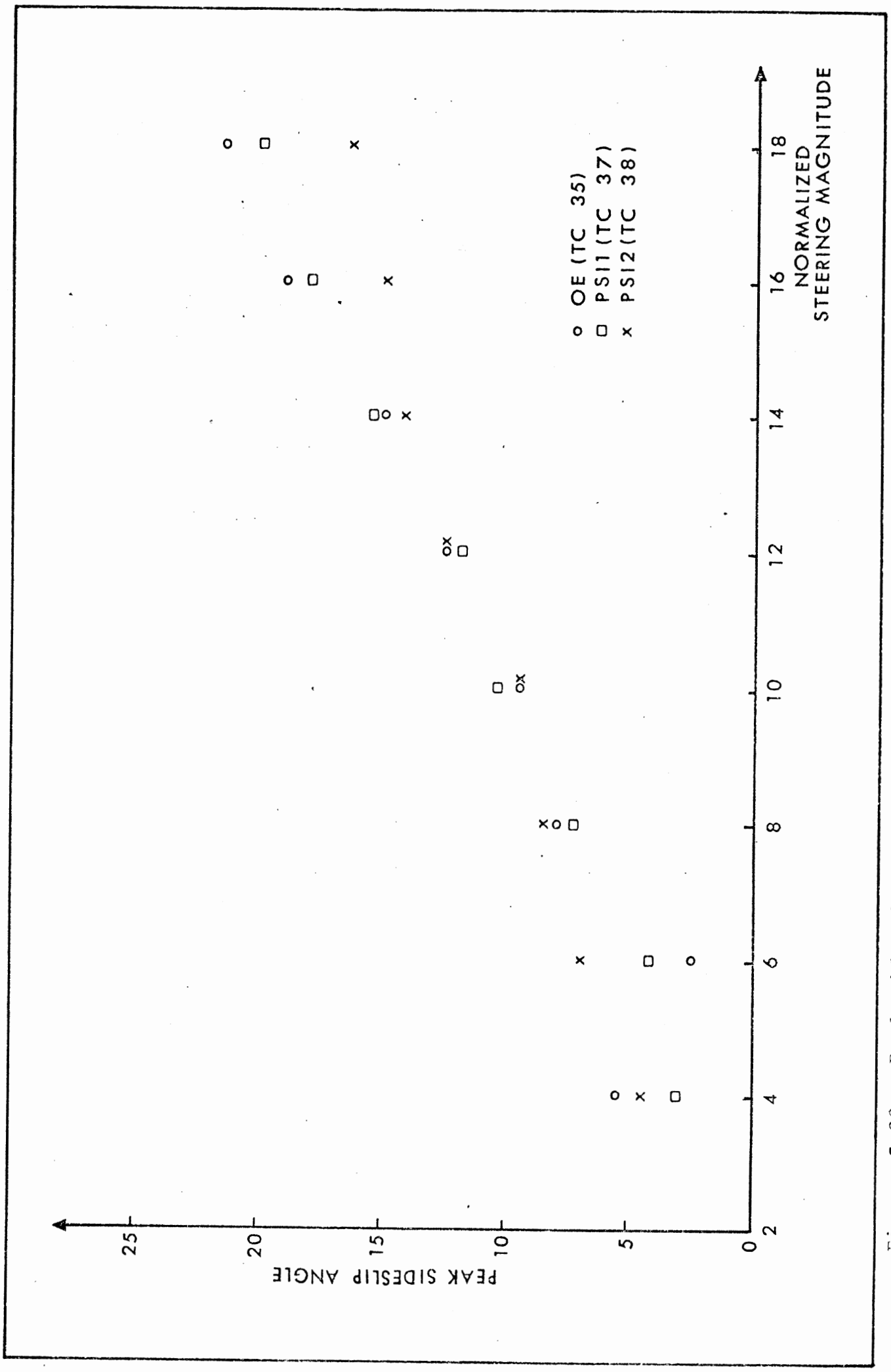

Figure 3-29. Peak sideslip angle vs. normalized steering magnitude, Buick, sinusoidal steer.

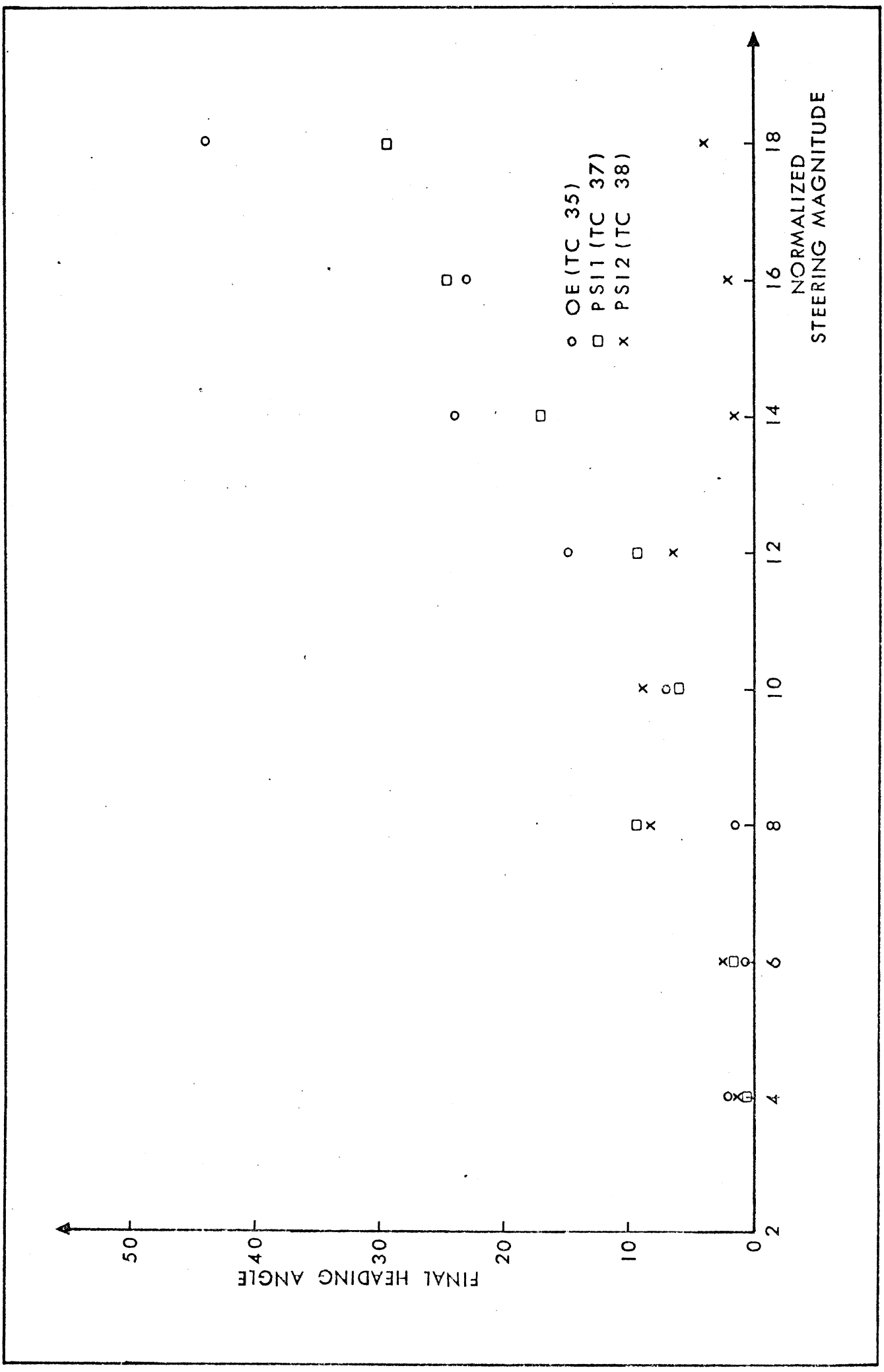

Figure 3-30. Final heading angle vs. normalized steering magnitude, Buick, sinusoidal steer.

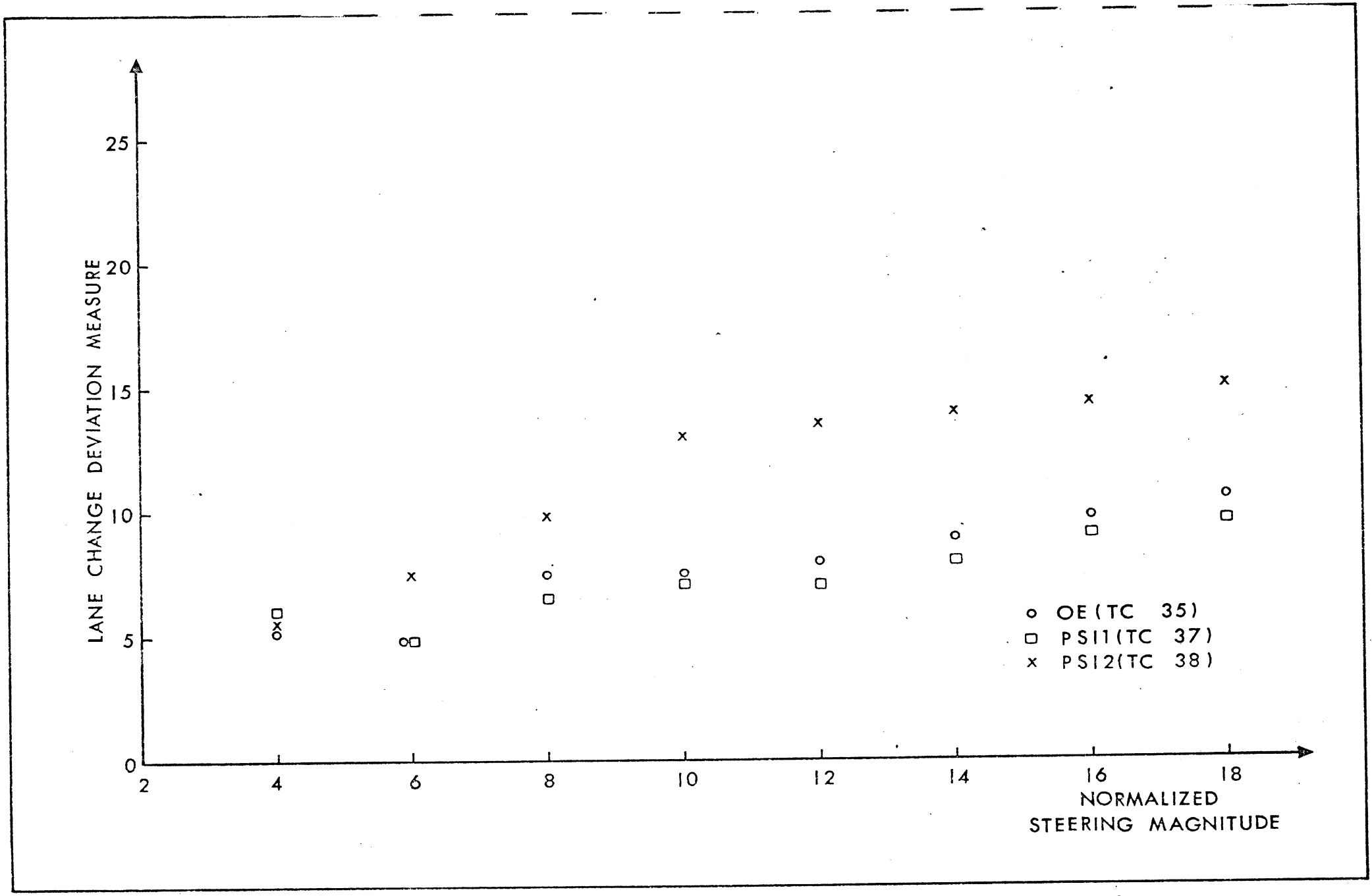

Figure 3-31. Lane change deviation vs. normalized steering magnitude, Buick, sinusoidal steer.

may be gained from Figures 3-32 and 3-33. For the higher steer levels, the increasing TINF values indicate that the PSI2 condition maintains the initial polarity of path curvature through almost the entire second half of the steer cycle. (The second half of the steer cycle starts at time t = 1 second and ends at t = 2 seconds.) It is evident from the YINF values (see Figure 3-33) that this behavior results in extreme lateral motions, far in excess of what might be expected from the OE vehicle.

These same trends have been observed for the loaded Buick. Consider Table 3-20 in which the numerics for the loaded Buick (26 psi front, 32 psi rear, test configuration #39) and the loaded Buick PSI condition (26 psi front, 20 psi rear, test configuration #40) are given. While the magnitude of the peak sideslip angles at all steer levels are somewhat higher in the loaded PSI case, the change deviations, Δ, and the final heading angles, $\Delta\psi$, indicate a serious trend toward under-corrections in the loaded PSI condition. Finally, the values of TINF and YINF indicate that the loaded PSI case is essentially out of control for even reasonably small steer amplitudes, showing lateral acceleration in the direction of the attempted lane change long after steering in either direction has stopped.

The data presented in Table 3-20 are illuminated by the plots of peak lateral acceleration obtained during the first and second half of the response to the steering input which are presented in Figures 3-34(a) and 3-34(b). Note that the acceleration levels resulting from the first half sine wave of steer are quite comparable for the loaded OE and the loaded PSI configurations. However, the values resulting from the second half steer exhibit satisfactory symmetry for the OE vehicle whereas a drastically reduced corrective response is obvious in the loaded PSI case.

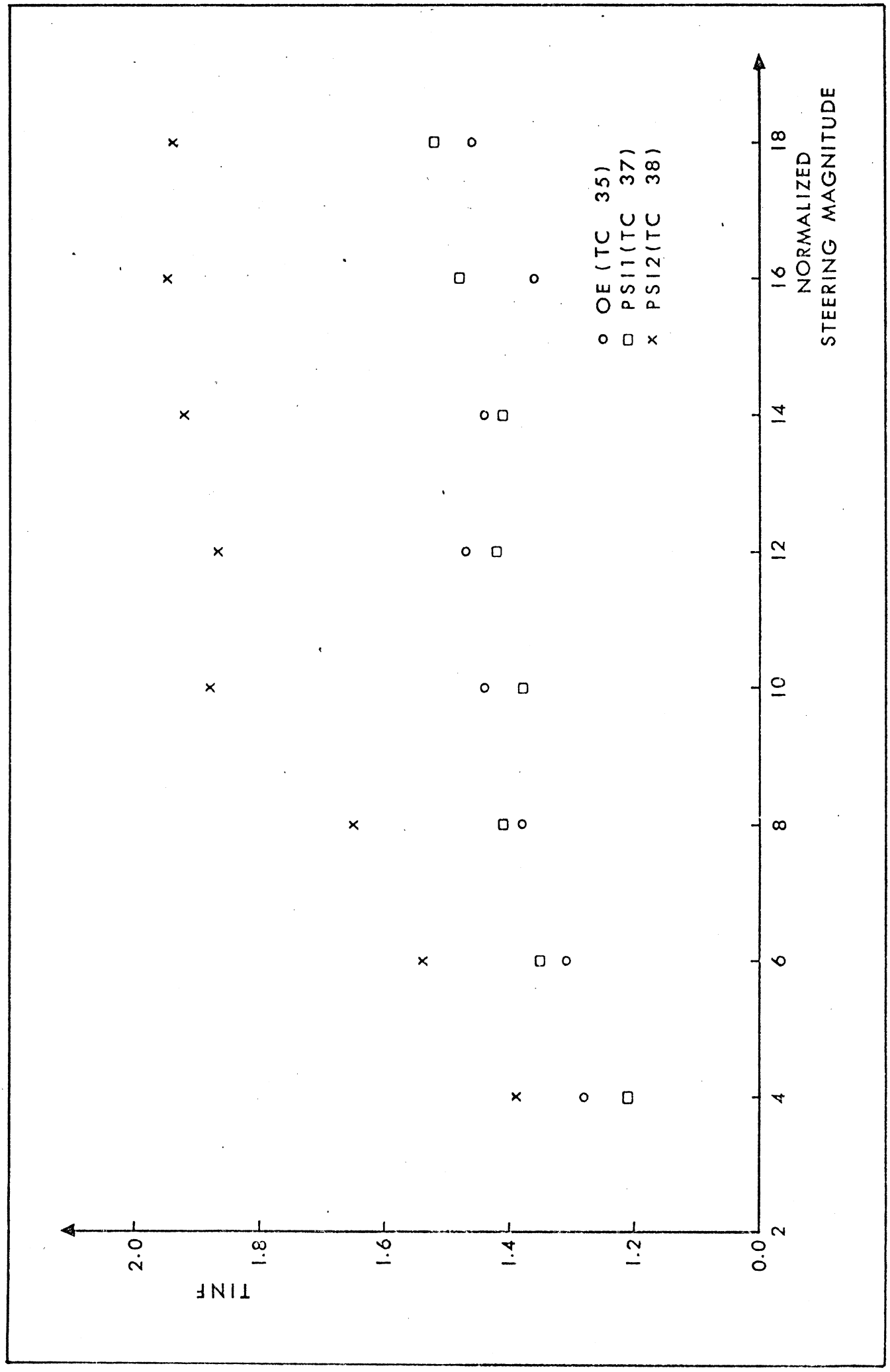

Figure 3-32. Inflection time vs. normalized steering magnitude, Buick, sinusoidal steer.

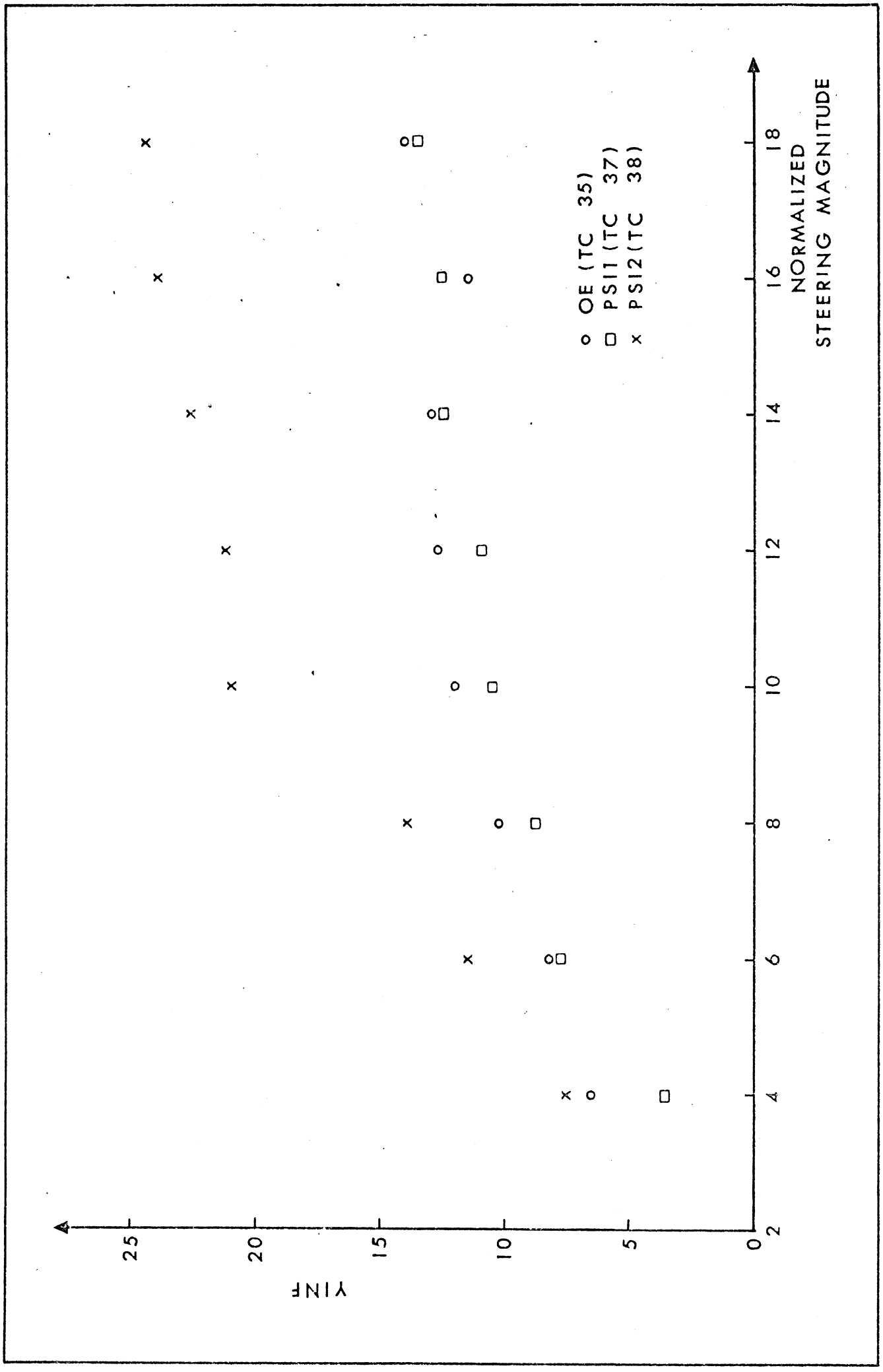

Figure 3-33. YINF vs. normalized steering magnitude, Buick, sinusoidal steer.

Table 3-20. Sinusoidal Steer Metrics for the Loaded Buick OE (TC #39) and Loaded Buick PSI (TC #40).

σ	δ_{sw}	TC#	TINF	YINF	BMAX	TBMX	PSIF	MSRE
	- 95.0	39	1.38	- 7.23	- 3.96	2.00	- 2.02	5.50
4	+ 95.0	39	1.29	4.80	- 3.31	0.94	- 0.70	6.90
	- 95.0	40	1.56	-10.26	4.07	1.11	- 6.03	7.80
	+ 95.0	40	1.34	5.25	- 4.12	0.96	- 4.37	6.12
	-140	39	1.49	-11.25	- 6.41	2.13	- 1.20	8.02
6	+140	39	1.43	9.63	5.50	2.10	- 1.84	6.67
	-140	40	2.05	-21.72	9.84	1.31	-19.06	13.37
	+140	40	1.61	11.64	- 6.98	1.14	- 4.80	8.14
	-175	39	1.53	-13.38	- 8.23	2.18	- 0.36	9.81
8	+175	39	1.53	11.91	- 7.17	1.14	- 2.29	8.23
	-175	40	2.82	-47.85	11.77	1.39	-30.16	17.54
	+175	40	2.06	24.39	-12.01	1.34	18.87	15.20
	-210	39	1.66	-17.07	- 9.67	2.30	- 0.25	12.21
10	+210	39	1.58	14.13	- 9.21	1.16	- 5.59	9.81
	-210	40	2.97	-57.93	15.16	1.46	-39.15	19.54
	+210	40	2.77	45.87	-15.15	1.24	27.72	9.87
	-240	39	1.78	-20.76	10.08	1.26	- 3.88	14.41
12	+240	39	1.63	14.34	-10.96	1.21	- 9.20	9.42
	-240	40	2.77	-51.72	15.37	1.41	-34.63	19.84
	+240	40	2.97	55.29	-17.87	1.46	41.04	18.60
	-280	39	1.76	-20.46	11.95	1.29	1.92	14.00
14	+280	39	1.68	17.49	-12.02	1.26	-19.12	11.84
	-280	40	2.97	-57.81	15.74	1.41	-36.78	7.48
	+280	40	2.67	46.77	-18.94	1.46	36.38	19.19
	-310	39	1.78	-22.14	-15.15	2.55	8.58	14.85
16	+310	39	1.66	16.41	-14.46	1.26	-30.68	11.13
	-310	40	2.67	-47.91	18.32	1.46	-33.39	16.56
	+310	40	2.97	56.43	-22.85	1.48	42.36	19.10
	-340	39	1.80	-22.80	15.09	1.34	7.75	15.26
18	+340	39	1.71	17.85	-15.43	1.29	-31.46	11.69
	-340	40	2.40	-39.24	18.24	1.44	-28.95	19.29
	+340	40	2.62	45.36	-20.97	1.46	34.70	34.70

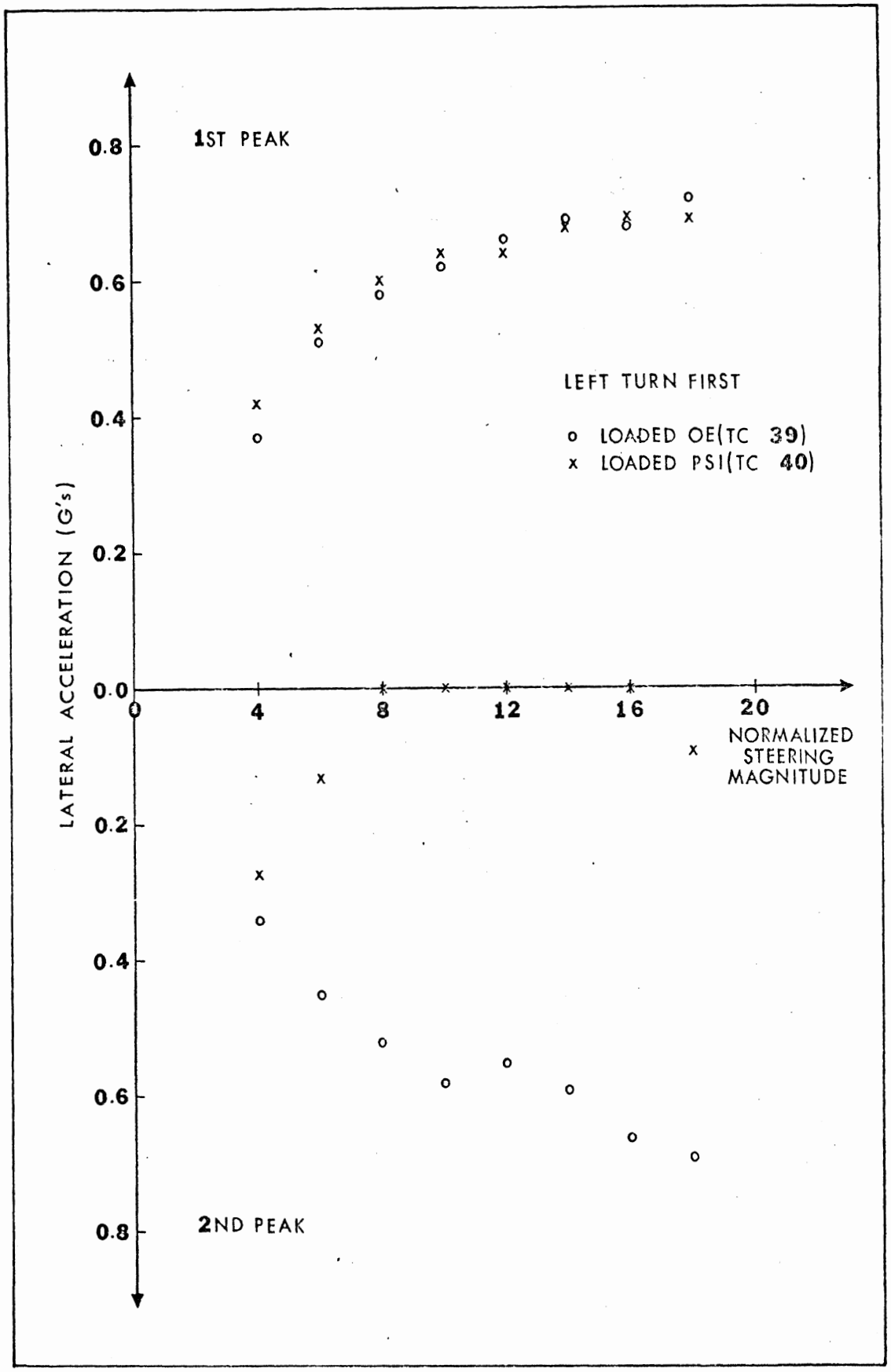

Figure 34(a). Peak lateral acceleration vs. normalized steering magnitude for the first and second half steer cycles, Buick, left polarity.

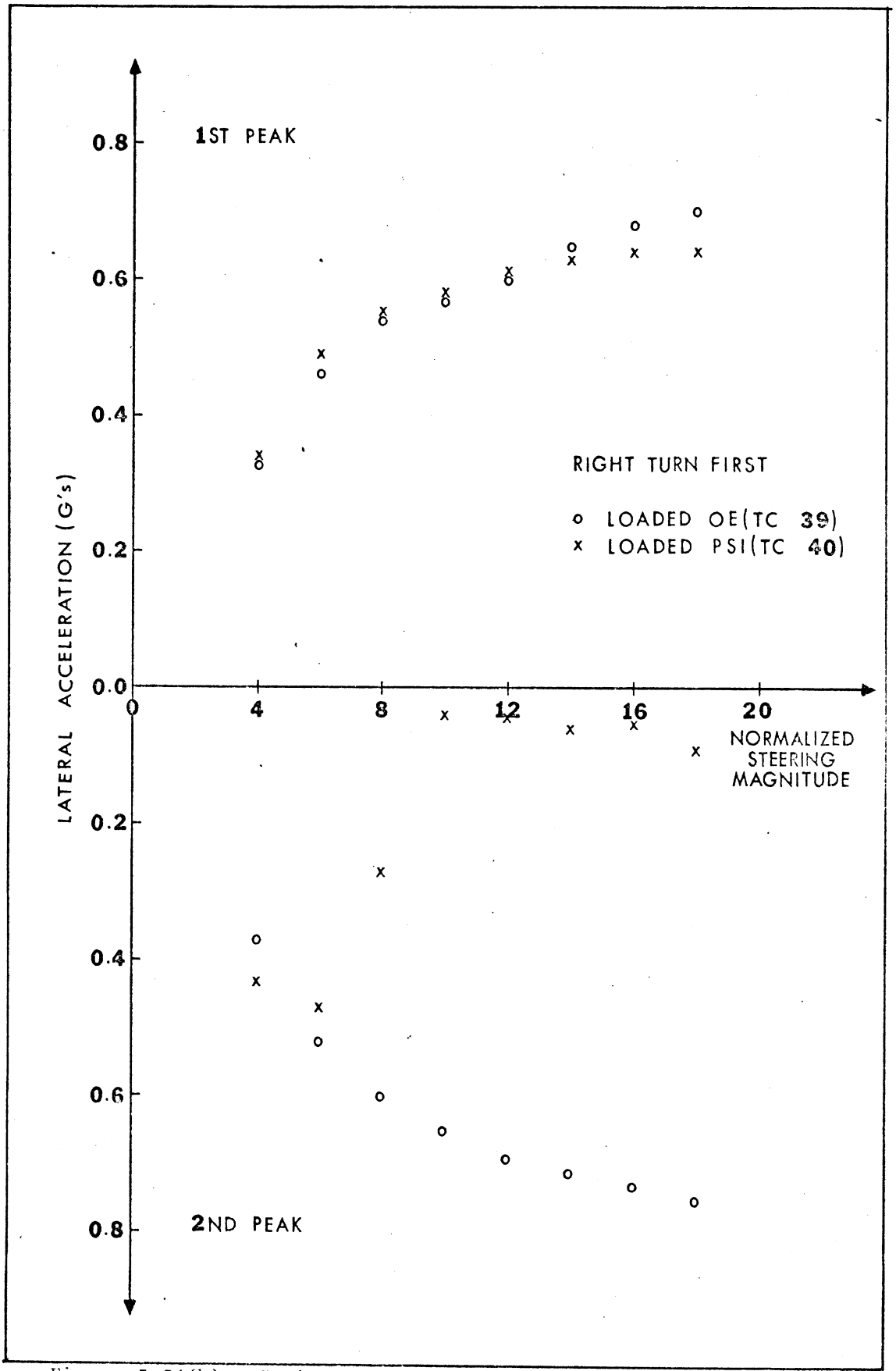

Figure 3-34(b). Peak lateral acceleration vs. normalized steering magnitude for the first and second half steer cycles, Buick, right polarity.

Finally, it will be instructive to examine certain time histories of the lane change maneuver for the loaded OE and loaded PSI configurations. In particular, in Figure 3-35, the measured steer angle, lateral acceleration, and sideslip angle are plotted versus time for a steer amplitude of $\sigma = 8$. This figure clearly contrasts the smooth initial and corrective response of the loaded OE vehicle with the extreme under-corrective response of the loaded PSI configuration.

The above results lead to the conclusion that the Buick PSI2 and the loaded PSI configurations do not perform well in the sinusoidal steer maneuver. To gain a comprehensive understanding of this performance, it has been necessary to examine in some detail all the traditional metrics and the newly introduced inflection time and lateral displacement, TINF and YINF, respectively. However, ample evidence of the nature of the lane change performance is provided by examining the peak lateral accelerations and TINF.

3.2.4.6 Drastic Steer/Brake. The objective of this maneuver is to impose the maximum challenge to the vehicle's roll stability that can be derived solely from tire-road shear forces and thereby obtain a binary characterization of roll potential under the defined conditions. A half sine wave of steering is applied, with no braking, with the vehicle coasting at an initial velocity of either 50 or 60 mph. A perusal of the response data from that run is made and the time is determined at which yaw rate attains 95% of its maximum value. Next, a run is made with the same velocity and steer input, but a brake input is initiated (such that all wheels lock) at the time at which 95% of the peak yaw rate is attained, with braking maintained for two seconds. In this second run, the free transient roll response is examined, such that the precise time for brake release in the following run can be determined.

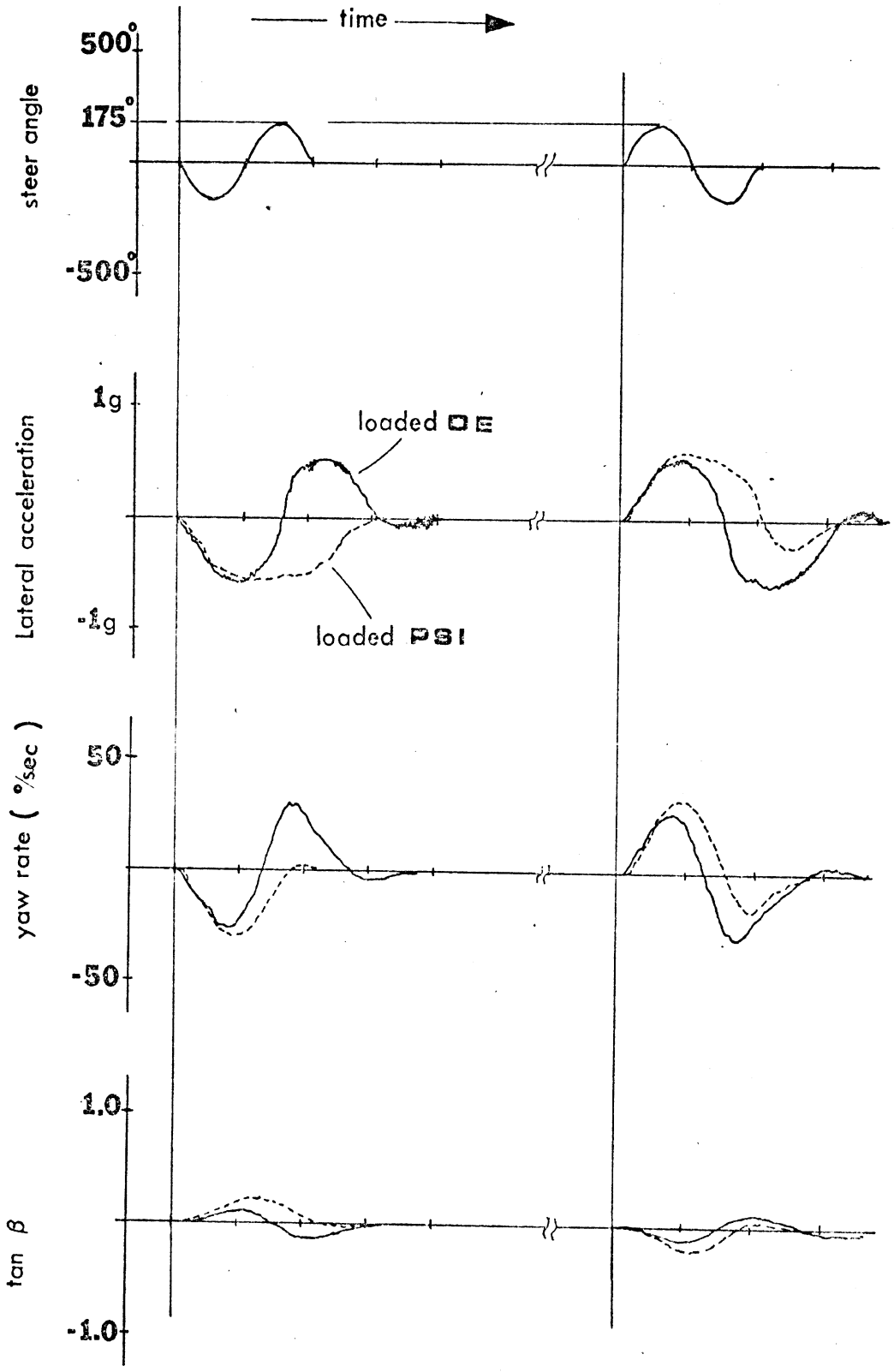

Figure 3-35. Time history of a lane change maneuver for the Buick.

In the next run, the brake release time is set to coincide with the peak in roll rate response of the proper polarity to contribute to the roll-over process.

The steering input, lasting for one second, provides sufficiently large yaw moments to cause the vehicle to achieve a significant angular momentum in yaw by the time wheels are unlocked (somewhere between 0.5 and 0.75 seconds). When all wheels attain 100% slip, the vehicle exhibits negligible directional sensitivity, and it slews in yaw, accumulating body sideslip at nearly constant rate. The sprung mass, of course, has responded to the initial roll moment by rolling clockwise, say, for a counterclockwise steering input. Since wheel lockup results in a loss in tire side force, the roll moment drops to near zero with brake application, and the sprung mass rebounds counterclockwise in roll. Being an undamped mode of response, the sprung mass overshoots in roll and rebounds again, now rolling clockwise. Upon release of the brake, the wheel spin up to their freely rolling spin velocity under a condition of high slip angle at all four tires (between 10° and 30°, generally). The step-like quality of the side force buildup which follows is crucial to the determination of roll overshoot, because of the requirement to provide maximum net roll moment while the sprung mass is passing through zero roll angle, with peak roll rate.

On most passenger vehicles, sufficient roll energy is accumulated to carry the roll motion into the region of bump stop contact, at which time the roll moment can be further increased as the roll momentum of the sprung mass is reacted with an impulse that immediately increases the vertical tire load on the outside wheels. At this time, the summation of vertical loads will be greater than the vehicle static weight and a commensurate increase in side force is realized. If the total overturning moment in roll at this juncture exceeds

the gravity moment, the vehicle will lift its inside wheels; if not, the vehicle will not roll over in this maneuver.

Vehicle performance would be judged as being degraded in comparison with a non-roll-over baseline performance, if it exhibited roll-over in response to the indicated steer and brake inputs.

In the present investigation, the drastic steer and brake procedure was run for the Mustang in the OE and the PSI conditions. While slightly higher peak roll angles were attained in the PSI condition (8.5° versus 8° in the OE configuration), these configurations exhibited, by and large, remarkable similarity in their measured responses. These data are presented in detail in Appendix F.

3.2.5 SUMMARY. Drastic changes in the mechanical properties of tires occur as a result of inflation pressure deviations which have been shown to occur rather routinely in the vehicle population. These changes are particularly marked in the low and mid range of slip angles, causing decreasing lateral force with decreasing inflation pressure and increasing load.

Inflation pressure deviations had a marked effect on the response of the Buick and Mustang in the sinusoidal and trapezoidal steer maneuvers. In particular, it was shown that significant and potentially dangerous deviations from OE performance can derive from inflation pressure on the rear tires being lowered below the level recommended by the manufacturer, while leaving the front tires inflated to the pressure recommended by the vehicle manufacturer.

3.3 IN-USE TIRE MIXTURES

The consequences of mixing tires of dissimilar construction on passenger-car handling performance have recently been receiving some attention with regard to both the normal driving range [7] and limit performance [4]. For example, data presented in Reference 7 indicate that first-order changes in the understeer/oversteer of a "typical compact sedan" may result from replacing the original equipment bias-belted tires on the front wheels with radial tires, with the OE bias-belted tires remaining on the rear wheels. As is pointed out in [4] and [7], however, the radial tires which were the basis for these changes were "representative of one end of the spectrum of radial tires presently marketed." Further, "cornering stiffness and aligning torque stiffness effects (of radial tires) can be quite variable." The key issue is the comparison between such mechanical properties as cornering stiffness, aligning stiffness, and camber stiffness of the radial and non-radial tire.

Similar statements may be made regarding limit maneuvers. For example, it was shown in Reference 4 that the peak side-slip angles measured in trapezoidal steer tests were substantially increased through the use of bias-belted tires on the front wheels and bias tires on the rear wheels. Again, the point was not that all bias-belted/bias tire mixes would cause this change in performance. Rather, the mechanical properties of the front and rear tires—and here we must include the peak force levels as well as the stiffness properties—were significantly disparate, and thus serious departures from the OE performance resulted.

A precise definition of tire intermix has been given in [7]: "Tire intermix is a term which describes the practice of applying tires to a vehicle that are not identical in generic type, brand, aspect ratio, size, or wear state." It

is clearly impossible to consider all possibilities for tire intermix, even when our permutations are limited to tires routinely available for the test Buick and Mustang. Rather, we have chosen certain discrete tire combinations, as listed in Table 3-21, to illustrate the various changes in performance that result from mixing tires. Initially considered here are changes in performance that result from the use of stiff radial tires in front, with OE tires remaining on the rear wheels.

Table 3-21. Tire Combinations Used in Testing and/or Simulation.

Buick: OE, Firestone Deluxe Champion Sup-R-Belt H78-14

OE - Bridgestone 225SR-14 (steel-belted radial)

OE - Firestone 500 H78-14 (bias)

OE - Firestone Town & Country H78-14 (bias, snow)

Mustang: OE, Goodrich Silvertown Belted E78-14

OE - Pirelli 185-14 (radial)

OE - Goodyear Custom Power Cushion Polyglas Belted E78-14

In Figures 3-36 and 3-37, longitudinal force* data are compared for the Bridgestone 225R-14 and the OE Firestone Deluxe Champion Sup-R-Belt H78-14 used on the Buick. Similar data are presented in Figures 3-38 and 3-39 for the Pirelli 185R-14 and the OE B.F. Goodrich Silvertown Belted E78-14 used on the Mustang. Clearly, the longitudinal force data are similar for both sets of tires. Thus it is not surprising that very little change in braking performance was measured for

*Note that the Bridgestone was inflated to the manufacturer's recommended front inflation pressure, 24 psi, for the vehicle testing. The Bridgestone data shown in Figures 3-36 and 3-37 were obtained at 28 psi, as were all of the non-OE mobile tire data for H78-14 tires.

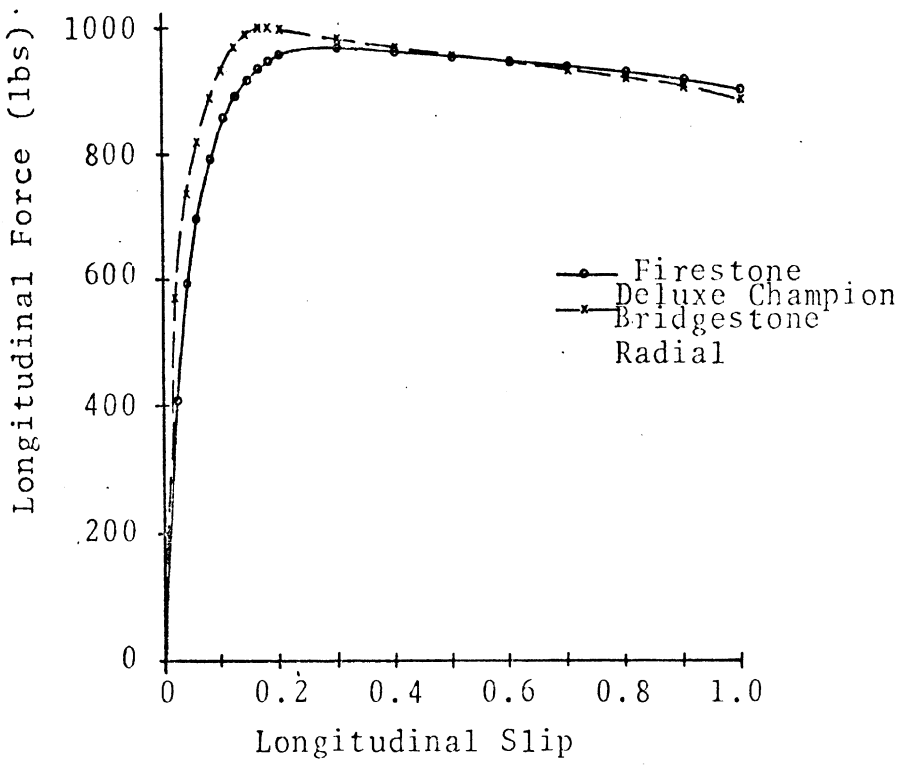

Figure 3-36. Longitudinal force vs. slip, 1100 lbs. load, dry asphalt, 40 mph, 28 psi.

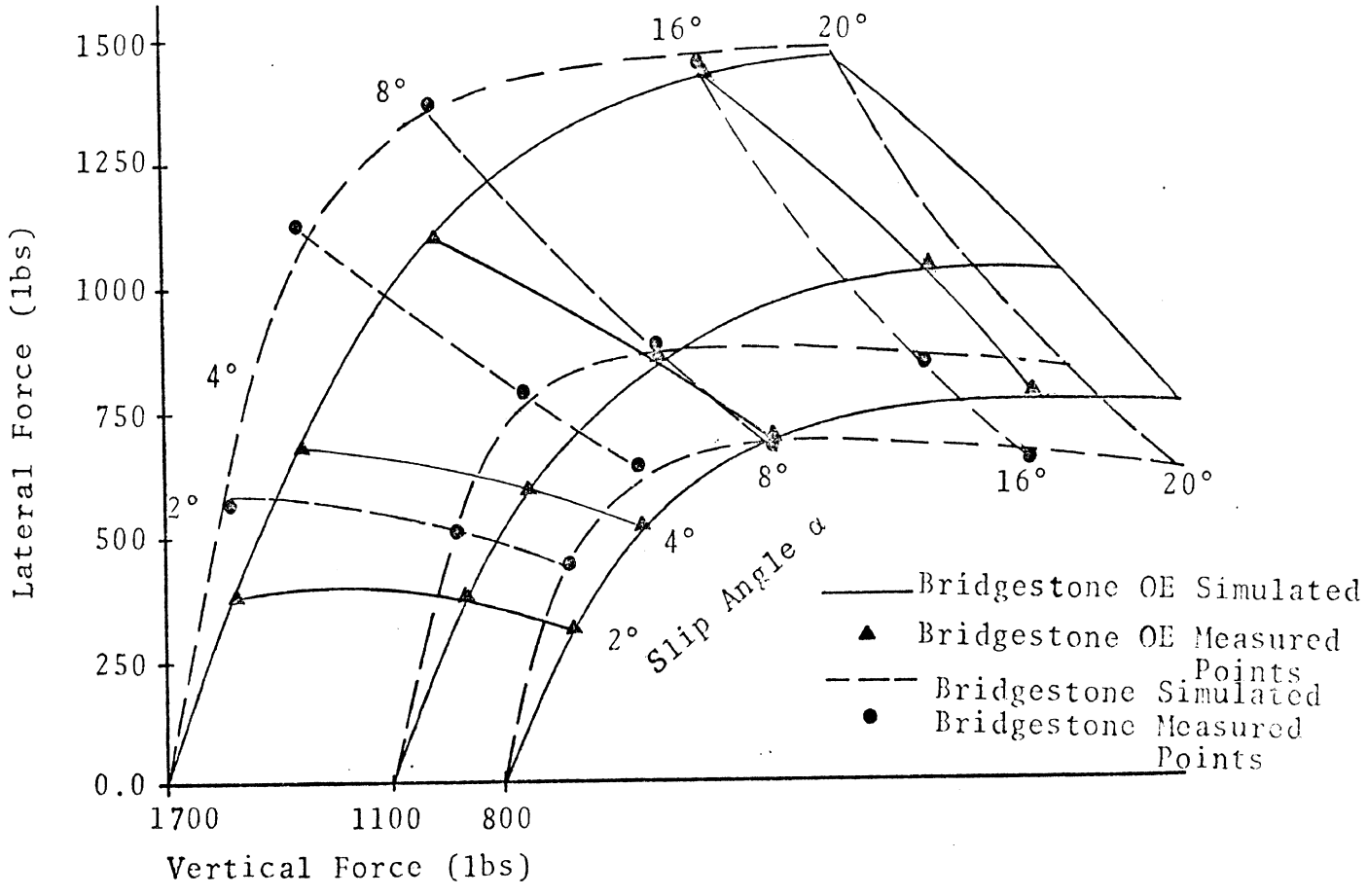

Figure 3-37. Lateral force vs. slip angle and load, dry asphalt, 40 mph, 28 psi.

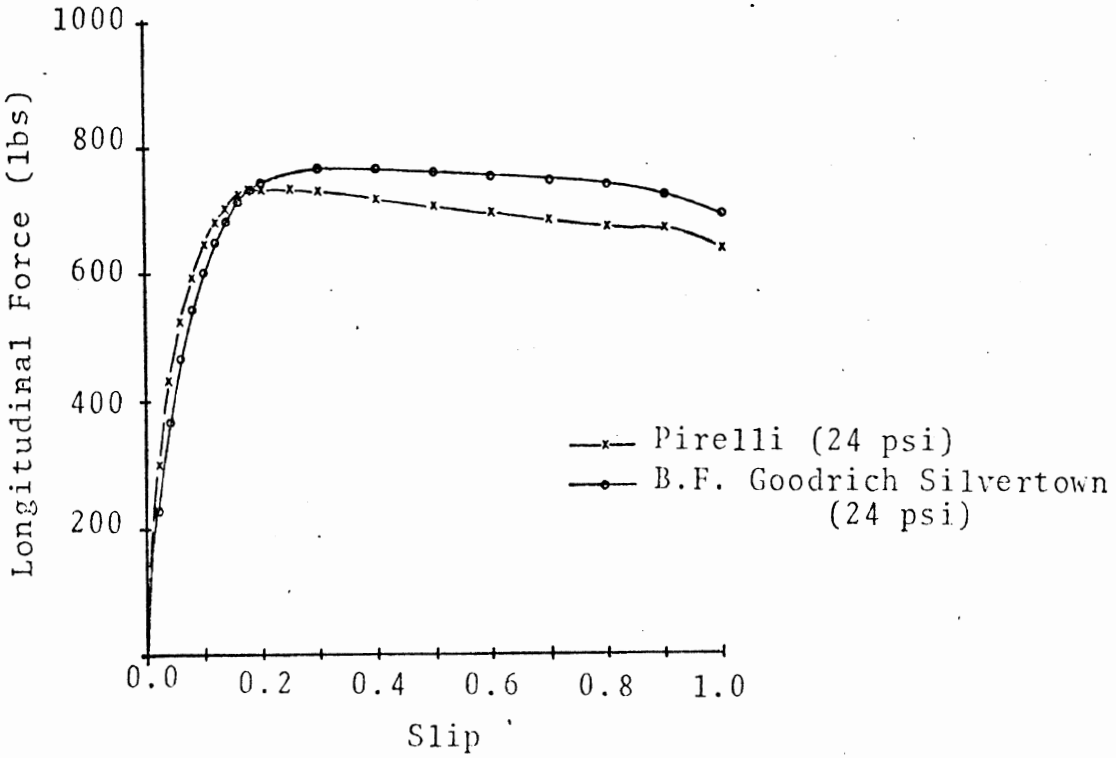

Figure 3-38. Longitudinal force vs. slip, 800 lbs. load, dry asphalt, 40 mph, 24 psi.

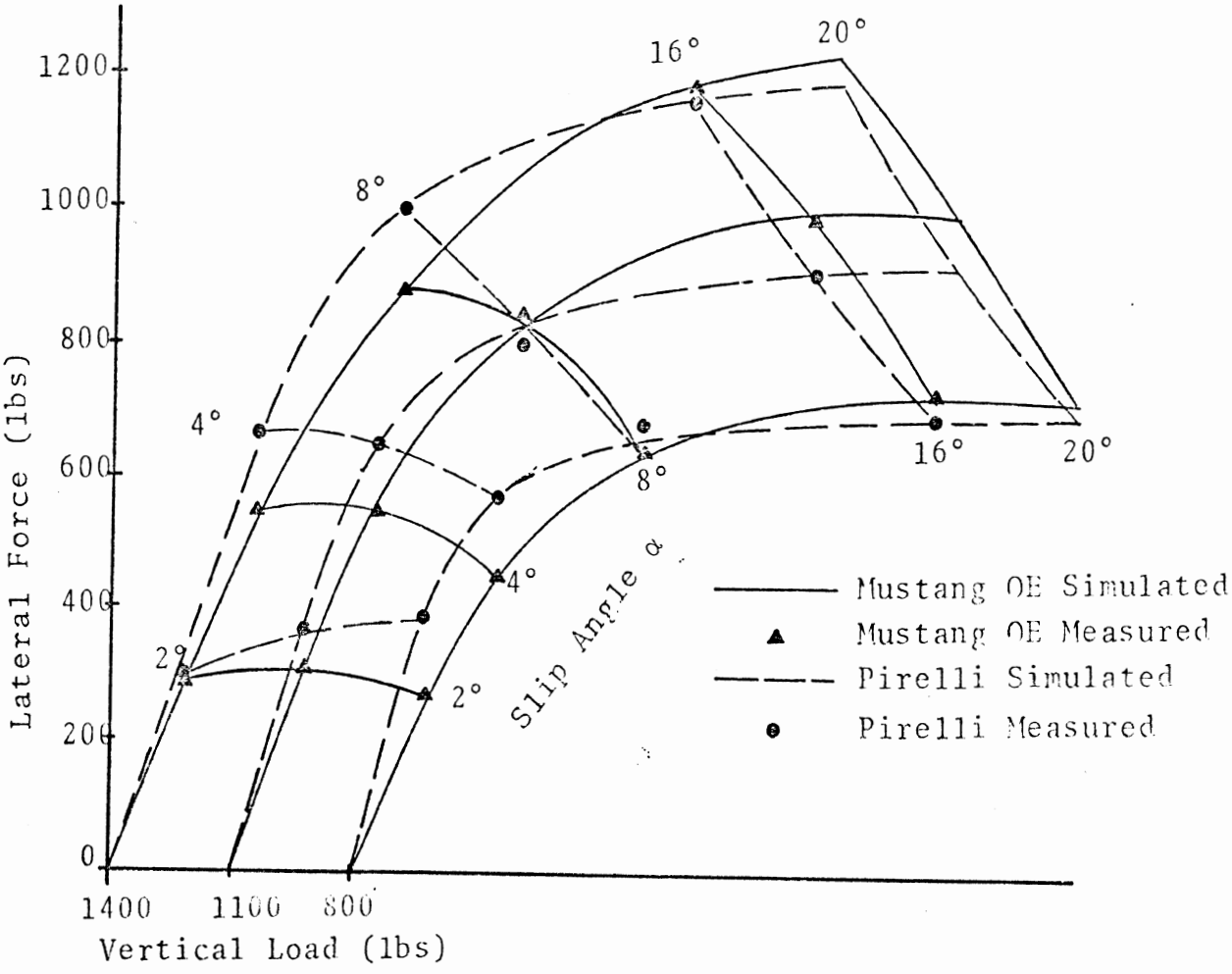

Figure 3-39. Lateral force vs. slip angle and load, dry asphalt, 40 mph, 24 psi.

either vehicle when the OE tires on the front wheels were replaced by a corresponding stiff radial tire. (A summary of these measurements is presented in Appendix F.) Note also that both vehicles locked rear tires first on dry pavement, a fact that further attenuated changes accruing from radial tires mounted in front.)

As one might expect from an examination of Figures 3-37 and 3-39, the replacement of an OE tire should lead to significant departures from OE performance when the sinusoidal-steer and trapezoidal-steer test procedures are conducted producing a maneuver in which the tires routinely operate in the mid-slip-angle range. Consider, for example, Table 3-22, in which a list of the sinusoidal steer metrics for the Buick with the Bridgestone tires mounted in front (test configuration #42) is compared to the metrics for the OE configuration (test configuration #35). The extreme values of TINF, YINF,* and Δ at low steer amplitudes indicate the handling problems of the test configuration with the Bridgestone and OE tires.

Note also that the response of this same test configuration was quite asymmetric. The measured asymmetry is, of course, of some import, because it prevents the clear characterization of the lane-change procedure by simple metrics. Thus we concur with the suggestion in Reference 4 that this phenomenon is an appropriate matter for further research.**

Computer simulation was used as a tool to aid in understanding the response of the Buick with this tire configuration. While the computed results did not, of course, predict the measured asymmetries, the computations did further quantify the effects to be expected due to the use of such a stiff

---

*The metrics TINF and YINF are discussed in detail in Section 3.2.

**An attempt was made to gain insight into this asymmetry by repeating the Bridgestone-OE runs with the Bridgestone tires switched from side to side. Details of these measurements are presented in Appendix E.

Table 3-22. Buick: Sinusoidal Steer Metrics

σ	δ_{sw}	TC#	TINF	YINF	BMAX	TBMX	PSIF	MSRE
	-95°	35	1.28	- 6.63	- 5.56	2.27	- 2.18	5.47
4	-95°	42	1.61	-12.93	- 4.53	1.95	- 8.54	10.45
	+95°	42	1.34	9.00	3.51	2.10	-10.09	5.53
	+140°	35	1.31	8.07	- 3.11	0.96	- 0.03	4.97
6	-140°	42	2.03	-21.93	- 7.46	2.14	-16.69	14.95
	-175°	35	1.38	-10.23	- 8.19	2.0	1.63	7.58
8	-175°	42	2.03	-28.29	9.04	1.29	-21.58	18.02
	+175°	42	1.57	16.20	-10.99	1.22	-25.56	11.63
	-210°	35	1.51	-13.17	-11.24	2.27	4.90	7.61
10	+210°	35	1.38	10.95	7.86	2.27	- 9.25	7.06
	-210°	42	1.72	-20.88	11.56	1.34	-22.19	17.51
	+210°	42	1.66	19.63	14.96	2.94	-34.98	13.38
	-240°	35	1.56	-13.89	-13.92	2.35	10.64	8.63
12	+240°	35	1.38	11.85	10.57	2.37	-19.26	7.56
	-240°	42	1.81	-22.53	13.50	1.38	-24.85	18.09
	+240°	42	1.75	23.97	15.41	3.01	-27.66	17.68
	-280°	35	1.33	-11.22	-17.52	2.50	18.78	9.69
14	+280°	35	1.51	14.10	13.99	2.60	-29.60	8.51
	-280°	42	1.61	-18.15	11.75	1.35	- 6.78	16.79
	+280°	42	1.70	20.40	34.46	4.08	-61.37	14.11
	-310°	35	1.36	-11.55	-19.01	2.55	23.24	9.72
16	-310°	42	1.66	-19.95	-12.55	2.42	3.89	15.73
	+310°	42	1.61	19.77	45.00	3.73	-75.64	14.62
	-340°	35	1.41	-12.99	-27.12	2.92	45.75	11.09
18	+340°	35	1.51	14.97	25.63	3.53	-44.06	10.39
	-340°	42	1.60	-18.87	-20.44	2.80	29.02	15.0
	+340°	42	1.71	22.89	45.02	3.46	-88.44	14.67

TC #35 refers to the OE Buick, lowest steer level run first.

TC #42 refers to the original set of Bridgestone front-OE rear tests.

radial tire on the front wheels. Note, however, that in all the computed results presented in this section the input tire data were obtained at 28 psi, not 24 psi (as is recommended by the manufacturer for the front tires of the Buick).

In Figures 3-40(a) and 3-40(b), simulated time histories of yaw rate and sideslip angle are presented for the Buick in a high-level sinusoidal steer maneuver. Three tire configurations are compared, namely, Bridgestone-front/OE rear, Bridgestone front and rear, and OE front and rear. Clearly, the Bridgestone-front/OE-rear configuration yields a spin-out response, while the OE configuration and the vehicle with all four Bridgestone tires do not.

It can be demonstrated that even one very stiff front tire can yield marked changes in performance. This is shown in Figures 3-41(a) to 3-41(c), in which results for the OE configuration are compared to results computed with (1) the Bridgestone tire on the right front, the OE on the left front; (2) the Bridgestone tire on the left front, the OE tire on the right front; and (3) Bridgestone tires on both front wheels. These runs clearly indicate that the lane-change results for combinations (1) and (2) should be expected to be asymmetric, and may deviate markedly from OE performance.

Similar trends may be observed in the measured and computed responses to a trapezoidal steer input. Consider, for example, Figures 3-42 and 3-43, in which measured values of peak lateral acceleration for each OE vehicle are compared to the corresponding values measured with stiff radial tires replacing the OE front tires. The obvious disparity in lateral acceleration at low steer angles is a clear result of the increased cornering stiffness of the radial tires over the OE tires. The results at high steer angles are quite similar, a finding quite in accord with the tire test data which indicated similar peak levels of lateral shear forces (see Figures 3-37 and 3-39).

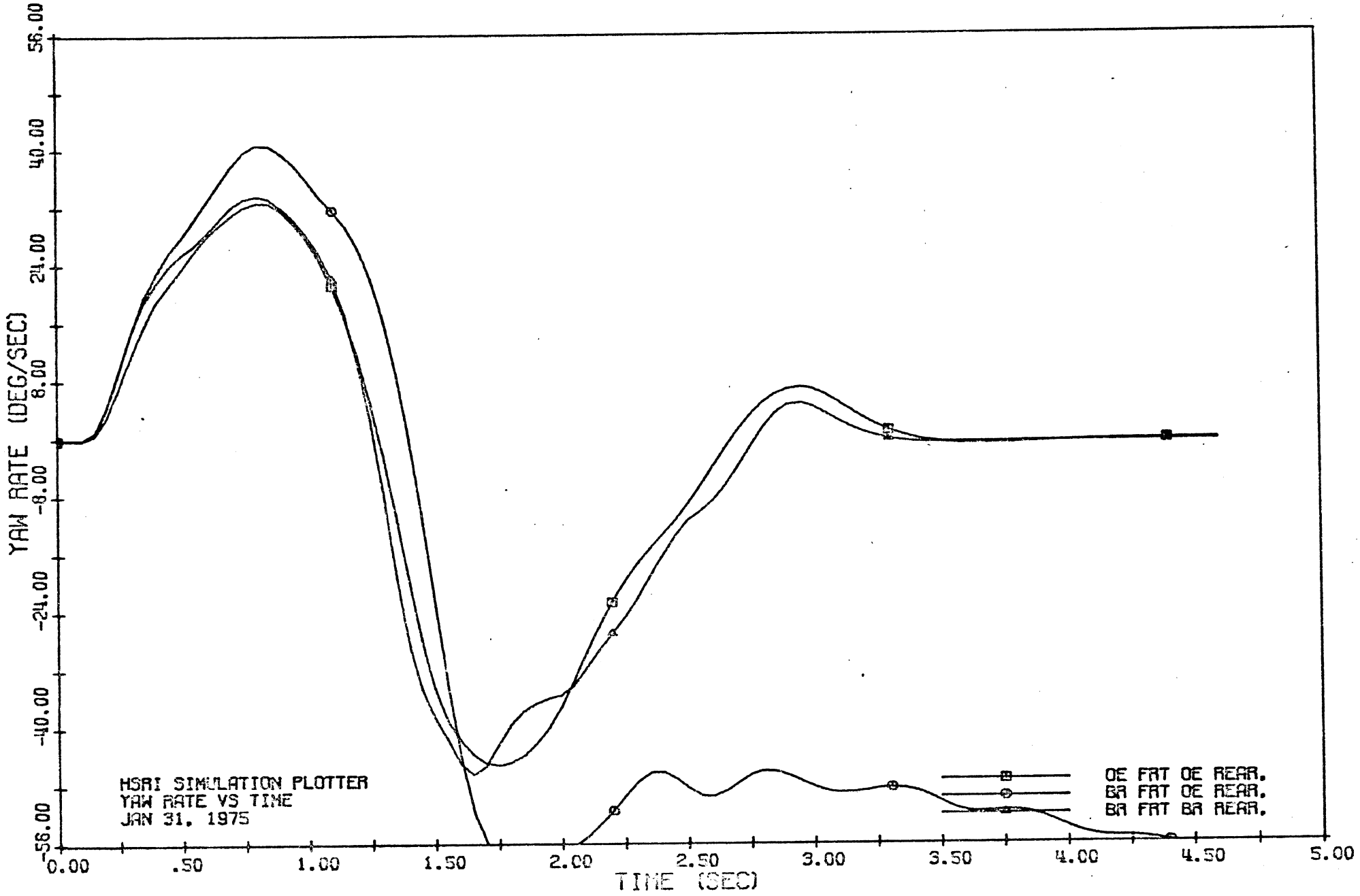

Figure 3-40(a). BUICK WAGON: 360. DEG SINE. TIRE MIX RUNS

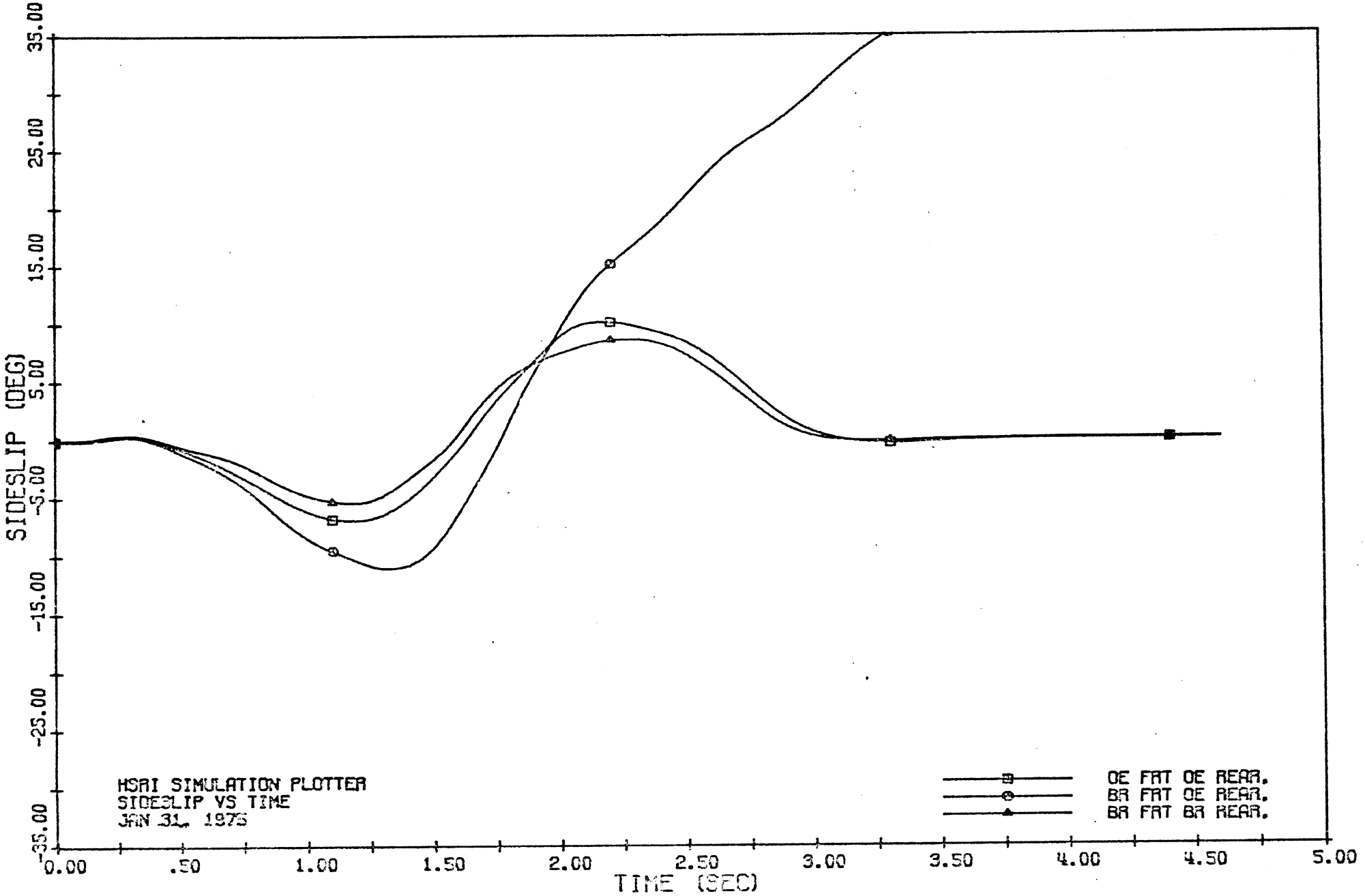

Figure 3-40(b). BUICK WAGON: 340. DEG SINE. TIRE MIX RUNS

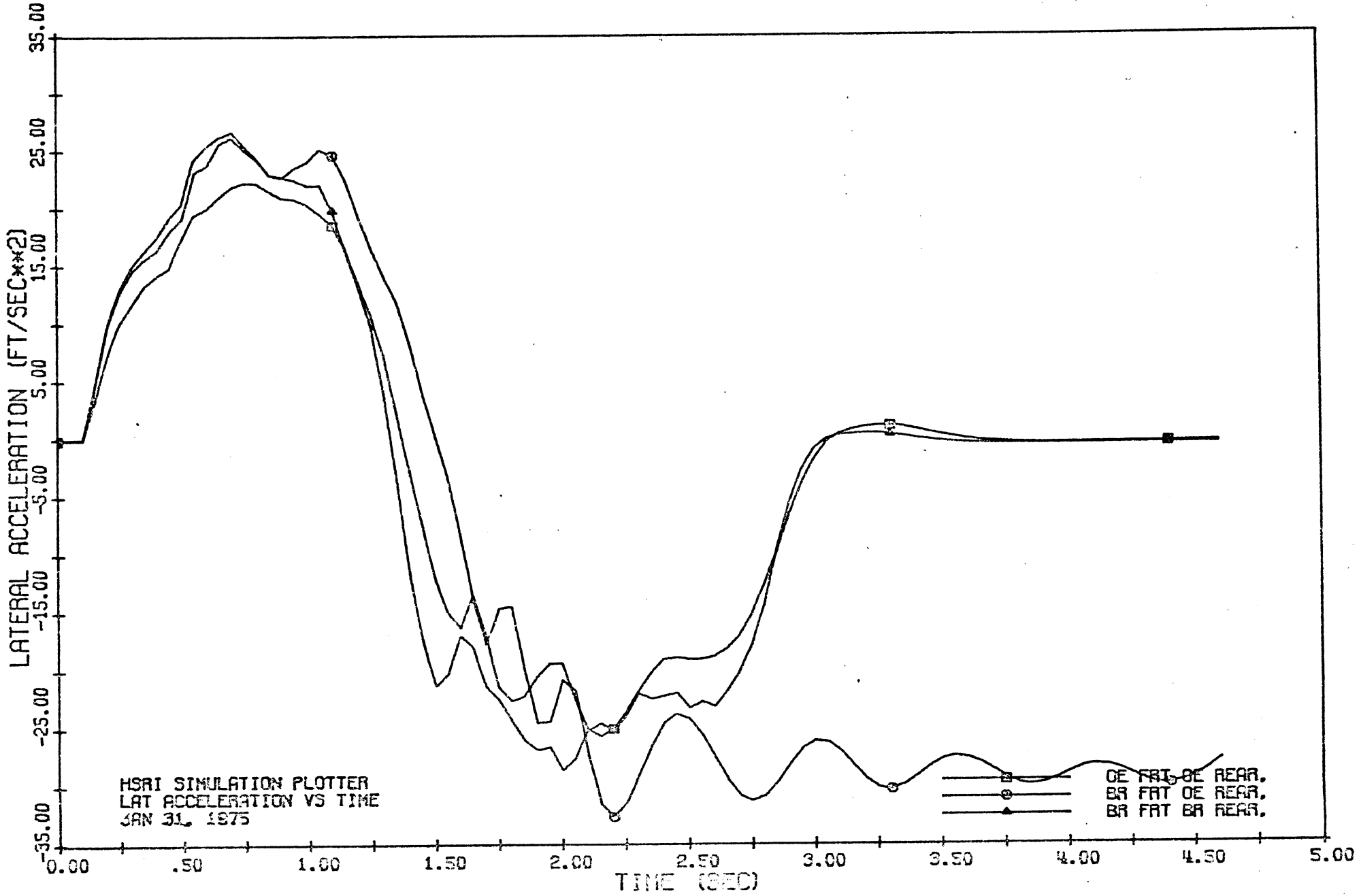

Figure 3-40(c). BUICK WAGON: 3.0. DEG SINE, TIRE MIX RUNS

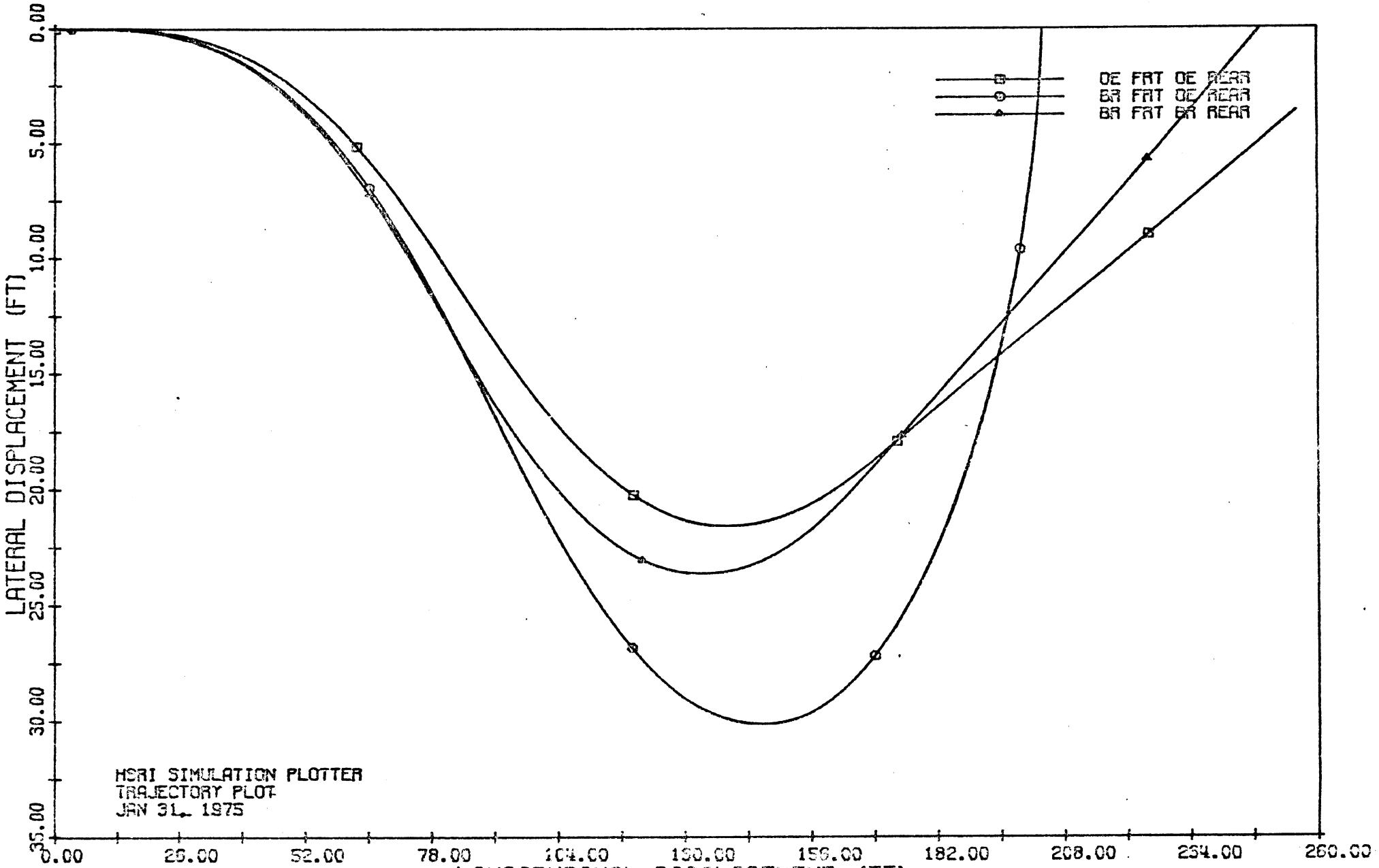
0.00
5.00
10.00
15.00
20.00
25.00
30.00
35.00
LATERAL DISPLACEMENT (FT)
0.00
26.00
52.00
78.00
104.00
130.00
156.00
182.00
208.00
234.00
260.00
LONGITUDINAL DISPLACEMENT (FT)
DE FRT DE REAR
BR FRT DE REAR
BR FRT BR REAR
HSRI SIMULATION PLOTTER
TRAJECTORY PLOT
JAN 31, 1975
BUICK HARDTOP: 340. DEG SINE, TIRE MIX RUNS

Figure 3-40 (d).

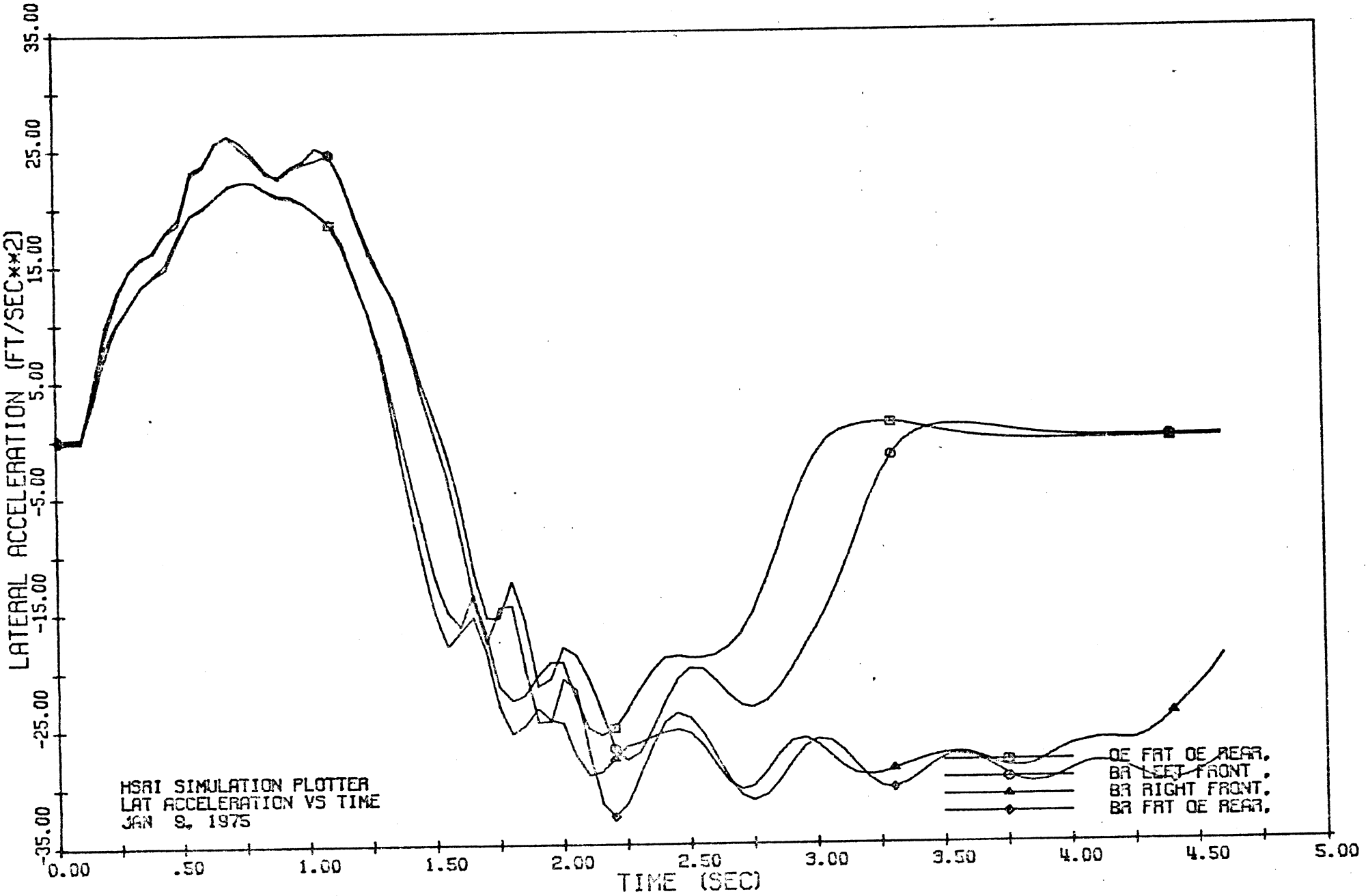

Figure 3-41(a) Buick Wagon: 340 deg sine asymmetry runs

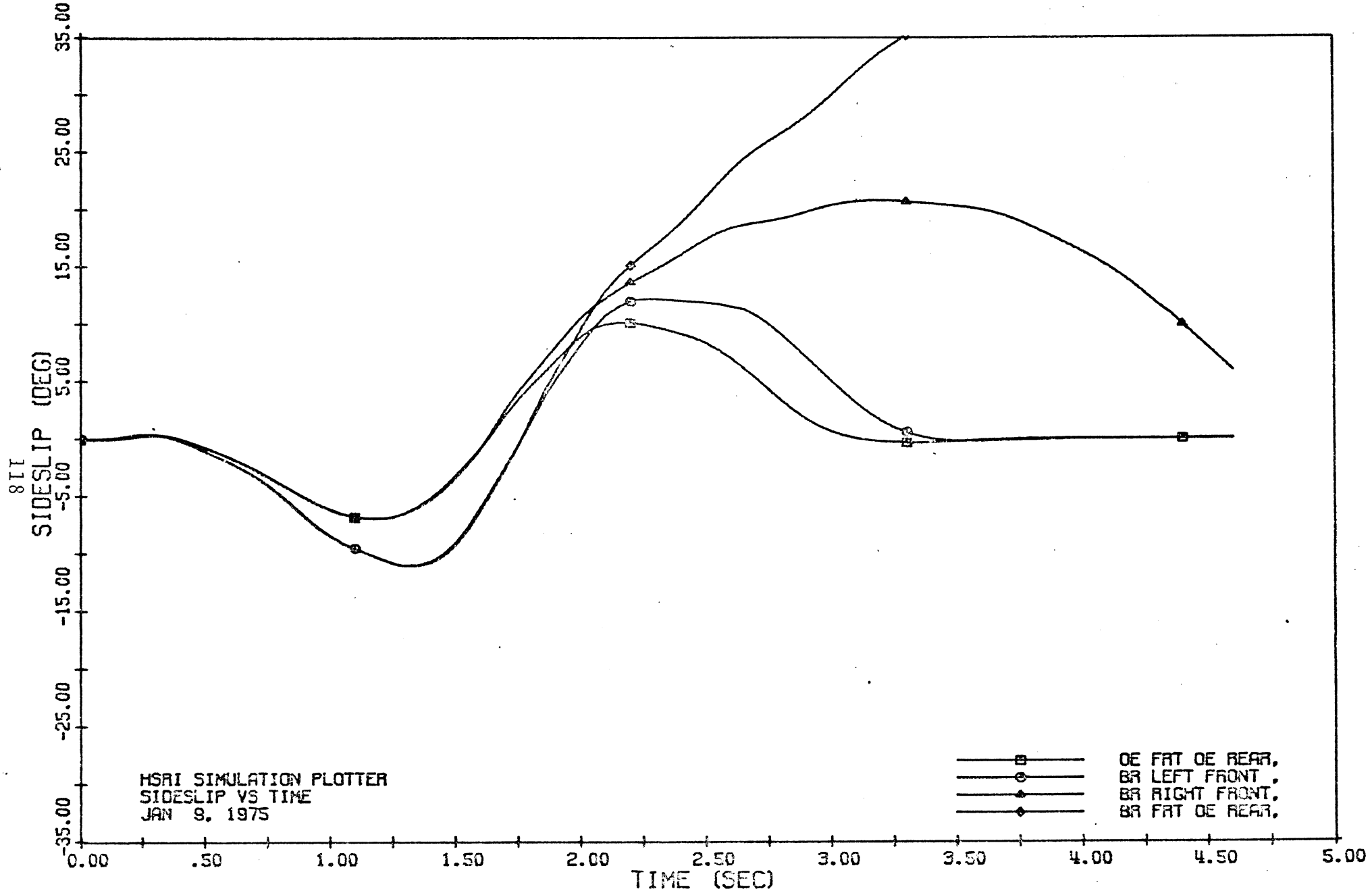

Figure 3-41(b). Buick Wagon: 340 deg. sine asymmetry runs

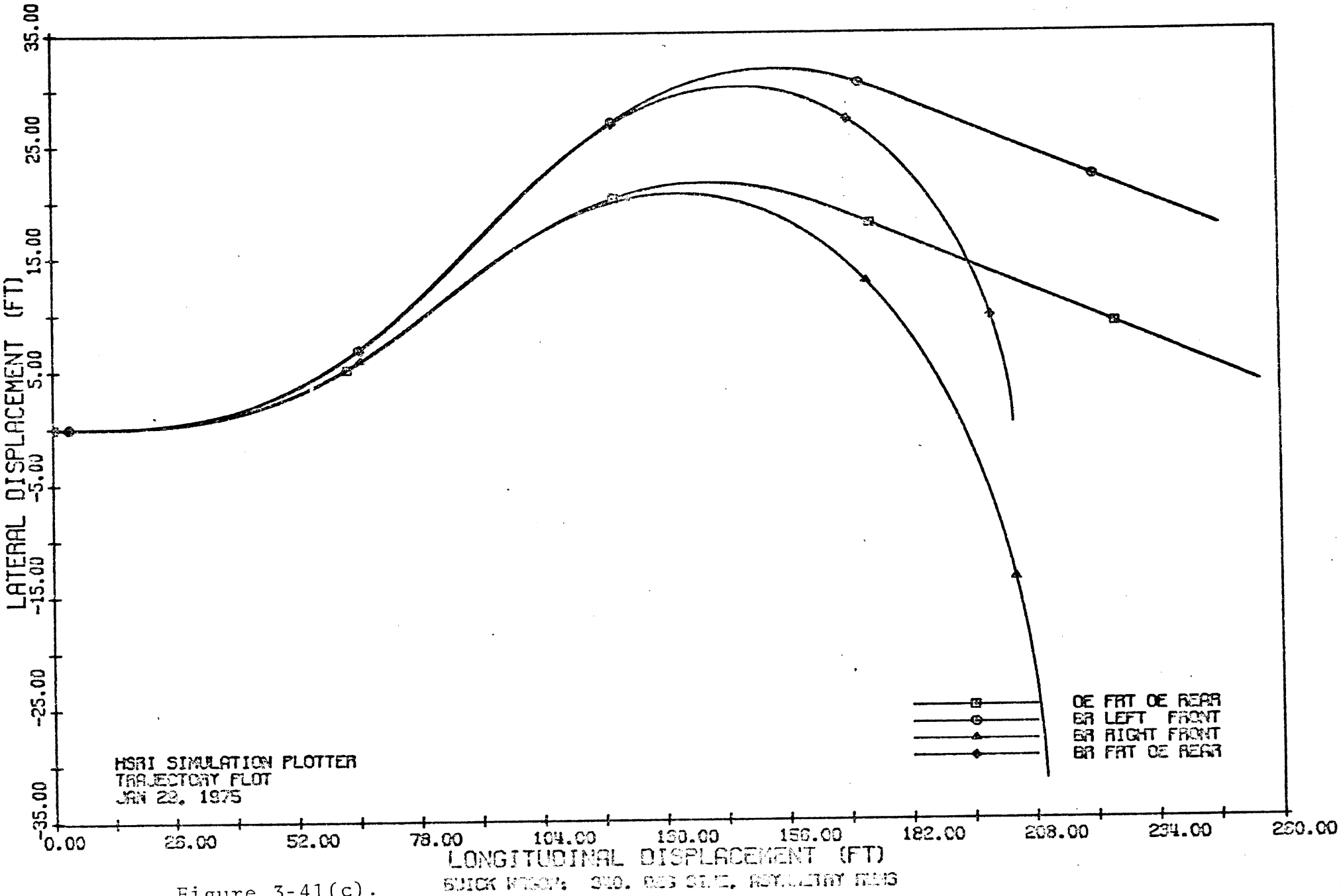
LATERAL DISPLACEMENT (FT)
35.00
25.00
15.00
5.00
-5.00
-15.00
-25.00
-35.00
0.00
26.00
52.00
78.00
104.00
130.00
156.00
182.00
208.00
234.00
260.00
LONGITUDINAL DISPLACEMENT (FT)
HSRI SIMULATION PLOTTER
TRAJECTORY PLOT
JAN 23, 1975
OE FRT OE REAR
BR LEFT FRONT
BR RIGHT FRONT
BR FRT OE REAR

Figure 3-41(c).

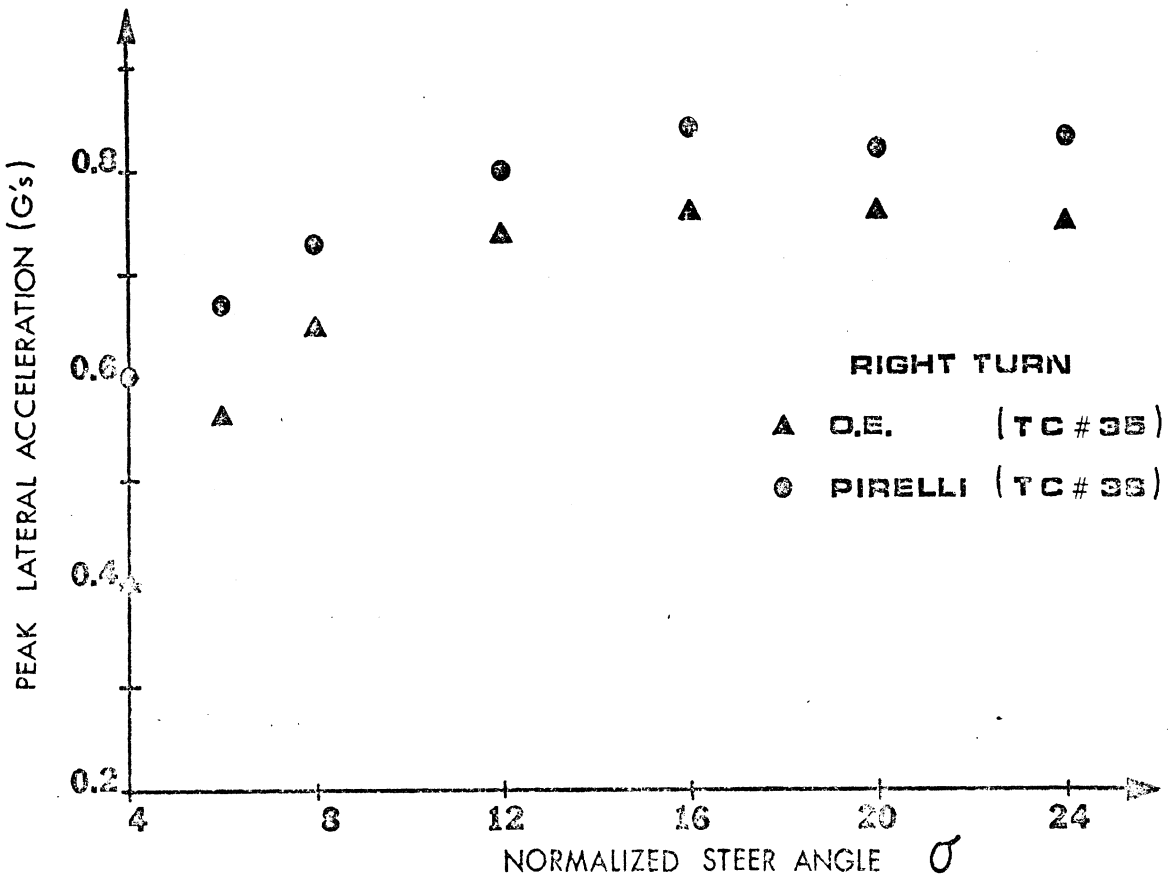

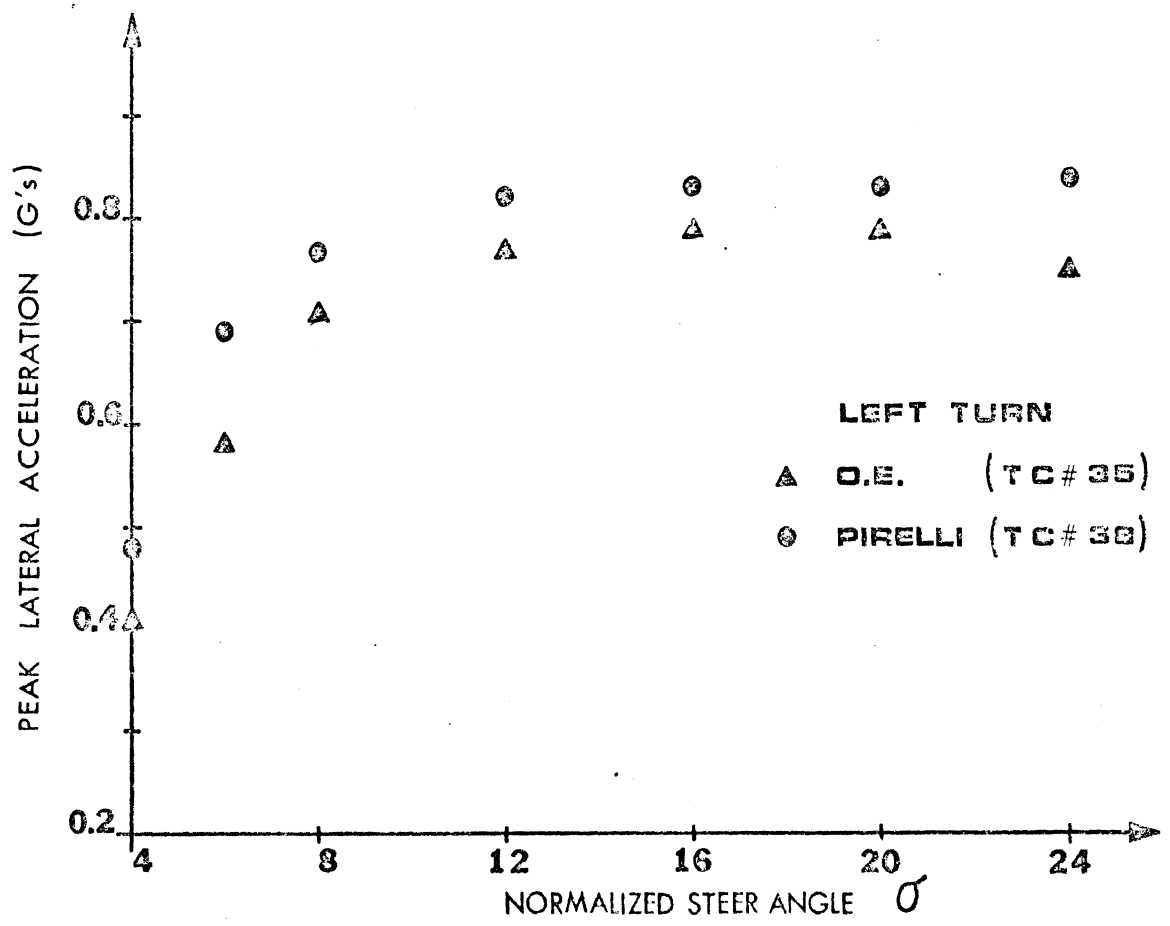

Figure 3-42. Peak lateral acceleration vs. normalized steer angle, Mustang trapezoidal.

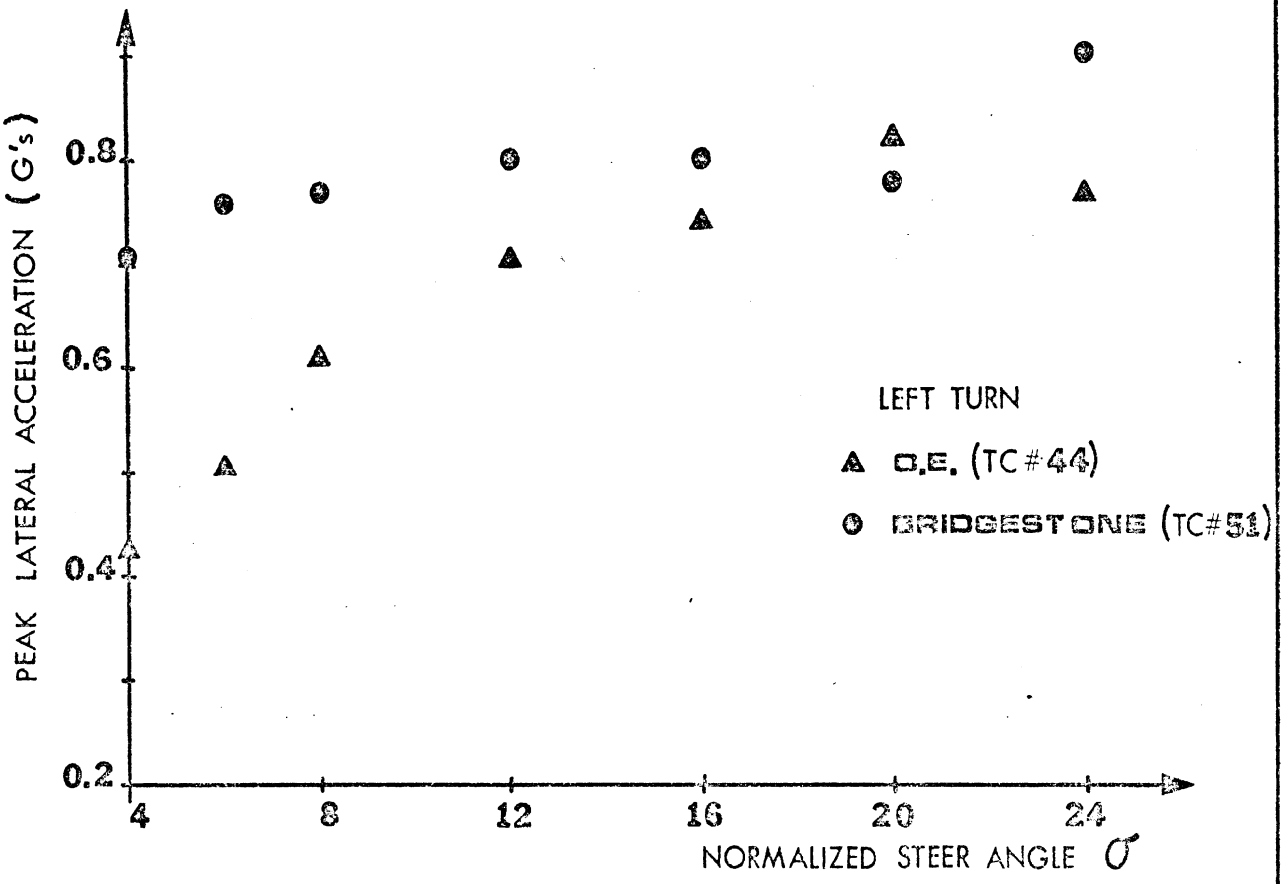

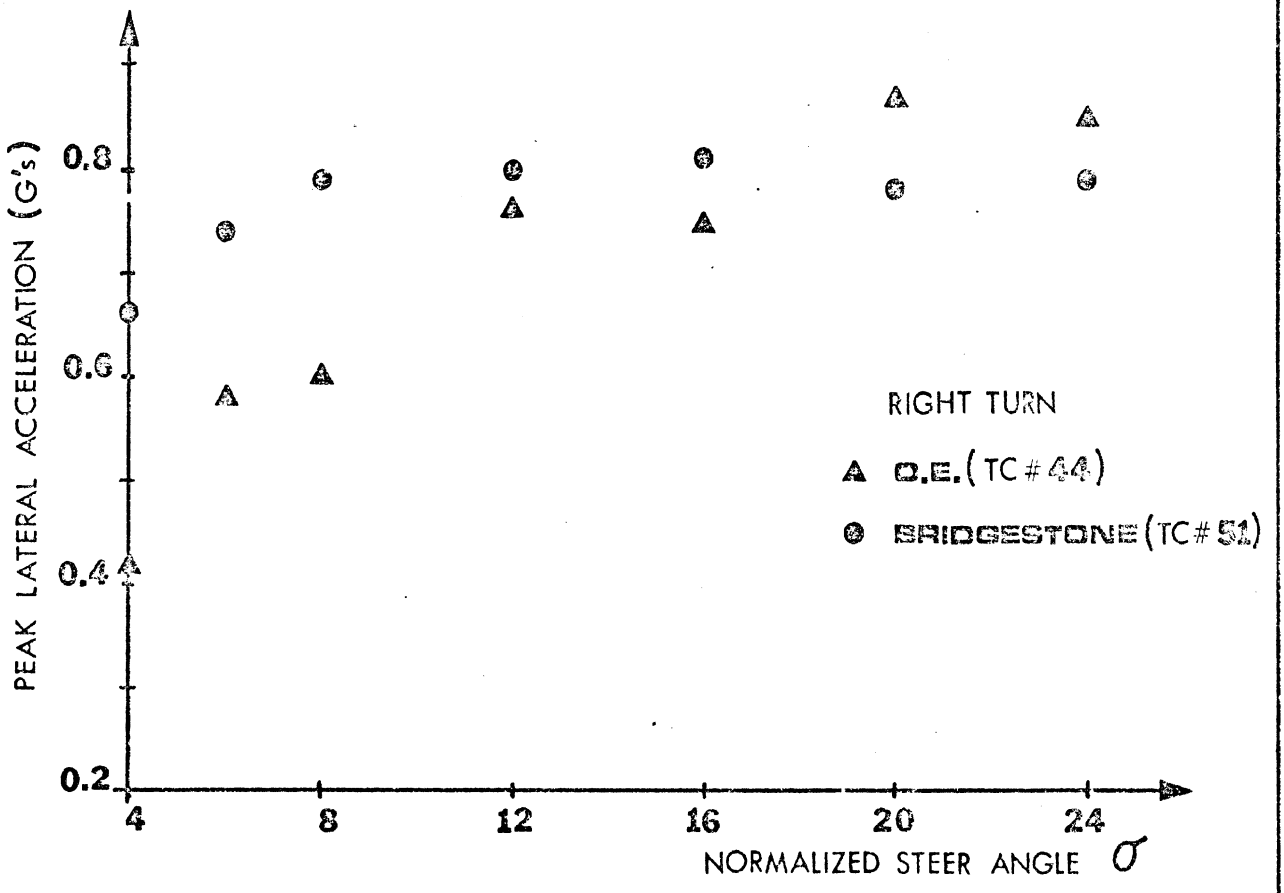

Figure 3-43. Peak lateral acceleration vs. normalized steer angle, Buick trapezoidal.

Additional computations shed some light on the trapezoidal steer response of other stiff radial-OE combinations. Consider in particular Figure 3-44, in which lateral acceleration, calculated for the Buick in a 175° trapezoidal steer maneuver is plotted for (a) the OE configuration; (b) Bridgestone front, Bridgestone rear; (c) OE front, Bridgestone rear; (d) Bridgestone front, OE rear. The trend is as anticipated*—the extremes are configurations (c) and (d), with the other combinations at intermediate values.

It is important to emphasize at this point that the measured and computed disparities between the OE configurations and the configuration with stiff radial tires on the front wheels and OE tires on the rear wheels do not result from differences in aligning or camber stiffness between the radial tires and the OE tires. Rather, these disparities occur mainly because the lateral forces generated by the Bridgestone and the Pirelli tire were greater than the corresponding OE tire in the mid range of slip angles, that is, from four to ten degrees. The differences in camber stiffness and aligning stiffness between the OE and the radial tires, which are quite important in normal driving maneuvers are much less important in severe maneuvers.

It is, of course, true that many radial tires do tend to be stiffer than the bias-belted or bias tire of comparable size and load rating (see, for example, Reference 12). Thus it seems that one must expect, in probablistic terms, that the replacement of fewer than all four of the OE tires with radial tires may lead to significant changes from OE performance, as produced in severe maneuvers. But the possibility

---

*Note that the computed values of peak lateral acceleration are very close to the measured data presented in Figure 3-43 at $\sigma = 8$. This leads to some confidence in our use of the 28 psi Bridgestone tire data for the Buick front tires, rather than the more desirable but unavailable 24 psi data.

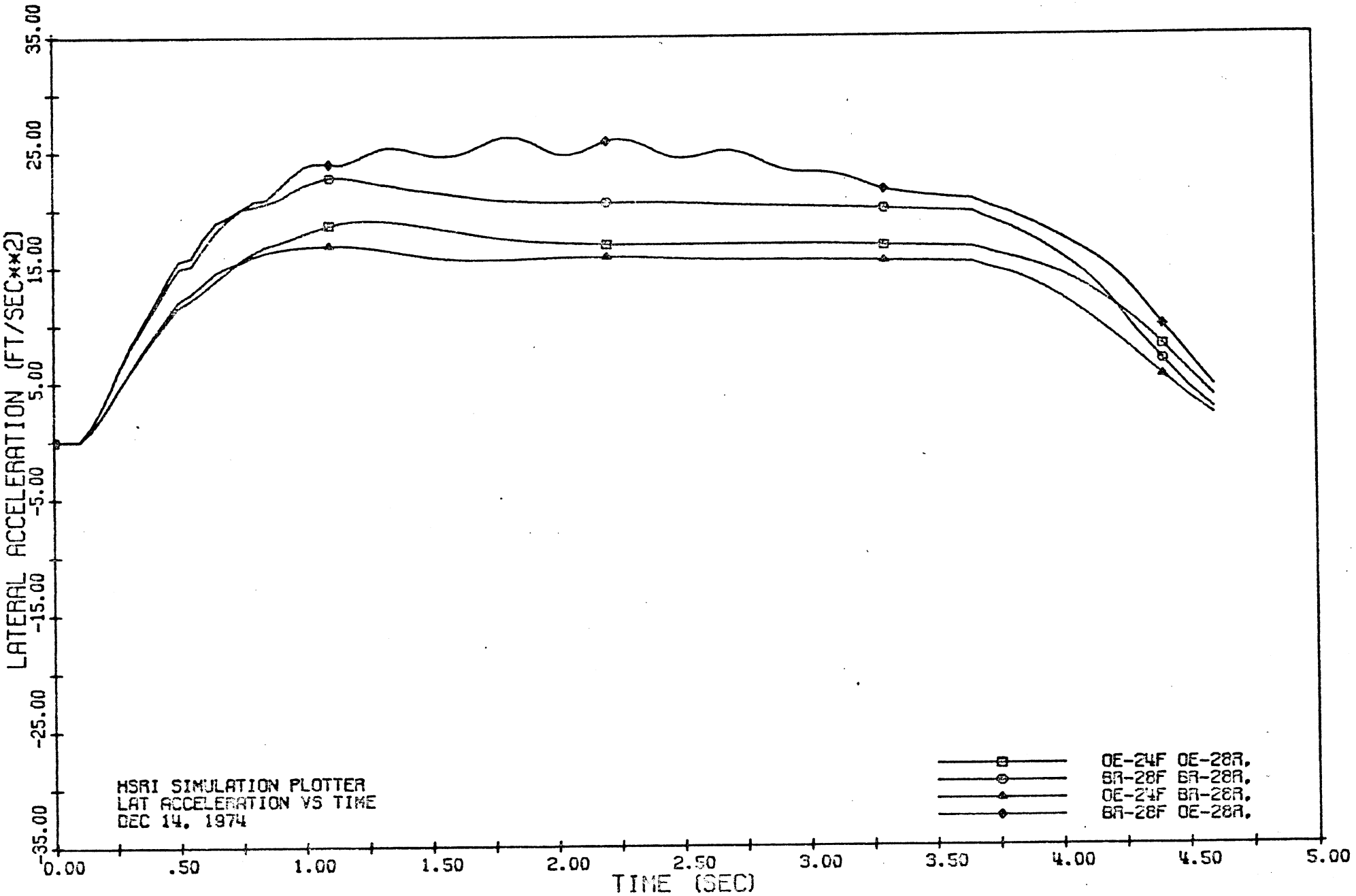

Figure 3-44. BUICK WAGON: 175.0 DEG TRAP TIRE MIX VARIATION RUNS

of such changes is by no means restricted to permutations involving radials. This will be demonstrated through simulations of Buick performance with a very stiff bias tire—the Firestone 500 H78-14—mounted on the front wheels, with the OE bias-belted Firestone Deluxe Champion H78-14 mounted on the rear wheels. The carpet plots for these two tires are presented in Figure 3-45.

In Figure 3-46(a) and 3-46(b), the yaw rate and sideslip angle responses computed for this Buick configuration are plotted for comparison with the results previously computed for the OE Buick and the Bridgestone-front/OE-rear configuration. Clearly, stiff tires of bias construction on the front wheels can also lead to significant changes from OE performance. This finding does not, of course, indicate that combinations of bias tires on front wheels and bias-belted tires on rear wheels lead to significant deviations from the OE response. (The opposite combination (viz., bias-belted on front, bias on rear) was shown, in Reference 4 , to lead to drastic changes.) Rather, the indication is that replacement of one or more OE front tires by any tires which tend to generate higher lateral forces than the OE tires, while leaving the OE tires on the rear, is likely to lead to significant deviations from the response of the OE vehicle.

The corollary to the above argument is also worth noting. Replacement of one or more rear OE tires by tires tending to generate lower lateral forces than the OE tires, while leaving OE tires on the front, is likely to lead to significant deviations from the OE response. This result is difficult to demonstrate for the test vehicles and tires used in the present investigation, since the test tires were, by and large, chosen because they were stiffer than the OE tires. However, this statement is obviously supported by the findings presented earlier with respect to the influence of low inflation pressure in the rear tires.

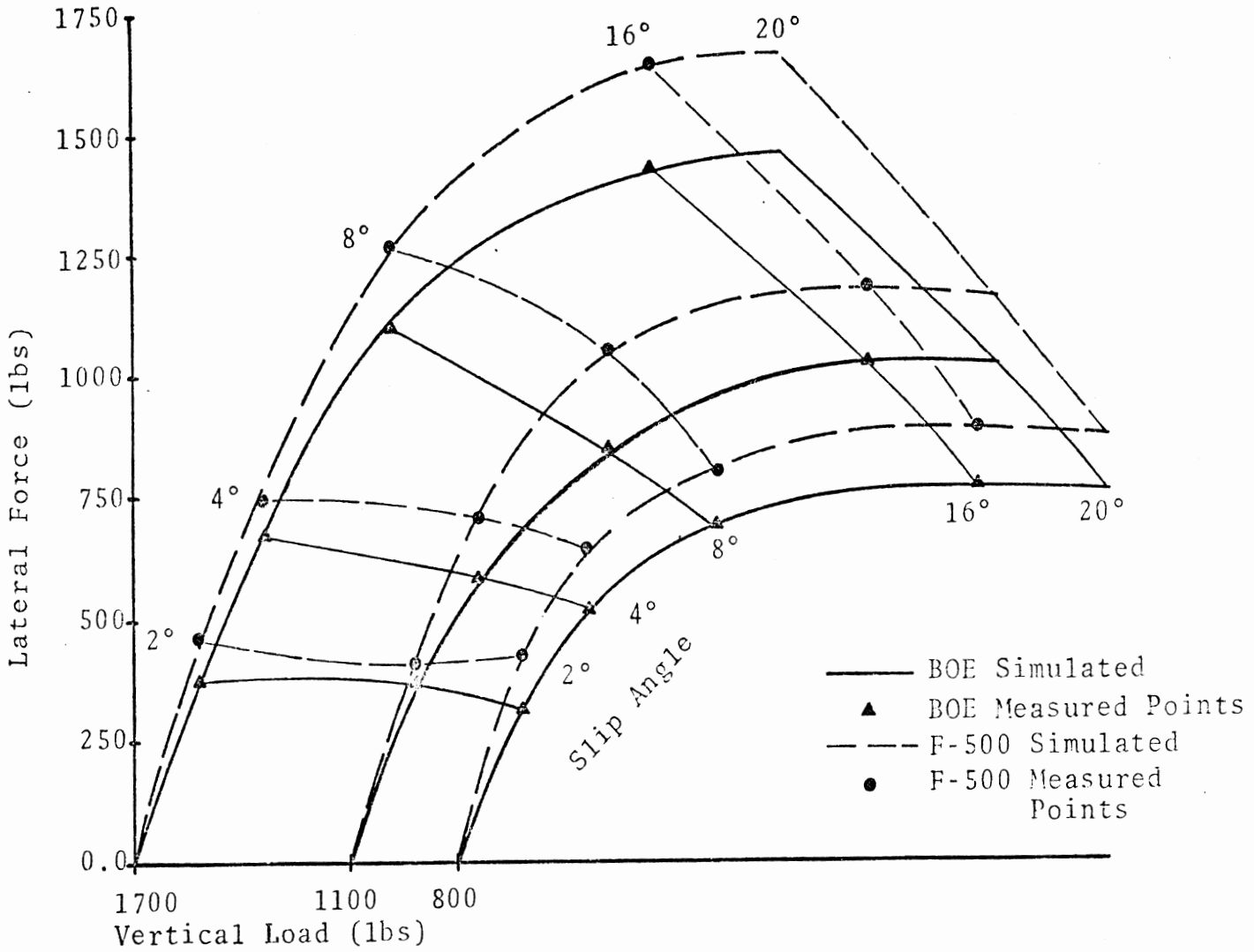

Figure 3-45. Lateral force vs. slip angle and load, dry concrete, 40 mph, 28 psi.

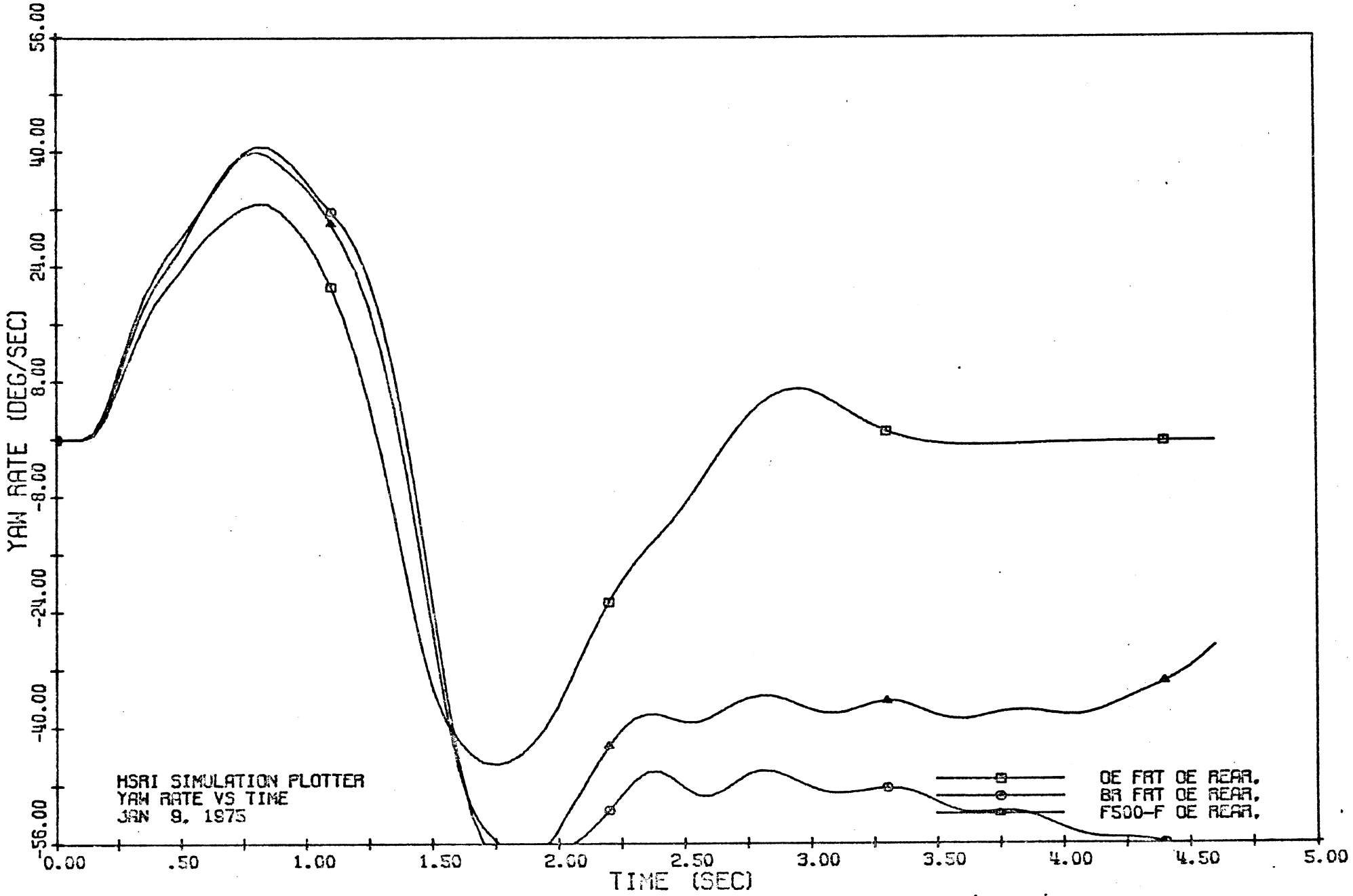

Figure 3-46(a). Buick Wagon: 340 deg sine, construction mix.

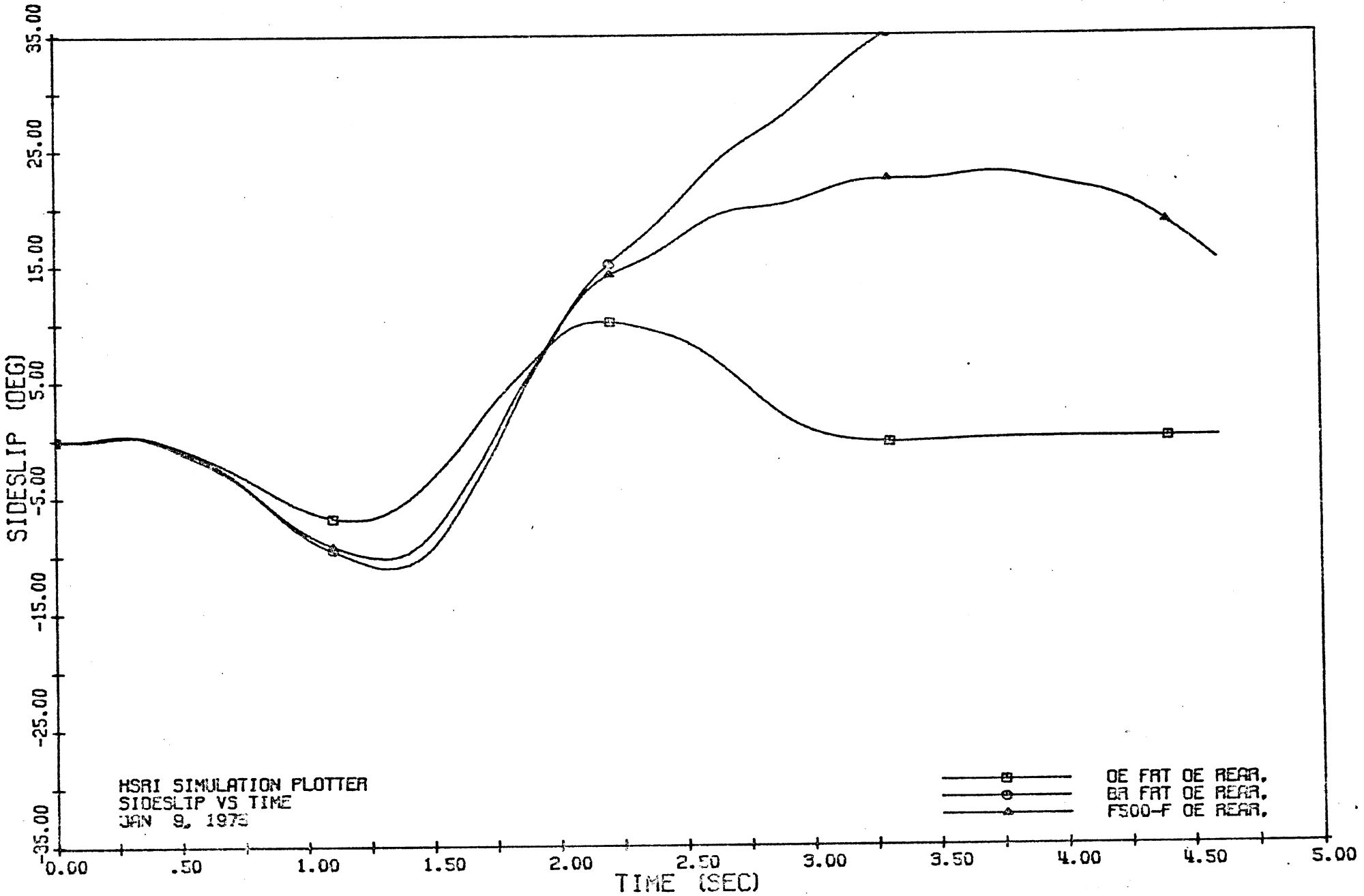

Figure 3-46(b). Buick Wagon: 340 deg sine, construction mix.

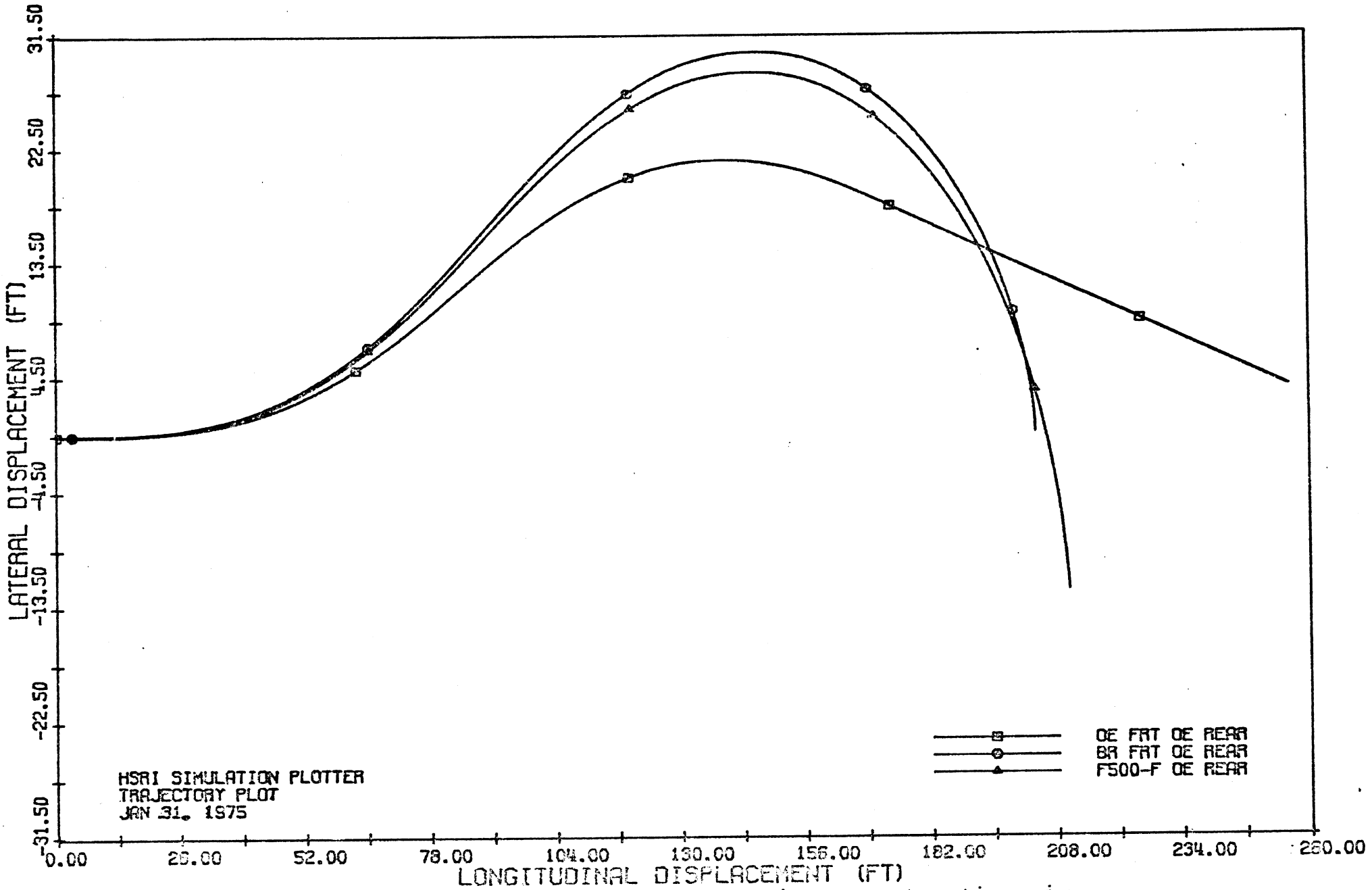

Figure 3-46(c). Buick Wagon: 340 deg. sine, construction mix.

The above discussion should not be interpreted as supporting the view that the replacement of less than all four OE tires will always lead to significant deviations from OE performance. In fact, there were two mix sets which led to OE-like performance in the vehicle testing program. These sets were (1) OE on front wheels, Firestone Town and Country H78-14 (a bias-snow tire) on rear wheels of the Buick; and (2) Goodyear Custom Power Cushion Polyglas on the front wheels, and OE tires on the rear wheels of the Mustang.

Consider Figures 3-47 and 3-48, in which the peak values of lateral accelerations measured in the trapezoidal steer procedure for these configurations are compared with the corresponding OE measurements. In each case, the similarities in the measured values are obvious across the entire range of steer angles. Similarities between OE test results and test results obtained using these tire mixes were also evident in the braking, braking-in-a-turn, and sinusoidal steer metrics, as is shown in Appendix F. Clearly, these tire mix configurations should not be expected to produce noticeable changes in OE performance as measured by VHTP procedures conducted on a dry surface.

3.4 TREAD WEAR

One of the principal concerns inherent in the careful quantification of the effects of tread wear on vehicle handling performance is the definition of wear itself. Many varieties of wear are possible and probable. For example, Erlich and Jurkat have reported that 27.8 percent of the front tires and 17.8 percent of the rear tires which they examined showed some unusual tread wear pattern such as waves or step wear [13]. Baker and McIlraith have reported that 3.6 percent of the tires examined in their survey had differences of more than 4/32-inch groove depth between the inside, middle, and outside of the tread [14]. A summary of these and other pertinent data is given by Harvey and Brenner [11].

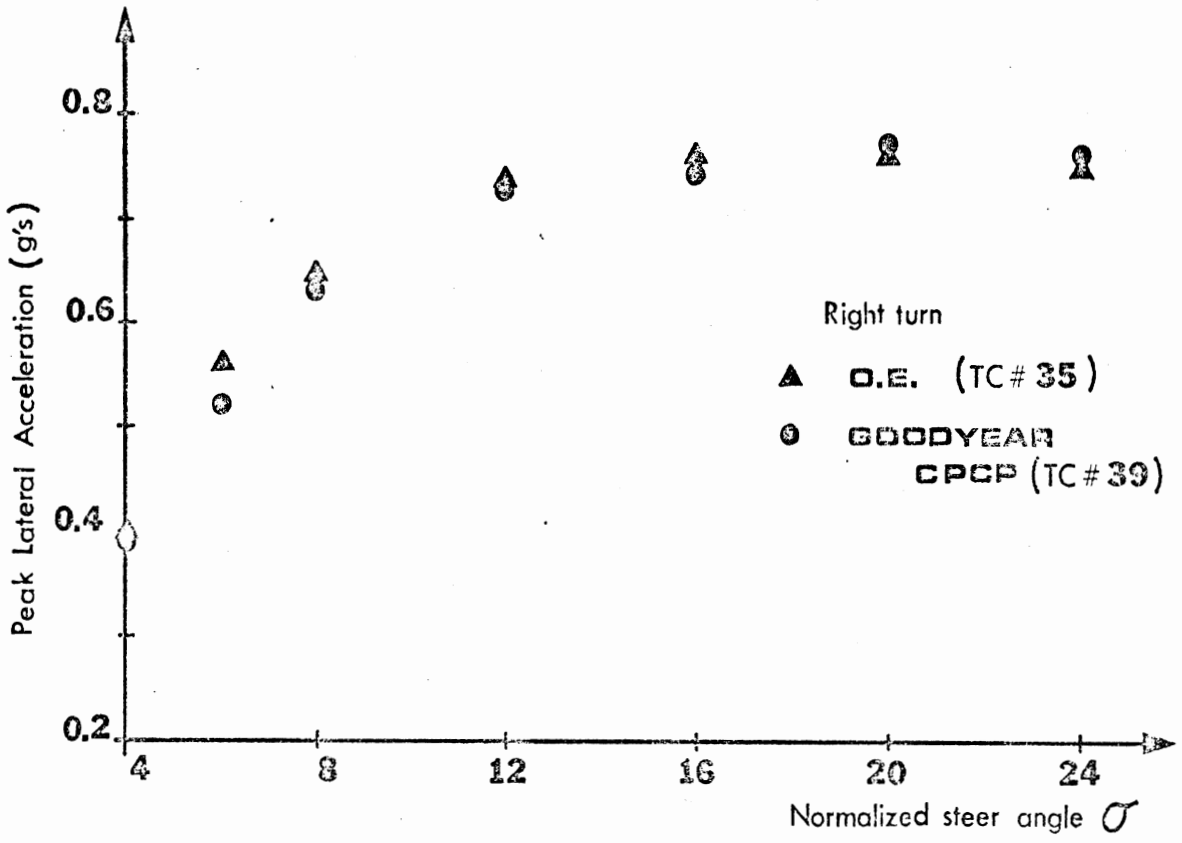

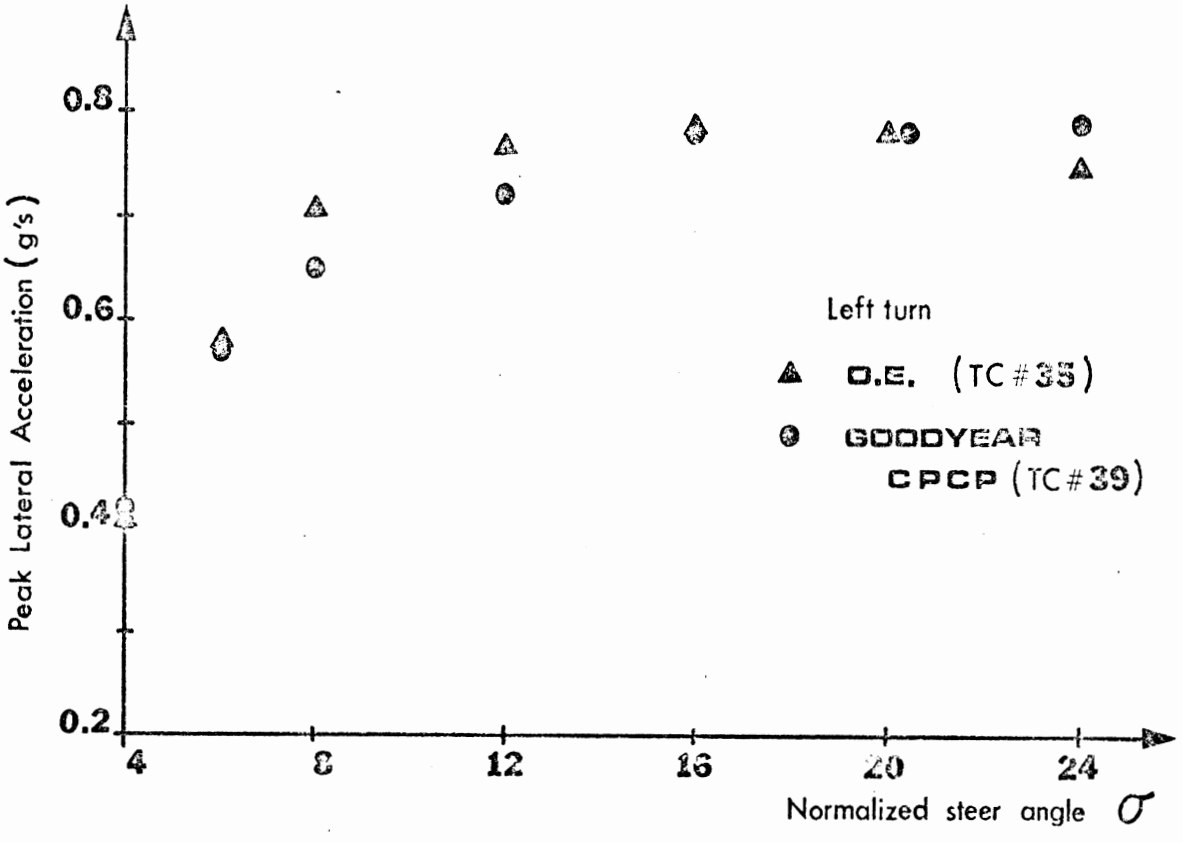

Figure 3-47. Peak lateral acceleration vs. normalized steer angle, Buick trapezoidal steer maneuver.

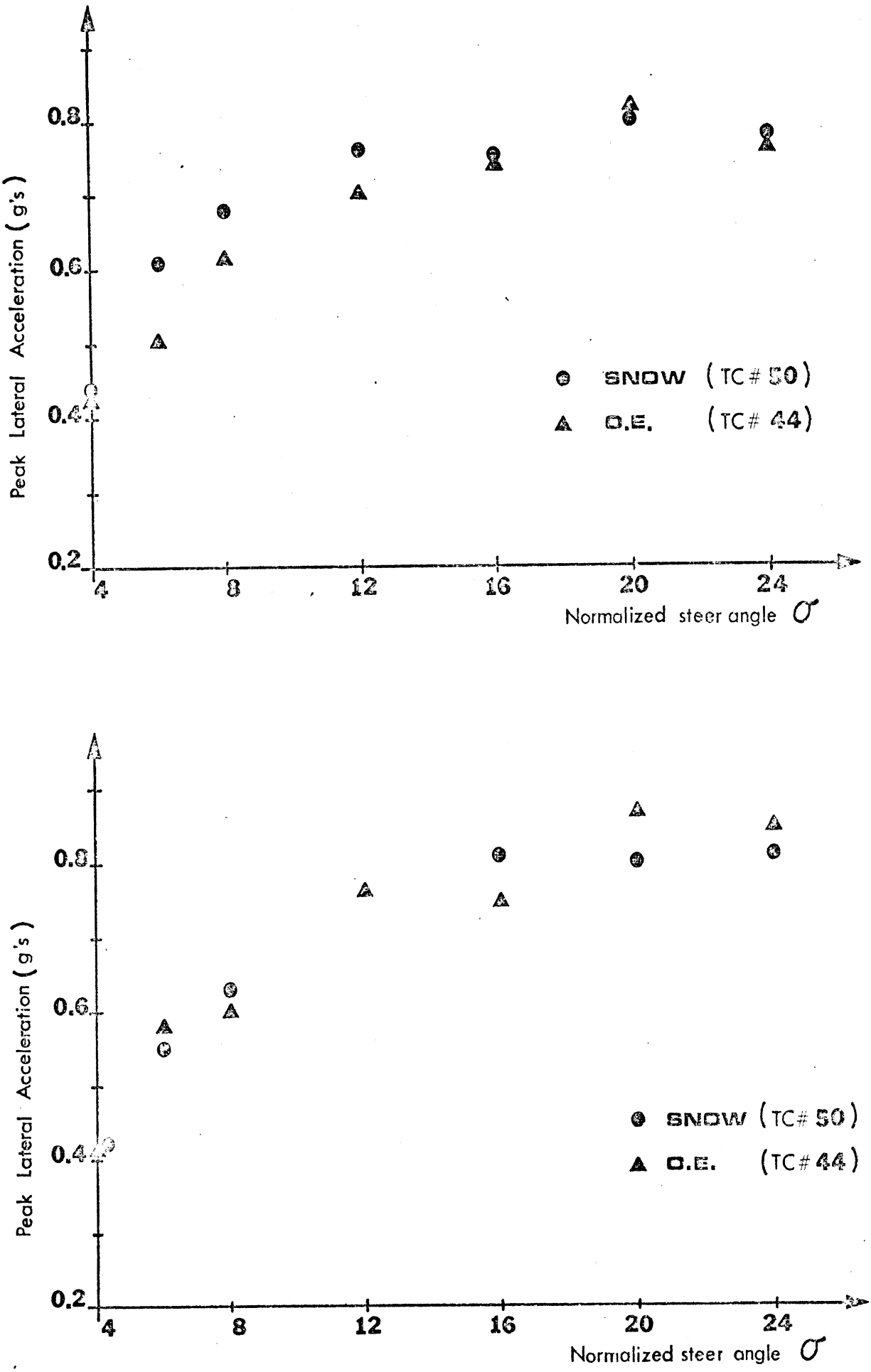

Figure 3-48. Peak lateral acceleration vs. normalized steer angle, Mustang trapezoidal steer maneuver.

Our goal in the investigation of the effects of tread wear was to quantify as clearly as possible the braking and handling of the test vehicles equipped with a particular set of worn tires with well-defined characteristics. These worn test tires were obtained by machining new tires down to the desired tread depth, with the depth held constant across all grooves. Thus the crown radius was determined by the tire carcass, and the worn tires were reasonably free of uneven wear patterns.*

The very necessity of defining a so-called worn tire leads to obvious questions concerning the relationship between the test vehicles equipped with these carefully controlled tires and vehicles on the highway. Indeed, it has been shown that the crown radius on a machined tire can have a first-order effect on the shear forces generated by that tire on a dry surface [15]. In addition, it is a matter of some concern that the chemical changes due to aging which may accompany on-vehicle tire wear have been neglected in this study. However, the basic cause-and-effect relationship underlying the tire tests and vehicle tests, namely, that worn tires tend to deliver higher shear forces on dry surfaces, is well accepted. (See, for example, [15].) Thus the vehicle test results obtained for the worn tires on the dry surface should be considered indicative, if not typical, of the performance to be expected on the highway.

Tire tests were performed for each of the OE tires machined to tread depths of 6/32 inch, 4/32 inch, and 2/32 inch. Some of that data is presented in Figures 3-49 and 3-50, in which

---

*The tires were "worn" using a truing machine. Thus the radius of the worn tire is measured from the wheel center, not the tire center. Usually this practice led to only small variations in tread depth around the tire. In the few cases when the circumferential variation in groove depth resulting from out-of-round tires exceeded 1/32-inch, the tires were not used for tire testing or vehicle testing.

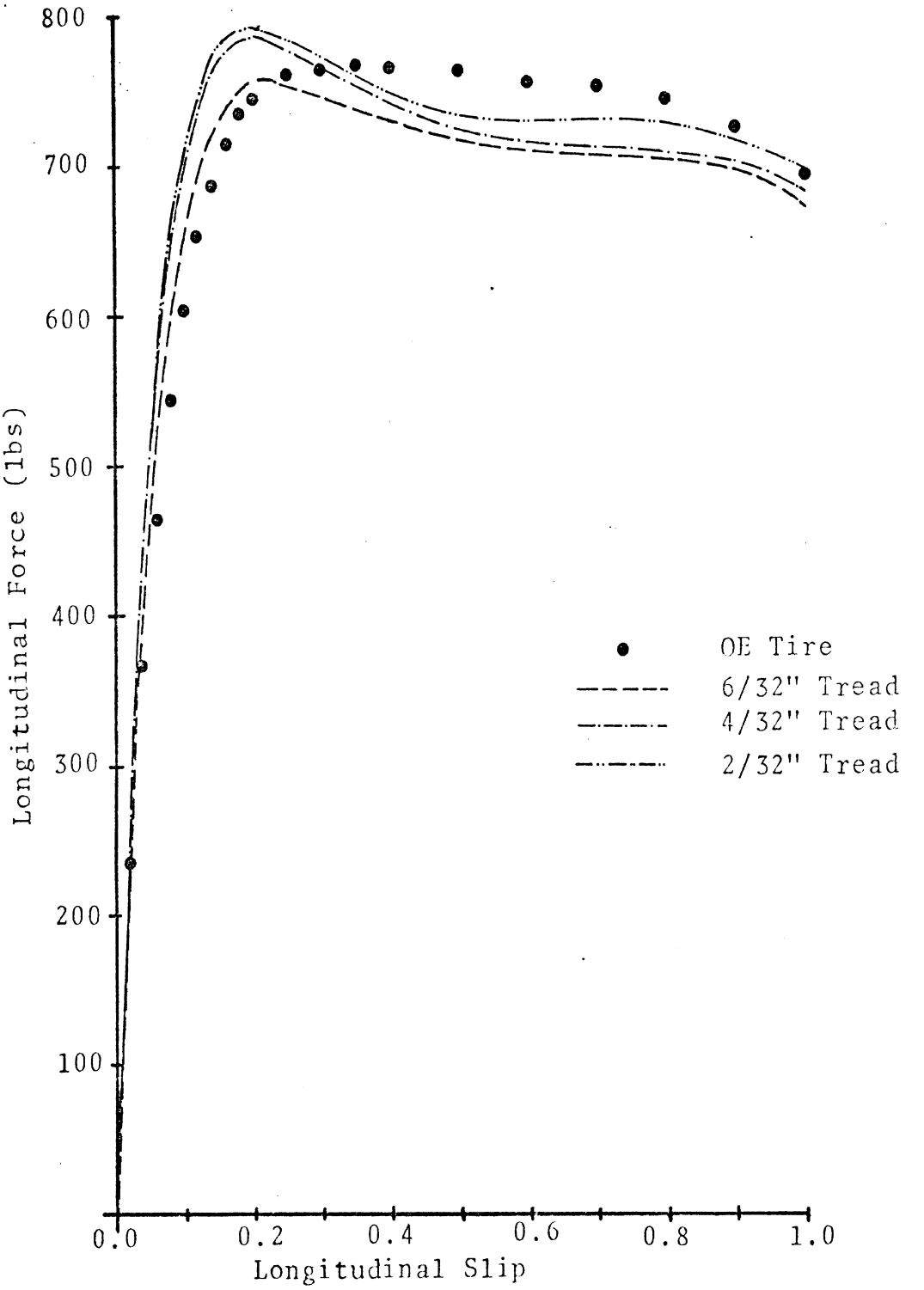

Figure 3-49. Longitudinal force vs. slip for various tread depths, B.F. Goodrich Silvertown at 800 lbs, 24 psi.

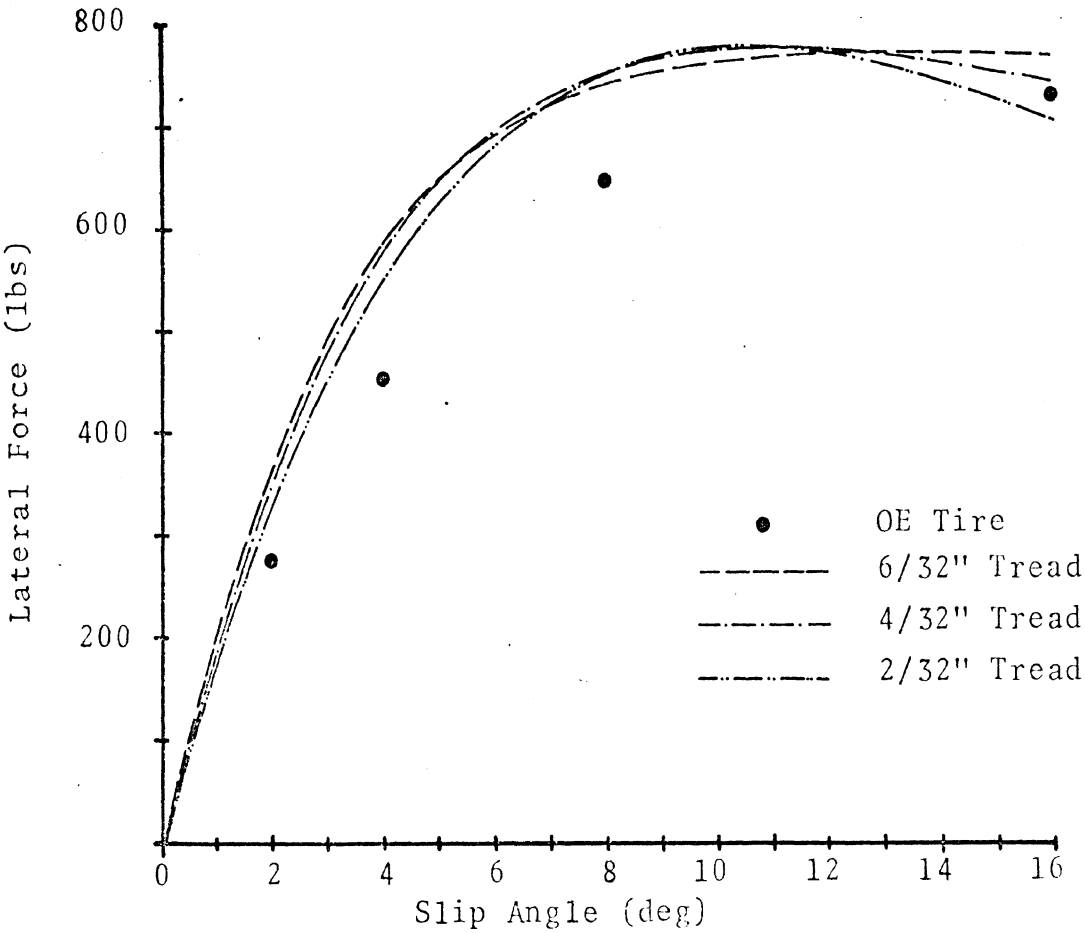

Figure 3-50. Lateral force vs. slip angle for various tread depths, B.F. Goodrich Silvertown, 800 lbs. 24 psi.

measurements of longitudinal and lateral force versus longitudinal and lateral slip are compared for each depth.

The similarities in the longitudinal force data led to the expectation of little or no change in the braking performance of the Mustang on the dry surface. This turned out to be the case: When the OE Mustang was tested on the dry surface in the straight-line braking procedure, a wheels-unlocked peak acceleration of 0.73 g was measured; with tires cut to 2/32-inch tread depth, 0.75 g was measured. In the braking-in-a-turn performance, there was again little difference noted between the performance of the OE vehicles and the corresponding worn-tire configurations. A complete summary of all these data is presented in Appendix F.

In the case of lateral force data, however, differences were noted (see Figure 3-50). To achieve the largest possible change from the performance of the OE vehicle, the tests for each vehicle on the dry surface were run with 2/32-inch-tread tires on the front and OE tires on the rear. This configuration led to marked changes from the OE performance in the limit steering procedures, sinusoidal steer and trapezoidal steer.

Consider, for example, Figures 3-51 and 3-52, in which the measured value of maximum lateral accelerations obtained for each of the test vehicles is compared to the corresponding OE data. The effects of increased stiffness possessed by the 2/32-inch-depth front tires are readily apparent. A summary of the data measured in the trapezoidal-steer and sinusoidal-steer tests, is presented in Appendix F.

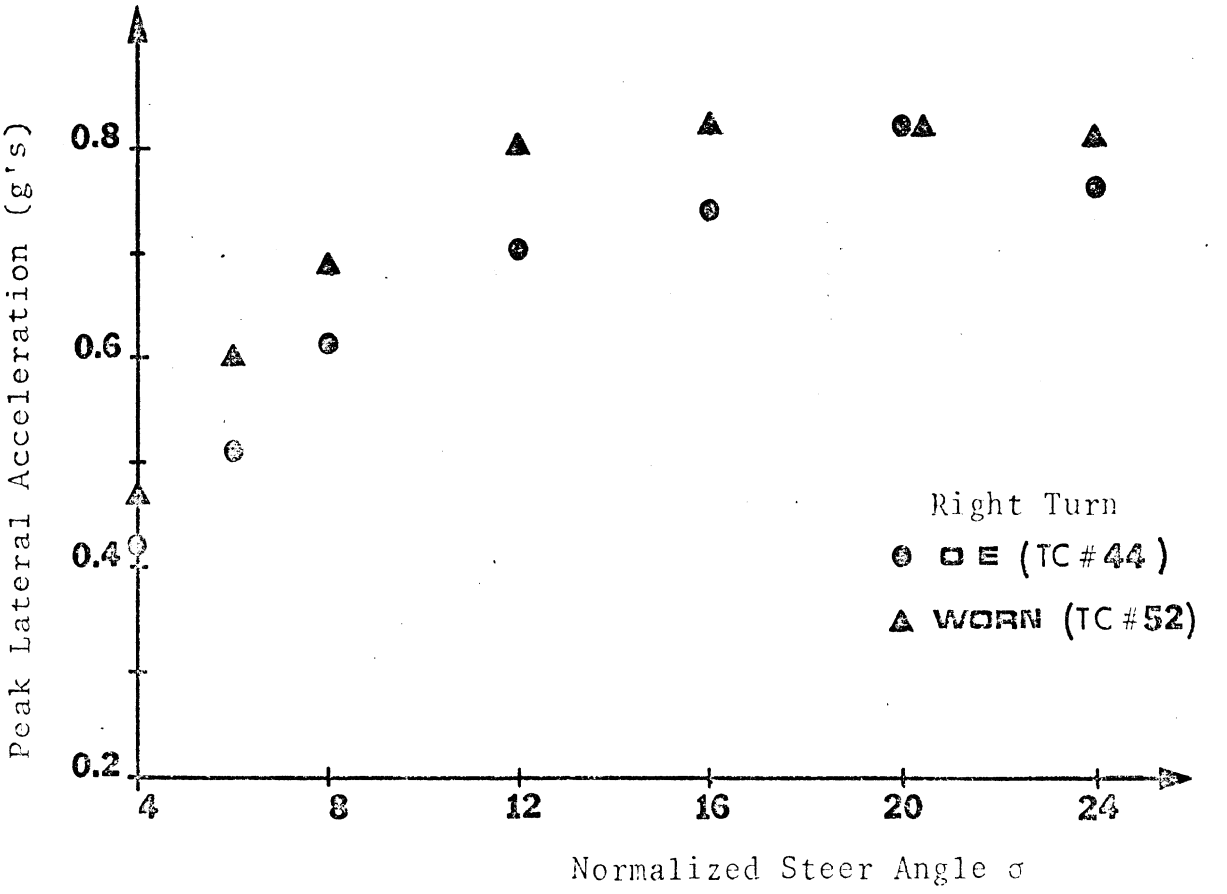

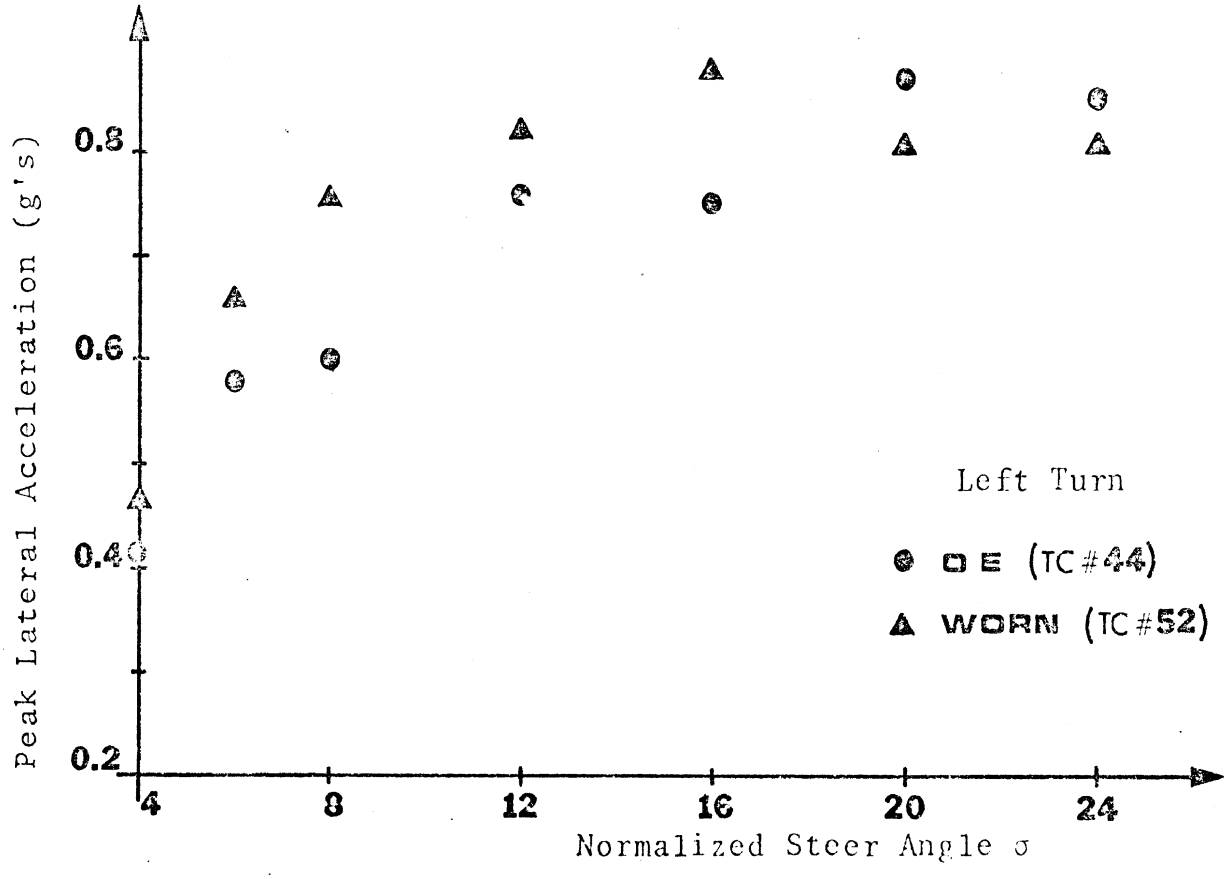

Figure 3-51. Buick trapezoidal steer peak lateral acceleration vs. normalized steer angle.

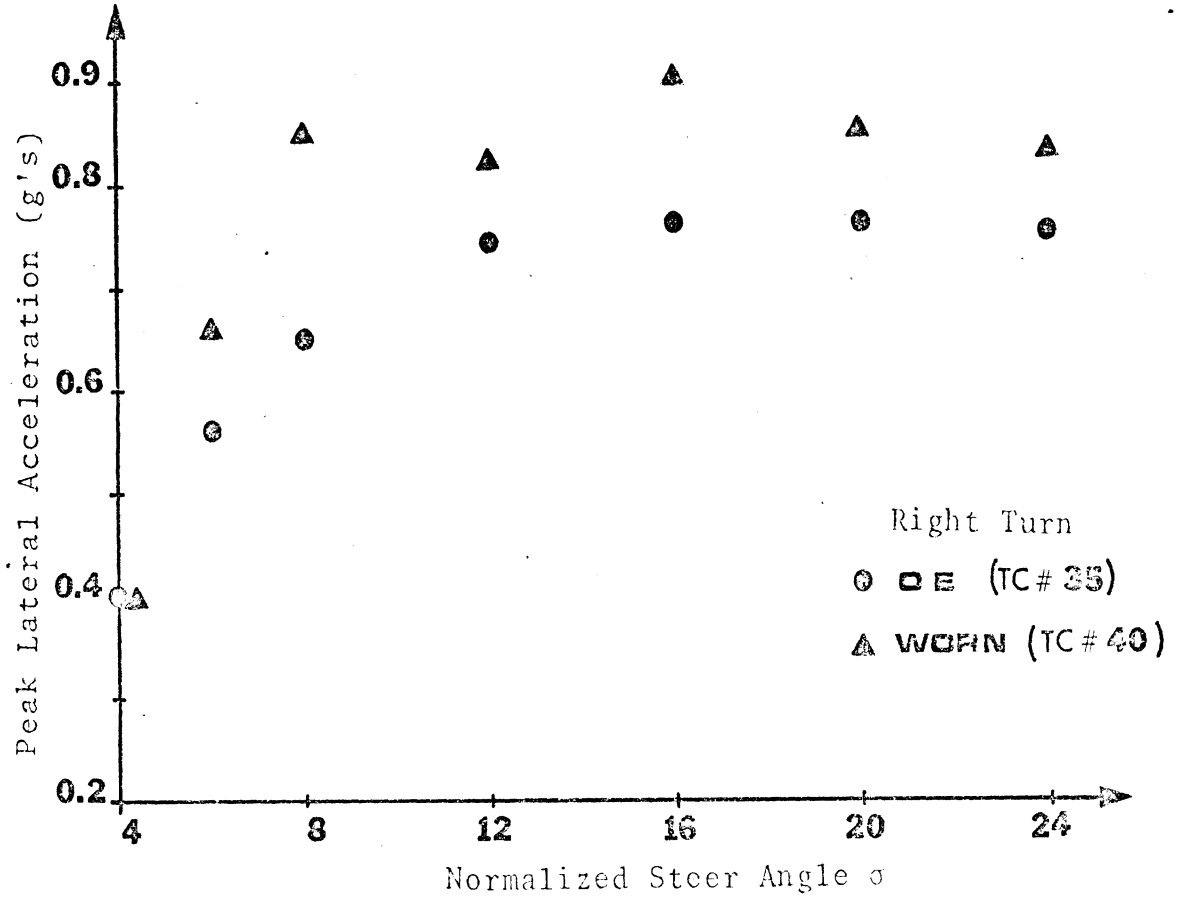

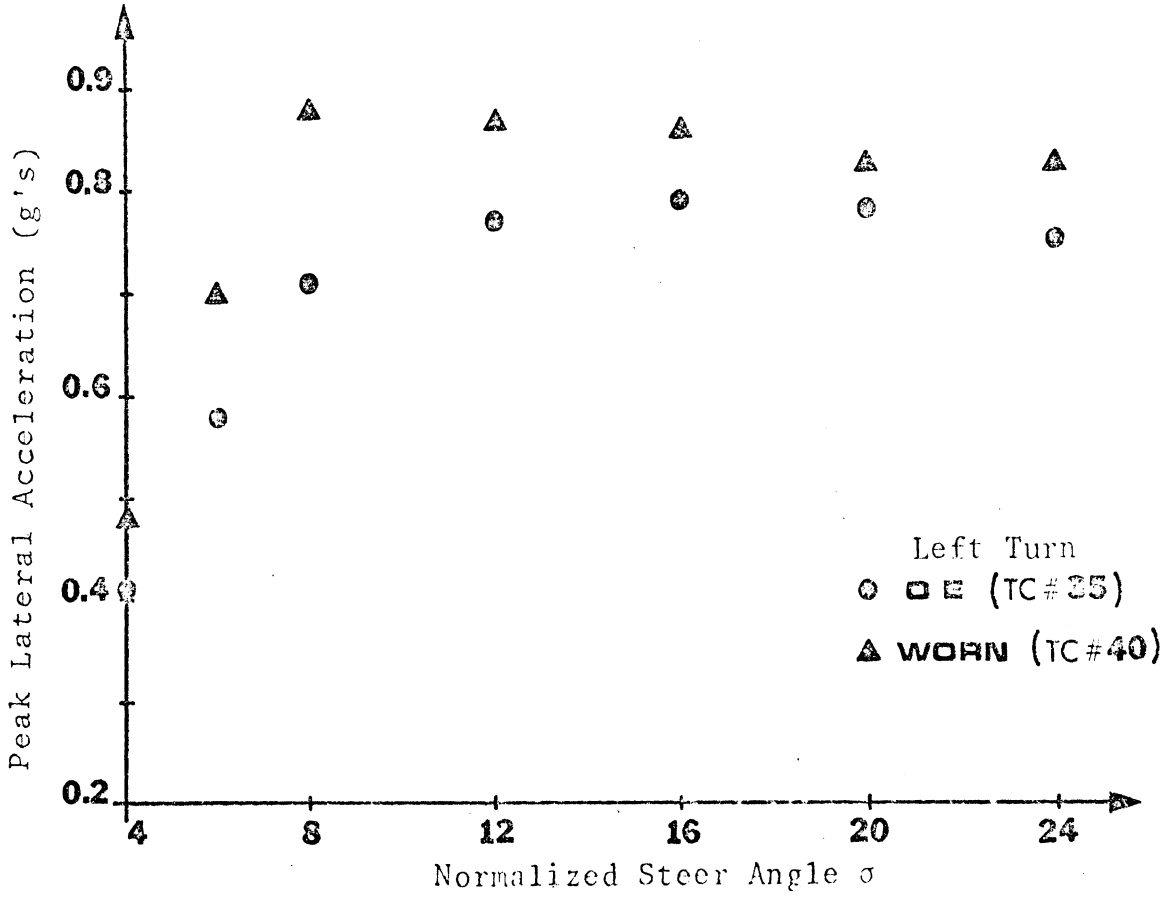

Figure 3-52. Mustang trapezoidal steer peak lateral acceleration vs. normalized steer angle.

4.0 LIMIT MANEUVERING PERFORMANCE ON WET SURFACES

4.1 COMPLICATIONS INHERENT IN WET TESTING

There is ample incentive for study of the effects of tire-in-use factors on tire performance on certain wet surfaces. For example, Reference 16 points out that the "accident history [at a site on the Ohio Turnpike] appears (sic) to be highly associated with wet pavement, and to a degree with heavily worn tires." However, while it is desirable to measure the shear forces generated for the wet surface-tire combination of interest itself rather than resorting to laboratory techniques, it is well known that serious difficulties arise in over-the-road tire testing on a wet surface.

Some documentation of these difficulties is given in Figure 4-1, which has been reproduced from Reference 17. The scatter in these data, which were measured by using a brake trailer with external watering, resulted from "nonuniform water cover caused by irregularities in the road elevation profile."

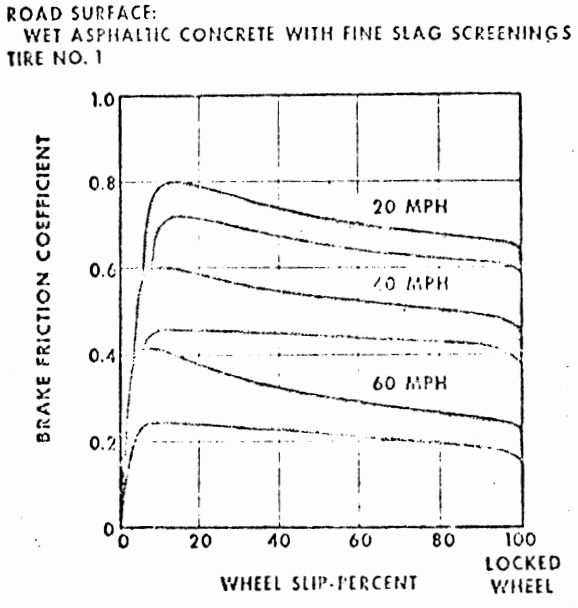

Figure 4-1. Variability of transient μ-slip curves measured on wet asphalt.

Some scatter in the measured data can be eliminated through the use of on-board watering, since external effects such as wind disturbances are effectively eliminated. Although it is reasonable to assume that the water depth encountered by the test tire remains reasonably constant during any single test run, the actual depth is difficult to determine accurately. Thus it seems reasonable to assume that for both external and internal watering "the water depths quoted for [over-the-road] traction test results must be considered very approximate." [18].

Vehicle tests on a wet surface are subject to the same confounding problems as tire testing using external watering. However, the scatter in the measurements due to a nonuniform water cover is a more serious issue in open-loop vehicle testing than in over-the-road tire testing since a larger wetted-surface area is required for vehicle testing.

In addition, the front tires of the vehicle obviously disturb the water in the path of the rear tires, leaving little hope of an accurate estimation of the water depth to which the rear tires are exposed. Thus, as is pointed out in Reference 19, the simulation of vehicle maneuvers on a wet surface by computation is a "speculative undertaking."

In spite of these obstacles, this study included a program of tire testing and vehicle testing on wet surfaces. Although the tire and vehicle tests were performed on the same jennite surface, different watering systems were used in the two test programs. Water used in the vehicle tests was provided by a system of irrigation pipes, whereas the tire tests were run using the internal watering capability of the mobile tire tester. This practice suggests that, whereas the mobile tire measurements conducted on the wet surface may, indeed, indicate trends in the wet traction performance of the test tires, there is not a precise relationship between the tire

data (as measured on the wet surface) and the shear forces generated at the tire-road interface while the vehicle was tested on the wet surface.

Wet-surface testing was performed on TTI's jennite-surfaced skid pad. (See Figure 4-2.) In wetting the pad, water is expelled from pipes positioned on the north end of the pad (the lower left portion of Figure 4-2). Natural drainage (resulting from the built-in grade) causes the water to run off the pad to the south. However, the pad is not flat enough to drain the water uniformly, and thus water depth in the vehicle tests varied from nearly zero to at least 1/4 inch.

The above-described test conditions do not lead to data of sufficient resolution to detect subtleties in vehicle performance resulting from variations in tire-in-use factors. However, certain of the test results demonstrated that a sudden and radical departure from OE-like performance can, in some cases, result from tire-in-use factors. The detection of these cases made the wet-testing phase of the present investigation a productive endeavor, with results that certainly bear on tire-inspection criteria.

4.2 TIRE TESTS CONDUCTED ON THE WET SURFACE

Tire tests were performed on the wet jennite surface for each of the OE tires and selected non-OE tires. The tires that were tested and the test matrix are identified in Tables 4-1 and 4-2. Table 4-3 presents the more limited* test program conducted with the tread-worn tires.

A complete set of wet-test data is presented in Appendix D of this report. These results verify that the shear forces tend to drop with both speed and tread wear. Further, since the peak levels of shear force are a complicated function of

*A breakdown in the tire truing equipment precluded the delivery of the tread-worn tires in time for conducting the complete test matrix.

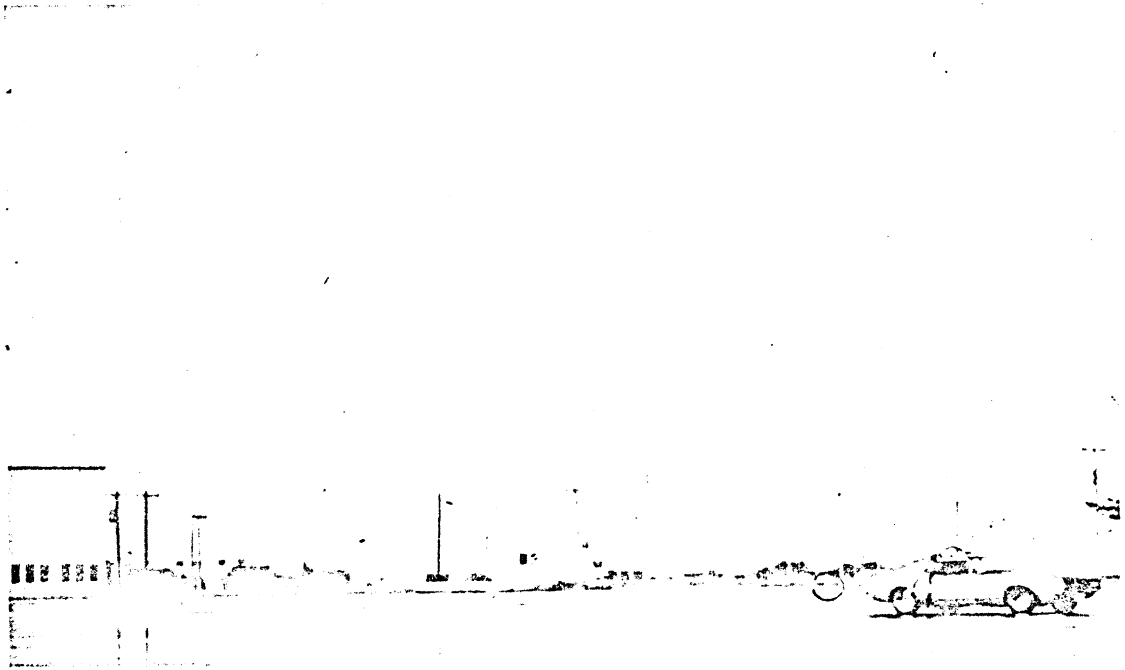

Figure 4-2. The wet test pad

Table 4-1. Tires Tested Through the Full Wet Test Matrix

B.F. Goodrich Silvertown E78-14 (4 inflation pressures)
Bridgestone 225R-14, 28 psi
Firestone Deluxe Champion H78-14 (4 inflation pressures)
Firestone 500 H78-14, 28 psi
Firestone 500 E78-14, 24 psi
Goodyear Custom Power Cushion Polyglas E78-14, 24 psi
Pirelli 185R-14, 24 psi

Table 4-2. The Wet Test Matrix

E78-14 tires

	Load		
Speed	800	1100	1400
20 mph	μ, x		
40 mph	μ, x	μ, x	x
50 mph	x		

H78-14 tires

	Load		
Speed	800	1100	1700
20 mph		μ, x	
40 mph	μ, x	μ, x	x
50 mph		x	

---

x = free rolling

μ = μ-slip curves at $\alpha = 0$ and $\alpha = 4$.

Table 4-3. Wet Tests for the Tread-Worn Tires.

B.F. Goodrich Silvertown E78-14, 24 psi

Tread Depth	
2/32	40 mph - 800 lbs, 1100 lbs
4/32	40 mph - 800 lbs
6/32	40 mph - 800 lbs

Firestone Deluxe Champion H78-14, 28 psi

2/32	40 mph - 800 lbs, 1100 lbs

---

tread pattern, speed, and water depth, it is not surprising that the highest peak forces measured on the wet surface are not necessarily associated with the same tires as the highest peak forces measured on the dry surface.

4.3 FINDINGS FROM VEHICLE TESTS CONDUCTED ON A WET SURFACE

Three of the vehicle handling test procedures were performed on a wet surface, namely, straight-line braking, braking in a turn, and sinusoidal steer. The results of the straight-line braking tests are considered first.

The straight-line braking test procedure employed during wet-surface testing was similar to the dry-surface procedure. However, the initial velocity was reduced to 30 mph, rather than using 40 mph as was done in the tests conducted on the dry surface.

Table 4-4 presents the straight-line braking data for the OE Mustang and for various Mustang tire-in-use configurations. The OE vehicle reached almost .6 g before locking both front

Table 4-4a. Wheel Locks for the Straight Line Braking Tests. Mustang, Wet Jennite.

Tire Configur. \ P_b (psi)	300	325	350	375	400	425	500
11 (O.E.)	None				None	1,2,4 1,2 1,2,4	1,2,4
12 (psi all 18)				1 1	None 1,2	None 1,2 1,2,4	
15 (Wear all 6/32)	None None	1,2	1,2	1,2	1,2	1,2 1,2	
14 (Wear all 4/32)				1,2 2 2	1,2	1,2 1,2	
13 (Wear all 2/32)	2 2	2 1,2	1,2	1,2	1,2,4	1,2,4 1,2,4	

VEHICLE - MUSTANG NUMERIC - WHEEL LOCK

VHTP - #7, Straight-Line Braking (Wet)

P_b = brake line pressure

1 = left-front lockup

2 = right-front lockup

3 = left-rear lockup

4 = right-rear lockup

Table 4-4b. Average Deceleration (g's) for the Straight-Line Braking Tests, Mustang, Wet Jennite.

Tire Configur. \ P_b (psi)	300	325	350	375	400	425	500
11 (O.E.)	.38				.53 .58	.45 .50 .46	.46
12 (psi all 18)				.52 .56	.63 .50	.64 .50 .45	
15 (Wear all 6/32)	.41 .39	.38	.38	.43	.42	.47 .46	
14 (Wear all 4/32)				.43 .45 .41	.40	.43 .39	
13 (Wear all 2/32)	.37 .36	.39 .39	.41	.44	.45	.44 .41	

VEHICLE - MUSTANG NUMERIC - AX_{AV}

VHTP - #7, Straight-Line Braking (Wet)

wheels (and one rear wheel in some cases).* Though no degradation in the decelerations was recorded due to lowered inflation pressure (in fact, in one case .64 g was measured), the vehicle with worn-tire configurations performs quite poorly by comparison. In the extreme case, the Mustang with 2/32-inch tread depth on all four wheels, the vehicle could not reach 0.4 g's without locking both front wheels.

In the case of the Buick, straight-line braking and braking-in-a-turn procedures did not lead to clear-cut results. This was because the Buick locked its rear wheels first on the wet surface. Since the rear tires of the Buick were exposed to a surface whose water depth is disturbed by the front tires, it is not surprising that more scatter was obtained in the Buick tests than in the Mustang tests. The Buick test results were further complicated because extreme sideslip angles were often attained when the rear wheels locked. Under these conditions, the longitudinal deceleration and speed, as measured by a fifth wheel, are difficult to interpret.

The braking-in-a-turn metrics used for the Mustang are summarized in Table 4-5. Since a 0.3 g steady turn is difficult to maintain on wet jennite, the braking-in-a-turn measurements were taken starting from an initial 0.2 g turn rather than the 0.3 g turn specified for the dry surface. (The entire data set is presented in Appendix F.)

The RATIO metric indicates the quotient of the pre-braking steady-turn path curvature divided by the average path curvature from the time of the brake application until the vehicle decelerates to ten miles per hour. The negative RATIO values in Table 4-5c indicate a sign change between the initial value

*Dynamometer test results indicate that the front-to-rear brake proportioning varies with brake line pressure for the Mustang. At 400 psi, the front brake torque is approximately twice the rear brake torque. Simplified braking calculations for the Mustang show that the front wheels will lock for decelerations below approximately 0.59 g and the rear wheels will lock for decelerations above 0.59 g.

Table 4-5a. Wheel lockup for the braking-in-a-turn tests. Mustang, Wet Jennite.

Tire Configur.	P_b (psi) 275	300	325	350	375	400	425	450	475	500
11 (O.E.)		2 None None	None 2	2		1,2,4				
12 (psi all 18)			2 2	2 1,2 2	1,2	1,2,4				
16 (Mix PR F)	1	1,2 1,2 1,2 1	1,2 1,2	1,2,4	1,2 1,2 1,2	1,2,4 All				
17 (Mix CPCP F)			1 1		1,2 1,2	1,2,4 1,2,4				
18 (Wear 2/32 R)						2,4 2,4	2,4 2,4	All 1,2,4		
19 (Wear 4/32 R)						2,4 1,2,4 2,4 2 2	1,2,4 2,4 1,2,4 2,4 2	1,2,4 1,2,4		
20 (Wear 6/32 R)		1,2 2 1 1 1,2	1,2	1,2	2 1,2 1,2	2 2,4 1,2,4 1,2 1,2	1,2,4 2,4		2,4	1,2,4

VEHICLE - MUSTANG DIRECTION - RIGHT

VHTP - #8, Braking in a Turn (Wet) NUMERIC - WHEEL LOCK

Wheel Lock Code

1 left front

2 right front

3 left rear

4 right rear

Table 4-5b. Average Deceleration for the Braking-In-A-Turn Maneuver. Mustang, Wet Jennite.

Tire Configur.	P_b (psi) 275	300	325	350	375	400	425	450	475	500
11 (O.E.)		.47 .40 .40	.46 .43	.44		.40				
12 (psi all 18)			.49 .47	.50 .43 .50	.47	.44				
16 (Mix PR F)	.38	.42 .40 .40 .41	.44 .43	.41	.48 .46 .46	.45 .43				
17 (Mix CPCP F)			.42 .43		.43 .41	.40 .40				
18 (Wear 2/32 R)						.46 .47	.49 .46	.37 .44		
19 (Wear 4/32 R)						.47 .40 .46 .51 .47	.41 .50 .45 .48 .53	.44 .43		
20 (Wear 6/32 R)		.36 .38 .38 .39 .35	.38	.41	.55 .45 .44	.48 .42 .40 .45 .46	.41 .48		.51	.44

VEHICLE - MUSTANG DIRECTION - RIGHT

VHTP - #8, Braking in a Turn (Wet) NUMERIC - AX_{AV}

Average Deceleration in g's

Table 4-5c. Path Curvature RATIO. Mustang, Wet Jennite.

Tire Configur.	P_b (psi) 275	300	325	350	375	400	425	450	475	500
11 (O.E.)		.74 1.64 1.61	1.65 .88	.99		.14				
12 (psi all 18)			.68 .25	.69 .55 .60	-.21	1.5				
16 (Mix PR F)	1.41	.25 .12 .22 1.50	.08 .08	0.0	.15 .10 .24	-.14 -.10				
17 (Mix CPCP F)			1.64 1.68		.23 .24	-.08 -.12				
18 (Wear 2/32 R)						.64 .89	.66 .49	-.12 .09		
19 (Wear 4/32 R)						.64 .04 .75 .88 .99	-.19 .50 .13 .52 1.30	.20 .15		
20 (Wear 6/32 R)		.45 1.30 2.0 1.8 .33	.21	.15	.66 .54 .62	.81 .82 .31 .77 .55	.15 .73		0.0	0.0

VEHICLE - MUSTANG DIRECTION - RIGHT

VHTP - #8, Braking in a Turn (Wet) NUMERIC - RATIO

and the average value of path curvature, i.e., negative values of RATIO mean that the vehicle mass center began to veer to the left rather than continuing the initial right turn. In each case, this behavior was symptomatic of the lockup of both front wheels, thus effectively removing the tendency to turn right. The left-turning behavior was either initiated by imbalance of the longitudinal forces due to the locking up of only the left rear wheel (as in configuration #17, 400 psi), or by the variations in friction existing at the tire-road interface due to variations in water depth.

The braking-in-a-turn results are interesting and informative for pointing out the difficulties in performing wet-surface testing. However, they did not provide useful findings with respect to tire-in-use factors. In contrast, the sinusoidal steer maneuvers yielded such startling and repeatable disparities between the worn and non-worn tire configurations that the results retain their impact for tire-surface combinations only remotely similar to the conditions at TTI.

Before discussing these data and findings, some remarks are in order concerning the choice of the test conditions selected to conduct the sinusoidal steer maneuvers on the wet surface. First, note that calculations can yield useful insights into the class of response characteristics that would be considered statistically probable for given vehicles on a "typical" wet surface. However, computer simulation is not as effective a tool for the design of a wet-test program as it is for a dry-test program, since the wet-surface tire data to be loaded into the simulation is likely to be substantially different from the conditions prevailing in a particular test. Thus, whether simulation is used or not, vehicle test programs on a wet surface must be based only on past experience and an intuitive sense of the wet surface properties expected to occur during vehicle testing.

For the present investigation, it was originally decided to run the sinusoidal steer tests from an initial speed of 30 mph, rather than 45 mph, as on the dry surface. In addition, the $\sigma = 2$ steer amplitude was to be included, since it was felt that interesting results might be found even at such a low steer level. The very highest steer level was dropped as a meaningless extreme on a surface with such a low shear stress limit.

The Buick was the first test vehicle outfitted with the controller, and thus was the first vehicle to be run through the above sinusoidal steer test matrix. (All of the measured results from this testing are presented in Appendix F.) The results of this exercise were nondescript—every tire configuration yielded a creditable performance under these conditions. This, of course, did not indicate that each of the configurations would perform similarly well in the lane-change maneuver on other wet surfaces or at higher speeds.

To try to gain more insight into the wet-surface performance of the various tire configurations, an additional test program was performed for the OE and the worn tire configurations. In the additional program, mid-range sinusoidal steer maneuvers were run on the wet surface as speed was varied. At 40 mph initial speed, a vehicle with the 2/32-inch tread condition was found to spin out violently at 175° steer ($\sigma' = 8$) and above, while the other conditions remained under control. At 45 mph, however, the OE as well as all the worn tire configurations were found to spin out.

Based on these results, all the Mustang lane-change maneuvers on the wet surface were performed at 40 mph rather than 30 mph. In this case, the findings from the Buick tests were duplicated; that is, all configurations except the 2/32-inch rear tires yielded a creditable performance. Mustang testing had to be suspended in the mid-range for the 2/32-inch

tread depth configuration, however, to ensure the safety of the test personnel and preserve the test equipment. This is reflected in the peak sideslip angle metrics presented in Table 4-6. Note that the vehicle is very well behaved for configuration #25 (OE front, 2/32-inch of tread on rear tires) at $\sigma' = 8$ (155° steer), but that at $\sigma' = 10$ (193° steer) a violent "spin out" occurs. The suddenness of this transition from a reasonable lane-change response to a dramatic spin out is apparent in the time histories of yaw rate and lateral acceleration presented in Figure 4-3. Note that the first and second half of the lane-change cycle are nearly identical for the σ' equal to 8, and for $\sigma' = 10$ up to a point in the second half of the lane change (i.e., in the recovery half). At this point the yaw rate suddenly diverges for the $\sigma' = 10°$ case, approaching the extreme value of 60 degrees/second.

Table 4.6 Mustang, Peak Sideslip Angle in Sinusoidal Steer Maneuvers on a Wet Surface.

Tire Configur. \ σ'	4°	6°	8°	10°	12°	14°	16°	18°
21 (O.E.)	3/4	4/3	6/4	7/5	X/5	7/4	7/6	7/7
22 (psi 18 rear)	3/2	4/3	7/4	10/5	X/X	12/X	10/6	8/6
23 (Mix PR front)	3/3	5/4	4/6	5/4	6/5	6/5	6/4	5/4
24 (Mix CPCP front)	3/4	X/3	5/4	4/4	6/3	X/4	6/2	X/4
25 (Wear 2/32 rear)	2/1	X/1	4/3	S/S	S/	—	—	—
26 (Wear 4/32 rear)	2/X	3/4	4/3	4/X	X/X	X/X	5/6	4/5
27 (Wear 6/32 rear)	3/4	4/4	6/X	6/3	5/5	5/6	5/6	5/6
28 (Shoulder	1/2	2/X	3/3	5/5	4/4	3/3	4/3	3/3

VEHICLE - MUSTANG

VHTP - #9, Sine Steer (Wet)

NUMERIC - $|\beta_p|$

S - Denotes Spin-out

β_p in degrees

X indicates no data available

S indicates a dramatically increasing sideslip angle response (spin out)

Note: The dual entries (e.g., 3/4) indicate the maximum sideslip angle obtained in lane changes to the left and to the right, respectively.

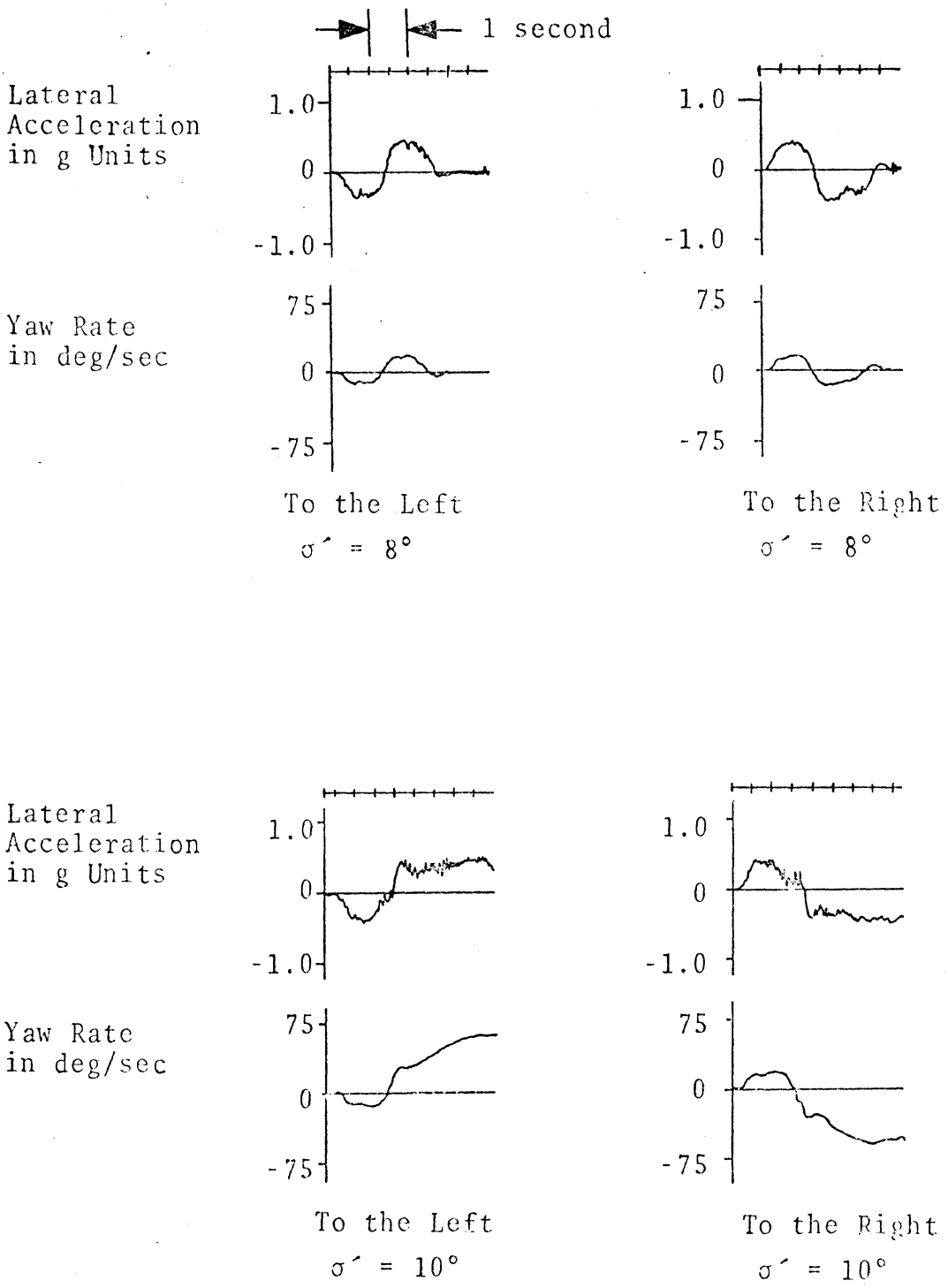

Figure 4-3. Mustang lane changes on a wet surface with rear tires worn to 2/32" groove depth.

5.0 INFLUENCE OF IN-USE TIRE FACTORS ON NORMAL DRIVING MANEUVERS

Tire-in-use factors can have a first-order influence on linear-range tire-stiffness properties (i.e., cornering stiffness, C_α, camber stiffness, C_γ, and aligning torque stiffness, AT_α). Large changes in these stiffness properties can cause the directional stability and response of the motor vehicle to depart from that intended by the manufacturer to an extent that the human operator may experience control difficulties during the execution of ordinary driving tasks. Accordingly, this section deals with changes in vehicle stability and response that, presumably, could degrade the pre-crash safety quality of a motor vehicle during normal driving.

In the next section, a theoretical discussion of the meaning of the understeer/oversteer factor, K, is presented. In Section 5.2, the experimental approach used in this study to measure K is described, followed by a comparison of calculated and measured values of K in Section 5.3. Finally, in Section 5.4, calculated values of understeer/oversteer factor are used in an examination of the influence of inflation pressure, tread wear, and replacement tire-mix on the performance of the 1971 Mustang and 1973 Buick in the normal driving range.

Although the understeer/oversteer factor, K, is primarily a measure of steady-state turning performance, qualitative insight into the transient response of a particular vehicle may be obtained from the value of K. Accordingly, the understeer/oversteer factor has been used in this study to provide an indication of the change in normal driving performance caused by tire-in-use factors. Admittedly, transient response is not entirely determined by the value of K, but for the vehicles and tire conditions considered in this investigation K proves to be a meaningful indicator of changes in vehicle directional response in the normal driving range resulting from tire-in-use factors. This matter is discussed in greater detail in Section 5.4.4.

5.1 THEORETICAL CONSIDERATIONS

5.1.1 INTERPRETING NORMAL DRIVING PERFORMANCE USING AN UNDERSTEER/OVERSTEER FACTOR. The results of linear analysis [5] show that the steady turning performance of passenger cars can be summarized by an equation of the form:

$$\frac{\delta_{sw}}{N_g} = \frac{57.3\ell}{R} + K\frac{A_y}{g} \qquad (5.1)$$

where

δ_{sw} = steering wheel angle (deg)

N_g = total steering ratio

ℓ = wheel base (ft)

R = radius of the path (ft)

K = the understeer/oversteer factor (deg/G)*

g = gravitational constant (ft/s^2)

A_y = lateral acceleration (ft/s^2)

The value of the understeer/oversteer factor, K, which is dependent upon many tire and vehicle parameters, can be determined both theoretically and experimentally. (The experimental determination of K will be discussed in Sections 5.2 and 5.3.)

A vehicle's motion sensitivity to steering wheel inputs can be readily derived from Equation (5.1) using the basic relationships for travel on a circular path at constant velocity, viz.,

$$A_y = u^2/R = ur \qquad (5.2)$$

*Capital "G" represents units of lateral acceleration expressed in normalized non-dimensional form. The normalizing factor used is the gravitational constant, g.

where r is the yaw rate (rad/s) and u is the velocity. The path-curvature gain is defined as:

$$\left(\frac{\left(\frac{1}{R}\right)}{\delta_{sw}}\right) = \frac{1}{N_g\left(57.3\ell + \frac{Ku^2}{g}\right)} \tag{5.3}$$

The lateral-acceleration gain is defined as:

$$\left(\frac{A_y}{\delta_{sw}}\right) = \frac{1}{N_g\left(\frac{57.3\ell}{u^2} + \frac{K}{g}\right)} \tag{5.4}$$

and the yaw-rate gain is:

$$\left(\frac{r}{\delta_{sw}}\right) = \frac{1}{N_g\left(\frac{57.3\ell}{u} + \frac{Ku}{g}\right)} \tag{5.5}$$

For a particular vehicle for which steering ratio, N_g, and wheel base, ℓ, are fixed the steering gains are functions of the velocity, u, and the understeer/oversteer factor, K (see Equations (5.3), (5.4), and (5.5)). Large positive values of K, corresponding to a highly understeer vehicle, tend to make the path curvature gain low at high velocities. On the other hand, small values of K can cause the lateral acceleration gain to become large at high speed.

Furthermore, for negative values of K, corresponding to an oversteer vehicle, there exists a speed, called the "critical speed," for which the path-curvature gain is infinite. At this speed the vehicle becomes dynamically unstable.* In the vicinity of this stability limit, the

*See Appendix C for a mathematical discussion of the linear analysis of passenger-car directional response.

average driver would find the path-curvature gain to be very high. Consequently, he would have great difficulty maintaining a steady path in the presence of any external disturbances.

The understeer/oversteer factor can also be used to gain insight into the dynamic response of the vehicle. Linear analysis shows that the directional response of an oversteer vehicle operated above the critical speed is characterized by an exponential instability [5]. When operated at speeds below the critical speed, the transient response of the oversteer vehicle dies out slowly taking a relatively long time to reach steady state. In contrast, the highly understeer vehicle approaches its equilibrium response rapidly, but the response may be lightly damped, creating the possibility of overshooting the steady-state path at high speeds of travel.*

The understeer/oversteer factor, K, is primarily a measure of steady-state turning performance. Qualitative insights into vehicle transient response may be obtained from the value of K, but a quantitative evaluation requires a more detailed analysis. For evaluating transient response the methods of linear analysis presented in Appendix C can be used to obtain root loci, frequency response plots, and step steering responses. In the time domain, factors such as response time, percentage overshoot, and settling time can be used to measure transient performance.

Recently, a "cornering compliance concept" [6 , 7] has been used to examine transient response time. In this concept, the understeer/oversteer factor is separated into two components—a cornering compliance of the front wheels and a cornering compliance of the rear wheels (i.e., the front and rear contributions to understeer). The results of this work

*Note, however, that the path-curvature gain (see (5.3)) is lower for the understeer vehicle than for the oversteer vehicle. Thus the response to steering of the oversteer vehicle is not necessarily more "sluggish" than the response of the understeer vehicle.

indicate that "shorter response times are more effectively obtained through added understeer at the rear suspension than with front suspension understeer" [6]. Recently, this approach has been used to study the influence of tire intermix (as caused by replacement and usage) on vehicle performance [7].

In the next section, an expression relating K to tire and vehicle parameters is presented in a form that clearly indicates the contribution to understeer from the front and rear running gear.

5.1.2 THE INFLUENCE OF TIRE AND VEHICLE PARAMETERS ON THE UNDERSTEER/OVERSTEER FACTOR. The purpose of this section is to provide a theoretical basis for explaining the results obtained in the linear performance study. In this section an algebraic expression for K is presented to specify (1) how tire parameters influence K (and thus, normal maneuvering performance) and (2) how vehicle properties can alter the influence of the tire parameters.*

The tire parameters of importance in the normal driving range are cornering stiffness, C_α, the camber (inclination) stiffness, C_γ, and the aligning torque stiffness, AT_α. These parameters are defined as follows:

$$(1) \qquad C_\alpha = \left. \frac{-\partial F_y}{\partial \alpha} \right|_{\alpha=0,\ \gamma=0}$$

(Thus, cornering stiffness is the negative of the slope of the lateral force, F_y, versus slip angle (α) curve for a tire evaluated at inclination (camber) angle, γ, and slip angle, α, equal to zero.)

*Readers interested in more fundamental discussions should find references 5 and 6 useful. For the expert, this material defines the point of view used in this study.

$$(2) \qquad C_\gamma = \left.\frac{\partial F_y}{\partial \gamma}\right|_{\alpha=0,\ \gamma=0}$$

(Thus, camber stiffness is the rate of change of lateral force with respect to inclination angle, γ, evaluated at $\gamma=\alpha=0$.)

$$(3) \qquad AT_\alpha = \left.\frac{\partial M_z}{\partial \alpha}\right|_{\alpha=0,\ \gamma=0}$$

(Thus, aligning torque stiffness is the rate of change of the moment about a vertical axis through the wheel center with respect to slip angle evaluated at $\alpha=\gamma=0$.) More detailed definitions of these parameters are given in SAE Special Publication J-670c [20].

The forces and moments created by the tires installed at the front and rear of the vehicle are determined by the above-defined stiffnesses and the slip angles and camber angles created by vehicle motion. In the classical "bicycle model," the average slip angle for the front wheels is given by:

$$\alpha_F = \beta + \frac{ar}{u} - \delta_F \qquad (5.6)$$

where

β is the vehicle sideslip angle

a is the distance from the center of gravity to the front wheels

r is the yaw rate

u is the forward velocity

δ_F is the average front-wheel steer angle.

The average front-wheel steer angle, at a given steering-wheel angle, depends mainly on steering gear ratio, but suspension

roll properties and steering and suspension-system compliances can be important factors.

The average front-wheel steer angle is given by the following expression:

$$\delta_F = \frac{\delta_{sw}}{N_g} + K_{frs}\,\phi + \left(\frac{AT_F}{K_{ss}}\right)\alpha_F + \left(E_{YF}\right)Y_F \qquad (5.7)$$

where

K_{frs} is the front roll-steer coefficient, relating front-wheel toe angles to the sprung mass roll angle

ϕ is the roll angle of the sprung mass

AT_F is the total aligning torque stiffness for both front wheels (i.e., $AT_F = 2AT_\alpha$ assuming equal aligning torque stiffnesses for both front tires)

K_{ss} is the total steering-system stiffness

E_{YF} is the lateral-force compliance-steer coefficient of the front wheels

Y_F is the total lateral force on both front wheels.

The average camber angle of the front wheels is given by:

$$\gamma = K_{\gamma\phi}\,\phi + K_{\gamma F}Y_F \qquad (5.8)$$

where $K_{\gamma\phi}$ is the rate of change of average camber angle with roll angle of the sprung mass and $K_{\gamma F}$ is the rate of change of average camber angle with lateral force applied at the front wheels. Finally, the total lateral force acting on the front tires is given by:

$$Y_F = -C_{\alpha F}\alpha_F + C_{\gamma F}\gamma \tag{5.9}$$

where

$C_{\alpha F}$ is the sum of the cornering stiffnesses of both front tires (i.e., $C_{\alpha F} = 2C_\alpha$, assuming identical front tires)

$C_{\gamma F}$ is the sum of the camber stiffnesses of both front tires (i.e., $C_{\gamma F} = 2C_\gamma$, assuming identical front tires).

Equations (5.6) through (5.9) may be solved simultaneously to express lateral force acting on the front tires as a function of (1) the basic motion variables, β, r, and ϕ, and (2) the steering wheel angle, δ_{sw}. In order to single out the interaction of front suspension and steering system properties with the linear tire properties, it is useful to write the expression for the lateral force created at the front tires in the following form:

$$Y_F = -C^*_{\alpha F}(\beta + \frac{ar}{u} - \delta - K^*_{frs}\phi) + C^*_{\gamma F}K_{\gamma\phi}\phi \tag{5.10}$$

where

$$C^*_{\alpha F} = \frac{C_{\alpha F}}{(1-C_{\gamma F}K_{\gamma F})(1 + \frac{AT_F}{K_{ss}}) - E_{YF}C_{\alpha F}} \tag{5.11}$$

$$\delta = \delta_{sw}/N_g$$

$$K^*_{frs} = K_{frs} + \frac{E_{YF}C_{\gamma F}K_{\gamma\phi}}{1-C_{\gamma F}K_{\gamma F}} \tag{5.12}$$

$$C^*_{\gamma F} = \frac{C_{\gamma F}}{1-C_{\gamma F}K_{\gamma F}} \tag{5.13}$$

The quantity $C^*_{\alpha F}$ given by (5.11) is defined here to be the "equivalent front cornering stiffness." Similarly, $C^*_{\gamma F}$ is defined to be the "equivalent front camber stiffness." The lateral force compliance effects denoted by E_{YF} and $K_{\gamma F}$ are usually negative. Thus E_{YF} tends to reduce the influence of the cornering stiffness as shown in (5.11), and $K_{\gamma F}$ tends to reduce the influence of both the cornering and camber stiffnesses as shown in (5.11) and (5.13).* In addition, the ratio of the aligning-torque stiffness to the steering-system stiffness reduces the equivalent front cornering stiffness of the vehicle.

For many solid rear axle suspensions, the lateral-force compliances are small. In addition, the rear wheels do not camber significantly when the body rolls. Under these circumstances, we can state that the lateral force created at the rear wheels is given by:

$$Y_R = -C^*_{\alpha R}(\beta - \frac{br}{u} - K^*_{rrs}\phi) \tag{5.14}$$

where

$$C^*_{\alpha R} = \frac{C_{\alpha R}}{(1+\frac{AT_R}{K_{ssR}})} \tag{5.15}$$

---

*The quantities E_{YF} and $K_{\gamma F}$ were not measured in this program, since they are difficult to measure without special apparatus of the type described in [21]. They are believed, however, to be of negligible importance in the case of the Mustang. For the Buick station wagon, these quantities may be important in establishing the absolute value of the understeer/oversteer factor. However, in this investigation, results demonstrating the influence of tire-in-use factors on normal driving performance were obtained through calculations in which E_{YF} and $K_{\gamma F}$ were ignored. Calculations using estimated values of E_{YF} and $K_{\gamma F}$ showed that the basic conclusions concerning tire-in-use factors were not significantly changed by the inclusion or omission of E_{YF} and $K_{\gamma F}$.

$C^*_{\alpha R}$ is the equivalent rear cornering stiffness

$C_{\alpha R}$ is the sum of the cornering stiffnesses of the rear tires

AT_R is the sum of the aligning-torque stiffnesses of the rear tires

K_{ssR} is the steering stiffness of the rear axle

K^*_{rrs} is the roll steer coefficient of the rear axle

and b is the distance from the center of gravity to the rear axle.

The average slip angle of the rear wheels, α_R, is given by:

$$\alpha_R = \left(\frac{\beta - \frac{br}{u} - K^*_{rrs}\phi}{1 + \frac{AT_R}{K_{ssR}}} \right) \tag{5.16}$$

In a steady turn, static equilibrium requires that the following three equations be satisfied, viz:

(a) The lateral force equation: $m \cdot u \cdot r = Y_F + Y_R$ (5.17)

(b) The yaw moment equation: $0 = aY_F - bY_R + N_F + N_R$ (5.18)

(c) The roll equation: $\phi = K_\phi (\frac{ur}{g})$ (5.19)

where

m is the total mass of the vehicle

N_F is the aligning moment from the front wheels ($N_F = AT_F\alpha_F$)

N_R is the aligning moment from the rear wheels ($N_R = AT_R\alpha_R$)

and K_ϕ is the roll coefficient in degrees roll per G of lateral acceleration.

(The roll coefficient, K_ϕ, is a function of the total suspension roll stiffness, the weight of the sprung mass, and the height of the sprung mass center of gravity above the roll axis. Note that K_ϕ is always a negative quantity since a positive acceleration produces a negative roll angle.)

By combining the equilibrium equations into a single expression relating steering wheel angle to path curvature and lateral acceleration (that is, by expressing the equilibrium equations in the form of Equation (5.1)), the understeer/oversteer factor, K, can be identified as a function of tire and vehicle parameters. The resulting algebraic expression for K is presented here as the sum of three main terms for ease of application and interpretation, viz.:

$$K = K_1 + K_2 + K_3 \tag{5.20}$$

where

$$K_1 = -mgB \tag{5.21}$$

$$\text{where} \quad B = \left(\frac{C_{\alpha F}{}^* a^* - C_{\alpha R}{}^* b^*}{(a^*+b^*) C_{\alpha F}{}^* C_{\alpha R}{}^*} \right)$$

$$K_2 = K_\phi (B)(C) \tag{5.22}$$

$$\text{where } C = C^*_{\alpha F} K^*_{frs} + C^*_{\gamma F} K_{\gamma\phi} + C^*_{\alpha R} K^*_{rrs}$$

and $K_{\gamma\phi R}$ is assumed to be negligibly small

and

$$K_3 = -K_\phi (D)(E) \tag{5.23}$$

$$\text{where} \quad D = \frac{C^*_{\alpha F} + C^*_{\alpha R}}{C^*_{\alpha F} C^*_{\alpha R} (a^*+b^*)}$$

$$\text{and} \quad E = aC^*_{\gamma F} K_{\gamma\phi} + a^* C^*_{\alpha F} K^*_{frs} - b^* C^*_{\alpha R} K^*_{rrs}$$

The dimensions a* and b* are the values of a and b modified to take into account the influence of pneumatic trail on the point of application of the tire forces. Specifically,

$$a^* = a - (1-C_{\gamma F}K_{\gamma F})\left(\frac{AT_F}{C_{\alpha F}}\right)$$

$$b^* = b + \left(\frac{AT_R}{C_{\alpha R}}\right)$$

Usually, $C_{\gamma F}K_{\gamma F}$ is a relatively small quantity and

$$a^* \approx a - X_{PF}$$

where X_{PF} is the pneumatic trail of the front tires, $X_{PF} = \frac{AT_F}{C_{\alpha F}}$

and $$b^* = b + X_{PR}$$

where X_{PR} is the pneumatic trail of the rear tires, $X_{PR} = \frac{AT_R}{C_{\alpha R}}$.

The quantity K_1 in Equation (5.20) is determined by the most basic properties of the vehicle-tire system that govern understeer. As such, it may be expressed as the difference between the front and rear cornering compliance coefficients, D_F and D_R, defined here as

$$K_1 = D_F - D_R \tag{5.24}$$

where

$$D_F = \frac{mg\ b^*}{(a^*+b^*)}\left(\frac{1}{C^*_{\alpha F}}\right) \tag{5.25}$$

and

$$D_R = \frac{mg\ a^*}{(a^*+b^*)}\left(\frac{1}{C^*_{\alpha R}}\right) \tag{5.26}$$

Note that since

$$\frac{b^*}{a^* + b^*} \approx \frac{b}{a + b}$$

and

$$\frac{a^*}{a^* + b^*} \approx \frac{a}{a + b} ,$$

$$D_F \approx \frac{W_F}{C^*_{\alpha F}}$$ where W_F is the sum of the static loads on the front wheels

and

$$D_R \approx \frac{W_R}{C^*_{\alpha R}}$$ where W_R is the sum of the static loads on the rear wheels.

Thus, K_1 is the contribution to understeer deriving from the location of the center of mass and the values of the equivalent front and rear cornering stiffnesses.

The values of K_2 and K_3, given by (5.22) and (5.23), depend on the total roll stiffness, K_ϕ, and all the other roll related parameters. These terms describe the influence of the vehicle's roll properties on the understeer/oversteer factor.

As can be seen by examining Equations (5.20) through (5.23), many vehicle and tire parameters have an influence on the value of the understeer/oversteer factor. For the vehicles and in-use tire factors considered in this investigation, this degree of complexity is needed to explain the results obtained. All three tire stiffnesses and the steering and suspension-system compliances, which contribute to the equivalent front cornering stiffness, are important.

5.2 EXPERIMENTAL METHOD

The constant steering-wheel-angle test procedure was used to evaluate the understeer/oversteer factor for several different tire-in-use conditions and the original equipment

condition for both the Buick station wagon and the Mustang. This particular test method was chosen primarily because the outfitting of the vehicles for the driver-controlled limit maneuver tests was most suitable for conducting constant steer-wheel-angle tests. Other advantages of this method are (1) very little driver skill is required to perform this test, and (2) the understeer/oversteer factor can be determined without complications due to lash in the steering system or variable steering-gear ratio.

The transducers selected for limit maneuver testing were also used in the linear range vehicle tests. The quantities measured in the linear range tests were yaw rate, velocity, and lateral acceleration. The accelerometer was mounted on a stable platform, thereby eliminating the need for measuring roll angle. The proper operation of the test instruments was checked throughout the program by comparing the product of the yaw rate and velocity with the lateral acceleration measured in a steady turn. The estimated error tolerances of the transducers were as follows:

Lateral acceleration:	$\pm$ 0.02 g
Longitudinal velocity:	$\pm$ 0.5 mph
Yaw rate:	$\pm$ 1.0 deg/sec.

Satisfactory results were obtained by averaging readings from a large number of data samples. However, higher quality results can be obtained by using instruments with narrower error tolerance bands.

The steering wheel limiter built for the driver-controlled limit-maneuver tests [1] was used to set the steer angle. The driver's primary function was to modulate the throttle to vary vehicle speed.

FM analog tape recordings of the test data were made for subsequent computer processing.

A method of checking based on a procedure suggested in [22] was used to help ensure meaningful results. In this procedure a constant radius path marked on the test pad is followed by the driver while gradually increasing speed. Path curvature computed from the test data (i.e., r/u and A_y/u^2) was compared with the known path curvature to provide an additional check on the transducers and data recording equipment.

Extremely accurate measurements of vehicle motion are needed to determine the understeer/oversteer factor accurately. All the checks used in this program proved to be helpful for ensuring proper evaluation of the test data.

5.3 COMPARISON OF VEHICLE TEST RESULTS WITH CALCULATED VALUES OF UNDERSTEER/OVERSTEER FACTOR

Vehicle tests were performed to (1) provide experimental evidence of the influence of tire-in-use factors on normal driving performance and (2) verify the validity of the theoretical calculations. (The validity of the theoretical calculations depends not only on the quality of the vehicle model but on the accuracy with which vehicle and tire parameters have been measured.)

The 1971 Mustang, equipped with OE tires, produced the data plotted in Figure 5-1, which data derive from the constant steering-wheel test procedure. Note that the data points for path curvature have been plotted versus lateral acceleration over a range extending from 0.20 g to 0.32 g. This range of lateral acceleration was chosen because (1) the percentage errors in the measured data become large at lower levels of lateral acceleration, and (2) the vehicle's roll parameters were evaluated at a roll angle corresponding to about a 0.25 g turn.

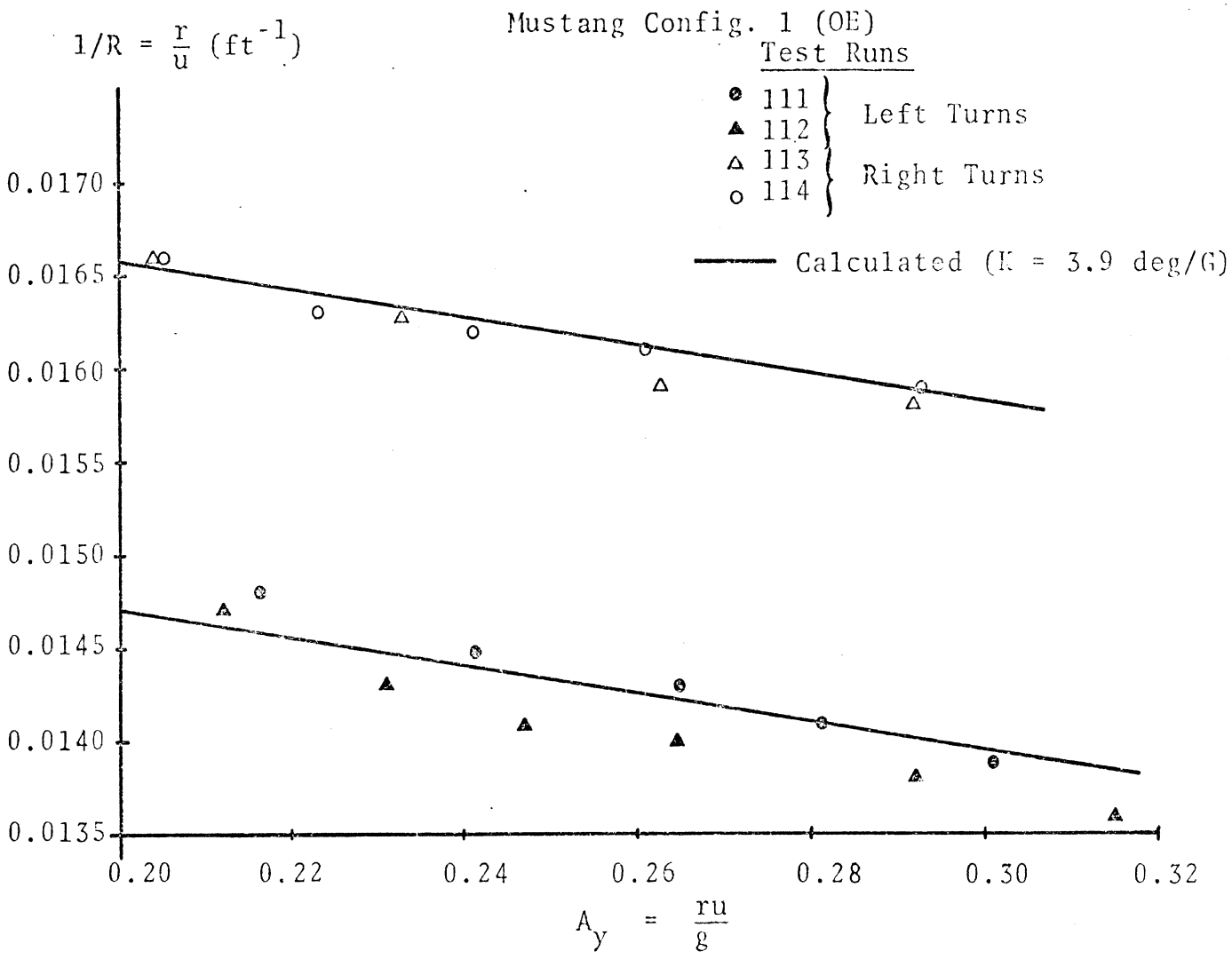

Figure 5-1. Calculated and measured results for the OE Mustang.

The slope of the solid line superimposed on the test data in Figure 5-1 was determined by the value of K calculated by using the digital computer program described in Appendix C. (The slope, S, of this line is related to K by the equation:

$$K = -57.3\, S(\ell)$$

Examination of Figure 5-1 indicates that the test results are repeatable and that the test data fall along the calculated slope reasonably well for the original equipment vehicle.

Figure 5-2 shows results obtained with the Mustang using OE tires but with the front tires inflated to only 12 psi. The greater negative slope of the solid line indicates that the vehicle has much more understeer in this latter condition than in the OE condition. Again, the agreement between simulation and test is reasonably good up to a lateral acceleration of about 0.28 g. Note that the linear range of vehicle performance does not extend above a lateral acceleration of approximately 0.28 g, presumably because of the relatively large slip angles required at the front tires for equilibrium. Thus the vehicle becomes more understeer above 0.28 g due to nonlinearities in the relationship between lateral force and slip angle.

Further evidence of the agreement between calculated and measured results is presented in Figures 5-3, 5-4, and 5-5. These figures apply respectively to the following tire-in-use configurations: rear tires inflated to 12 psi, front tires reduced to a 2/32-inch tread depth, and the Pirelli radials* installed on the front wheels.

---

*In the case of the Pirelli tires, logistical problems made it necessary to purchase tires for vehicle testing which were not from the same production lot as the tires used for tire testing. The results shown in Figure 5-5 indicate that the tires used in the vehicle tests may have had a higher cornering stiffness than the tires used in the tire tests.

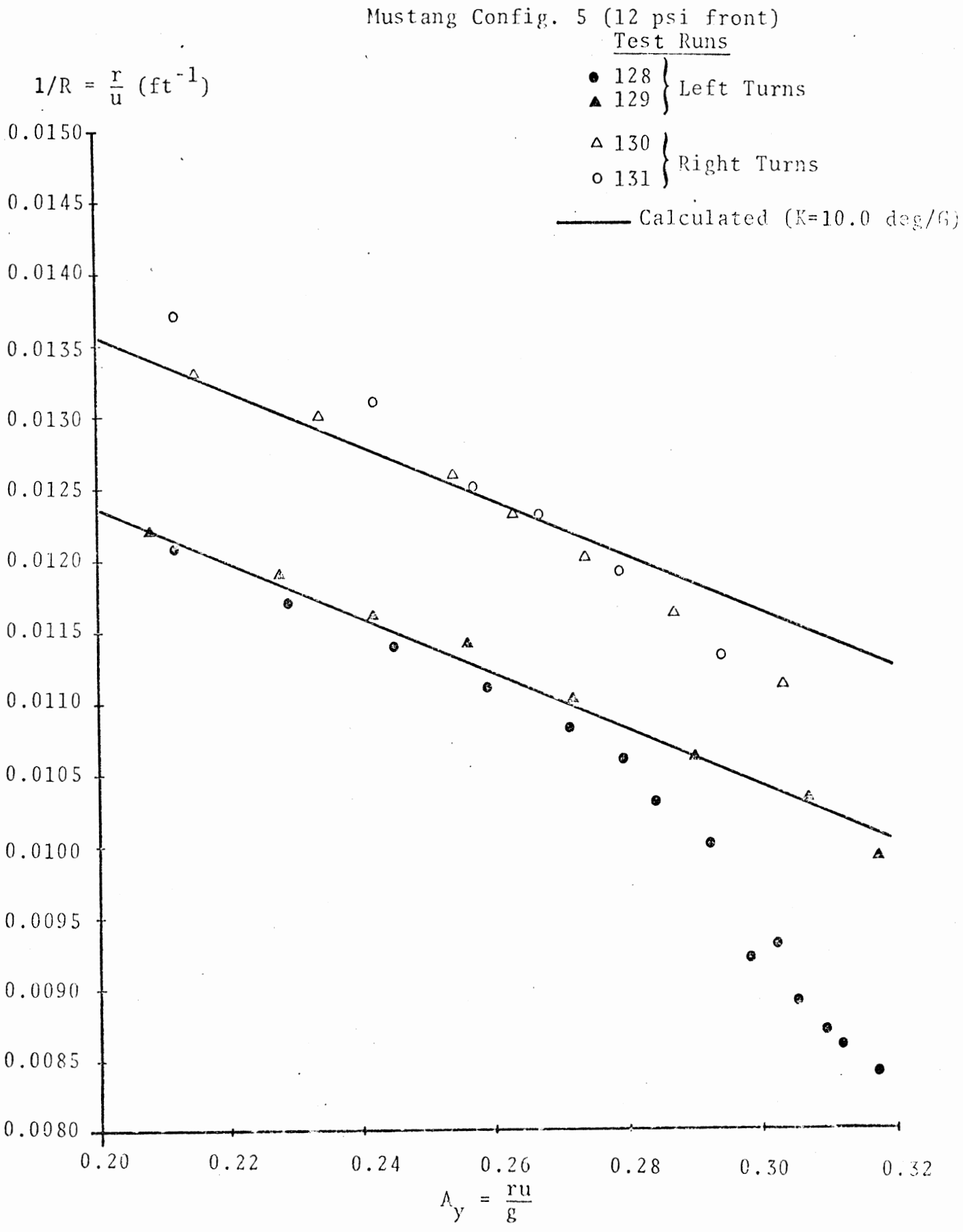

Figure 5-2. Calculated and measured results for the Mustang with underinflated front tires.

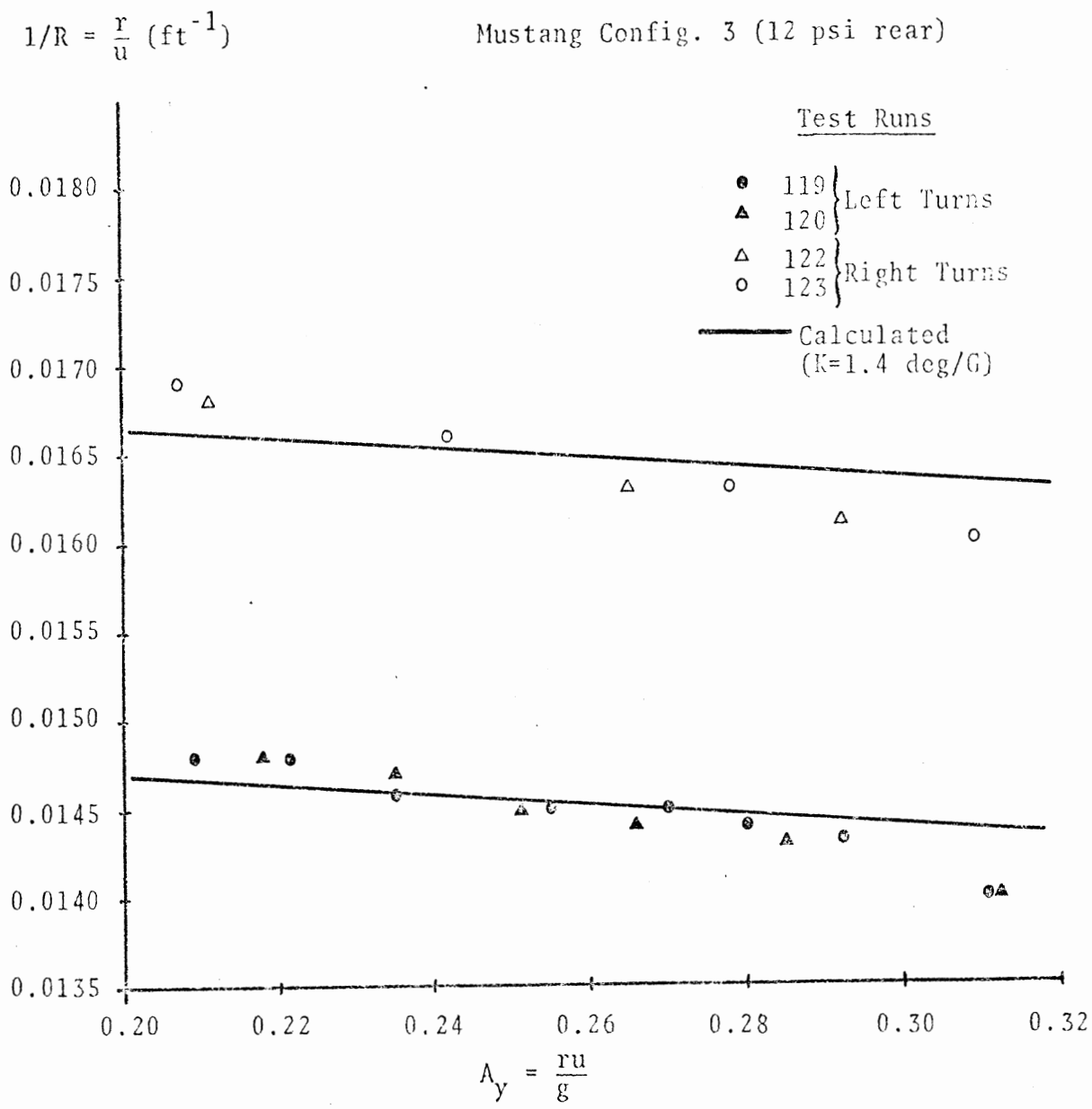

Figure 5-3. Calculated and measured results for the Mustang with underinflated rear tires.

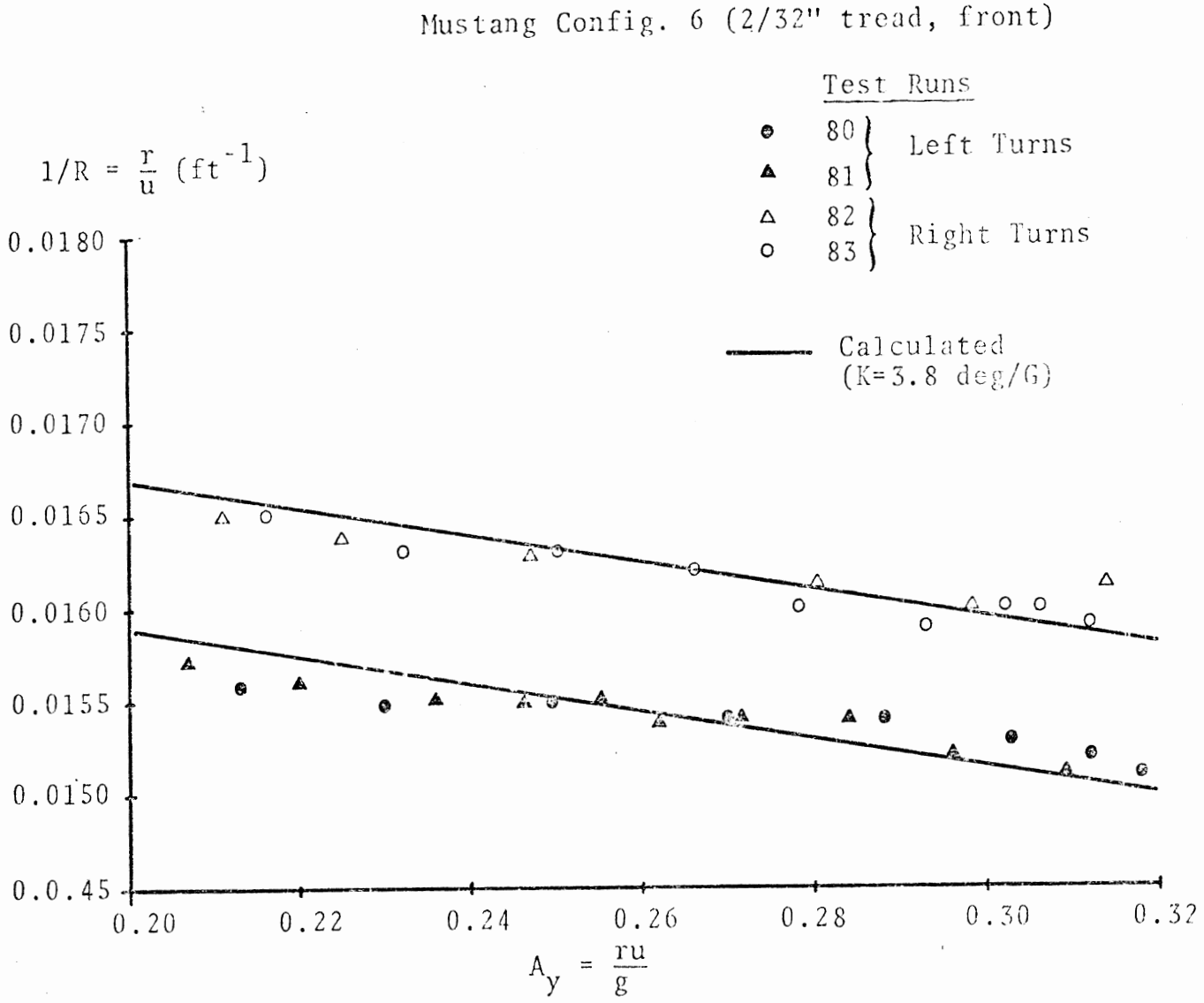

Figure 5-4. Calculated and measured results for the Mustang with front tires worn to 2/32" tread depth.

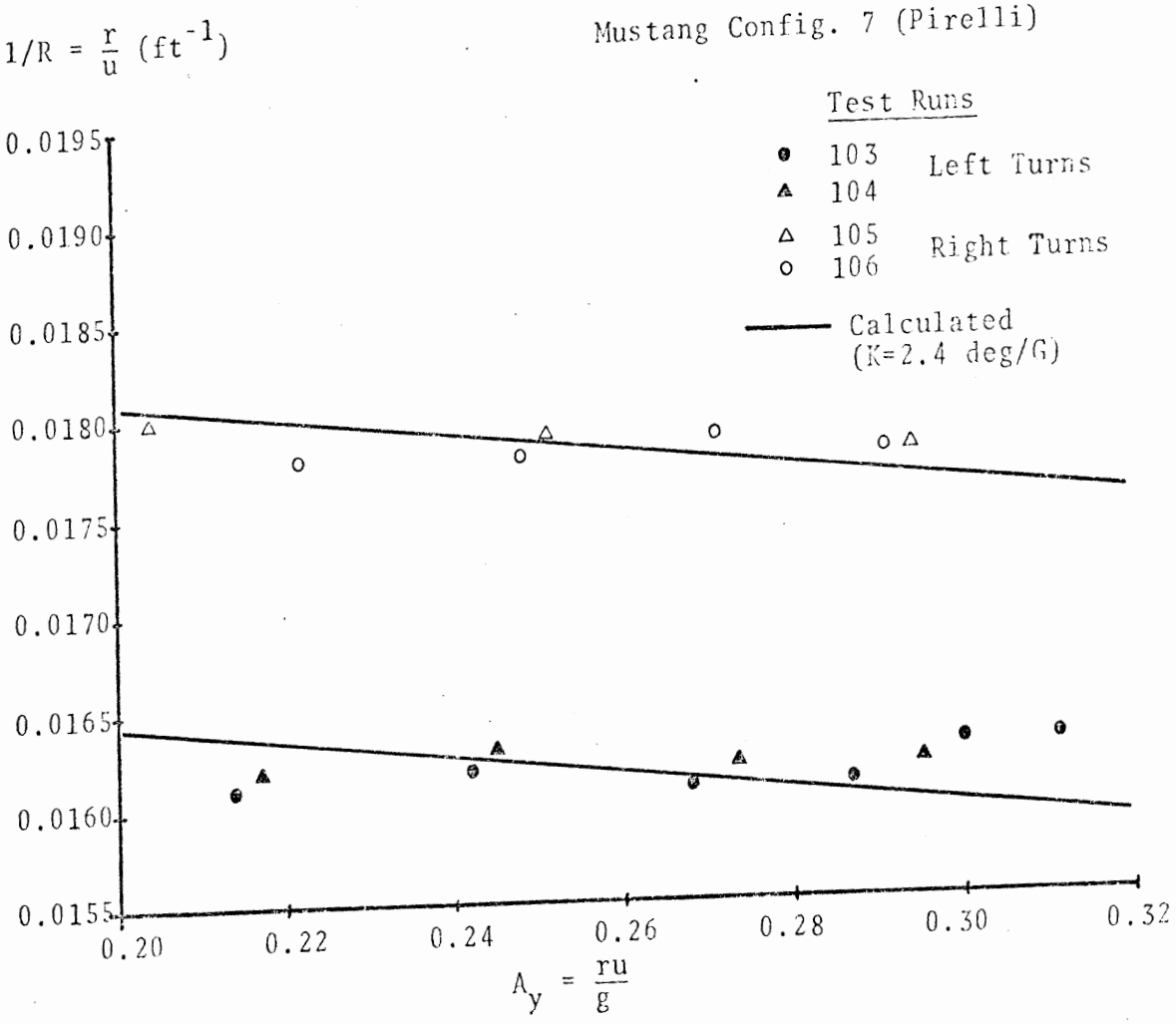

Figure 5-5. Calculated and measured results for the Mustang with Pirelli radial tires on the front wheels.

The constant-steer test data obtained with the 1973 Buick Century station wagon, in its OE configuration, are shown in Figure 5-6. The slopes of the lines shown in the figure were calculated from parameter data measured at HSRI. The agreement obtained between the calculated and measured results, as seen in Figure 5-6, is considered to be fair.

Figures 5-7 and 5-8 show a comparison of calculated and measured results for the Buick station wagon operated with rear tires inflated to 16 psi and with Bridgestone radial tires replacing the OE tires on the front wheels. The agreement between calculated and measured results is considered good enough to assert that calculations based on a linear analysis do predict the manner in which the steady turning performance of a motor vehicle is altered by tire-in-use factors.

The constant steer test is not easy to perform accurately. As pointed out in a recent SAE paper [7], <u>at best</u> this type of test is accurate to about 0.5 deg/G. Examination of the Mustang results indicate that they may be accurate within about 1.0 deg/G. The Buick results are probably no more accurate than 1.5 deg/G.

Basic statistical considerations indicate that a very high quality (i.e., low error tolerance) yaw rate gyro should be used in the constant steering wheel angle method. For example, simplified theoretical calculations for a typical vehicle making a 0.3 g turn on a radius of 100 feet show that the standard deviation of the yaw rate gyro, σ_r, is related approximately to the standard deviation of the understeer/oversteer factor of σ_K by the following expression:

$$\sigma_K \approx (85)\ \sigma_r \qquad (5.27)$$

where σ_K is in degrees/G and σ_r is in rad/sec.

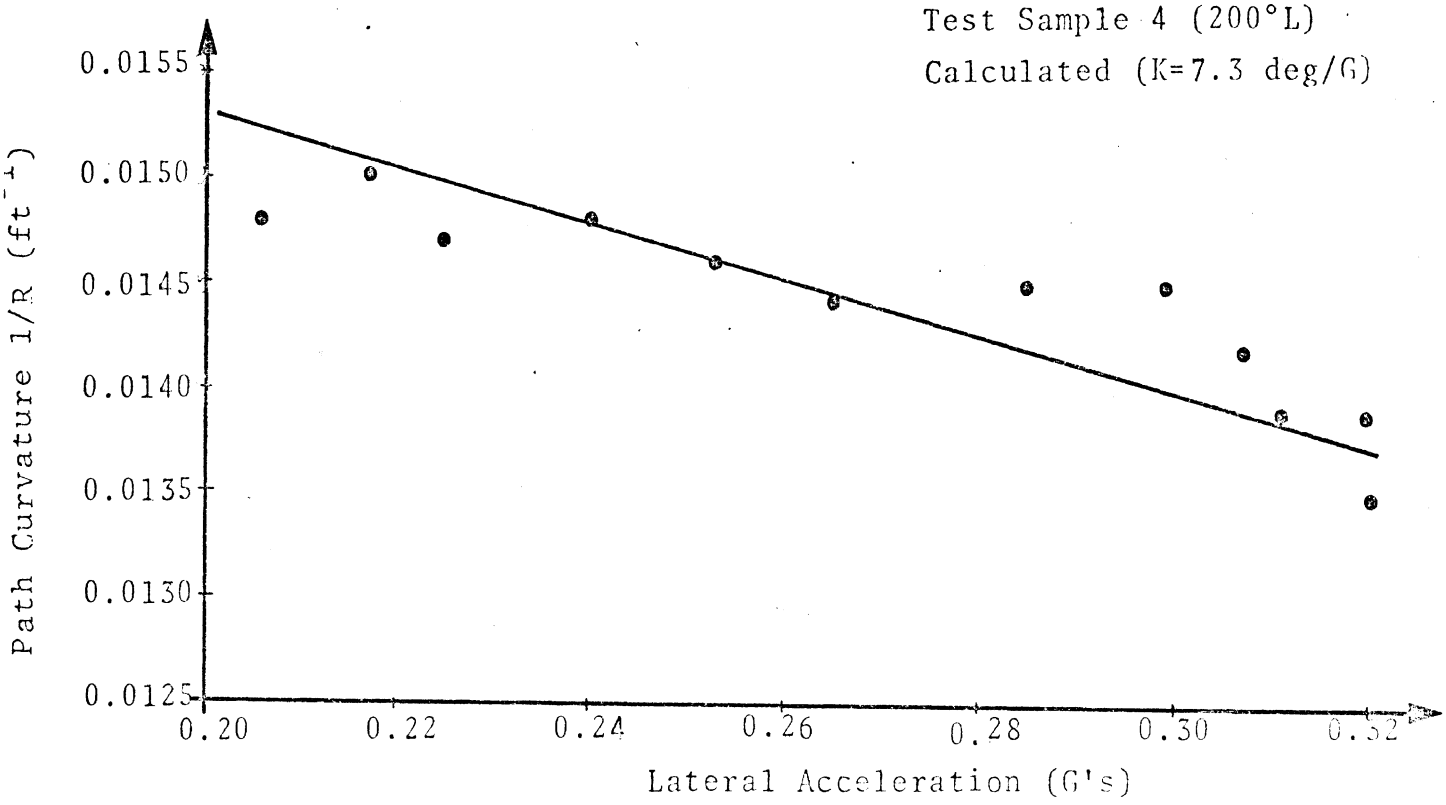

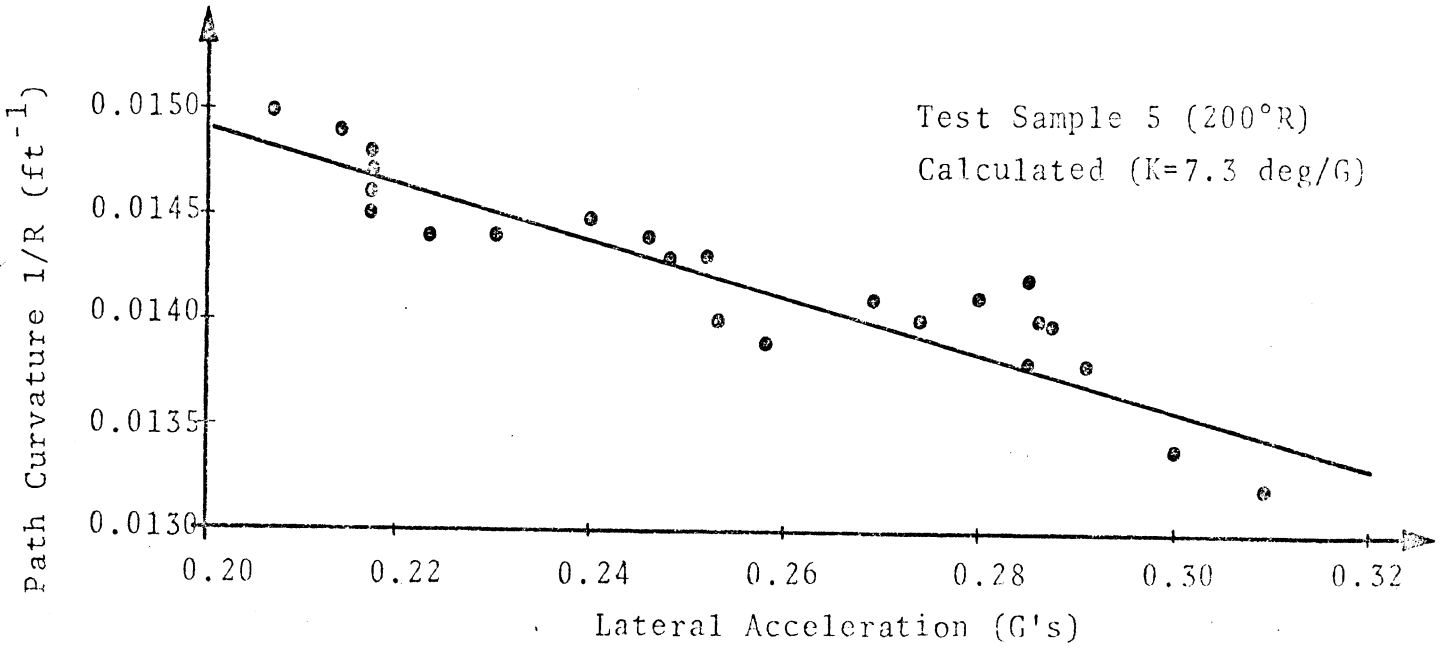

Figure 5-6. Calculated and measured results for the OE Buick station wagon.

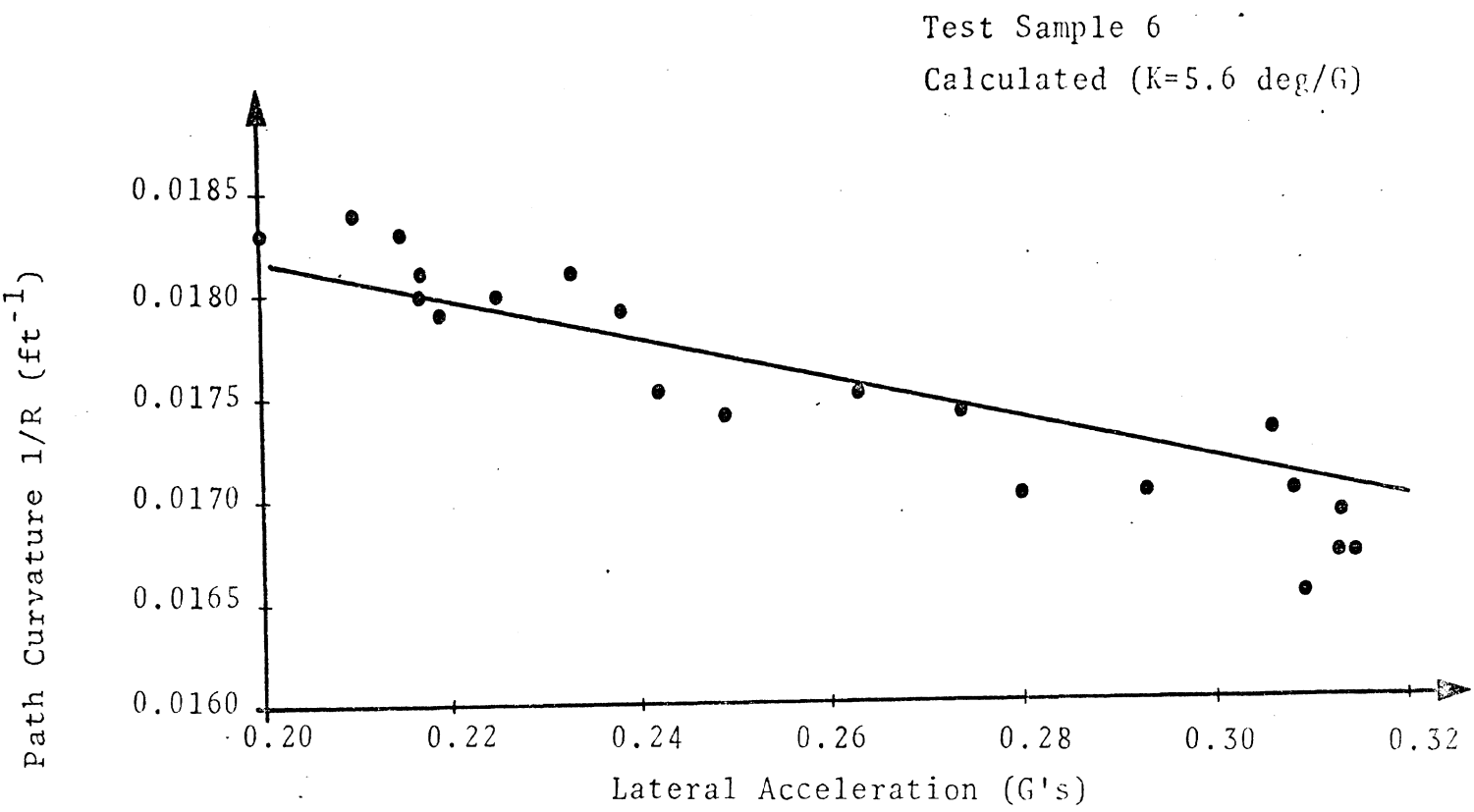

Figure 5-7. Buick results; 16 psi in rear tires.

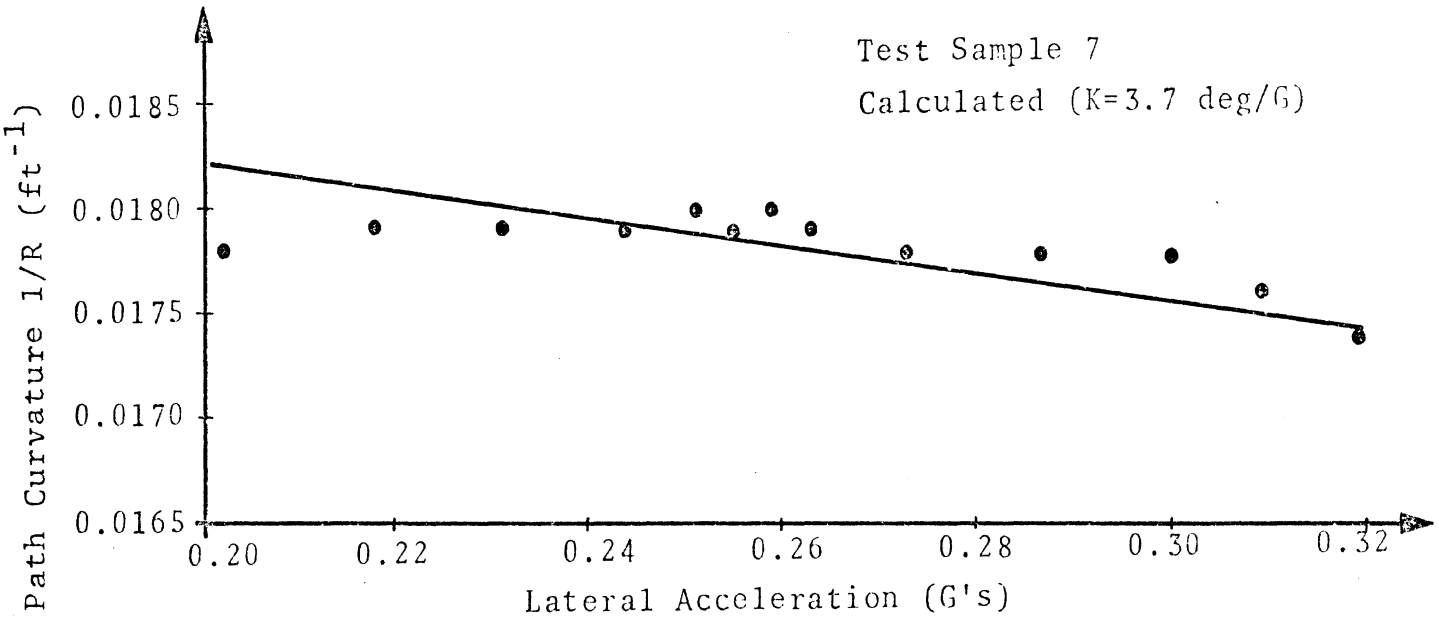

Figure 5-8. Buick results; Bridgestone radial tires on the front wheels.

Equation (5.27) indicates that for σ_K = 0.2 degrees/G, σ_r should be approximately 0.002 rad/sec (i.e., about 0.1 degrees/second),* a finding which says that the tests conducted in this program were handicapped by yaw rate measurements of insufficient accuracy. On the other hand, the accuracy of the forward velocity measurements were more than adequate for measuring K.

In the material that follows, calculated values of understeer/oversteer factor are used to assess the importance of changes in tire mechanical characteristics caused by tire-in-use factors. Measured tire properties are used as a basis for these calculations. The advantages of this analytical approach are that (1) many more cases can be examined quickly and efficiently by calculation than by test, (2) the results may be readily analyzed using theoretical equations (see Section 5.1), and (3) spurious results due to experimental inaccuracies are avoided.

5.4 FINDINGS

In this section, we use calculated values of the understeer/oversteer factor to examine how inflation pressure, tread wear, and replacement tire-mix influence the maneuvering performance of the 1971 Mustang and 1973 Buick in the normal driving range with approximately a two-person load.

5.4.1 INFLATION PRESSURE. Cornering, aligning torque, and camber stiffnesses are highly dependent upon inflation pressure. The extent to which the Mustang OE tires exhibit

*SAE proposed recommended practice XJ 266 calls for rate gyros with an accuracy of 0.05 degrees/second. This accuracy specification appears to be well justified.

this dependency is illustrated by the measured stiffnesses presented in Table 5-1. Clearly, the cornering and camber stiffnesses decrease and the aligning-torque stiffness increases as inflation pressure is reduced.

Table 5-1. C_α, AT_α, and C_γ Versus Inflation Pressure for the Mustang OE Tire (i.e., a Goodrich Silvertown E78-14 Tire).

Note: The static loads on the Mustang tires are 1020 lbs. front and 810 lbs. rear.

	Normal Load (lbs)	Inflation Pressure (psi)	C_α (lbs/deg)	AT_α (in.lbs/deg)	C_γ (lbs/deg)
	1020	24	143	300	22.0
Front	1020	18	120	345	17.4
	1020	12	90	368	14.4
	810	24	142	208	20.0
Rear	810	18	124	259	16.5
	810	12	95	300	13.3

The data given in Table 5-1 have been used to compute the understeer/oversteer factor, K, for the five tire-in-use configurations listed in Table 5-2. Case #1 in Table 5-2 represents the OE vehicle. Comparison of cases 1 and 3 indicates that a 2.5 deg/G reduction in K takes place when the inflation pressure in the rear tires is reduced to 12 psi. From cases 1 and 5 it can be seen that a 6.1 deg/G increase in K is obtained when the inflation pressure in the front tires is reduced to 12 psi.

Table 5-2. The Influence of Underinflated Tires on Mustang Normal Driving Performance

Case Number	Tire Configuration	Understeer/ Oversteer Factor (deg/g)
1 (OE)	Front 24 psi, Rear 24 psi	3.9
2	Front 24 psi, Rear 18 psi	3.2
3	Front 24 psi, Rear 12 psi	1.4
4	Front 18 psi, Rear 24 psi	5.9
5	Front 12 psi, Rear 24 psi	10.0

Decreasing the inflation pressure in the front tires produces more understeer, not only because the cornering stiffness of the front tires is reduced but also because the aligning-torque stiffness of these same tires is increased. The aligning-torque stiffness of the front tires interacts with steering-system compliance to reduce the equivalent cornering stiffness of the front tires and thereby to increase the understeer level (see Equations (5-11) and (5.20)).

A "contour" plot showing lines of constant K as a function of front- and rear-inflation pressures is presented in Figure 5-9. This plot applies to the Mustang with OE tires. Since the indicated range of inflation pressures (12 psi to 30 psi) covers almost all of the conditions likely to be encountered in practice, this plot summarizes the influence of off-design inflation pressure on directional performance in the normal driving range.

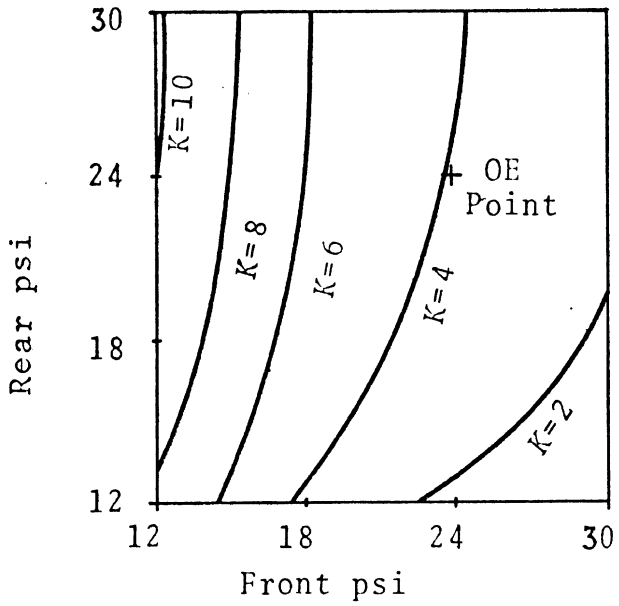

Figure 5-9. Influence of inflation pressure on understeer/oversteer factor for the Mustang.

Reexamination of Figure 5-9 indicates several interesting facts:

(1) At low front inflation pressure, rear inflation pressure has very little influence on the understeer level.

(2) In the neighborhood of the "OE" point, front to rear differences in inflation pressure are more significant than simultaneous equal reductions (or increases) in both front and rear inflation pressure.

(3) Changes in rear inflation pressure are about as important as changes in front inflation pressure at low understeer levels.

Similar calculations were performed for the Buick station wagon. Tables 5-3 and 5-4 present tire parameters and calculated

Table 5-3. C_α, AT_α, and C_γ Versus Inflation Pressure for the Buick OE Tire (i.e., a Firestone Deluxe Champion H78-14 tire)

	Normal Load	Inflation Pressure*	C_α (lbs/deg)	AT_α (in.lbs/deg)	C_γ (lbs/deg)
	1277	24	189	440	36.5
Front	1277	20	168	475	33.1
	1277	12	127	522	26.0
	1143	28	203	346	37.0
Rear	1143	20	171	418	32.7
	1143	12	129	472	24.5

*Recommended inflation pressures are 24 psi front and 28 psi rear.

Table 5-4. The Influence of Underinflated Tires on Buick Normal Driving Performance

Case Number	Tire Configuration	K
1 (OE)	Front 24 psi, Rear 28 psi	7.3
2	Front 24 psi, Rear 20 psi	6.3
3	Front 24 psi, Rear 12 psi	4.6
4	Front 20 psi, Rear 28 psi	9.0
5	Front 12 psi, Rear 28 psi	13.8

values of understeer/oversteer factor for five representative inflation-pressure configurations.

The major difference between the findings obtained for the Buick and the Mustang is that the OE Buick has more understeer than the OE Mustang (7.3 deg/g versus 3.9 deg/g, by our calculations). Otherwise the influences of changes in inflation pressure on understeer level are comparable, as demonstrated by the calculated results presented in Figure 5-10.

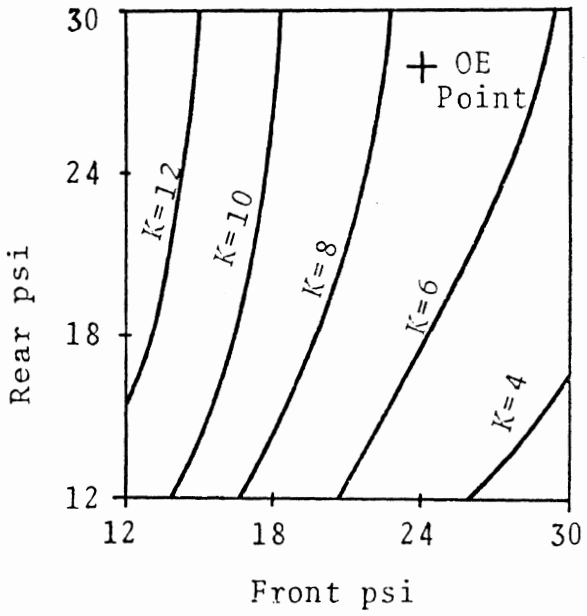

Figure 5-10. Influence of inflation pressure on understeer/oversteer factor for the Buick station wagon.

The above presented findings are believed to be representative of the passenger car population, in general, because (1) changes in inflation pressure affect almost all tires in approximately the same way (although some tires may be more sensitive to inflation pressure changes than others), and (2) vehicle design cannot substantially compensate for the influence of drastic changes in inflation pressure.

5.4.2 TREAD WEAR. Because several tire replacements are ordinarily required during the useful life of a vehicle, and approximately 30% of the tires sold are purchased in pairs [7], it is likely that a tire-wear intermix situation exists on many vehicles in use on the road.

At small slip angles, a worn tire will usually produce higher cornering forces, aligning moments, and camber forces than another less worn tire operated under the same conditions. The results presented here apply only to maneuvers in which small slip and inclination angles are involved. They differ considerably from the limit maneuver findings obtained on a wet surface.

Table 5-5 presents the tire parameters determined from flat-bed measurements for the Mustang OE tire at four levels of tread depth (including the OE condition). These data show that the cornering, camber, and aligning-torque stiffnesses all increase as tread is worn to a lesser depth.

Calculations of the understeer/oversteer factor are given in Table 5-6 for the Mustang operated at the four extremes of wear (i.e., OE tires front and rear, 2/32" groove depths on the front and rear tires, 2/32" groove depth on the front tires with nonworn OE rear tires, and nonworn OE front tires with 2/32" groove depth rear tires). The surprising feature of these results is the relative insensitivity of the understeer/oversteer factor to all combinations of tread wear. Comparison of cases 1 and 2 in Table 5-6 shows that a 1.4 deg/g increase in understeer level is caused by a change from OE tires to fully worn tires on the rear wheels. The use of fully worn tires on the front wheels (case 3) has even less influence, causing only a 0.7 deg/g decrease in understeer.

These results may seem to contradict the fact that tread wear causes relatively large increases in cornering stiffness.

Table 5-5. C_α, AT_α, and C_γ Versus Tread Wear for the Mustang OE Tire.*

	Normal Load	Groove Depth	C_α	AT_α	C_γ
Front	1020	OE	135	315	22.4
	1020	6/32	160	406	24.3
	1020	4/32	160	444	30.0
	1020	2/32	159	460	25.0
Rear	810	OE	136	225	19.9
	810	6/32	172	315	25.3
	810	4/32	174	346	30.3
	810	2/32	178	393	27.1

*All these data are for 22 psi. Thus the "OE" parameters are not the same as in Table 5-1.

Table 5-6. The Influence of Tread Wear on Mustang Normal Driving Performance.

Case Number	Tire Configuration	K (deg/G)
1	Front OE, Rear OE	4.3
2	Front OE, Rear 2/32"	5.7
3	Front 2/32", Rear OE	3.6
4	Front 2/32", Rear 2/32"	4.9

However, an increase in rear tire cornering stiffness from the OE value has little influence on K for the Mustang. This is illustrated graphically by the dashed vertical line in Figure 5-11. (Figure 5-11 is a contour plot showing the influence of front and rear cornering stiffnesses on K as calculated for the 1971 Mustang.)

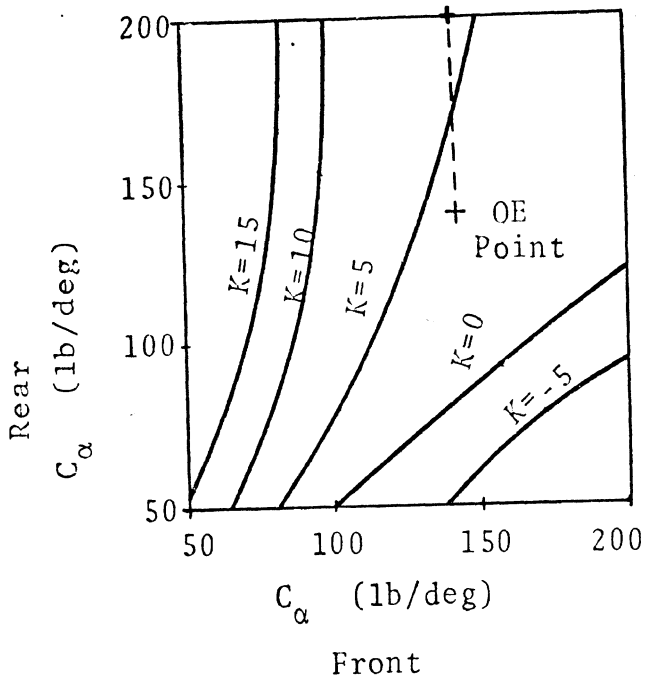

Figure 5-11. The influence of cornering stiffness values on understeer/oversteer factor for the Mustang.

The numerical results shown in Figure 5-11 indicate that an increase in front cornering stiffness (with all other parameters held the same) will cause a significant decrease in K for the Mustang. But an increase in tread wear not only increases cornering stiffness, it also causes increases in aligning-torque and camber stiffnesses. The increase in aligning-torque stiffness reduces the equivalent front cornering stiffness (see Equation (5.11)) and, thereby, partially compensates for the increase in cornering stiffness.

In addition, an increase in the camber stiffness of the front tires contributes to an increase in understeer level (see Equation (5.20)). A numerical evaluation of these effects shows that the use of tread-worn tires on the front wheels has little effect on the total resultant understeer of the Mustang.

Table 5-7 presents the three stiffnesses exhibited by the Buick OE tire at four groove depths. The indicated trends are the same as those found for the Mustang OE tire as tabulated in Table 5-5.

Table 5-7. C_α, AT_α, and C_γ Versus Groove Depth for the Buick OE Tire.*

	Normal Load (lbs)	Groove Depth (inches)	C_α lbs/deg	AT_α in.lbs/deg	C_γ lbs/deg
Front	1277	OE	200	423	38.3
	1277	6/32	242	588	46.1
	1277	4/32	253	643	53.0
	1277	2/32	277	815	58.4
Rear	1143	OE	200	361	37.8
	1143	6/32	246	522	47.3
	1143	4/32	261	574	54.4
	1143	2/32	285	741	60.2

*All these data are for 26 psi.

The influence of tread wear on the understeer/oversteer factor for the Buick is given in Table 5-8. As was true for the Mustang, tread wear does not have a marked influence on the understeer/oversteer factor.

Table 5-8. The Influence of Tread Wear on Buick Normal Driving Performance (all tires at 26 psi)

Case Number	Tire Configuration	K (deg/G)
1	Front OE, Rear OE	6.5
2	Front OE, Rear 2/32"	8.2
3	Front 2/32", Rear OE	6.2
4	Front 2/32", Rear 2/32"	7.9

Figure 5-12 shows the influence of cornering stiffness on K as calculated for the Buick station wagon. The dashed vertical line in Figure 5-12 shows that increasing rear cornering stiffness from its OE value on the Buick, with all other parameters held fixed, does not change K in a very marked manner. Thus the increase in cornering stiffness caused by worn tires should not be expected to have much influence on K. Note that the increases in camber and aligning torque stiffnesses accompanying rear tire wear are not significant, since the solid axle rear suspension has very little compliance steer or camber.

It is conceivable that vehicles designed with a low value of K (near neutral steer) would have their understeer level changed by a significant amount if tread-worn tires are mounted on the rear wheels. But the results calculated for the Mustang and Buick station wagon indicate that the understeer level of most passenger cars is insensitive to rear tire wear.

Calculations show that the steering-system stiffnesses of the Buick and the Mustang are a major factor in reducing the influence of front tire wear on understeer. Given the increasing aligning moment stiffness with tire wear, only

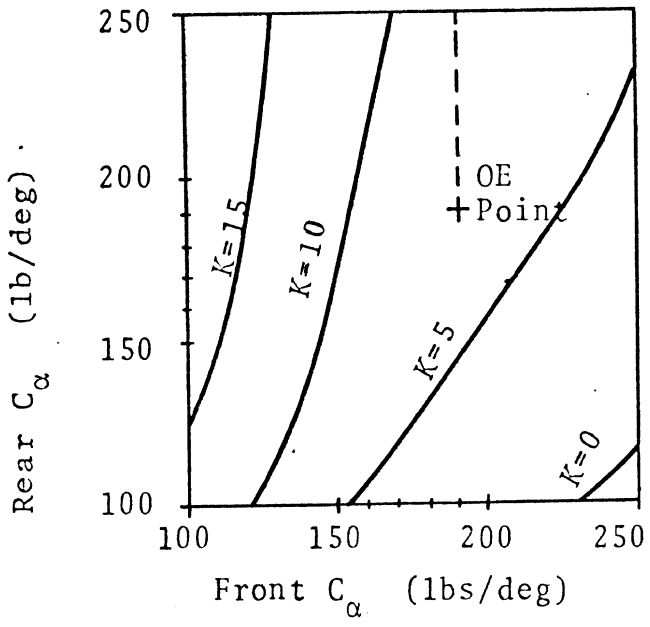

Figure 5-12. Influence of cornering stiffness on understeer/oversteer factor for the Buick.

vehicles with extraordinarily stiff steering systems would exhibit a significant change in understeer with increased wear of the front tires.

For some vehicles the changes in understeer caused by tire wear are just barely discernible when currently available test procedures are used. For example, if fully worn tires are used to replace the OE tires on the front wheels of the Mustang, K is reduced by 0.6 deg/g, but under the best of circumstances K may be determined to within about 0.5 deg/g using the constant steering wheel angle method.

5.4.3 REPLACEMENT TIRE MIX. On the average, radial tires have higher cornering and aligning torque stiffnesses and a much lower camber stiffness than belted-bias tires [12]. Two radial tires were selected for extensive use in this investigation. The mechanical properties of these radial

tires and their corresponding belted-bias OE tires are given in Table 5-9. The two radial tires were selected primarily because they had high cornering stiffnesses. Inspection of the values given in Table 5-9 shows that the low camber stiffnesses of these tires are representative of values typically exhibited by radial tires.

Table 5-9. Radial Versus OE Tire Parameters (all data are at 24 psi)

Vehicle	Tire	Front Tire Load	C_α	AT_α	C_γ
Mustang	OE	1020	143	300	22.0
Mustang	Pirelli Radial	1020	163	368	5.6
Buick	OE	1277	189	440	36.5
Buick	Bridgestone Radial	1277	273	558	15.0

Calculations show that (1) the use of Pirelli radial tires on the front wheels of the Mustang will change the OE value of K from 3.9 deg/g to 2.4 deg/g, and (2) the use of Bridgestone radial tires on the front wheels of the Buick will change the OE value of K from 7.3 deg/g to 3.7 deg/g. These are significant changes in understeer/oversteer factor.

Mounting these radial tires on the rear wheels of the appropriate vehicle (Mustang or Buick) will have little influence on K because, as shown in Figures 5-11 and 5-12, increases in rear cornering stiffness from the OE level will have a small influence on K.

Since a wide variety of replacement tires are available, it is difficult to concisely summarize the influence of all possible replacement tire mixes on normal driving performance. In this study, the tire parameters used for summarizing replacement tire mix situations were selected to represent typical bias, bias-belted, and radial tires.

The contour plots shown in Figures 5-13 and 5-14 for the Mustang and Buick, respectively, are based on the following scheme for selecting tire parameters:

(1) Tire B is the OE tire for the vehicle with OE tire parameters symbolized by $C_{\alpha B}$, $AT_{\alpha B}$, $C_{\gamma B}$.

(2) Tire C represents a hypothetical radial tire with tire properties given by

$$C_{\alpha C} = 1.2\ C_{\alpha B}$$

$$AT_{\alpha C} = 1.2\ AT_{\alpha B}$$

$$C_{\gamma C} = 0.2\ C_{\gamma B}$$ (Note the low level of $C_{\gamma C}$.)

(3) Tire A represents a hypothetical cross-bias, belted-bias, or snow tire with lower stiffness properties than the OE tire, viz.,

$$C_{\alpha A} = 0.8\ C_{\alpha B}$$

$$AT_{\alpha A} = 0.8\ AT_{\alpha B}$$

$$C_{\gamma A} = 0.8\ C_{\gamma B}$$

The values of K presented at points other than the nine points, specified by coordinates (A,A), (A,B), --------- (C,B), (C,C), in Figures 5-13 and 5-14 were obtained by interpolating between the values calculated at the points (A,A) through (C,C).

The following general statements are based on the findings diagrammed in Figures 5-13 and 5-14:

(1) If all tires are replaced with four identical tires of a different construction, not much change in K occurs.

(2) If the rear OE tires are replaced with "average" radial tires (i.e., tire C), not much change occurs.

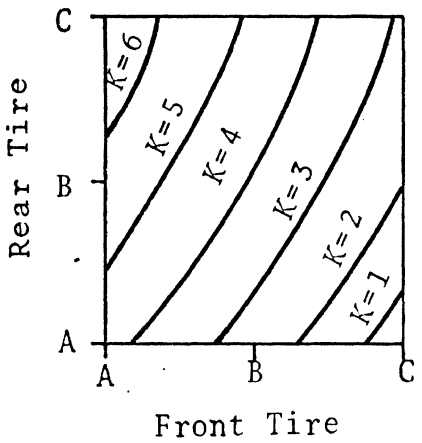

A	B	C
$0.8C_{\alpha}$	C_{α}	$1.2C_{\alpha}$
$0.8AT_{\alpha}$	AT_{α}	$1.2AT_{\alpha}$
$0.8C_{\gamma}$	C_{γ}	$0.2C_{\gamma}$

Figure 5-13. The influence of replacement tire mixes for the Mustang.

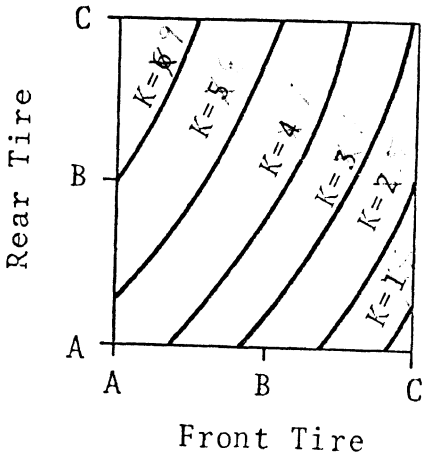

A	B	C
$0.8C_{\alpha}$	C_{α}	$1.2C_{\alpha}$
$0.8AT_{\alpha}$	AT_{α}	$1.2AT_{\alpha}$
$0.8C_{\gamma}$	C_{γ}	$0.2C_{\gamma}$

Figure 5-14. The influence of replacement tire mixes for the Buick.

(3) If the rear OE tires are replaced with tires with lower stiffness properties (i.e., tire A), a noticeable change in K occurs.

(4) If the front OE tires are replaced with "average" radial tires, a significant change in K occurs.

(5) If the front OE tires are replaced with tire A, a noticeable change in K occurs.

(6) The most significant changes in K occur when the OE tires are replaced by front-to-rear mix of tires A and C.

The above list of statements applies to either a 1973 Buick or a 1971 Mustang. Both of these vehicles have belted-bias original equipment tires. Clearly, the situation is different for vehicles specifically designed to use radial tires.

A first-order estimate of the influence of replacing OE radial tires with non-radial tires can be obtained by treating "tire C" in Figures 5-13 and 5-14 as the OE tire. In this case significant changes in K are obtained by (1) changing from tire C to tire A or B on the front wheels, and (2) changing from tire C to tire A on the rear wheels. Again, if all tires are replaced with four tires of the same construction type, much less severe changes occur.

5.4.4 SYNOPSIS AND CONCLUDING OBSERVATIONS. There are interesting and significant differences in the manner that inflation pressure, tread wear, and carcass construction influence the mechanical properties of the tires used on the Mustang and the Buick station wagon. These differences are illustrated by the parametric data presented in Table 5-1 for the Mustang tires and in Table 5-3 for the Buick tires.

Examination of the measured tire characteristics presented in Tables 5-1 and 5-3 leads to the following observations:

(1) When the inflation pressure is reduced, the cornering and camber stiffnesses are decreased and the aligning-torque stiffness is increased.

(2) When the tread depth is reduced, the cornering, camber, and aligning-torque stiffnesses are all increased.

(3) The radial tires used in this investigation to replace the belted-bias original-equipment tires have higher cornering and aligning stiffnesses and a much lower camber stiffness than the OE tires.

The generality of these observations is supported by the comprehensive set of tire data presented in Appendix D. Evidence showing the generality of the findings based on the third observation presented above can be found in the statistical comparison of radial versus belted-bias tires given in [12].

Cornering stiffness is the tire parameter which has the greatest influence on vehicle behavior in the normal driving regime. Calculations showing the influence of changing the front and rear cornering stiffnesses for the Buick and the Mustang are shown in Figures 5-11 and 5-12. Clearly, large variations in understeer/oversteer factor can be caused by widely differing values of front and rear cornering stiffnesses. However, the calculations used to make Figures 5-11 and 5-12 do not reflect the influence of changes in aligning torque stiffness and camber stiffness. For the tire-in-use factors and vehicles studied in this program, the aligning torque and camber stiffnesses are important and their influences must be considered along with the influence of cornering stiffness.

Results quantifying the important influence of under-inflated tires on normal driving performance are given in Figures 5-9 and 5-10. On the other hand, results given in Tables 5-6 and 5-8 show that the influence of tread wear on normal driving performance is almost insignificant for the Buick and the Mustang.

Results summarizing a variety of tire replacement-mix configurations are given in Figures 5-13 and 5-14. For the Mustang and the Buick, replacing the front OE (belted-bias) tires with radial tires was found to cause significant changes in the understeer/oversteer factor. However, replacing the rear OE tires with radial tires did not cause significant changes in the understeer/oversteer factor.

Finally, some observations on (1) the influence of tire-in-use factors on the dynamic response of vehicles in the normal driving range, and (2) the effect of load variation on directional response are in order.

As discussed earlier in Section 5.1, the understeer/oversteer factor can be used to make qualitative statements about dynamic response. Note that the analytic method described in Appendix C can readily be used to compute the response to a unit amplitude step steering input.

Typical responses to a unit step input of steer are given in Figures 5-15 and 5-16 for the Mustang and Buick in the OE configuration. Figures of this type can be used to determine numerics such as response time, percentage overshoot, and settling time. (Note that these numerics vary with speed.)

Response times calculated for the Buick and Mustang are given in Table 5-10. In this instance, response time is defined as the time required to reach 90% of the steady-state value. Note that since the yaw rate gain changes with changes

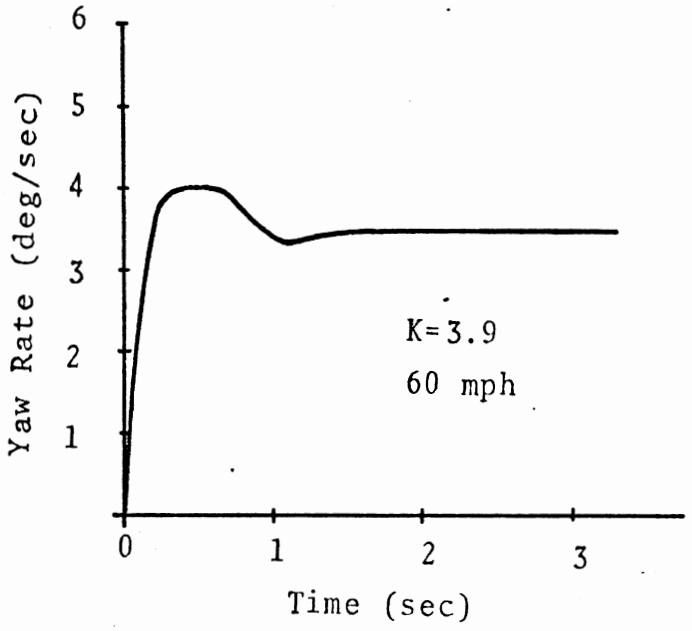

Figure 5-15. Step function response for the OE Mustang.

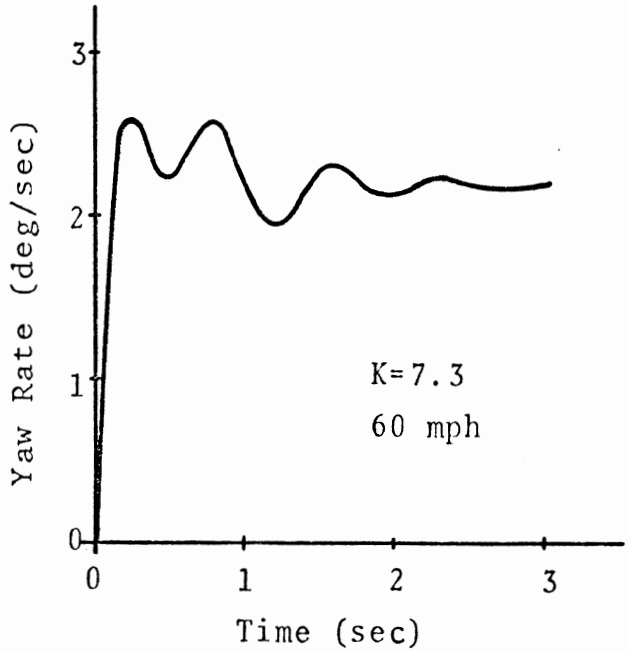

Figure 5-16. Step function response for the OE Buick.

Table 5-10. Calculated Yaw Rate Response Measures for Vehicle Speed of 60 mph.

Vehicle	Tire-In-Use Factor	K deg/g	Yaw Rate Steady-State Response Level (deg/sec)	Response Time (sec)
Mustang	OE	3.9	3.47	0.15
Mustang	12 psi rear	1.4	5.86	0.41
Mustang	12 psi front	10.0	1.73	0.13
Mustang	2/32" tread & 22 psi front	3.8	3.42	0.15
Mustang	Pirelli Radial front	2.4	4.60	0.22
Buick	OE	7.3	2.19	0.11
Buick	12 psi rear	4.5	3.10	0.23
Buick	12 psi front	13.8	1.30	0.10
Buick	2/32" tread & 26 psi front	6.3	2.45	0.12
Buick	Bridgestone Radial front	3.7	3.48	0.18

in tire-in-use factors, the steady-state response levels presented in Table 5-10 are functions of the understeer/oversteer factor. The results presented in Table 5-10 indicate that high values of K yield short response times and low steady-state yaw rate levels and, conversely, low values of K yield long response times and high steady-state yaw rate levels. Because of the qualitative correspondence between transient response and the value of K for a particular vehicle, it was assumed in this study that the understeer/oversteer factor characterizes the dynamic response of the vehicle in addition to quantifying the steady-state response levels.

However, a lower K does not necessarily mean a longer response time. For example, the Buick results shown in Table 5-10 indicate that (1) K is 4.5 deg/G and the response time is 0.23 seconds in the 12 psi rear case, and (2) K is 3.8 deg/G and the response time is 0.18 seconds for the case with Bridgestone radial tires on the front wheels.

Since the understeer/oversteer factor depends heavily on the static loads on the front and rear wheels (see Equations (5.24) to (5.26)), the effects of unfavorable loading combined with tire-in-use factors should be considered, particularly for the station wagon. Table 5-11 presents an example set of tire pressures, loads, and stiffness parameters for the normally and fully loaded Buick station wagon.

Table 5-11. Example Conditions for the Normally and Fully Loaded Buick Station Wagon.

Configuration		Load (lbs)	Pressure (psi)	C_α (lbs/deg)	AT_α (in.lbs/deg)	C_γ (lbs/deg)
Normal	Front	1277	24	189	440	37
	Rear	1143	28	203	346	37
Full	Front	1240	26	200	406	38
	Rear	1535	32	220	484	39

Calculations for the fully loaded station wagon with original equipment tires inflated to the manufacturer's recommended levels for the heavily loaded vehicle show that K = 6.2 deg/G for the fully loaded vehicle, compared to a K of 7.3 deg/G for the normally loaded vehicle (two-passenger load) with original equipment tires inflated to the manufacturer's recommended levels. These numerical results show that increases in inflation pressure have effectively offset the influence of the unfavorable load distribution for the fully loaded vehicle.

If the inflation pressure in the rear tires of the fully loaded vehicle is decreased to 12 psi, then K equals 1.6 deg/G. The change in directional response characteristics due to low inflation pressure in the rear tires of the fully loaded vehicle is dramatically illustrated by the change in yaw-rate response time. The response times for the normally loaded

vehicle and the fully loaded vehicle with 12 psi in the rear tires are given in Table 5-12.

Table 5-12. Calculated Yaw Rate Response Times for 60 mph Versus Load and Inflation Pressure.

Vehicle	Pressures, psi Front	Rear	Yaw Rate Response Time (seconds)
Normally Loaded	24	28	0.11
Normally Loaded	24	12	0.23
Fully Loaded	26	32	0.12
Fully Loaded	26	12	0.63

Clearly, the influence of inflation pressure can be amplified by unfavorable loading of the vehicle.

6.0 CONCLUSIONS AND RECOMMENDATIONS

This section contains:

(1) a list of specific findings extracted from the results of this investigation,

(2) general conclusions drawn from these findings,

(3) a discussion of the implications of the conclusions, and

(4) recommendations based on all of the above.

6.1 SUMMARY OF RESULTS (SPECIFIC FINDINGS)

In the course of conducting this study of the influence of tire-in-use factors on limit and normal maneuvering performance, findings were developed in six areas, viz:

- Test-Induced Tire Wear
- Inflation Pressure
- Replacement Tire Mixes
- Tread Wear
- Mathematical Modeling of Tires
- Vehicle-Testing Procedures

Each area is discussed separately below.

6.1.1 TEST-INDUCED TIRE WEAR. (When tires are operated at the high lateral force conditions commonly occurring in limit steering maneuvers, they tend to wear at the tread shoulder. Such wear does not occur with normal use, consequently, it is herein referred to as "test-induced wear.")

Findings:

(1) Mobile-tire-tester results show that a barely discernible amount of test-induced tire wear causes a significant increase in the peak lateral

force capabilities of the original-equipment, bias-belted tires installed on the 1971 Mustang and the 1973 Buick station wagon.

(2) Mobile-tire-tester results show that the lateral force characteristics of the radial tires used in this study were only slightly influenced by test-induced wear.

(3) Flat-bed tire-tester results show that test-induced wear causes significant alterations in tire shear force characteristics in the sub-limit range of lateral force levels for those tires whose peak lateral force levels are susceptible to shoulder-wear effects.

(4) The influence of test-induced wear can be controlled to an acceptable level by limiting high-speed tire testing on a dry surface to no more than one test run per tire at the highest slip angle used in this study (i.e., 16°).

(5) Test results for the Buick station wagon indicate that test-induced tire wear accrued during one sequence of the trapezoidal-steer maneuver is sufficient to markedly increase the maximum lateral acceleration attained in this maneuver with the Buick.

(6) Trapezoidal steer results for the Mustang show that the amount of wear accrued in one sequence of testing has little influence on the performance of this vehicle. However, if the OE tires used on the Mustang are fully shoulder-worn by 20 high-level trapezoidal-steer maneuvers, then the maximum lateral acceleration obtained with

shoulder-worn tires is approximately 20% higher than the lateral acceleration obtained with the same tires in the non-shoulder-worn (original equipment) condition.

(7) Many of the sinusoidal steer results were nearly identical for test configurations using four OE tires versus tests in which four shoulder-worn tires were employed.

(8) No significant changes from OE performance were obtained in tests performed on a wet surface using shoulder-worn tires.

6.1.2 INFLATION PRESSURE

Findings:

(1) Flat-bed tire-tester results verify that for all the tires tested in this investigation a reduction in inflation pressure causes:

   (a) a decrease in cornering stiffness,

   (b) a decrease in camber stiffness, and

   (c) an increase in aligning torque stiffness.

(2) Mobile-tire-tester results show that maximum longitudinal tire-force levels drop slightly with decreasing inflation pressure. However, straight-line braking and braking-in-a-turn test results indicate that the magnitude of this change in tire force characteristics is not large enough to cause detectable changes in vehicle braking performance. This finding is verified by analytical considerations.

(3) Mobile-tire-tester results verify that lateral tire force capability at high slip angles (8 to 16 degrees) and high vertical loads (such as occur on the outside tires in a severe turn) decreases significantly with reductions in inflation pressure.

(4) Limit-maneuver test results for the Buick station wagon show that a reduction in inflation pressure, from the manufacturer's specified levels of 24 psi front and 28 psi rear to 20 psi for all four tires, does not cause significant changes in limit performance for the normally loaded vehicle.

(5) Significant changes from original-equipment lateral-acceleration and sideslip-angle responses were obtained in trapezoidal steer tests with the Buick operated with 24 psi in the front tires and 16 psi in the rear tires. Simulation results agreed with this finding, and simulation was used to extend this finding to show that if only one rear tire (the one on the outside of the turn) is operated at 16 psi, the Buick will develop large sideslip angles in a trapezoidal steer maneuver.

(6) Trapezoidal-steer-test results and computer calculations indicate that the sublimit performance of the Buick station wagon is strongly affected by a reduction in the inflation pressure of the rear tires.

(7) In the trapezoidal-steer maneuver, the fully loaded station wagon with reduced inflation pressures in the rear tires elicited lateral accelerations and slip angles far in excess of those obtained from vehicle tests with the proper inflation pressure in the rear tires. (The proper inflation pressures

for the fully loaded Buick are 26 psi front and 32 psi rear. When the loaded vehicle was operated with 26 psi in the front tires and 20 psi in the rear tires, the outside rear tire came off the rim during several severe trapezoidal steer tests.)

(8) In the sinusoidal steer tests, significant and potentially dangerous deviations from the OE performances of the Buick and the Mustang were caused by lowering the inflation pressure in the rear tires below the level recommended by the manufacturer, while leaving the front tires inflated to the manufacturer's recommended pressure. The fully loaded station wagon with 26 psi in the front tires and 20 psi in the rear tires was essentially out of control in a sinusoidal steer maneuver for even reasonably small steer amplitudes, showing lateral acceleration in the direction of the attempted lane change long after steering in either direction has stopped.

(9) No degradations from OE performance were obtained in vehicle tests using under-inflated tires on a wet surface.

(10) Test results and calculations pertaining to the normal-driving-range performance of the Buick and the Mustang (i.e., for lateral accelerations less than about 0.3 g on a dry surface) indicate that

(a) Decreasing the inflation pressure in the front tires (while retaining the recommended rear pressure) produces significantly more understeer, not only because the front cornering stiffness is reduced, but because the front aligning torque stiffness is increased.

(b) At the recommended front inflation pressure, increases in rear inflation pressure have very little influence on the linear understeer level, but decreases in rear inflation pressure can cause a significant reduction in understeer level.

(c) With front tires at low inflation pressure, the inflation pressure of rear tires has very little influence on the understeer level.

(d) In the neighborhood of the OE-inflation-pressure conditions, front-to-rear differences in inflation pressure are more significant than simultaneous equal reductions (or increases) in both front and rear inflation pressures.

(11) Of all the tire-in-use configurations investigated, the configuration with normally inflated front tires and under-inflated rear tires (12 psi in this case) produced the longest yaw-rate response times measured on either the Mustang or the Buick.

6.1.3 REPLACEMENT TIRE MIXES. Due to the wide variety of replacement tire choices available (including different construction types and snow tires), an immense number of replacement tire mixes is possible. Several important mixes of replacement tires were investigated in this study.

Findings:

(1) Based on flat-bed tire-test results, "stiff" radial tires were chosen to replace the OE bias-belted tires used on the Buick and the Mustang. These tires had

(a) a higher cornering stiffness,

(b) a higher aligning torque stiffness, and

(c) a much lower camber stiffness than the OE tires.

(2) Mobile-tire-tester results show that the maximum-braking-force capabilities of the radial tires used in this investigation are nearly equal to the maximum-braking-force capabilities of the equivalent-size OE bias-belted tires.

(3) Mobile-tire-tester results show that the radial tires used in this investigation produced higher forces than the OE bias-belted tires in the 2° to 6° slip angle range and significantly lower forces than the OE belted-bias tires in the high slip angle range (i.e., near 16°).

(4) Simulation and test results indicate that the replacement of one or more front tires by any tires (whether radial, bias-belted, or bias ply) which generate higher lateral forces than the OE tires in the low to mid slip angle range (up to 10°), while leaving the OE tires on the rear, leads to significant deviations from the OE response in sinusoidal and trapezoidal steer maneuvers. (Conversely, replacement of one or more rear tires by tires generating lower lateral forces than the OE tires, while leaving the OE tires on the front, is likely to lead to significant deviations from the OE response in the sinusoidal and trapezoidal steer maneuvers.)

(5) Limit-maneuver test results show that insignificant deviations from OE limit performance were obtained for the Buick when operated with the bias-belted

OE tires on the front wheels and bias-ply snow tires on the rear wheels. (This result is not surprising, since the tire test results show that this snow tire has shear force properties very similar to the properties of the OE tires.)

(6) No significant changes from OE performance were obtained in tests performed on a wet surface using radial or snow tires to replace the bias-belted OE tires.

(7) Test results and analytical calculations show that

(a) the use of stiff radial tires on the front wheels of the Mustang or Buick will cause significant reductions in the understeer/oversteer factors for these vehicles,

(b) replacing only the rear OE tires with stiff radial tires does not produce a significant increase in the understeer of the Buick or Mustang (in fact, an increase from the OE value in rear tire cornering stiffness—as might occur due to tire replacement, wear, or inflation pressure—has little influence on the understeer/oversteer factor for either the Mustang or the Buick).

6.1.4 TREAD WEAR. The results summarized here pertain to uniform wear across and around the tread of the tire. Tires with tread groove depths of 6/32, 4/32, and 2/32 of an inch were used in this investigation to study the influence of varying levels of tread wear.

Findings:

(1) Flat-bed tire-tester results verify that a reduction in tread depth causes the cornering, camber, and aligning torque stiffnesses to increase.

(2) Mobile-tire-tester results show that the maximum longitudinal force capabilities of the tires tested on a dry surface increase slightly with increased tread wear (reduced-tread groove depth). However, the magnitude of this change in tire performance does not cause significant changes in vehicle braking performance.

(3) Mobile-tire-tester results show that in the intermediate to large slip angle range (i.e., from approximately 2° to 10°) the lateral force levels for tread-worn Mustang and Buick OE tires are significantly higher than the lateral force levels for the OE tires tested on a dry surface. However, the maximum lateral force capabilities of the OE and tread-worn tires are nearly equal.

(4) Marked differences from OE performance were obtained in sinusoidal- and trapezoidal-steer tests for both the Buick and the Mustang operated on a dry surface with front tires having 2/32" tread groove depths and rear tires having OE (new tire) groove depths. These differences in vehicle performance were largest at an intermediate normalized steer angle of about 8°.

(5) Vehicle tests and calculations show that the influence of tread wear on normal driving performance (as quantified using an understeer/oversteer factor in degrees/G) is insignificant for the Buick and the Mustang. (The reasons for this insensitivity to tread wear are (1) when worn tires are used on the front wheels, the increase in cornering stiffness is offset by the increase in aligning torque stiffness accompanying tread

wear; and (2) increasing the cornering stiffness of the rear tires has very little influence on the understeer/oversteer factor of these vehicles.)

(6) The Mustang, when operated on the wet surface with 2/32" groove depth tires on all four wheels, could not reach 0.4 g deceleration without locking both front wheels in a straight-line braking maneuver. (The vehicle equipped with new OE tires achieved almost 0.6 g before locking both front wheels.)

(7) Sinusoidal steer maneuvers performed on wet surfaces yielded startling and repeatable disparities between results obtained with worn and non-worn tire configurations. Both the Mustang and the Buick exhibited a violent "spin-out" behavior in a mid-range sinusoidal steer maneuver at 40 mph when the vehicles were equipped with OE front tires and rear tires which were worn to 2/32" tread groove depth. (This response was not obtained with 4/32" groove depth tires on the rear wheels at 40 mph, but a violent spin was obtained at 45 mph with 4/32", 6/32", and OE groove depth tires.)

6.1.5 MATHEMATICAL MODELING OF TIRES. In this study, a semi-empirical tire model [23] was refined and augmented to provide an accurate mathematical representation of measured tire data. Typical results from calculations using this model are presented in Figures 3-18, 3-19, 3-37, and 3-39. A complete description of the tire model is presented in Appendix B.

Findings:

(1) To obtain computed results within 5% of measured lateral shear force data across the entire range of slip angles and loads routinely encountered in limit maneuvers requires

   (a) the use of nonlinear functions to describe rates of change of heretofore assumed constant tire parameters such as lateral spring rate,

   (b) recognition of the differing pressure distributions at the tire-road interface for radial and non-radial tires, and

   (c) the use of load-sensitive stiffness and peak-friction descriptors.

(2) The refined tire model provided improved prediction of limit-maneuver response for two vehicles (a 1971 Dodge Coronet and a 1971 Chevrolet Brookwood station wagon) which were tested in a previous program. In addition, the new tire model was found useful both for extrapolating tire data to more extreme values and for simulating limit maneuvers, particularly trapezoidal and sinusoidal steer.

6.1.6 VEHICLE TESTING PROCEDURES. This section presents observations made concerning the process of collecting, examining, analyzing, and interpreting data from normal-driving-range and limit-maneuver testing activities. The findings bear on the results of this program and on future research activities.

Findings:

(1) For the constant-steering-wheel-angle method used to assess normal driving performance, it was found that

(a) the results are highly susceptible to measurement errors at low lateral accelerations (i.e., below 0.15 g),

(b) very accurate measurements of vehicle-response variables, particularly yaw rate, are needed to accurately determine the understeer/oversteer factor, and

(c) a great deal of care and checking by testing personnel is required.

(2) The limit-maneuver tests performed on a wet surface indicate that

(a) variations in water depth estimated to be from 0 to 0.25 inches made it very difficult to interpret results from braking tests, because the order and position of wheel lock-up was not repeatable;

(b) the Buick straight-line-braking and braking-in-a-turn tests did not lead to clear-cut findings, because extreme sideslip angles were often obtained due to an imbalance of braking force and a propensity for the rear wheels to lock before the front wheels on this vehicle on this wet surface;

(c) in braking-in-a-turn maneuvers on a wet surface, the path curvature of the Mustang changed from an initial right turn to a left turn in some extreme cases where both front wheels locked; and

(d) the sinusoidal-steer tests on the wet surface are useful for illustrating gross changes in directional stability (such as violent spin-outs) but they are not useful for quantifying the subtleties of directional response.

(3) The dry-surface limit maneuvers that proved to be most useful in the investigation of tire-in-use factors were straight-line braking, trapezoidal steer, and sinusoidal steer.

(4) The time to the inflection point of the trajectory of a vehicle in a sinusoidal steer maneuver was found to be a useful measure for interpreting the results of this test. (Note that the inflection point indicates the transition to the recovery half of the lane-change maneuver. The time to the inflection point is nearly equivalent to the time of the zero-crossing of the lateral-acceleration time history.)

(5) An under-corrective response in a sinusoidal steer maneuver is easily identified by the difference between the peak magnitude of the lateral accelerations obtained during the first and second halves of the maneuver.

(6) Asymmetric responses between left-then-right and right-then-left lane changes on a dry surface were obtained on occasion in this study. (This finding is in conformance with that observed in previous studies [1], [4].)

(7) Variability in sideslip-angle data caused difficulties in using this information for making fine distinctions in directional-response characteristics.

6.2 GENERAL CONCLUSIONS

The following general conclusions were drawn from the evidence gathered in this research investigation.

Inflation Pressure

• Vehicles in use on the highway often exhibit significant inflation-pressure deviations below the manufacturer's recommendations. Such deviations can severely degrade the directional response of the vehicle in emergency maneuvers, particularly when the rear inflation pressure is lower than the manufacturer's recommendation and the front inflation pressure is properly maintained.

• In the normal driving range, improper maintenance of inflation pressure leading to under-inflated front or rear tires can cause significant deviations from the vehicle stability and control properties intended by the manufacturer.

• Tire test results verified that cornering stiffness drops rapidly with decreasing inflation pressure, and this effect is more pronounced at high vertical loads. Also, aligning torque stiffness increases and camber stiffness decreases slightly with decreasing inflation pressure.

Tire Replacement Mix

• The mixing of tires that are not of the same generic type, brand, aspect ratio, and size can (1) degrade the directional response of passenger cars in limit-turning maneuvers, and (2) alter significantly the stability and

control properties intended by the manufacturer. This degradation and/or change is likely to be serious if very stiff tires are mounted in front, with relatively less stiff tires in the rear.

Uniform Tread Wear

• On a dry surface, tire wear is likely to degrade the directional-response characteristics of passenger cars only if the wear is asymmetric, with severely worn tires in front and non-worn tires in the rear. This degradation is more likely to be evident in limit maneuvers than in the normal driving range.

• On a wet surface, severe tread wear will lead to much lower peak shear forces than those obtained from corresponding non-worn tires. Thus, braking performance may be significantly degraded due to tread wear of any tire. Furthermore, if the rear tires are severely worn while the front tires are not, potentially disastrous yaw instability may result.

Test-Induced Wear (Including Shoulder Wear)

• Tire testing and vehicle testing at high speeds and high slip angles may rapidly change the measured lateral shear force characteristics of some, but not all, passenger car tires. The lateral force capabilities of radial tires (with rounded shoulders do not appear to be sensitive to this phenomenon.

• Vehicles equipped with tires with test-induced wear will not necessarily have the same directional-response characteristics as the same vehicles euipped with new tires or tires worn in routine service.

• In the present investigation, tire-test and vehicle-test-induced wear were limited to tolerable levels by

frequently changing tires. The influence of test-induced wear can be controlled by subjecting test tires to no more than one severe turning maneuver or no more than one high-slip-angle, high-speed tire test.

Vehicle Testing

• Testing in the normal driving range can provide much-needed insight into passenger vehicle performance. However, such testing requires much-higher-quality instrumentation than limit-maneuver testing and a great deal of care by testing personnel.

• The most useful limit maneuvers for the purposes of the present investigation were straight-line braking, trapezoidal steer, and sinusoidal steer.

• New sinusoidal steer metrics were developed in the present investigation. The use of these new metrics allow a reasonable understanding of the lane-change maneuver, using only the lateral-acceleration time history, thus obviating complicated data processing.

• An appropriate methodology for detecting the subtleties of vehicle directional response on a wet surface is not currently available. However, in the present program the wet-surface test results provide graphic insight into the instability that may result from using new front tires with severely worn rear tires.

Mathematical Modeling of Tires

• The semi-empirical tire model developed in this investigation to compute the shear forces at the tire-road interface is capable of (a) reasonable estimations of the tire-traction field, based on very few input tire/surface descriptors; or (b) extremely accurate matching of measured data based on more detailed user input.

6.3 IMPLICATIONS OF THE FINDINGS AND CONCLUSIONS

The stability, control, and accident-avoidance capability of passenger cars are significantly influenced by tire-in-use factors. In particular, differences in front-to-rear tire shear force characteristics due to improper inflation pressure, poor choices for replacement tires, or front-to-rear mixing of new tires with worn tires can cause potentially dangerous directional performance characteristics which do not exist in properly maintained original equipment vehicles.

Furthermore, surveys of (a) the condition of tires in use on the highway [11] and (b) tire replacement practices [7] indicate that many vehicles-in-use are operated with undesirable tire configurations. Clearly, proper tire maintenance and replacement practices could eliminate a number of potentially hazardous vehicle conditions from highway driving.

The research objectives of this study were addressed and fulfilled, but not without some difficulty. Further investigations are needed to reduce these difficulties. Specifically, further research is needed to

(1) Evaluate the influence of the steady-state and transient response characteristics of passenger cars on the performance of the driver-vehicle system in normal driving.

(2) Develop a test methodology suitable for studying vehicle directional response and control on wet surfaces.

(3) Improve the utility of the sinusoidal-steer maneuver by (a) identifying the causes for asymmetric response, and (b) developing simpler measures for interpreting the results.

(4) Improve the utility of the trapezoidal-steer maneuver by (a) developing a better understanding of the meaning of the absolute level of the sideslip angle response, and (b) improving the accuracy of sideslip angle measurements.

(5) Extend the state of knowledge concerning the type of wear induced by high-speed tire testing or drastic turning maneuvers to include a deeper understanding of (a) the physical mechanisms involved in lateral-force generation, and (b) the relevance of this type of wear to vehicle-in-use safety.

6.4 RECOMMENDATIONS

The results of this study indicate that departures from inflation pressures recommended by the manufacturer introduce significant vehicle-response problems. Low inflation pressure in the rear tires with proper inflation pressure in the front tires is particularly hazardous. For example, the limit-maneuvering performance of the Mustang was degraded by reducing the inflation pressure in the rear tires from 24 psi to 18 psi, and the Buick limit performance was seriously degraded by reducing the rear inflation pressure from 28 psi to 16 psi.

Since inflation pressure is easily adjusted, quite often low in vehicles in use, and extremely important in vehicle maneuvering, it is recommended that inflation pressures be set as closely as possible to the manufacturer's recommended levels (corrected for tire temperature). They should be set within ±1 psi, and inspection stations should be equipped with air pressure gages which are accurate to ±1 psi. Results from studies of service-station air towers show that a

simple periodic calibration is sufficient to maintain this accuracy [11].

Maintaining inflation pressure to close tolerance is fairly difficult because inflation pressure changes as the tire absorbs heat during usage (or even due to changes in ambient temperature). Traditionally, cold inflation pressures have been specified, and currently the recommended cold inflation pressures are labeled on new vehicles. However, a tire can go from cold to hot very quickly in use. Furthermore, twenty minutes may be needed for a tire to cool to ambient conditions [11]. Consequently, inflation-pressure inspection criteria need to take tire-temperature into account.

Since inflation pressure is not difficult or costly to set, vehicles passing through inspection facilities should exit with the manufacturer's recommended inflation pressures.

There may be some question as to the proper inflation pressure if the vehicle owner has replaced his original equipment tires with another type of tire. Inspection station personnel should note any change from OE tires and indicate to the vehicle owner that the recommended inflation pressures labeled on the vehicle do not necessarily apply to the currently installed tires.

The results of this study indicate that tire tread depth has little influence on directional response in normal driving. But asymmetric wear (front-to-rear) can degrade braking and/or directional performance in limit maneuvers. In particular, severely worn front tires with OE rear tires can lead to directional control problems in severe turning maneuvers on a dry surface, and worn rear tires can lead to directional response problems on a wet surface. In addition, severe tread wear of any or all four tires will significantly degrade braking performance on a wet surface.

Setting an optimum level of tread groove depth is a tradeoff between the costs inherent in observing a high minimum groove depth and the resulting benefits in improved braking and directional performance. Our recommendation, based on the results of this investigation and tempered by our perception of the economics involved, is that tires should be replaced when they reach a groove depth of 2/32 of an inch.

Data collected on the flat-bed tire tester show that a major change in lateral force characteristics takes place between OE and 6/32" (approximately half-worn) tread groove depths, and a significantly smaller change in lateral force characteristics takes place between 6/32" and 2/32" of tread groove depth. In addition, on a heavily wetted surface, a 5-mph increase in speed from 40 to 45 mph was found to be sufficient to cause poor vehicle directional response in lane-change maneuvers with 2/32", 4/32", and 6/32", and OE tread groove depths on the rear tires. These results indicate that the gains obtained by requiring groove depths higher than 2/32" may not be very large. (Only the 2/32" condition caused poor directional response at 40 mph.)

Tread groove depth is not the only tire factor determining the ability of a tire to operate satisfactorily on a wet road. Recent research investigations [24] and [25] have used measures of flow rate or pressure rise to quantify the capacity of tread grooves for handling water. Tread pattern geometry, contact patch width (or area), and groove width are all tire factors which can influence the shear force capability of a tire on a wet road.

Due to the relatively large number of wet-weather accidents, research into inspection methods for assessing the capacity of a vehicle's tires to provide a path for expelling water is recommended. Possibly a simple device can be invented which would apply water to a vehicle's tires and measure

groove flow-capacity directly (or indirectly using pressure measurements). The devices described in [24] or [25] provide a foundation for this work.

In some cases, test-induced tire wear causes significant deviations from the lateral force characteristics of normally broken-in, original-equipment tires. For tire test programs whose purpose is to determine the lateral force capabilities of a tire in the first (and possibly only) emergency turning maneuver to which that tire is subjected, it is recommended that no more than one high-force-level, high-speed test be made on a single tire sample.

Replacement tire mixes which result in very stiff tires mounted on the front wheels and relatively less stiff tires on the rear wheels are likely to cause significant and potentially dangerous changes from the directional response characteristics of the vehicle with original equipment tires. Since replacing tires two at a time is often done for economic reasons, many replacement tire mixes exist on the road.

However, there does not appear to be any worthwhile alternative to having tire lateral force data to decide if a given tire mix is likely to cause a significant change in vehicle behavior. For example, radial tires are on the average stiffer than belted-bias tires, but many radial tires are less stiff than some belted-bias tires. Unless the lateral force characteristics of the tires are known, the buyer or the inspector cannot identify unfavorable construction mixes.

An obvious course of action would be to require the tire manufacturer to supply the needed data. Whether this is a reasonable course of action cannot be determined from the results of this study. Furthermore, the longitudinal traction numerics used in the uniform tire quality grading system are not sufficient for evaluating lateral shear force characteristics. Consequently, further research is recommended for determining a cost-effective methodology for specifying the range of lateral traction performance provided by replacement tires.

REFERENCES

1. Ervin, R.D., et al., Vehicle Handling Performance, Highway safety Research Institute, Univ. of Michigan, Ann Arbor, 3 Vols., a Report to NHTSA, Contract No. DOT-HS-031-1-159, November 1972.

2. Dugoff, H. and Brown, B.J., "Measurement of Tire Shear Forces," SAE Paper No. 700092, January 12-16, 1970.

3. Tielking, J.T., Fancher, P.S., and Wild, R.E., "Mechanical Properties of Truck Tires," SAE Paper No. 730183, January 8-12, 1973.

4. Roland, R.D., et al., The Influence of Tire Properties on Passenger Vehicle Handling, Final Report to NHTSA, Calspan Corp., Buffalo, N.Y., 4 Vols., June 1974.

5. Segel, L., et al., Motor Vehicle Performance—Measurement and Prediction, Univ. of Michigan Engineering Summer Conference, July 22-26, 1974.

6. Bundorf, R.T. and Leffert, R.L., "The Cornering Compliance Concept for Description of Directional Control (Handling) Properties," General Motors Proving Ground Engineering Publication No. 2771, 1971.

7. Leffert, R.L., Riede, P.M., and Rasmussen, R.E., "Understanding Tire Intermix Through the Cornering Compliance Concept," SAE Paper No. 741104, October 21-25, 1974.

8. Segel, L., "Theoretical Prediction and Experimental Substantiation of the Response of the Automobile to Steering Control," Proceedings of the Automobile Division, The Inst. of Mech. Eng., No. 7, 1956-57, p. 310.

9. Experimental Validation of the Calspan Tire Research Facility, Final Report to the Rubber Manufacturers Association, Calspan Report ZM-5269-K-1, December 21, 1973.

10. Olsson, P.L. and Bauer, H.J., "A Survey of Practices in Automobile Inflation Pressures," General Motors Corp., Warren, Mich., Research Publication GMR-433, December 6, 1974.

11. Harvey, J.L. and Brenner, F.C., "Tire Use Survey," National Bureau of Standards Technical Note 528, May 1970.

12. Peterson, K.G. and Rasmussen, R.E., "Mechanical Properties of Radial Tires," SAE Paper No. 730500, May 14-18, 1973.

13. Erlich, I.R. and Jurkat, M.P., "Characteristics of Tire Usage in the Eastern United States, A Survey," Davidson Laboratory Report R-1336, October 1968.

14. Baker, J.S. and McIlraith, G.D., "Use and Condition of Tires on Four-Tired Vehicles on the Illinois Tollway—Tire Study 2," Traffic Institute, Northwestern University, June 1968.

15. Rasmussen, R.E. and Cortese, A.D., "The Effect of Certain Tire-Road Interface Parameters on Force and Moment Performance," General Motors Proving Ground Publication A-2526, July 1969.

16. Dunlap, D.F., et al., Influence of Combined Highway Grade and Horizontal Alignment on Skidding, Highway Safety Research Institute, Univ. of Michigan, Prepared for Transportation Research Board, NCHRP Project 1-14, September 1974.

17. Harned, J.L., Johnston, L.E., and Scharpf, G., "Measurement of Tire Brake Force Characteristics as Related to Wheel Slip (Antilock) Control Systems Design," SAE Paper No. 690214.

18. Tielking, J.T., "Tire Traction Research," HIT Lab Reports, Vol. 3, No. 4, December 1972.

19. Bernard, J.E., "A Digital Computer Method for the Prediction of the Directional Response of Trucks and Tractor-Trailers," SAE Paper No. 740138.

20. SAE Handbook Supplement, J 670c, January 1973.

21. Nedley, A.L. and Wilson, W.J., "A New Laboratory Facility for Measuring Vehicle Parameters Affecting Understeer and Brake Steer," SAE Paper No. 720473, May 22-26, 1972.

22. Leffert, R.L., "Instrumentation for Characteristic Speed Measurement," General Motors Technical Center Publication A-2264, February 5, 1968.

23. Dugoff, H., Fancher, P., and Segel, L., "An Analysis of Tire Traction Properties and Their Influence on Vehicle Dynamic Performance," SAE Paper No. 700377, 1970 International Automobile Safety Conference Compendium, Society of Automotive Engineers, New York.

24. Sinnamon, J.F. and Tielking, J.T., Hydroplaning and Tread Pattern Hydrodynamics, Highway Safety Research Institute Report UM-HSRI-PF-74-10, October 1974.

25. Dijks, A., "A Multifactor Examination of Wet Skid Resistance of Car Tires," SAE Paper No. 741106, October 21-25, 1974.